

ENGINEERING DESIGN HANDBOOK

SABOT TECHNOLOGY ENGINEERING

DEPARTMENT OF THE ARMY
HEADQUARTERS, UNITED STATES ARMY MATERIEL COMMAND
Washington, DC 20315

AMC PAMPHLET
No. 706-445

10 July 1972

Engineering Design Handbook

SABOT TECHNOLOGY ENGINEERING

<i>Paragraph</i>	<i>Page</i>
LIST OF ILLUSTRATIONS	v
LIST OF TABLES	vii
PREFACE	viii

CHAPTER 1. INTRODUCTION

1-0	List of Symbols	1-1
1-1	Background	1-1
1-2	Sabots	1-5
1-2.1	Definition	1-5
1-2.2	Classification	1-6
1-2.3	Action Inside the Gun Tube	1-6
1-2.4	History of Sabot Use	1-12
1-3	Guns	1-14
1-3.1	Definition	1-14
1-3.2	Classification	1-14
1-3.3	Action Inside the Gun	1-14
1-3.4	Pressure-travel Curves	1-16
	References	1-16

CHAPTER 2. SABOT SYSTEM ANALYSIS

2-0	List of Symbols	2-1
2-1	Geometric Classification of Sabots	2-1
2-1.1	Generic Types of Cup Sabots	2-2
2-1.2	Generic Types of Ring Sabots	2-6
2-2	Sabot Design Constraints	2-6
2-3	The Comparison Between Cup and Ring Sabots	2-12
2-4	Fluid Buoyancy Support of Gun-launched Structures	2-13
2-5	Obturation and Sabot Seal Dynamics	2-18
2-5.1	General	2-18
2-5.2	Obturation Methods	2-18
2-5.3	Sabot Seal Dynamics	2-19
	References	2-20

TABLE OF CONTENTS (Con't.)

CHAPTER 3. STRUCTURAL DESIGN
CONSIDERATIONS

<i>Paragraph</i>		<i>Page</i>
3-0	List of Symbols	3-1
3-1	Structural Design Fundamentals	3-2
3-2	Material Characterization	3-3
3-2.1	Linear Elastic Behavior	3-4
3-2.2	The Fitzgerald Modification of Hooke's Law for Incompressible Media	3-5
3-2.3	Loading Rate Effects	3-6
3-2.3.1	Linear Viscoelasticity	3-6
3-2.3.2	Behavior of Materials at High Loading Rates	3-9
3-2.3.3	Other Observations	3-9
3-2.4	Failure Criteria	3-9
3-3	Elementary Design Considerations for Cup Sabots	3-12
3-3.1	Standard Cup Sabot	3-12
3-3.1.1	Bending of Base Plate	3-14
3-3.1.2	Crushing of the Base Plate	3-14
3-3.1.3	Buckling of the Sabot Wall	3-15
3-3.2	Cup Sabot With External Undercut	3-15
3-3.3	Cup Sabot With Internal Undercut	3-15
3-3.4	Cup Sabot With Rider	3-16
3-3.5	Cup Sabot With Base Plate	3-17
3-3.6	Cup Sabot With Shear Plate Restraint	3-18
3-3.7	Special Considerations for Spin-stabilized Applications	3-18
3-3.7.1	Eccentrically Located Pin	3-18
3-3.7.2	Torque Key	3-19
3-3.7.3	Torque Key for Constant Twist	3-23
3-3.8	Special Cup Sabots	3-23
3-4	Elementary Considerations for Ring Sabots	3-23
3-4.1	Buckling of the Forward Portion of the Projectile	3-24
3-4.2	Tensile Failure in Projectile Aft Section	3-25
3-5	The Finite Element Technique	3-25
3-5.1	Background	3-25
3-5.1.1	Geometry	3-25
3-5.1.2	Materials	3-25
3-5.1.3	Boundary Conditions	3-26
3-5.1.4	Dynamic Problems	3-26
3-5.1.5	Miscellaneous Applications	3-26
3-5.1.6	Reliability and Accuracy	3-26
3-5.1.7	Summary	3-26

TABLE OF CONTENTS (Con't.)

<i>Paragraph</i>		<i>Page</i>
3-5.2	Theory of the Finite Element Method	3-26
3-5.2.1	Variational Principles	3-27
3-5.2.2	Finite Elements	3-27
3-5.2.3	Summary	3-29
3-5.3	Application of the Finite Element Method	3-29
3-5.3.1	Input Data	3-29
3-5.3.2	Output Data	3-30
3-5.3.3	Summary	3-31
3-5.4	Example Problems	3-31
3-5.4.1	Uniaxial Compression of a Right Circular Cylinder	3-31
3-5.4.2	Thermal Expansion of a Right Circular Cylinder	3-35
3-5.4.3	Centrifugal Loading of a Right Circular Cylinder	3-35
3-5.4.4	Internal Pressurization and Rotation of a Hollow Cylinder	3-35
3-5.4.5	Internal Pressurization of a Composite Cylinder	3-35
3-5.4.6	Cup Sabot With Metal Base Plate	3-42
3-5.5	Conclusions	3-42
	References	3-47

CHAPTER 4. EXPERIMENTAL METHODS
FOR SABOT DEVELOPMENT

4-0	List of Symbols	4-1
4-1	Introduction	4-1
4-2	Dynamic Failure Characterization of Materials Under Gun Loading Conditions	4-2
4-2.1	Structural Test Vehicle	4-2
4-2.2	Loading Analysis	4-3
4-2.3	Experimental Procedures	4-3
4-2.4	Results of Feasibility Study	4-7
	References	4-7

APPENDICES

Page

APPENDIX A

SUMMARY OF SABOT DESIGNS AND THEIR CHARACTERISTICS	A-1
---	-----

TABLE OF CONTENTS (Con't.)

	<i>Page</i>
APPENDIX B	
SUMMARY OF STRUCTURAL PROPERTIES FOR MATERIALS USED IN SABOTS	B-1
APPENDIX C	
A FINITE ELEMENT PROGRAM FOR DETERMINING THE STRESSES AND STRAINS IN AXISYMMETRIC, ELASTIC BODIES	C-1
Part A: Program Listing (UNIVAC 1108, FORTRAN IV)	C-2
Part B: Input Data	C-15
Part C: Additional Remarks and Output Data	C-21
APPENDIX D	
ABSTRACT BIBLIOGRAPHY OF SABOT TECHNOLOGY ..	D-1
Preface	D-2
Table of Contents	D-3
Abstracts	D-6

LIST OF ILLUSTRATIONS

<i>Fig. No.</i>	<i>Title</i>	<i>Page</i>
1-1	The Design Process	1-2
1-2	Examples of Group 1, Type 1 Sabots	1-7
1-3	Examples of Group 1, Type 2 Sabots	1-8
1-4	Examples of Group 1, Type 3 Sabots	1-9
1-5	Examples of Group 2 Sabots	1-10
1-6	Sabot in Gun Tube	1-11
1-7	Gun System	1-15
1-8	Pressure-travel (Solid Lines) and Velocity-travel (Dotted Line) Curves	1-19
2-1	Basic Cup Design	2-2
2-2	Basic Ring Design	2-2
2-3	Basic Cup Design	2-3
2-4	Cup With Rotating Band (imparts spin to projectile)	2-3
2-5	Cup With Obturator (seals launch tube)	2-3
2-6	Cup With Forward Bevel (augments aerodynamic separator of sabot and projectile)	2-3
2-7	Cup With Internal Taper (thrust and spin transmitted to the projectile through the tapered surface)	2-4
2-8	Cup With External Undercut (weight reduction)	2-4
2-9	Cup With Internal Undercut (weight reduction)	2-4
2-10	Cup With Rider	2-4
2-11	Cup With Base Plate (bearing surface multiplier)	2-4
2-12	Cup With Base Plate and Shock Absorber (for highly brittle projectiles)	2-5
2-13	Cup With Shear Plate Restraint	2-5
2-14	Cup With Support Sting (for thin-walled models)	2-5
2-15	Cup With Fluid Support (for fragile projectiles such as rocket-assisted projectiles)	2-5
2-16	Basic Ring Design	2-6
2-17	Ring With Obturator (seals launch tube)	2-6
2-18	Ring With Forward Bevel (augments aerodynamic separation of sabot and projectile)	2-6
2-19	Ring With Unsupported Forward Undercut (aero-augmented separation and weight savings)	2-7
2-20	Ring With Longitudinally-supported Forward Undercut	2-7
2-21	Ring With Circumferentially-supported Forward Undercut	2-7
2-22	Two-piece Ring	2-7
2-23	Two-piece Self-sealing Ring	2-7
2-24	Performance Limits and Capabilities of Different Sabot Designs	2-10

LIST OF ILLUSTRATIONS (Con't.)

<i>Fig. No.</i>		<i>Page</i>
2-25	Performance Limits and Capabilities of Different Sabot Designs	2-11
2-26	Comparison of Cup and Ring Sabots	2-12
2-27	Projectile, Gun Launch Schematic for Fluid Buoyancy Support System	2-14
2-28	Schematic Diagram of Gun Tube, Ring, and Sabot Projectile	2-20
3-1	Illustration of Possible Stress-strain Behavior	3-4
3-2	Response Characteristics of a Viscoelastic Material	3-8
3-3	Dynamic Stress-strain Relationship for a Polycarbonate Plastic ("Lexan")	3-11
3-4	Variation of $\Phi(h/R)$ With h/R	3-21
3-5	Variation of h/R With Stress Ratio τ_{SC}/τ_{SS}	3-22
3-6	Representative Axisymmetric Solid	3-28
3-7	Typical Idealization of Axisymmetric Solid	3-28
3-8	Quadrilateral Idealization of Solid	3-28
3-9	Setup of Simple Compression Problem	3-32
3-10	Input for Simple Compression Problem	3-33
3-11	Output for Simple Compression Problem	3-36
3-12	Input for Restrained Thermal Expansion Problem	3-37
3-13	Output for Restrained Thermal Expansion Problem	3-38
3-14	Stresses and Displacements for Rotating Solid Cylinder	3-39
3-15	Displacements and Stresses for Hollow Cylinder With Internal Pressure	3-40
3-16	Displacements and Stresses in Rotating Hollow Cylinder	3-41
3-17	Displacements and Stresses in Hollow Cylinder of Two Materials Under Internal Pressure	3-43
3-18	Simple Sabot	3-44
3-19	Element Layout for Sabot	3-44
3-20	Input Data	3-45
3-21	Selected Element Results for Sample Sabot Problem	3-46
4-1	Structural Test Vehicle	4-4
4-2	Structural Test Vehicle Schematic	4-5
4-3	Typical Chamber and Muzzle Pressure-time Response	4-6
4-4	Gun Launch Tested Steel and Aluminum Samples	4-9
4-5	Gun Launch Tested Polycarbonate ("Lexan")	4-10

LIST OF TABLES

<i>Table No.</i>	<i>Title</i>	<i>Page</i>
3-1	Results of Lockheed Propulsion Company (LPC) Tests for Material Strength Under Gun Launch Conditions	3-10
4-1	Experimental Results	4-8

PREFACE

The Engineering Design Handbook Series of the Army Materiel Command is a coordinated series of handbooks containing basic information and fundamental data useful in the design and development of Army materiel and systems. The handbooks are authoritative reference books of practical information and quantitative facts helpful in the design and development of Army materiel so that it will meet the tactical and the technical needs of the Armed Forces.

The purpose of this handbook is to compile meaningful engineering analysis information pertaining to sabots. Emphasis is on numerical techniques for practical stress analysis and methods for determining material strength properties under realistic gun-launch conditions. An exhaustive abstract and reference bibliography is included as Appendix D.

Acknowledgment is offered for the services of Utah Research and Development Corporation, to Mr. Dalton Cantey of Lockheed Propulsion Company, and to Mr. E. L. Bannister, Ballistic Research Laboratories, Aberdeen Proving Ground, Maryland, for the *Sabot Technology Engineering Handbook*, Second Edition, 29 August 1969, which is the document upon which this handbook is based.

The Engineering Design Handbooks fall into two basic categories, those approved for release and sale, and those classified for security reasons. The Army Materiel Command policy is to release these Engineering Design Handbooks to other DOD activities and their contractors and other Government agencies in accordance with current Army Regulation 70-31, dated 9 September 1966. It will be noted that the majority of these Handbooks can be obtained from the National Technical Information Service (NTIS). Procedures for acquiring these Handbooks follow:

a. Activities within AMC, DOD agencies, and Government agencies other than DOD having need for the Handbooks should direct their request on an official form to:

Commanding Officer
Letterkenny Army Depot
ATTN: AMXLE-ATD
Chambersburg, Pennsylvania 17201

b. Contractors and universities must forward their requests to:

National Technical Information Service
Department of Commerce
Springfield, Virginia 22151

(Requests for classified documents must be sent, with appropriate “Need to Know” justification, to Letterkenny Army Depot.)

Comments and suggestions on this Handbook are welcome and should be addressed to:

U.S. Army Materiel Command
ATTN: AMCRD-TV
Washington, D. C. 20315

CHAPTER 1

INTRODUCTION

1-0 LIST OF SYMBOLS

a	= longitudinal acceleration
A_B	= cross-sectional area of gun bore
d	= diameter of projectile
D	= diameter of bore
F	= force
KE	= kinetic energy
L	= length
m	= mass
m_s	= predicted sabot mass
m_o	= sabot mass design objective
m_p	= mass of projectile
P_c	= pressure of propellant gases acting on base of sabot projectile
P_f	= probability of failure
R_s	= structural reliability
v	= velocity or muzzle velocity
W	= weight or weighting factors
p, s	= subscripts referring to projectile and sabot, respectively

1-1 BACKGROUND

Sabots are used as supports for projectiles during gun tube travel. When high velocity is the desired characteristic of the supported projectile, the lightest weight sabot feasible is desired. Generally, engineering steps taken to minimize sabot weight increase the stress and deformation requirements imposed upon the sabot during its travel through the bore of the gun. This handbook presents engineering design procedures for sabots. It takes into consideration the conflicting criteria associated with maximum performance and maximum reliability.

The steps and decisions which must be made in the process of producing an engineering design are summarized in Fig. 1-1. It will be noted that the design process contains the following six different types of activities^{1-3*}:

- (1) To recognize need for the product (Block 1 in Fig. 1-1)
- (2) To establish criteria for evaluating alternatives (Blocks 2 and 3)
- (3) To generate one or more tentative designs or prototypes (Blocks 4 and 9)
- (4) To analyze each alternative (Blocks 5, 7, and 10)

*References are located at the end of each chapter unless specific reference is made to the abstract bibliography of Appendix D.

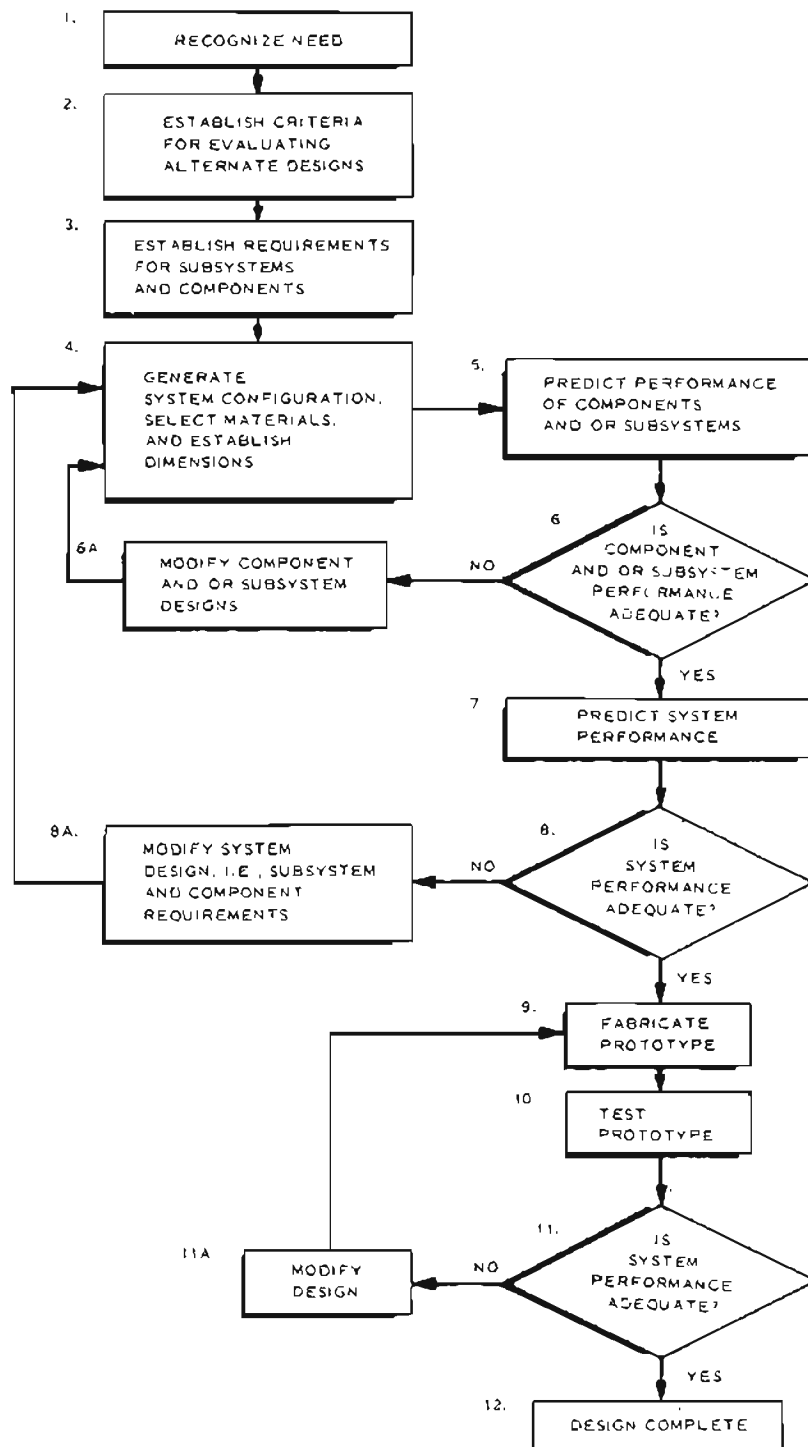


Figure 1-1. The Design Process

- (5) To compare alternatives with previously established criteria or requirements (Step 2) and, if necessary, modify the design and repeat the preceding step (Blocks 6, 6A, 8, 8A, 11, and 11A). This is the optimization phase of the design process
- (6) To implement the best alternative (Block 12).

Assume that the need for a sabot has been established; the next step in its design (Block 3) is establishment of the sabot design criteria. A sabot is a component of a weapon system designed for an ultimate goal to deliver a specified projectile to a target at a prescribed range and terminal velocity. The projectile should have an acceptable impact velocity and should reach the target within an acceptable dispersion. Qualitatively the sabot must accomplish the following:

- (1) Position and structurally support the projectile during its launch
- (2) Seal or obturate the powder gases within the launch tube
- (3) Minimize balloting of the projectile, i.e., undesired lateral or yawing motion produced by bore and/or projectile asymmetries, variations in bore friction, and powder burning phenomena
- (4) Impart rotation to spin-stabilized projectiles
- (5) After discharge from the launch tube, separate from projectile without disturbing the flight of the projectile and without creating a hazard to personnel in the immediate area.

The quantitative requirements for a specific sabot application can be established from a knowledge of weapon system performance goals,⁴ using the techniques of external⁵⁻⁹ and terminal ballistics.¹⁰⁻¹² The loads imposed upon the sabot can be predicted using

the analytical methods of interior ballistics.¹²⁻¹⁸ The output from this stage of the sabot design process (Block 3) should be (1) a definition of the projectile, i.e., mass, diameter, length, and other dimensional considerations; (2) gun configuration and performance requirements, i.e., bore diameter, muzzle velocity, etc.; (3) the sabot load environment, i.e., base pressure, acceleration, bore friction, etc.; and (4) permissible anomalies in launch conditions, primarily maximum allowable lateral displacement, lateral velocity, yaw angle, and yaw rate.

Having at least tentatively established the design criteria, the next step (Block 4) is to select a basic sabot configuration, materials, dimensions, and manufacturing processes considered capable of satisfying the design criteria. This step normally is performed in one or a combination of three different approaches to design — intuitively, empirically, or rationally². The intuitive approach defies description because it depends upon the designer's "feel" for the problem and his individual creativity. The empirical approach is the scaling to new requirements of proved designs and experimental results. The rational approach to design is the systematic application of established scientific laws, principles, and rules of logic to a properly defined problem. If it were possible to establish a general design; analyze it for all combinations of conditions; and produce a closed-form solution that could be solved for the various dimensions of the design in terms of material properties, performance requirements, loading conditions, etc.; complete rational design could be performed. Furthermore, there would be no need for succeeding steps (Blocks 5, 6, and 6A). In practice this is rarely possible, however, and the rational approach to design normally consists of establishing critical design parameters using complete solutions of idealized problems with limited but, hopefully, the significant loading or performance condition. Despite its shortcomings, the rational design approach permits the designer to establish without bias the "base" design required as an input to the subsequent

prediction, evaluation, and optimization phases. The rational approach may be thought of as providing precise solutions to approximate problems. Solutions of this type appropriate to sabot design are presented in a subsequent chapter of this handbook.

The "base" design established in Block 4 is a necessary input to the analysis or prediction stage of the design process (Block 5). This step consists of taking the specific design configuration, dimensions, detailed material properties, loading conditions, etc., and predicting the system's behavior. For example, in the case of a structural design problem, one would predict the stresses and strains induced in the body by the mechanical and thermal loads imposed upon it. Electronic computers have been a particularly useful asset in this phase of design. Their widespread availability and ability to perform computations at high speed makes it possible to achieve approximate solutions to "exact" problems which are more accurate than the exact solutions to "exact" problems which are more accurate than the exact solutions of approximate problems referred to above.^{17, 19, 21} Digital computer algorithms could be used for hand calculations but they are so lengthy that manual solution is neither economically feasible nor reliable, and would take too long to provide answers for design decisions on a timely basis.

The next step (Block 6) in the design process is to compare the predicted performance to the desired performance, i.e., the design criteria. In the traditional "go - no go" concept of structural design, the predicted stresses and/or strains are compared to the stresses and/or strains that the material is capable of withstanding to determine if a desired safety factor is achieved. If the desired safety factor is not achieved, design changes are made (Block 6A); whereas if an adequate safety factor is obtained, the design progresses to the system performance evaluation phase (Block 7).

Alternately, statistical techniques can be employed to combine the uncertainties in the

predicted stresses or strains with the random variations in the ultimate properties of the material to establish the probability of failure or the structural reliability. To employ this latter technique, a design criterion or figure of merit that uses both the structural reliability and an appropriate performance parameter should be used. For example, one might maximize the figure of merit formed by a linear combination of the structural reliability and the ratio of the desired sabot mass to the predicted sabot mass, each multiplied by a weighting factor, i.e.,

$$\text{Figure of Merit} = F \text{ or } M = W_1 R_s + W_2 \left(\frac{m_o}{m_s} \right) \quad (1-1)$$

where

$R_s = 1 - P_f = \text{structural reliability}$

$P_f = \text{probability of failure}$

$m_s = \text{predicted sabot mass}$

$m_o = \text{desired sabot mass (design objective)}$

$W_1, W_2 = \text{subjectively established weighting factors designed to give more or less emphasis on either the structural reliability or the sabot mass.}$

Optimization techniques can then be employed (Block 6A) to determine and implement those changes that improve the figure of merit. This technique is repeated until the figure of merit reaches an extreme value. Observe that the figure of merit is used for comparison purposes only and does not necessarily have a physical significance.

To avoid the problem of suboptimization, i.e., achieving an "optimum" component design that does not result in optimum system performance, it is important that the design procedure include prediction (Block 7), evaluation (Block 8), and optimization phases (Block 9) for the entire system. In the sabot design problem, the system evaluation phase

would consist of predicting the time-dependent motion, velocity, acceleration, chamber pressure, etc., for a given projectile-sabot design, charge configuration, gun barrel length, etc.^{13-17, 19} The figure of merit for system optimization must employ a system performance parameter such as muzzle velocity. In an expanded performance evaluation program, the figure of merit would be expanded to include obturation and/or seal dynamics considerations.

Once the optimal, or at least an acceptable, design has been achieved analytically, it generally becomes necessary to demonstrate the capability of the design. For this purpose, one or more prototypes are manufactured, tested, and the results are evaluated. The purpose of this phase of the design is to (1) verify the analysis, (2) determine the effect of phenomena not included in the analytical design, and (3) confirm that the design meets the design objectives. The similarity between the analytical and prototype sequences will be noted. Instead of developing an analytical model, a prototype is fabricated (Block 9). Instead of predicting the response of the component or system, the response is measured (Block 10). The evaluation and optimization phases also are similar to the analytical cycle. The primary difference is that measured data are used in lieu of theoretical predictions. Successful completion of all performance and qualification tests resulted in a completed design.

This handbook is organized in accordance with the previous discussion. Sabot design considerations covered include (1) structural considerations, (2) obturation, and (3) seal dynamics. Elementary, closed-form equations for preliminary design of sabots are presented as well as sophisticated computer programs for detailed analysis. More material is included under structural design considerations (Chapter 3) than for either obturation or seal dynamics. This is due to the fact that structural design is further advanced than either obturator design or the evaluation of dynamic phenomena excited during launch. This

should not be construed to mean that structural considerations are more important. It merely points out the need for additional work in the latter areas.

Chapter 2 is a preliminary chapter because it establishes the basic types of sabots, their classification, and the nomenclature used in this handbook. References are listed at the end of each chapter and a comprehensive bibliography is included as Appendix D.

The remainder of Chapter 1 is devoted to generalized background information pertinent to guns and sabots.

1-2 SABOTS

1-2.1 DEFINITION

The term "sabot" in this handbook is a derivative of a term referring to a wooden shoe. A military use of sabot is inherited from its description as "a piece of soft metal formerly attached to a projectile, to take the grooves of the rifling". In modern terms, a sabot is a device conforming on one surface to a gun bore and on the other surface to a projectile. It carries the projectile down the gun bore, under action of propellant gases. Nearly all sabots separate from the projectile after exit from the gun, leaving the projectile to fly to its target unaccompanied. In addition to being a projectile carrier, a sabot also may be designed to reinforce structurally or to protect the projectile under the high pressure, temperature, and acceleration environment in the gun bore. To satisfy its main function as a projectile carrier, the sabot not only must remain intact during bore travel, but also must serve as a gas seal. Even minute leakage of gun gas around or through a sabot structure is inimical because of the intense erosive power of the gas flow.

Generally, a sabot projectile is subcaliber with respect to the gun, i.e., a projectile with a diameter less than the bore diameter of the launch tube, and which uses the sabot as an adapter or carrier to support it during launch.

Because the sabot usually is separated or discarded from the projectile after it emerges from the launch tube, it also is referred to as "a discarding sabot projectile". When the basic objective to be achieved is the highest possible muzzle velocity (or projectile acceleration) for a given projectile weight, a performance improvement will be achieved only if the average cross-sectional density of the sabot is less than that for the projectile alone.

1-2.2 CLASSIFICATION

Sabot projectile applications can be grouped into two categories based upon the configuration and function of the projectile. The first group is characterized by high density, high ballistic coefficient projectiles designed for maximum impact kinetic energy, and terminal ballistic effects. Of outstanding importance in this group are kinetic energy penetrator rounds designed for defeat of medium and heavy armor. Literature review and initial analysis indicate that these configurations have been developed to a relatively high degree of sophistication on the basis of qualitative design procedures and an extensive background of experimental evaluation testing. Within this group, there are basically three different types of sabot projectiles: (1) spin-stabilized projectile with a cup sabot, (2) aerodynamically stabilized* projectile with a cup sabot, and (3) aerodynamically stabilized* projectile with ring sabot. Typical designs for these three types are depicted in Figs. 1-2 through 1-4.

A second group of sabot projectiles is characterized by medium- and low-density projectiles that may be gun-launched for many uses. Applications for this group include aeroballistic testing of a wide variety of aerodynamic models using light gas-gun techniques, weapon systems employing high explosive and shaped charge warhead configuration, gun-booster rockets, and a variety of tactical and research projectiles including flares, chaff, probes, electronic packages, and

liquid payloads. Typical sabot designs of the second group are shown in Fig. 1-5. Research studies show that fluid sabot buoyancy support techniques can provide significant structural design advantages for relatively low-density gun-launched structures. Projectile support during launch acceleration provided by the buoyancy and pressure distribution effect of the fluid can result in significant reductions in strength and weight requirements. Such projectiles, without fluid support, would be exposed to destructive acceleration loads during gun launch. Functional and design limitations imposed on buoyancy-supported projectiles are controlled primarily by configurational requirements, density, fluid compressibility, and hydrodynamic effects.

1-2.3 ACTION INSIDE THE GUN TUBE

Consider the simple sabot-projectile system shown in Fig. 1-6 as the system is acted upon by the propellant gas pressure P_c , accelerating the system to the right (as shown in the figure). The accelerating force F is given by

$$F = P_c A_B = P_c \left(\frac{\pi D^2}{4} \right) \quad (1-2)$$

where P_c is the pressure* acting upon the shot base area $A_B = \pi D^2/4$, A_B also equals the bore cross-sectional area. This force causes an acceleration a of the shot

$$a = \frac{P_c A_B}{(m_p + m_s)} = \frac{\pi D^2 P_c}{4(m_p + m_s)} \quad (1-3)$$

where m_p is the mass of the projectile and m_s is the mass of the sabot.

The acceleration gives rise to coupling stresses at the contact interfaces as indicated by the arrows in Fig. 1-6(B). The coupling stresses as indicated, over-simplified by comparison to reality, are a mixture of shears and normal stresses generated by force F and the differential inertial resistance to motion of

*Fins or flared aft sections.

*The "back pressure" at the forward end of the projectile (usually atmospheric condition) is neglected in comparison to the higher magnitude of P_c .

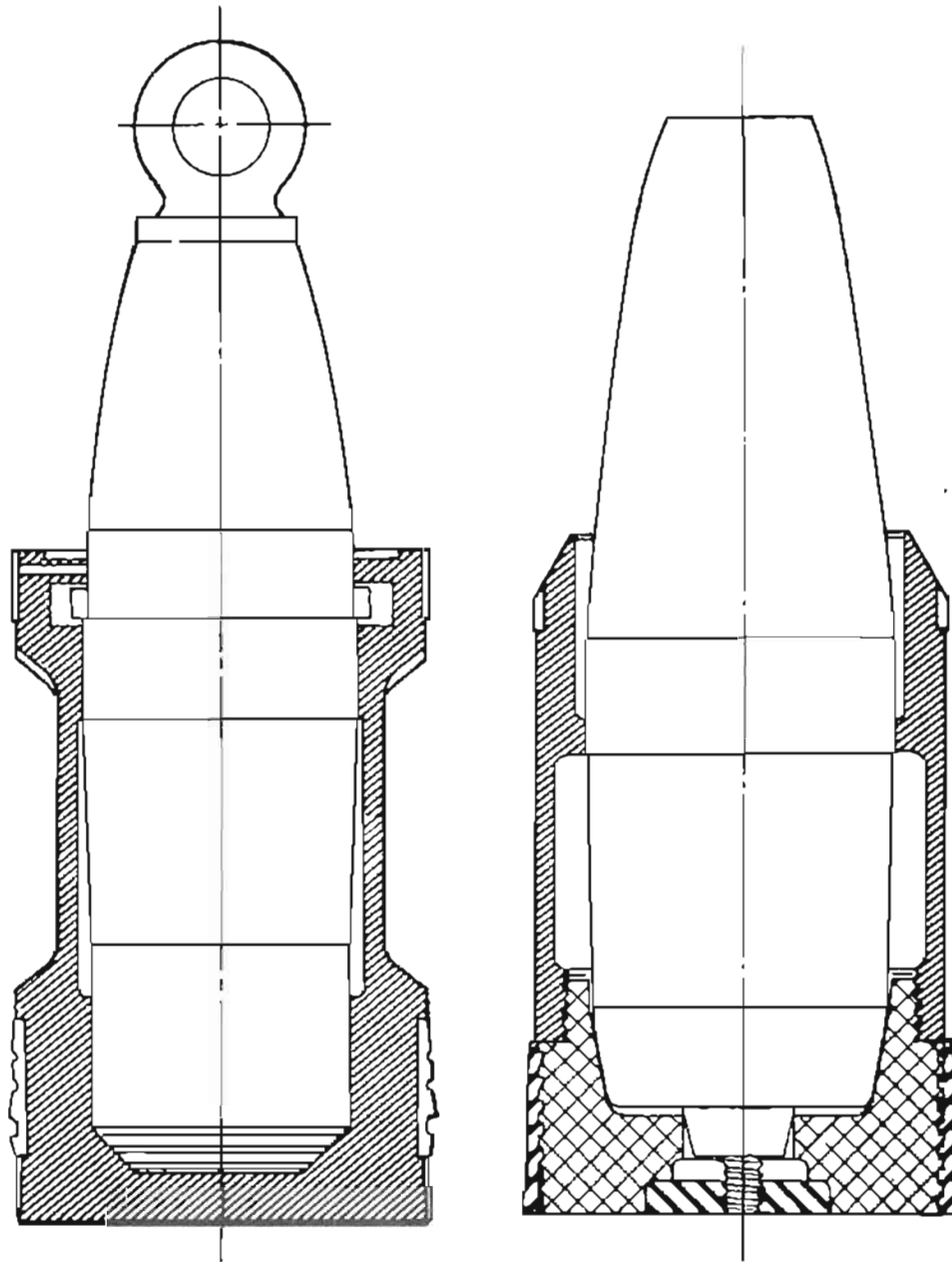


Figure 1-2. Example of Group 1, Type 1 Sabots

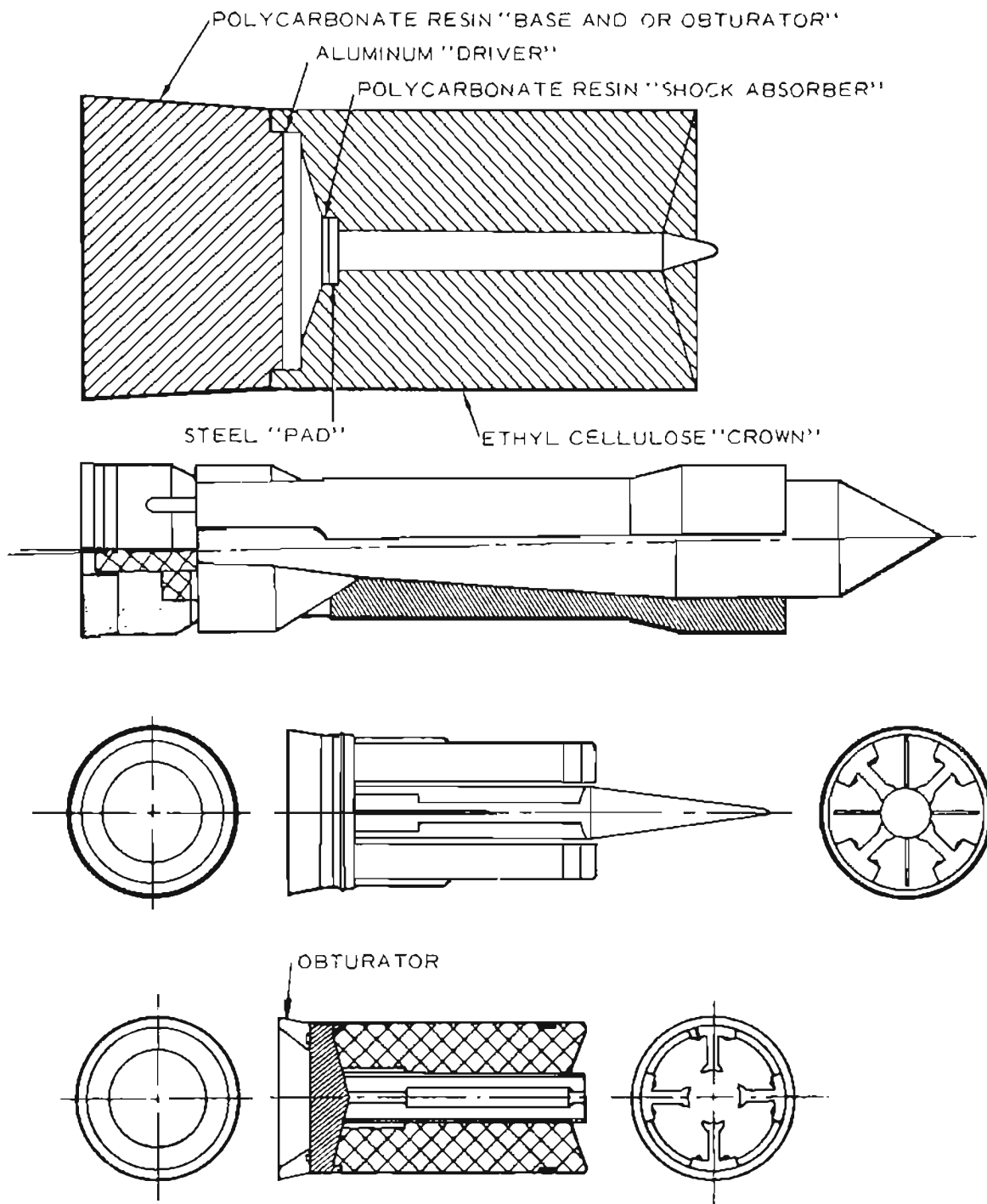


Figure 1-3. Examples of Group 1, Type 2 Sabots

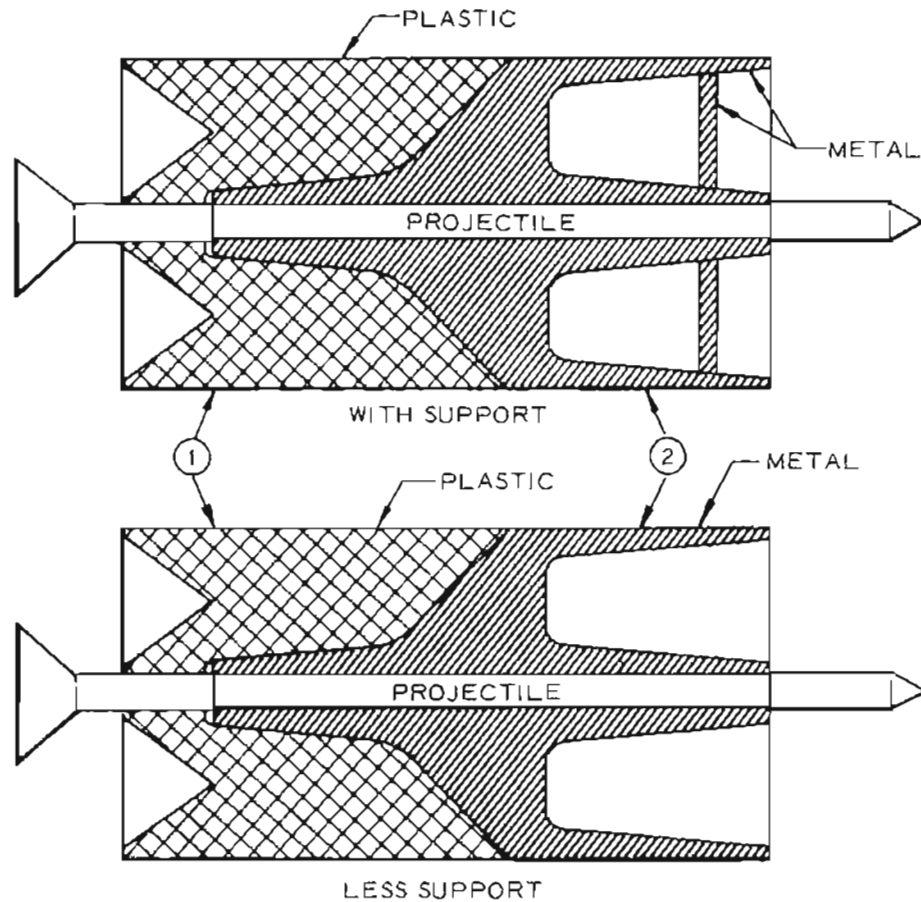
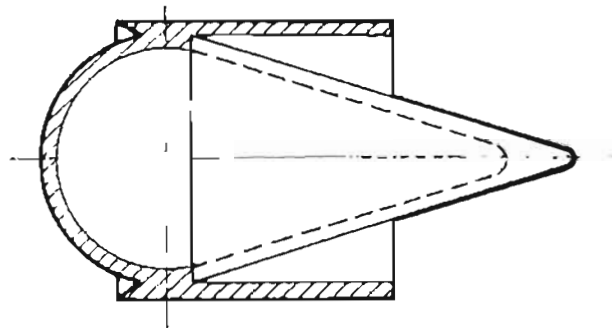
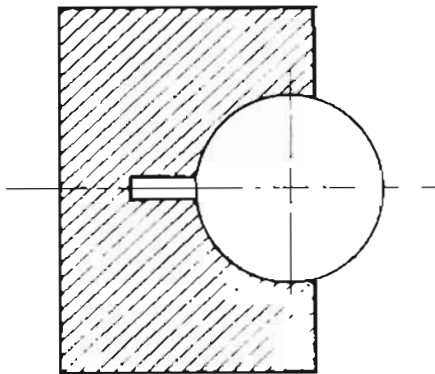


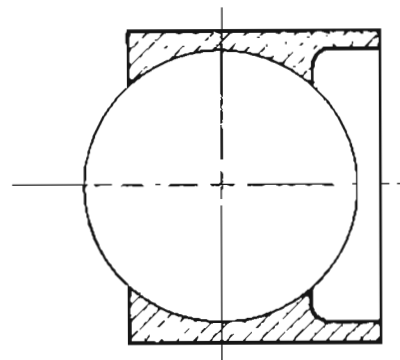
Figure 1-4. Examples of Group 1, Type 3 Sabots



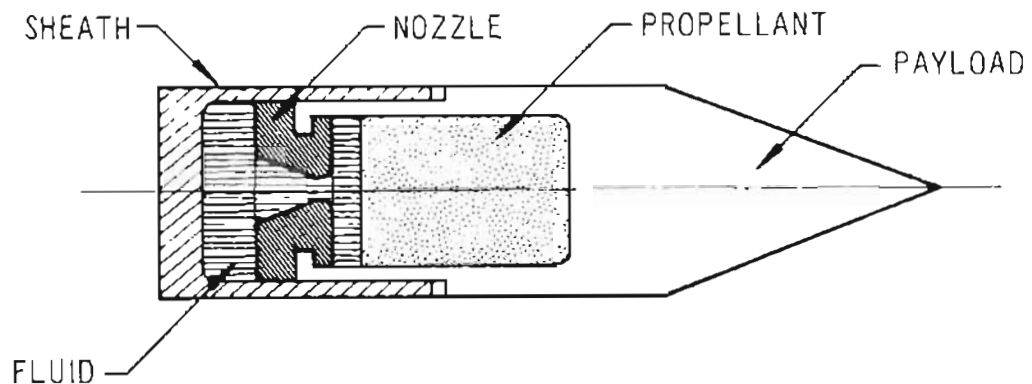
(A) MODIFIED CUP SABOT FOR LAUNCHING THIN WALLED AERODYNAMIC MODELS



(B) CUP SABOT FOR LAUNCHING SPHERICAL BODIES



(C) RING SABOT FOR LAUNCHING SPHERICAL BODIES



(D) FLUID SUPPORT SABOT FOR LAUNCHING ROCKET-ASSISTED PROJECTILES OR PROBES

Figure 1-5. Examples of Group 2 Sabots

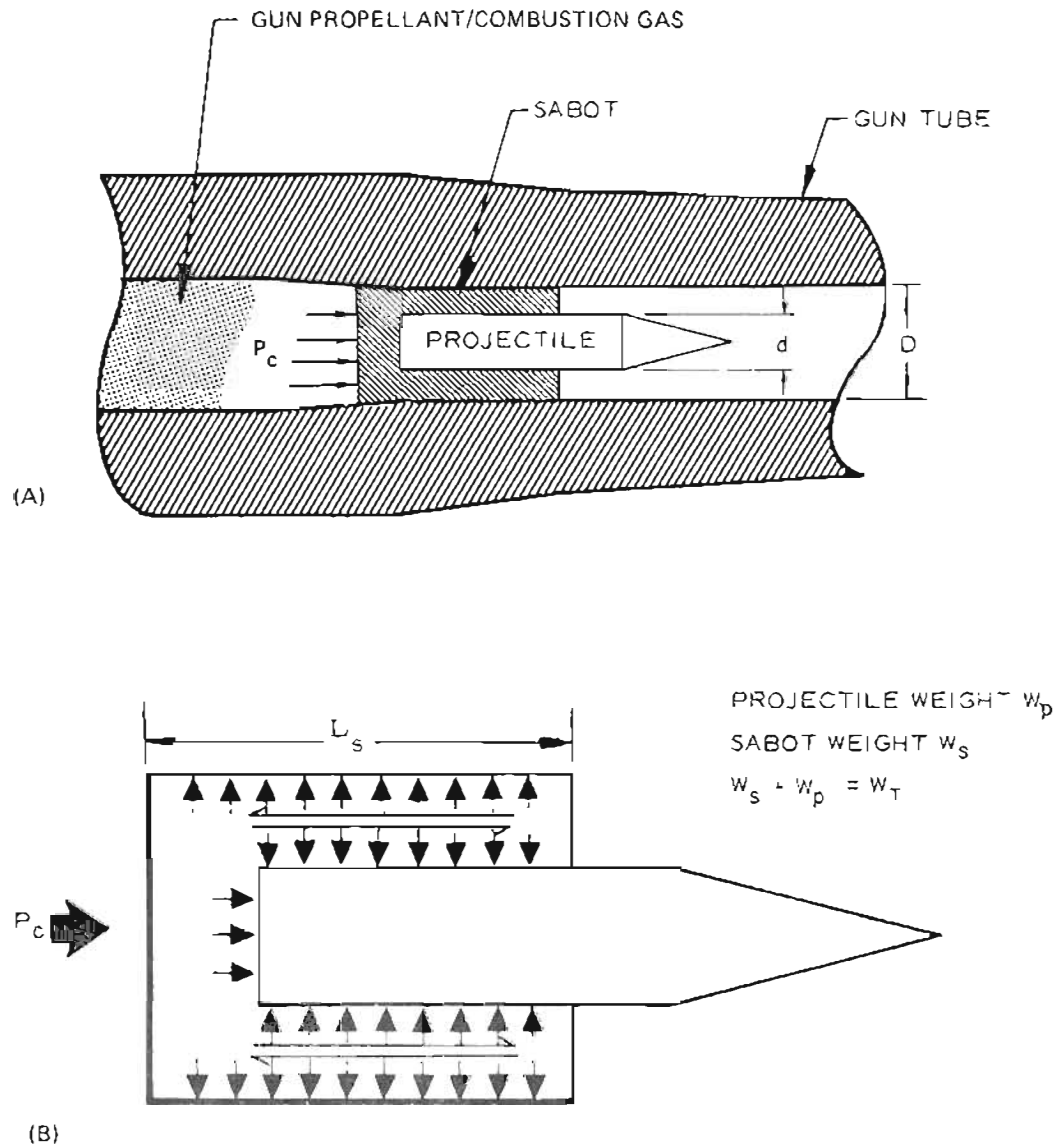


Figure 1-6. Sabot in Gun Tube

the projectile and sabot, as well as by the confinement of the barrel. The result of the action is to cause frictional shear gripping of the cylindrical surface of the projectile by the sabot and a push normal to its back (left) end. Thus, the acceleration force F is transmitted from the sabot through the interfaces as indicated to cause its acceleration along with the sabot. This scheme is operative until an allowable stress or deformation is exceeded in the material of the sabot or the projectile, causing failure of the parts. The objective of structural analysis of sabots is to deduce, formally, how the load F is distributed through the sabot and projectile, particularly near the contact surfaces between which failure is likely to be initiated. The stress analysis prediction then can be compared to the strengths of the materials and the design evaluated. Alternatively, the capability for adequate stress and strength analysis is synonymous with the capability for design optimization because the stress-strength analysis capability permits permuting design details to arrive at design optima.

The design depicted schematically in Fig. 1-6, while simple, is representative of approaches to many sabot applications. The complications arising in the details of an analysis by geometric variations in the sabot in no way alter the generic approach illustrated.

1-2.4 HISTORY OF SABOT USE

Sabot is the French word for wooden shoes worn by peasants in France, Belgium, and neighboring countries. Recently, however, the word has been applied to the "shoe" carrier used to launch various aerodynamic shapes and subcaliber projectiles at hypervelocity speeds.

The Canadians were among the first to apply the potentialities of sabot-launched projectiles. The success they achieved by 1949 in the development of an APDS (armor-piercing, discarding-sabot) shot for a 20-lb cannon encouraged the United States to

launch into the development of a 76 mm HVAPDS (hypervelocity, armor-piercing, discarding-sabot) shot in competition with the T66 rigid shot previously under development. The experimental version of this 76 mm HVAPDS shot was designated the T145. It subsequently was redesignated as the M331 when accepted for use by the U.S. Army.

Until 1953, sabots were made of metal, primarily aluminum and magnesium alloys because of their high strength-to-weight ratios. Sabot discard was achieved by designing the sabot so that when it was in the launch tube the centrifugal forces associated with spinning the sabot and projectile would expand the sabot out against the launch tube but would not fracture it. When the sabot and projectile emerged from the launch tube, removal of the radial restraint caused the sabot to disintegrate under the centrifugal loading.

In 1953, the advantages of plastic sabots were recognized and the development of a plastic version of the T145 sabot projectile, designated T89, was begun. This sabot projectile was highly successful and later became part of the M88 cartridge. Advantages of plastic sabots²² include:

- (1) Their strength is adequate for many applications.
- (2) They cost less because they are easier to manufacture.
- (3) They do not require critical materials.
- (4) They do not create as much wear on the launch tube.
- (5) They break into less lethal pieces.

The first plastic sabots were made of glass-fiber filled diallylphthalate sheathed in nylon and they included metal reinforcements whenever it was felt necessary to redistribute the stresses. The nylon sheath was necessitated by the abrasive nature of glass-filled

materials. Nylon also is used for rotating bands on projectiles and on metal sabots. Other plastics used for the structural portions of sabots include polypropylenes, polycarbonates, celluloses, epoxies, and phenolics. Polyethylene, neoprene, and silicone rubbers are used for seals and obturators.

The United States began development of a series of high L/D (length-to-diameter) fin-stabilized, high-density, kinetic-energy penetrators in 1951. This type projectile sometimes is called an "arrow" projectile and is typified by the T320 and T208 shot series.^{24,25} Because of the high L/D ratio, the traditional cup or push sabot was inadequate and ring or push-pull sabots were developed. This type of sabot wraps around the central or forward section of the projectile, and partially pulls, partially pushes the projectile through the launch tube. To transfer acceleration forces from the sabot to the projectile, a series of buttress-shaped, annular grooves are made on both the projectile body and mating sabot surface. These grooves interlock when the sabot and projectile are assembled. Because this type of projectile usually is fired from smoothbore guns*, centrifugal forces cannot be relied upon for separation. Ring sabots, therefore, are usually made in several segments and incorporate air scoops or bevels on the forward end of each segment so that aerodynamic forces and stored strain energy tend to peel or petal the sabot segments away from the projectile.

The aft end of both ring and cup sabots also are scooped out, permitting the high gas pressures generated by the burning powder to assist in sealing against gas leakage.

It also should be observed that the annular grooves on the projectile body increase its drag coefficient and, therefore, are objection-

able. Aircraft Armaments, Inc. (AAI) has developed a friction-type, ring sabot and demonstrated its use in both small (cal .22) and large (152 mm) caliber weapons.^{26,27}

Two serious disadvantages exist with the fin-stabilized, "arrow" projectile and ring sabot combination: (1) both the launch tube-sabot and the sabot-projectile interfaces must be sealed against gas leakage and the destructive erosion associated with gas leakage, and (2) the fins of the projectile are exposed to high temperature gases during both the launch and flight portions of operation. The latter results in extreme fin ablation which is extremely undesirable. To overcome these difficulties, a series of delta-finned projectiles was developed that can be launched from a modified cup sabot.²⁸ The modified cup sabot consists of a base plate upon which the weight of the projectile rests and four to six circumferentially spaced radial supports to position the projectile in the launch tube.

The possibility of employing gun-launched rockets and space vehicles as a means of obtaining improved performance at reduced cost has not gone unnoticed. The SPRINT high-speed interceptor missile is a typical example of a high-performance ejection-launched rocket. It uses a modified cup sabot. Studies also indicate the feasibility of launching space vehicles 14 ft in diameter using a mass-restrained atomic-powered cannon.²⁹

In 1964, in connection with Project HARP (Joint United States-Canadian High Altitude Research Program), interest was expressed in launches of high-performance rockets from guns of up to 16-in. in bore diameter³⁰⁻³⁵. In a typical high-performance rocket motor, axial accelerations of order only 10 or 10² g can be tolerated before axial buckling causes catastrophic failure. In 1964, Lockheed Propulsion Company and Ballistic Research Laboratories (BRL) cooperated to demonstrate survivability of high-performance rocket vehicles at $\approx 10^4$ gravities acceleration in 3- to 5-in. bore sizes. The support technique used

*Rifled barrels have been used but it is anticipated that there is sufficient slippage between the sabot and the projectile that the latter will not develop significant spin.

has been termed "fluid buoyancy support"* and consists, in essence, of neutral flotation of the structure in a gun tube, from which the rocket-containing fluid slug is expelled as a unit³⁷⁻³⁹.

A summary of sabots, sabot-projectiles, and their characteristics is included in Appendix A.

1-3 GUNS

1-3.1 DEFINITION

The term "gun" in this handbook, unless otherwise indicated, may be taken in its general sense — i.e., a projectile-throwing device consisting essentially of a projectile-guiding tube, with connected reaction chamber in which the chemical energy of a propellant is rapidly converted into heat and the hot gases produced expand to expel the projectile at a high velocity.

1-3.2 CLASSIFICATION

For convenience of discussion, guns are classified according to their salient features, functions, modes of operation, etc.⁴⁰ The boundaries of these classifications are not always clearly defined, and the classifications and nomenclature are often traditional. The classifications are useful, however, and are in common use. The principal one is based roughly on size and portability and classifies "gun" as small arms and artillery. Small arms are in general less than 30 mm in caliber. Artillery consists of the larger weapons usually mounted on carriages and moved by other than human power. Small arms are more variable in design and function. They include such weapons as rifles, machine guns, pistols, etc. Artillery weapons include guns (specific), howitzers, and mortars. Guns (specific) include those firing usually at lower elevation and higher velocity. Howitzers include those generally operating in a lower velocity range. The latter can be fired at high angles and use zoned charges, i.e., charges

loaded in separate increments and ones that can be varied within limits by the gunner. Mortars operate at high angles similar to howitzers. Mortars possess lower velocities and generally are loaded from the muzzle. They are not complex in design and may be taken apart and transported by foot soldiers.

Pistols, mortars, howitzers, and guns that produce medium or low velocities under ordinary circumstances are not ordinarily considered for use as projectors for high-velocity sabot projectiles. When sabot-support of subcaliber projectiles for attainment of muzzle velocities in excess of 4,000 fps is a design objective, the guns most suitable for use as launchers are typically long in caliber length and/or designed for high pressure operation ($\approx 75,000$ psi).

1-3.3 ACTION INSIDE THE GUN

Essentially, a gun is a heat engine. Its action resembles the power stroke of an automobile engine with the expansion of hot gases driving the projectile instead of a piston (Fig. 1-7). When the charge is ignited, gases are evolved from the surface of each propellant grain, and the pressure in the chamber increases rapidly. Resistance to initial motion of the projectile is great, and relatively high chamber pressures are attained before much motion of the projectile takes place. The chamber volume is increased by the movement of the projectile. This has the effect of decreasing the pressure. However, the rate of burning of the charge increases. The effect is a rapid increase in the propellant pressure until the point of maximum pressure is reached. This occurs at a relatively short distance from the origin of rifling. Beyond that point, pressure drops and, at the muzzle, reaches a value considerably less than maximum pressure, probably on the order of 10 to 30 percent thereof, depending upon the weapon design and the propellant. This muzzle pressure continues to act on the projectile for a short distance beyond the muzzle. Thus, the projectile continues to accelerate beyond the muzzle.

*Patent Numbers 3,369,455 and 3,369,485

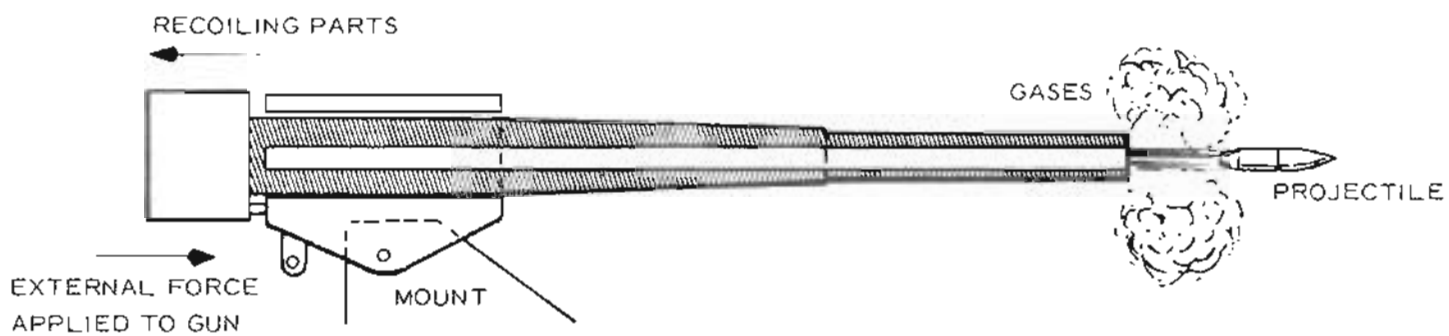


Figure 1-7. Gun System

1.3.4 PRESSURE-TRAVEL CURVES

In order for the projectile to acquire the designated muzzle velocity, and that the pressures developed to accomplish this not damage the weapon, all tubes are designed in accordance with a desirable pressure-travel curve for the proposed weapon⁴¹.

The pressure-travel curves (Fig. 1-8) indicate the pressure (or force if pressure is multiplied by the cross-sectional area of the bore) existing at the base of the projectile at any point of its motion. Hence, the area under any of the curves represents the work accomplished on the projectile per unit cross-sectional area, by the expanding gases.

If the areas under Curves A and B are equal, then the work performed in each of these cases will be equal, and the muzzle velocities produced by each of these propellants will be the same, since

$$\text{WORK} = KE = mv^2/2 \quad (1-4)$$

The fact that Curve A exceeds the permissible pressure curve cannot be tolerated.

Should it be desired to increase the muzzle velocity of a projectile, the work performed, or the area under some new curve, must be greater than the area under a curve giving a lower muzzle velocity. Such an increase in velocity is indicated by Curve C whose maximum pressure is equal to that of Curve B, but whose area is greater than that under Curve B. It appears that the ideal pressure-travel curve would be one coinciding with the curve of permissible pressure. However, if it were possible to design a propellant capable of producing such a result, many objectionable occurrences would take place. In addition to producing excessive erosion (a factor which would materially decrease the accuracy life of the gun), brilliant flashes and nonuniform velocities because of high muzzle pressure would result. Moreover, the chamber would have to be materially increased and this would affect the weight, and hence the mobility, of

the gun. As a result, the velocity prescribed for a particular gun always is somewhat below the maximum possible to obtain. The propellant grain most suitable for producing this result is one giving the prescribed velocity uniformly from round to round without exceeding the permissible pressure at any point in the bore.

For these, among other reasons, it is desirable to obtain high projectile velocities by sabot-support of a projectile light in weight as opposed to construction of a heavy, uneconomical gun capable of firing the unsupported projectile without a sabot.

REFERENCES

1. E. V. Krick, *Introduction to Engineering and Engineering Design*, John Wiley and Sons, N.Y., 1956.
2. L. Harrisberger, *Engineership: A Philosophy of Design*, Brooks/Cole Publishing Co., Belmont, California, 1966.
3. S.E. Elmaghraby, *The Design of Production Systems*, Reinhold Publishing Co., N.Y., 1966.
4. D. Dardick, et al., "Gun/Projectile Systems", *Space/Aeronautics* 47, No. 3, 92-99 (1967).
5. F.J. Zimmerman and L.A.C. Barbarek, "Analysis of Performance Requirements for Hypervelocity Guns", Appendix B of *Hypervelocity Weapon Feasibility Study*, Vol. II, Air Proving Ground Center, Report No. WADD-TR-61-203 II, April 1961.
6. R.C. Bullock and W.J. Harrington, *Summary Report on Study of the Gun-Boosted Rocket System*, Department of Mathematics, North Carolina State College, Raleigh, N.C., File No. PSR-9/8, 15 December 1962.

7. AMCP 706-140, Engineering Design Handbook, *Trajectories, Differential Effects, and Data for Projectiles*.
8. AMCP 706-242, Engineering Design Handbook, *Design for Control of Projectile Flight Characteristics*.
9. R.E. Carn and A.B. Stinson, *Handbook of Trajectory Data for Spin Stabilized Projectiles, Typical Fin Stabilized Flechettes, Spheres and Cubes*, BRL Report No. R-1336, August 1966.
10. a. AMCP 706-160(S), Engineering Design Handbook, *Elements of Terminal Ballistics, Part One, Kill Mechanisms and Vulnerability* (U).
 b. AMCP 706-161(S), Engineering Design Handbook, *Elements of Terminal Ballistics, Part Two, Collection and Analysis of Data Concerning Targets* (U).
 c. AMCP 706-162(S-RD), Engineering Design Handbook, *Elements of Terminal Ballistics, Part Three, Application to Missile and Space Targets* (U).
11. AMCP 706-245(C), Engineering Design Handbook, *Design for Terminal Effects* (U).
12. AMCP 706-107, Engineering Design Handbook, *Elements of Armament Engineering, Part Two, Ballistics*.
13. AMCP 706-150, Engineering Design Handbook, *Interior Ballistics of Guns*.
14. G.V. Parkinson, *Simple Internal Ballistics Theory for Single and Double Chamber Guns*, Space Research Institute, McGill University, Report No. SRI-H-TN-4, 26 August 1966.
15. J.M. Frankle, *An Interior Ballistic Study of a 24-inch Gun for Project HARP*, BRL Technical Note No. 1606, May 1966.
16. A.E. Seigel, *The Theory of High Speed Guns*, AGARDograph-91, May 1965.
17. L.A. DeStefano, *A Digital Computer Simulation of Breech-Launched Rockets*, Frankford Arsenal, Report No. M67-18-1, January 1967.
18. J.B. Goode, *Definitions of Pressures for use in the Design and Proof of Guns and Ammunition*, Royal Armament Research and Development Establishment, Memorandum No. 11/66, April 1966.
19. V. Oskay, *Proof Testing and Computer Analysis of BRL 81/26mm Light-Gas Gun*, BRL Memorandum Report No. 1855, July 1967.
20. E.B. Becker and J.J. Brisbane, *Application of the Finite Element Method to Stress Analysis of Solid Propellant Rocket Grains*, Rohm and Haas Company, Report No. S-76, November 1965.
21. E.L. Wilson and R.E. Nickell, "Application of the Finite Element of Heat Conduction Analysis", *Proceedings of the Fifth U.S. Congress of Applied Mechanics*, ASME, N.Y., 1966.
22. L.C. MacAllister, *On the Use of Plastic Sabots for Free Flight Testing*, BRL Memorandum Report No. MR-782, May 1954.
23. J.D. Peters, *Development Test of Plastic Discarding Sabot Shot for 76mm Gun, T91* (U), APG Report No. TAI-5002-8, 22 January 1958 (C).
24. E.W. Bailey, *Development of Shot, APFSDS, 90/40mm T320 for 90mm Smoothbore Guns*, APG Report No. TAI-1475, 21 November 1957.
25. S.J. Doherty, *Sabot Materials and Designs for High Velocity Kinetic-Energy Artillery Ammunition*, ARMA TR 67-11, April 1967 (C).

26. Aircraft Armaments, Inc., *Development of a Special Type Small Arms Cartridge (Sabot Supported)* (U), Report No. ER-1414, July 1958 (C).
27. W.L. Black, *Design and Fabrication of APDS Shot* (U), Aircraft Armaments, Inc., Report No. ER-4341, March 1966 (C).
28. E. Huchital, *Development of Delta Wing Armor Penetrating Shot* (U), Electro Mechanical Research Co., Report No. 2, September 1958; Report No. 11, March 1960; *Design and Development of Low-Drag, High-Energy, Armor-Penetrating Projectiles* (U), EMRC Report No. 16, 31 March 1961; Report No. 30, 31 October 1962 (C).
29. AVCO Corp., *Feasibility Study of a GASP Launch Payload Vehicle* (U), Report No. RAD-SR-26-60-54, 5 July 1960 (C).
30. G.V. Bull, D. Lyster, and G.V. Parkinson, *Orbital and High Altitude Probing Potential of Gun-Launched Rockets*, Space Research Institute, McGill University, Report No. SRI-H-R-13, October 1966.
31. F.W. Eyre, "The Development of Large Bore Gun Launched Rockets", Canadian Aeronautics and Space Journal, 12, 143-149 (1966).
32. F.M. Groundwater, *The Development of Gun Launched Rockets*, Space Research Institute, McGill University, Report No. SRI-H-R-6, February 1968.
33. J.A. Brown and S.T. Marks, "High Altitude Gun Probe Systems for Meteorological Measurements", *The Meteorological Rocket Network*, IRIG Document No. 111-64, February 1965, pp. 211-221.
34. G.V. Bull, "Development of Gun Launched Vertical Probes for Upper Atmosphere Studies", Canadian Aeronautics and Space Journal, 10, 236-247 (1964); "Project HARP", Ordnance, LII, 482-486 (1968).
35. C.H. Murphy and G. V. Bull, *Aerospace Application of Gun Launched Projectiles and Rockets*, Space Research Institute, McGill University, Report No. SRI-R-24, February 1968; "Gun Launched Missiles for Upper Atmosphere Research", *AIAA Preprint No. 64-18*, January 1964.
36. R. Rossmüller and M. Salsbury, *16-Inch HARP Work at Rock Island Arsenal-Summary Report*, Rock Island Arsenal, Technical Report No. 66-1493, April 1966.
37. D.E. Cantey, "Gun Launch of Rocket Vehicles by Fluid Support Techniques", Paper presented at the 3rd ICRPG/AIAA Solid Propulsion Conference held in Atlantic City, 4-6 June 1968.
38. D.E. Cantey, *RS-RAP Feasibility Demonstration, Phase I, Final Technical Report* (U), Lockheed Propulsion Company, Report No. 953-F, 25 October 1968 (C).
39. D.E. Cantey and F. Saam, *F-RAP Feasibility Demonstration, Phase I* (U), Lockheed Propulsion Company, Report No. 962-F, December 1968 (C).
40. AMCP 706-250, Engineering Design Handbook, *Guns-General*.
41. AMCP 706-252, Engineering Design Handbook, *Gun Tubes*.

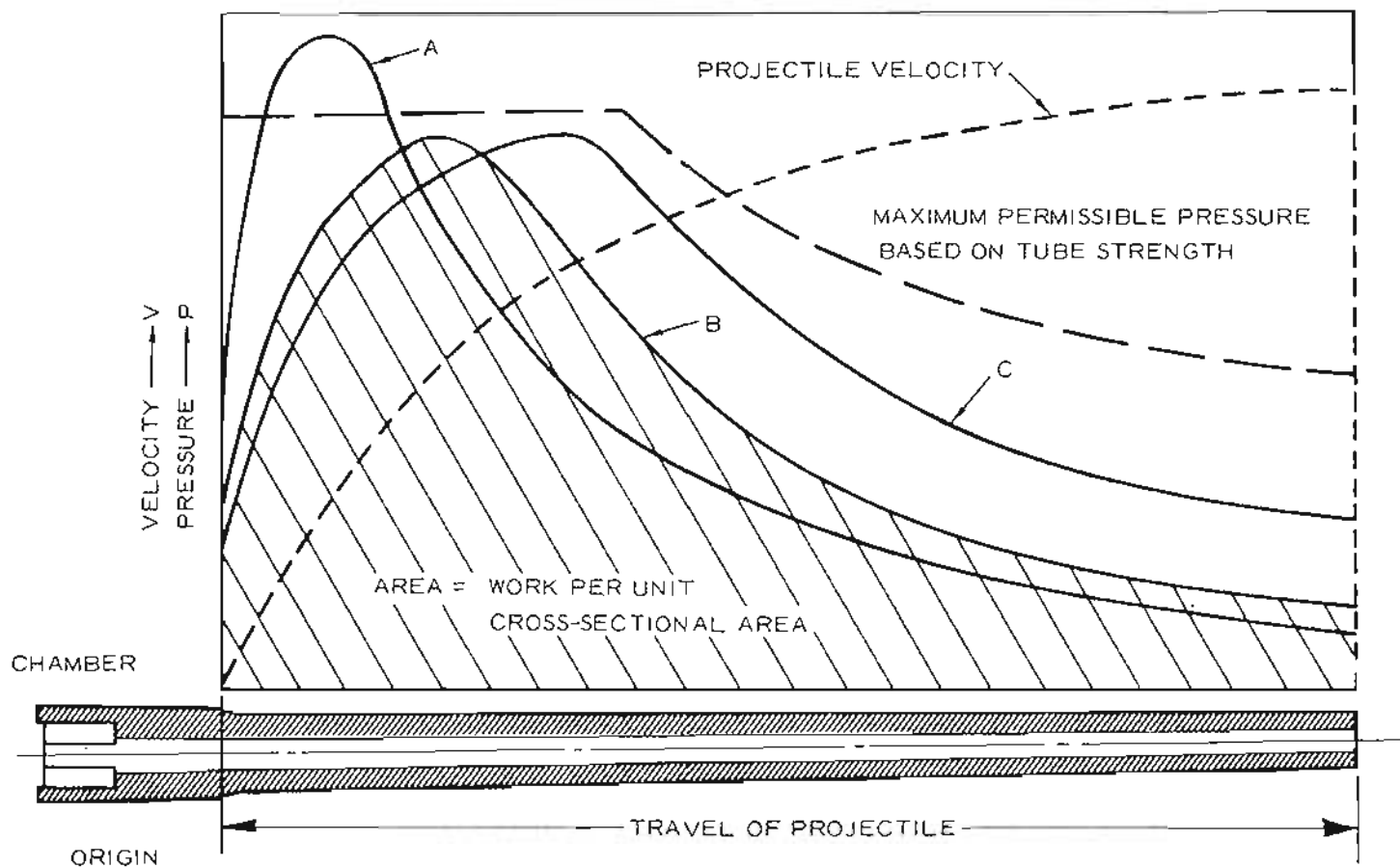


Figure 1-8. Pressure-travel (Solid Lines) and Velocity-travel (Dotted Line) Curves

CHAPTER 2

SABOT SYSTEM ANALYSIS

2-0 LIST OF SYMBOLS

 B = bulk compressibility d = projectile diameter D = gun bore diameter d = projectile diameter F = force g = acceleration k = gun tube length in bore diameters L = length m = mass p = hydrostatic pressure P = pressure s = surface area element S = stress tensor t = time V = volume or acceleration potential v = velocity x = distance ρ = density Φ = a pressure function of $\frac{p}{\rho}$ *Subscripts:* B = bore c = chamber f = fluid g = gravitational G = grain o = nominal p = projectile or propellant s = sabot t = total

Bar (—) over symbol indicates vector or tensor quantity

2-1 GEOMETRIC CLASSIFICATION OF SABOTS

For current purposes, the various sabot designs are divided into two main classes: (1) the cup type (Fig. 2-1), including both the spin-stabilized and nonspin-stabilized projectiles, and (2) the ring type (Fig. 2-2). Although 12 variations of the basic cup design and seven modifications of the basic ring design are identified and shown in the accompanying figures, the simple dual geometric

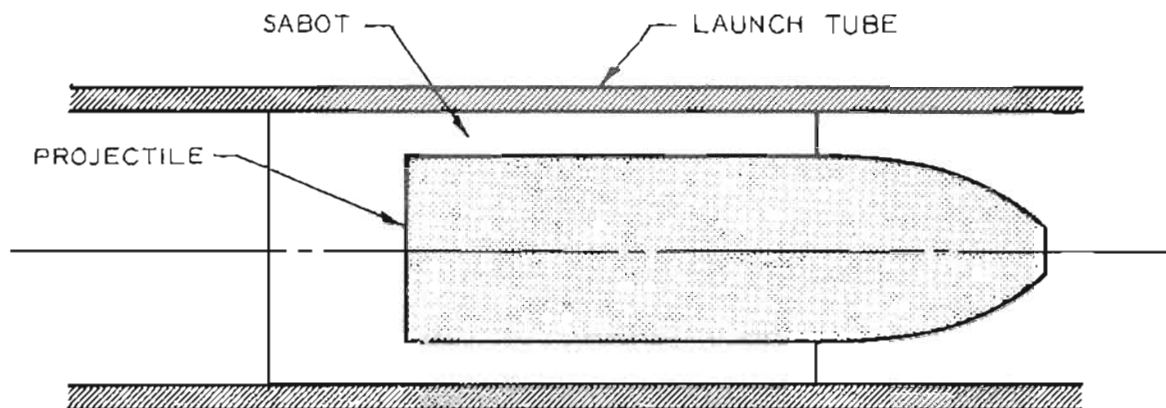


Figure 2-1. Basic Cup Design

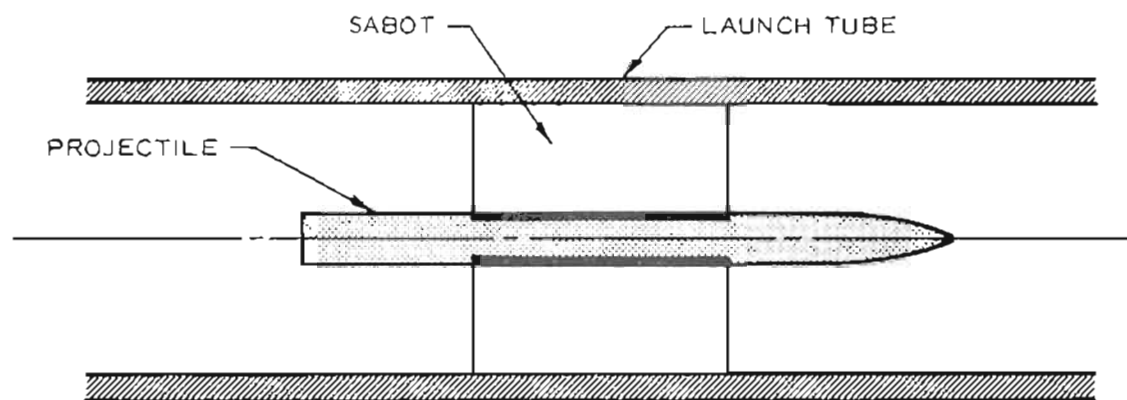


Figure 2-2. Basic Ring Design

classification with generic modifications has been adopted as a basis for the ensuing discussion.

2-1.1 GENERIC TYPES OF CUP SABOTS

The basic cup sabot and generic modifications are illustrated in Figs. 2-3 through 2-15. The simplest modifications of the basic cup include the addition of a rotating band to impart spin to the projectile; the addition of a separate obturator; and the additions of bevels, slots, and undercuts to reduce weight and/or improve discard characteristics. The designs illustrated in Figs. 2-11 and 2-12 incorporate truncated cones of a high shear strength material to adapt the cup design which is primarily suited to low L/D projec-

tiles of almost full caliber diameter to high L/D projectiles of relatively small diameter. A thin layer of plastic sometimes is used to mitigate the dynamic forces imposed on the projectile. The designs shown in Figs. 2-14 and 2-15 are unique because they are used to launch fragile objects. The design in Fig. 2-14 utilizes a rigid, internal sting to redistribute launch loads to less critical sections of the object being launched^{1*} while the design shown in Fig. 2-15 uses a fluid to accomplish the same task. The patented design shown in Fig. 2-15 also is unique because it is primarily used to launch full-caliber projectiles. The

*References are located at the end of each chapter.

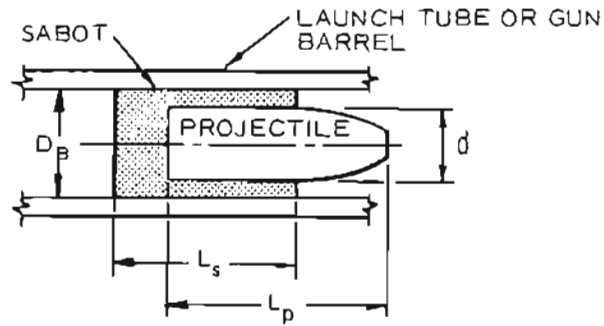


Figure 2-3. Basic Cup Design

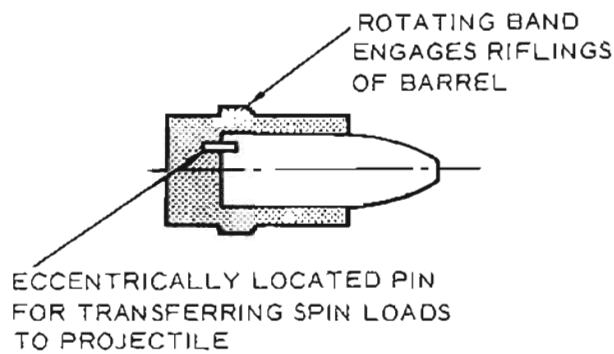


Figure 2-4. Cup With Rotating Band (imparts spin to projectile)

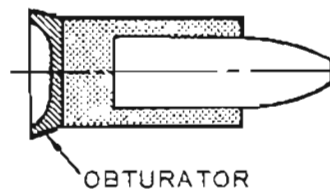


Figure 2-5. Cup With Obturator (seals launch tube)



Figure 2-6. Cup With Forward Bevel (augments aerodynamic separation of sabot and projectile)

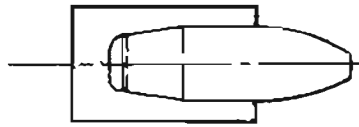


Figure 2-7. Cup With Internal Taper (thrust and spin transmitted to the projectile through the tapered surface)

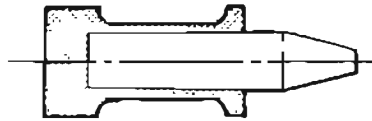


Figure 2-8. Cup With External Undercut (weight reduction)

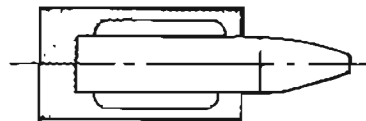


Figure 2-9. Cup With Internal Undercut (weight reduction)

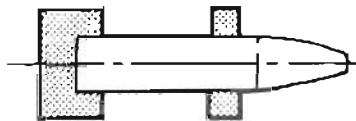


Figure 2-10. Cup With Rider

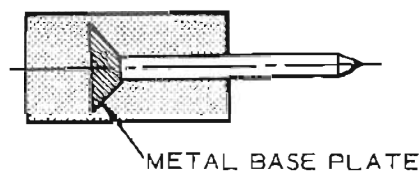


Figure 2-11. Cup With Base Plate (bearing surface multiplier)

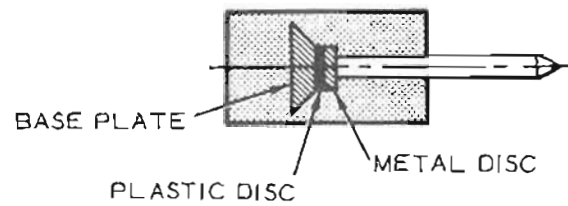


Figure 2-12. Cup With Base Plate and Shock Absorber (for highly brittle projectiles)

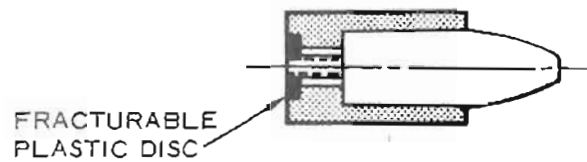


Figure 2-13. Cup With Shear Plate Restraint

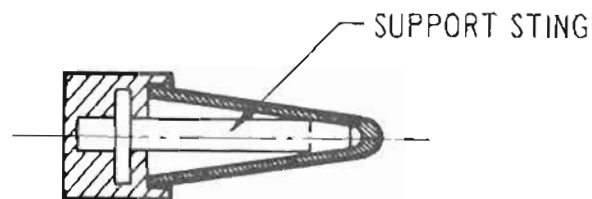


Figure 2-14. Cup With Support Sting (for thin-walled models)

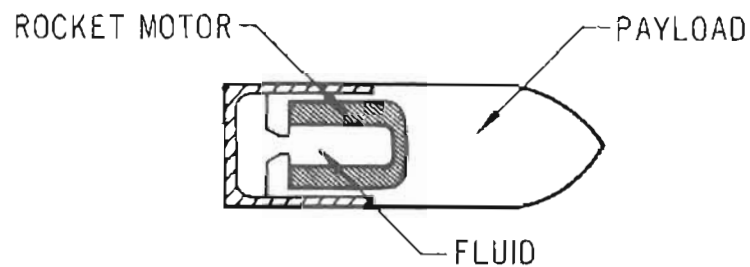


Figure 2-15. Cup With Fluid Support (for fragile projectiles such as rocket-assisted projectiles) (Patent Numbers 3,369,455 and 3,369,485)

objective of this sabot is to reduce the launch weight of the projectile instead of increasing the muzzle velocity.

2-1.2 GENERIC TYPES OF RING SABOTS

The basic configuration for the ring sabot and its generic variations is shown in Figs. 2-16 through 2-23. The simple modifications of adding obturators, bevels, slots, etc., to improve sealing characteristics and reduce sabot weight are illustrated. Figs. 2-22 and 2-23 incorporate the high shear-strength characteristics of a metal with the low density properties of plastics to achieve higher performance.

2-2 SABOT DESIGN CONSTRAINTS

The fundamental objective of a large class of sabot-projectiles is to achieve higher projectile muzzle velocity from guns which operate at some nominal efficiency level. The general design problem can be viewed from two alternate positions. Given a specific projectile of mass m_p and diameter d which achieves a muzzle velocity v_1 from a nominal gun of diameter d , it is desired to attain a higher muzzle velocity v_2 by using a larger gun (diameter D) and a sabot to fit the given projectile into the larger diameter tube. The problem is to determine the gun size and sabot configuration capable of achieving the

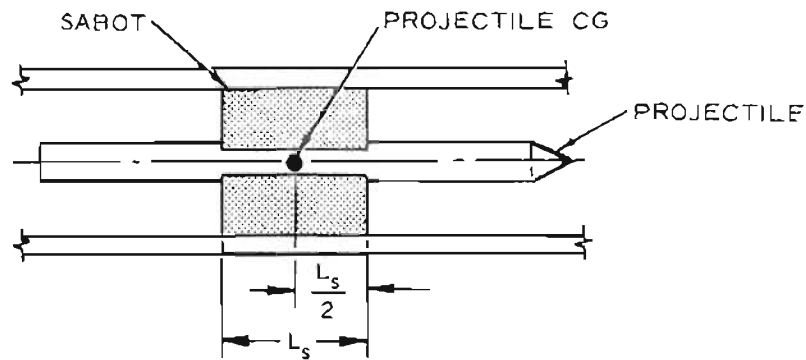


Figure 2-16. Basic Ring Design

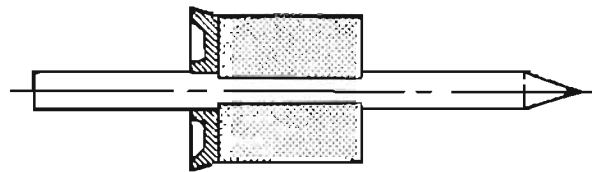


Figure 2-17. Ring With Obturator (seals launch tube)

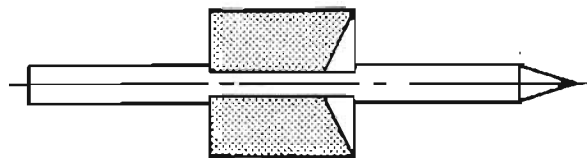


Figure 2-18. Ring With Forward Bevel (augments aerodynamic separation of sabot and projectile)

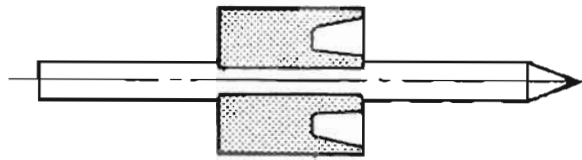


Figure 2-19. Ring With Unsupported Forward Undercut (aero-augmented separation and weight savings)

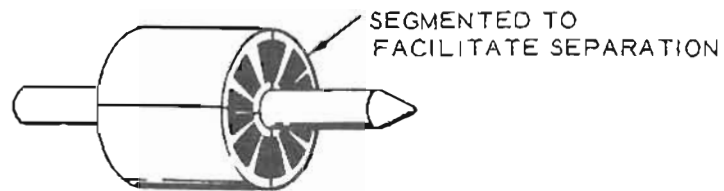


Figure 2-20. Ring With Longitudinally-supported Forward Undercut

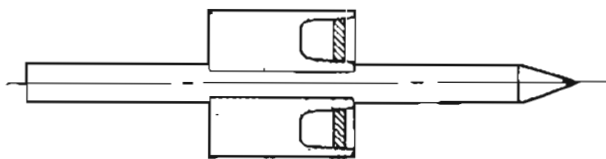


Figure 2-21. Ring With Circumferentially-supported Forward Undercut

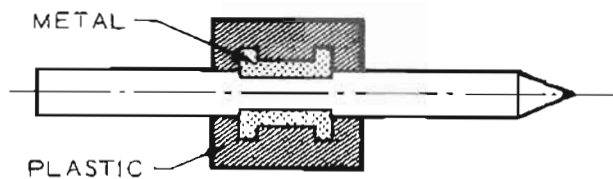


Figure 2-22. Two-piece Ring

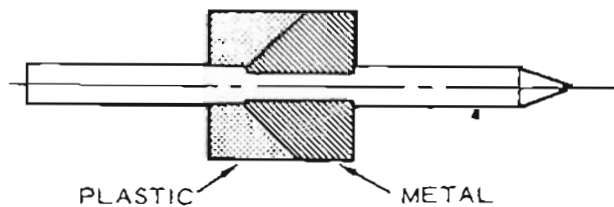


Figure 2-23. Two-piece Self-sealing Ring

desired performance. Alternatively, the designer may be given a specific gun of diameter D , capable of launching a nominal mass m_o at an initial velocity v_1 , and be required to determine the reduced projectile mass m_p and sabot configuration which will permit attainment of the desired higher velocity v_2 . The purpose of this paragraph is to illustrate the general constraints imposed upon the sabot design by these system performance requirements.

Consider first the problem of velocity increase for a given projectile mass by gun size increase and the use of a sabot. Neglecting bore friction and gas compression ahead of the projectile, the only force acting on the sabot projectile is the propellant gas pressure assumed to be uniformly distributed over the shot base. The kinetic energy delivered to the projectile of mass m_p by expansion of gas in the gun of diameter d is given by

$$\frac{\pi}{4} d^2 \int_0^{kd} p dx = \frac{1}{2} m_p v_1^2 \quad (2-1)$$

where k is the length of the launch tube in bore diameter or caliber lengths, v_1 is the muzzle velocity, and

$$\int_0^{kd} p dx$$

is the integral of the shot base-pressure travel curve for the gun. The velocity v_2 achieved by the same projectile mass m_p when fired from a gun of diameter D with the same caliber length k peak pressure, and piezometric efficiency is given by

$$\frac{\pi}{4} D^2 \int_0^{kd} p dx = \frac{1}{2} (m_p + m_s) v_2^2 \quad (2-2)$$

where m_s is the mass of the sabot required to support and transmit the additional kinetic energy to the projectile.

For equivalent peak pressure and piezometric efficiency – i.e., ratio of peak to average pressure, in the gun system – the integrals in Eqs. 2-1 and 2-2 are proportional to the bore diameters, d and D , respectively. Using this result, dividing Eq. 2-2 by Eq. 2-1 and rearranging, yields an expression for the sabot mass m_s and gun size D required to achieve the desired velocity v_2 as follows:

$$\frac{m_s}{m_p} = \left[\frac{1}{\left(\frac{d}{D}\right)^3 \left(\frac{v_2}{v_1}\right)^2} \right] - 1 \quad (2-3)$$

From the alternate point of view, in which the gun size is fixed and the projectile is reduced in size with a sabot to achieve higher velocity, an equivalent result can be obtained as follows: The kinetic energy delivered to a nominal projectile mass m_o by the gun of diameter D and caliber length k is given by

$$\frac{\pi}{4} D^2 \int_0^{kD} p dx = \frac{1}{2} m_o v_1^2 \quad (2-4)$$

For constant energy delivered by the gun, an increased muzzle velocity v_2 can be achieved by reducing the sum of the projectile and sabot mass as given by Eq. 2-2. Combining Eqs. 2-2 and 2-4 results in

$$\frac{v_2}{v_1} = \left[\frac{\frac{m_o}{m_p}}{\left(\frac{m_s}{m_p}\right) + 1} \right]^{\frac{1}{2}} \quad (2-5)$$

Assuming constant projectile shape and density (as its mass is reduced to achieve the velocity increase) results in the following proportionality:

$$\frac{m_o}{m_p} = \left(\frac{D}{d}\right)^3 \quad (2-6)$$

Substituting this result into Eq. 2-5 and rearranging yields the result previously obtained into Eq. 2-3.

It may be observed that Eq. 2-3 involves three dimensionless ratios. This permits the ratio of the sabot mass to the projectile mass to be plotted as a function of the ratio of the projectile diameter to the bore diameter, with the ideal velocity increment

$$\frac{\Delta v}{v_1} = \frac{v_2 - v_1}{v_1}$$

as a parameter (Fig. 2-24). Lines of equal velocity-increase for the ideal gun performance assumed are shown in the figure. One must remain on the left side of the zero velocity increment curve if there is to be any increase in the muzzle velocity due to the use of a sabot unless the gun is operated at an increased peak pressure or piezometric efficiency.

In general, choice of the gun system performance level is dictated by such other system constraints as tube material strength, erosion resistance requirements, system weight and length limits, interior ballistic effects, muzzle blast, and flash limitation requirements, etc., which will not be considered here. One important effect not included in the simple analysis discussed here is the decrease in piezometric efficiency that results as muzzle velocities are increased. This performance degradation is caused by the work necessary to accelerate the propellant gases themselves to high velocity. In the limit as shot weight approaches zero, the shot velocity approaches a fixed upper limit determined by the expansion properties of the gun propellant combustion products. Light gas guns are able to exceed the velocity limit imposed on powder gas guns by the use of low molecular weight gases in the expansion process.

The shaded area of Fig. 2-24 shows the region occupied by existing sabot-projectile designs as listed in Appendix A. Observe that this region was determined by plotting the sabot-projectile mass ratio versus the projectile-gun bore diameter ratio for representative designs. In general, the large ideal velocity increment increases indicated by the theoretic

cal calculations for the designs located at the left side of the shaded region (low projectile-to-bore diameter ratios) are not achieved for two reasons. First, the analysis resulting in Eq. 2-3 implicitly assumes constant projectile shape and composite density as the gun size is increased or the projectile size is decreased to achieve higher velocities. This assumption becomes increasingly poor as the projectile-to-bore diameter ratio decreases. In general, the projectile length-to-diameter ratio and composite density tends to increase because of aerodynamic flight stabilization and terminal ballistic requirements. Thus, the left part of the shaded region should be shifted to the right relative to the lines of constant velocity increase. Second, the gun efficiency problem at high velocity previously described causes severe degradation in velocity performance for the very light shotweight designs.

Another instructive way to consider the performance limits and capabilities of sabot-projectile designs is illustrated in Fig. 2-25, which shows the sabot-to-projectile mass ratio m_s/m_p plotted versus the projectile-to-nominal shot mass ratio m_p/m_o of Eq. 2-5. Plotted in this fashion, the effects of projectile shape and density are excluded from the analysis and the actual achieved velocity increases are closer to ideal values. Choice of the nominal projectile mass m_o is arbitrary and is associated with the efficiency level assumed for the gun systems. The existing sabot-projectile design data shown in Fig. 2-25 were obtained from the performance summary data of Appendix A, assuming m_o equal to 96 lb for a 155 mm gun (an artillery weapon). Values of m_o for other gun sizes were obtained by scaling 96 lb as the cube of the gun bore diameter which approximates equivalent gun peak pressure and piezometric efficiency.

These elementary system analysis considerations illustrate the general design requirements for velocity increase by the use of sabot-subcaliber projectiles. Projectile mass must be reduced to achieve velocity increase for constant gun performance. Generally, the

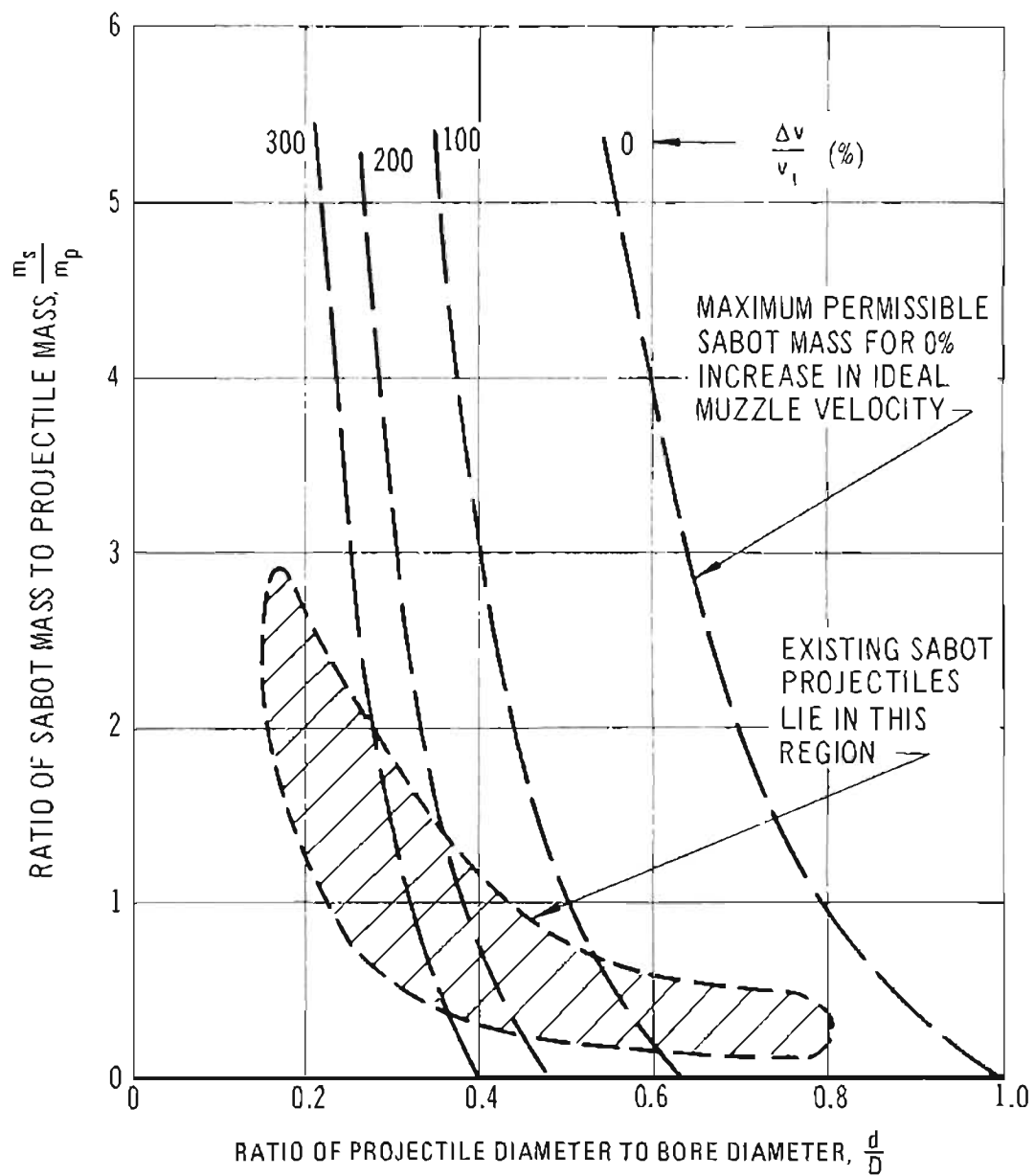


Figure 2-24. Performance Limits and Capabilities of Different Sabot Designs

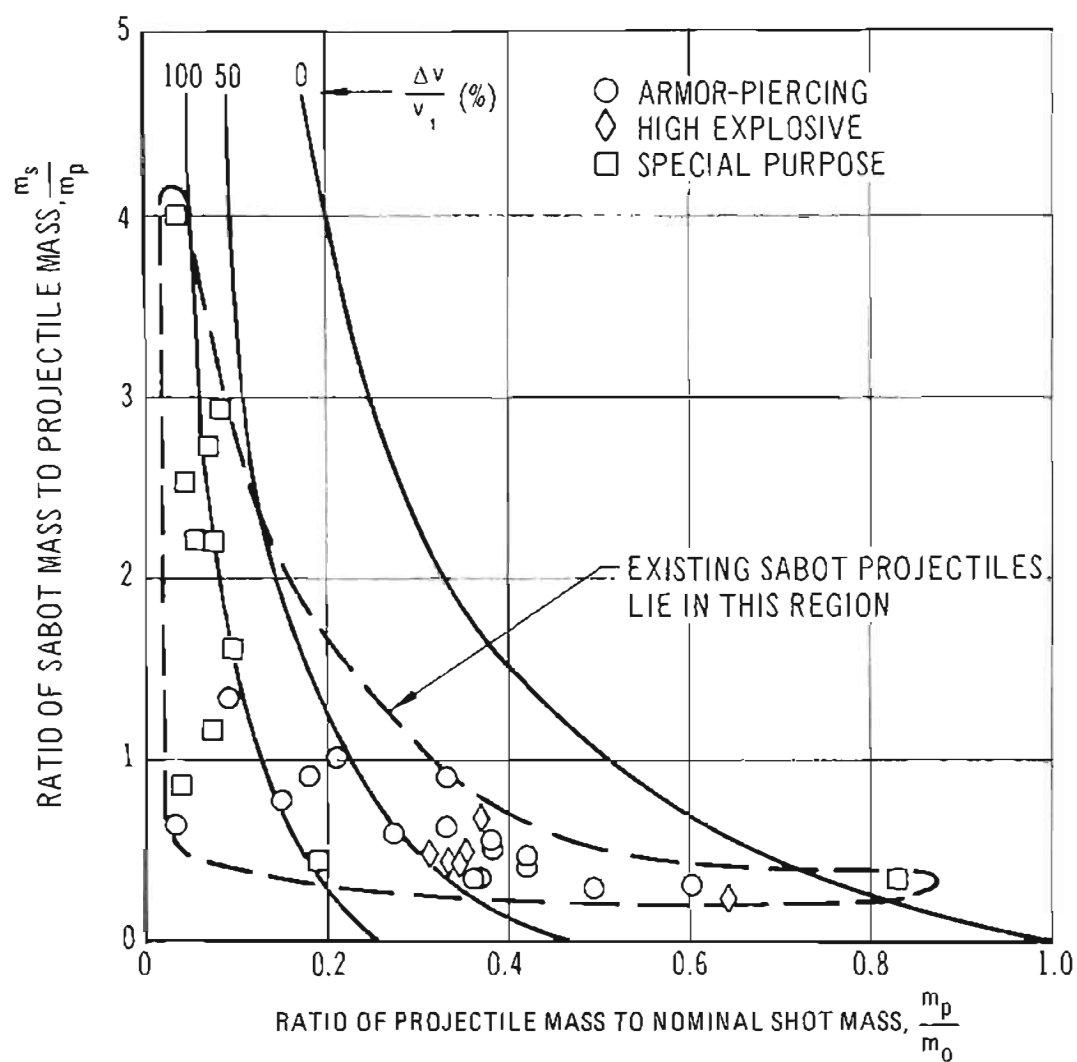


Figure 2-25. Performance Limits and Capabilities of Different Sabot Designs

projectile mass is the useful end product of the system and, therefore, there are system requirements to maximize the projectile mass. Additional velocity increase can be achieved for a fixed projectile mass by decreasing the weight of the sabot as illustrated in Fig. 2-25. This latter design goal is of primary importance in sabot-projectile technology.

2-3 THE COMPARISON BETWEEN CUP AND RING SABOTS

The first decision which the sabot designer must make is whether or not to employ a ring or a cup sabot configuration. Based upon empirical evidence, investigators at BRL established the following criteria²:

$$\frac{d}{D} > 0.40, \frac{L_p}{d} < 10$$

One-piece cup sabot (Figs. 2-3 through 2-9)

$$\frac{d}{D} > 0.40, \frac{L_p}{d} \geq 10$$

Cup sabot with bearing plate (Figs. 2-11 or 2-12)

$$\frac{d}{D} \leq 0.40$$

Ring sabot (Figs. 2-16 through 2-23)

The performance capability of a cup and ring sabot both designed to the same set of conditions using the same material are given in Fig. 2-26. It may be observed that although the ring sabot consistently gives better performance than the cup sabot, the amount of

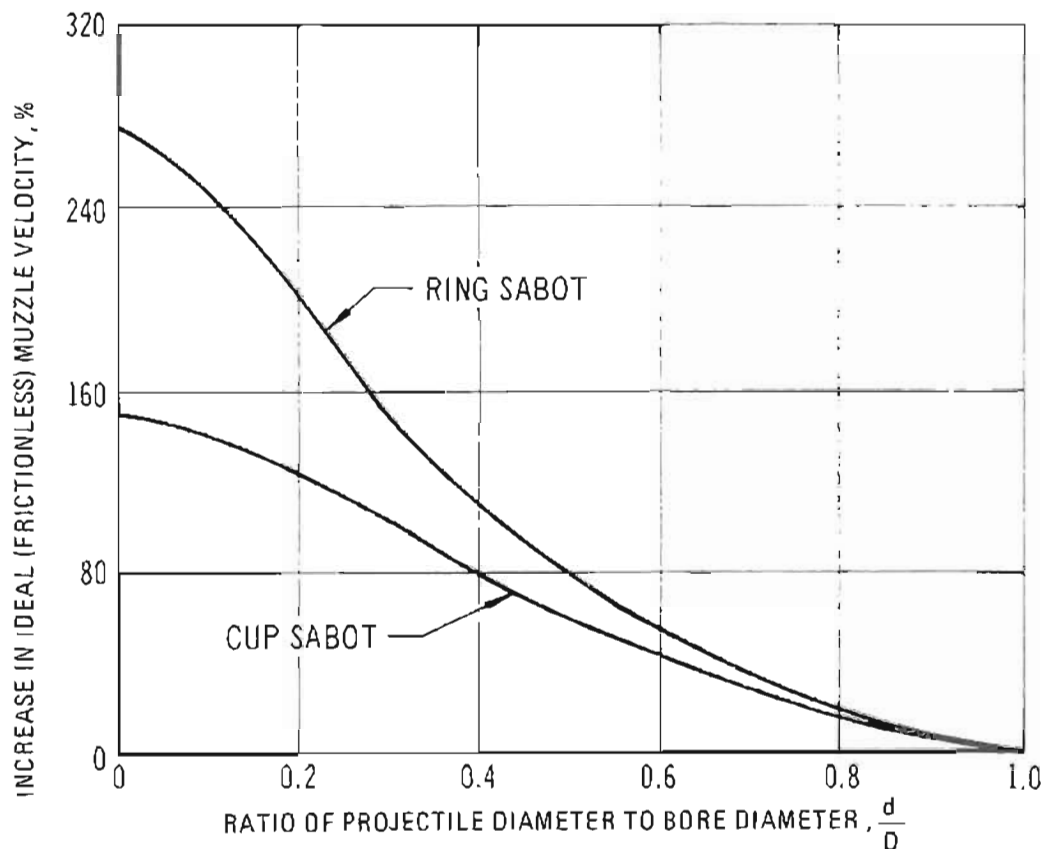


Figure 2-26. Comparison of Cup and Ring Sabots (6-in diameter bore, projectile $L/D = 10$, effective density of projectile = 0.260 lbm/in.³, maximum gas pressure = 50,000 psi, density of sabot = 0.040 lbm/in.³, and shear strength = 10,000 psi) (lbm = pounds mass)

improvement at relatively large projectile diameters ($\frac{d}{D} > 0.40$) is significantly less than at smaller diameters. This is sufficiently less so that one must consider other quantifiable criteria, i.e., cost of manufacture, reliability, etc.

In ring sabots the means normally employed to transfer the shear forces developed between the sabot and the projectile is a series of annular grooves shaped like a buttress thread. To ensure an effective transfer of these shear forces, the grooves on the projectile body must fit carefully into the grooves in the sabot. The manufacturing costs for producing a ring sabot, therefore, can be much higher than for an equivalent cup sabot.

In addition, the ring sabot has one more joint to seal than does the cup sabot, i.e., the joint between the sabot and the projectile. Failure to achieve an effective seal on this joint has been blamed for the failure of ring sabots to function properly. The exposure of the aft end of the projectile associated with ring sabots also is considered a problem area that must be considered. It is concluded that the BRL rule-of-thumb is a reasonable criterion for preliminary design of sabots but that a more detailed parametric study may be warranted for a specific set of performance criteria.

2-4 FLUID BUOYANCY SUPPORT OF GUN-LAUNCHED STRUCTURES

The fluid buoyancy sabot is a special development of the Lockheed Propulsion Company* and has application to the generic structure that is typically weak in longitudinal buckling, but which can be gun-launched to achieve some system advantage. One such structure is a rocket-assisted projectile — where the projectile may be considered to be in the range between an artillery bombardment projectile and an earth orbit satellite. System performance in all cases appears to be maximized by gun launch of a flight vehicle

incorporating a high mass fraction (ratio of propellant and total weight) propulsion unit.

It is desirable that the rocket propulsion unit be designed for its intrinsic operating parameters only. When this is accomplished, the resulting unsupported propulsion unit is too fragile for gun launch (except in the trivial case of a "blow gun"). Fluid immersion makes the rocket unit (and/or payload) rugged, rendering it virtually insensitive to gun bore loads. This paragraph presents a theoretical analysis of the fluid buoyancy, sabot system.

A schematic diagram of the fluid buoyancy support projectile and gun launch system is presented in Fig. 2-27. The thin-walled aft-section of the motor chamber is encased in a close fitting polymeric cup containing a fluid that fills the motor chamber cavity and nozzle assembly. The purpose of this fluid is to transmit pressure, resulting from gun propellant gas expansion and inertial reaction of the projectile, throughout the interior of the booster rocket, thereby counteracting forces tending to destroy the motor chamber and grain.

The ballistic trajectory can be divided into the following three regions for discussion purposes:

- (1) Gun tube acceleration
- (2) Transition from gun tube to exterior
- (3) Exterior ballistic flight.

Relative to an inertial frame of reference traveling with the projectile, the projectile can be considered to be at rest in a time-varying inertial acceleration field with equipotential planes oriented normal to the gun bore axis (neglecting spin effects for the moment). After transition of the projectile from the gun tube to the exterior, the acceleration field drops abruptly as the driving gun gas dissipates. For the case of exterior ballistic flight in an atmosphere, aerodynamic drag effects

*Patent Numbers 3,369,455 and 3,369,485.

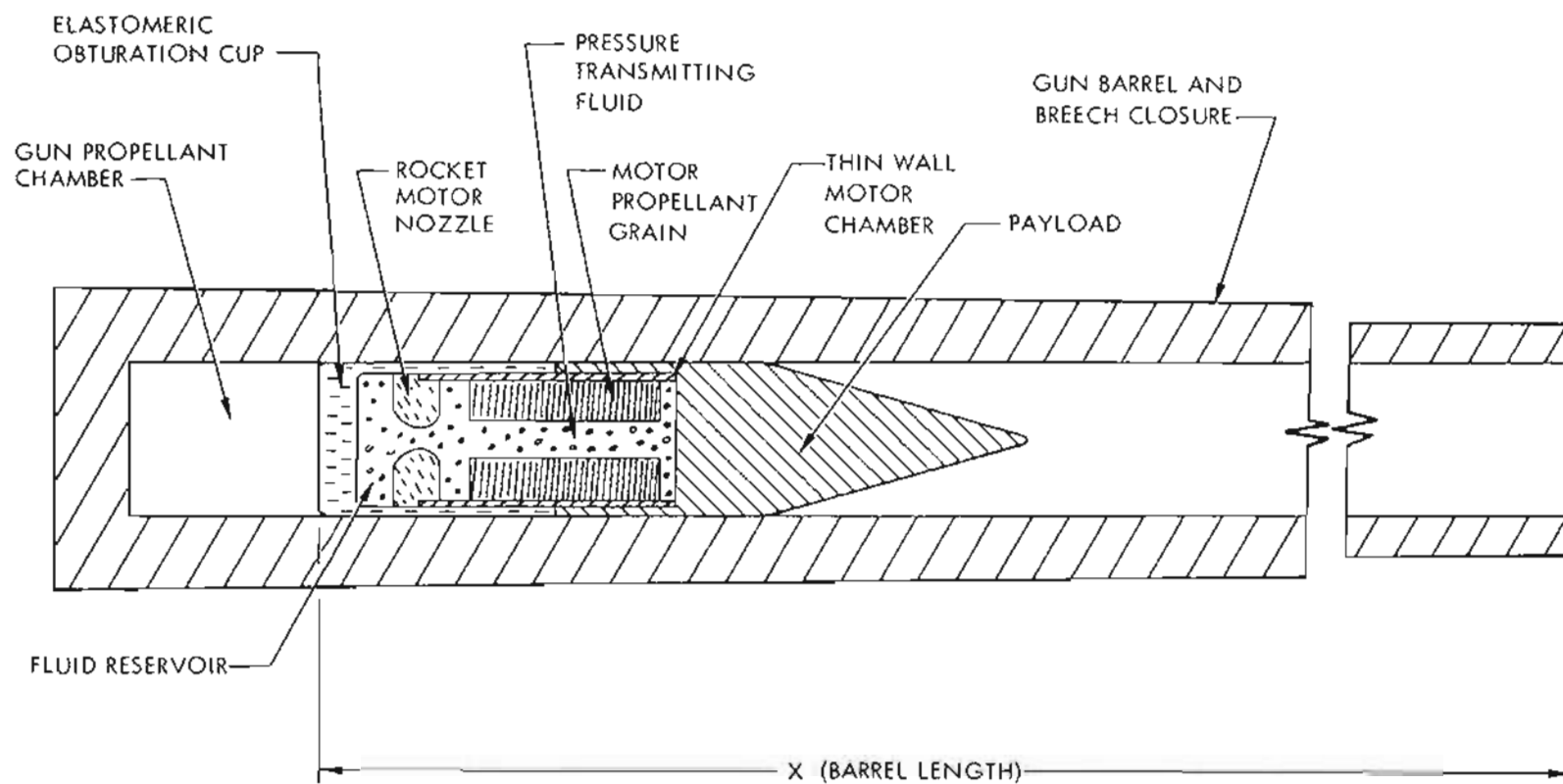


Figure 2-27. Projectile, Gun Launch Schematic for Fluid Buoyancy Support System

will cause the acceleration field to drop below zero, resulting in projectile deceleration. The orientation of the deceleration field with respect to the projectile is determined by projectile pitch and yaw. From the standpoint of projectile structural integrity, the primary effect of interest is the physical response of the projectile to this transient inertial acceleration field resulting from the gun launch and exterior ballistic flight.

In general, the equations of motion for a deformable body are obtained by equating the material density ρ times the convective derivative of velocity with respect to time, to the forces acting on unit volume³. The forces acting on any elemental volume are due partly to body forces, e.g., gravitational and inertial forces, and partly to the resultant of the surface tractions acting because of the state of stress of the body. Thus, using vector notation, the equation of motion can be written as:

$$\rho \frac{d\bar{v}}{dt} = \rho \bar{g} + \text{div } \bar{S} \quad (2-7)$$

Bars (—) over the symbols denote vector or tensor quantities. Symbols used are defined as follows:

ρ = average mass per unit volume (density)

\bar{v} = velocity field

\bar{g} = body force per unit mass (acceleration field)

\bar{S} = stress tensor

t = time

This basic equation is applicable to solids, liquids, and to materials that display characteristics of both limit conditions. The distinction among these various forms of matter is embodied in the nature of the internal stresses given by the stress tensor. An additional differential relationship, which must be satisfied by the density and velocity fields, results

from conservation of matter and is known as the equation of continuity, i.e.,

$$\frac{d\rho}{dt} + \rho \text{ div } \bar{v} = 0 \quad (2-8)$$

It should be emphasized that the indicated density derivative with respect to time is a so-called "convected derivative" defined as:

$$\frac{d\rho}{dt} = \dot{\rho} + \bar{v} \cdot \nabla \rho \quad (2-9)$$

where $\dot{\rho}$ is the ordinary variation with time of the material density at a fixed point in space. The second term accounts for the additional material density variation resulting from the motion of the observer traveling with the velocity field during unit time.

The material under consideration is said to be "incompressible" if changes in the material density with time are negligible for the physical process in question. In this approximation $d\rho/dt = 0$, and, therefore, the velocity field must satisfy the condition $\text{div } \bar{v} = 0$.

Before these relations can be applied to the specific problems involving real materials, a supplementary set of "material characterization" relationships is required expressing the stress \bar{S} in terms of the deformation, the rate of deformation or the history of the deformation, depending upon the complexity of the material. That is, a rheological equation of state must be obtained for each important material. Before discussing the required specific material characterization, it would be well to consider the projectile in the gun launch environment in greater detail to establish a qualitative understanding of the relative importance of the various effects.

Refer again to the projectile gun launch schematic, Fig. 2-27, and consider the instantaneous state of the projectile when it is near maximum acceleration in the gun barrel. Forces on the projectile under these conditions are primarily body forces resulting from inertial reaction of the various projectile elements to the very large acceleration field

(10^4 – 10^5 g). It is clear that gravity loading effects can be neglected under these conditions as contributing a negligible amount to the total body forces on the projectile. In addition to the body forces resulting from the linear acceleration field, another source of body forces is the angular acceleration resulting from the bore rifling in spin-stabilized projectiles. For the current discussion, body forces will be assumed to result only from the linear acceleration. Finally, surface tractions are introduced during the gun tube travel by frictional forces at the gun tube walls.

The general effect of the linear acceleration on the rocket motor portion of the projectile is intuitively clear. Pressure will be developed in the pressure transmitting fluid resulting from inertial reaction of the payload mass and body forces in the fluid. At the base of the projectile, pressure in the elastomeric obturation cup will precisely balance the gun propellant chamber pressure. Moving toward the forward end of the projectile along the axis of symmetry, the fluid pressure will decrease to a value determined by the payload mass as the fluid "surface" (located at the fluid-payload interface) is approached. The fluid, motor chamber, and obturation cup walls are constrained by the gun barrel walls in exactly the same way that water in a stand pipe tank is constrained by the pipe walls.

Considering the dynamics of the gun tube acceleration process now, it is clear that for the limit case of incompressible behavior for all materials, adequate protection of the thin-walled motor chamber during the gun tube travel requires only that the velocity of transmission of the pressure wave through the fluid be at least as large as the propagation velocity of a deformation wave in the obturation cup walls or the velocity of gun gases around the outsides of the cup walls. The situation is complicated, however, by the compressible nature of real materials. Because adequate protection of the motor chamber and nozzle assembly requires that the internal volume remain reasonably constant, it is evident that bulk compression of the fluid

and motor propellant as pressure increases means that the extra volume must be filled with fluid flowing into the chamber through the nozzle from an external reservoir. To scale the effect, consider the case of the rocket motor shown in Fig. 2-27 where the propellant volume V_p occupies 50 percent of the total chamber volume V_i with the remainder filled with fluid V_f . Assume that bulk compressibilities of the fluid B_f and propellant B_p are 3×10^{-6} and 0.9×10^{-6} psi⁻¹, respectively, and that the average maximum fluid pressure ΔP is 15,000 psi. For equilibrium conditions, the total volume change, $\Delta V/V$, is:

$$\frac{\Delta V}{V}(100) = \Delta P \left[\left(\frac{V_p}{V_i} \right) B_p + \left(\frac{V_f}{V_i} \right) B_f \right] (100) = 2.9\%$$

Thus, for this example, a volume of fluid at 15,000 psi equal to 2.9 percent of the total internal chamber volume must flow through the nozzle from the reservoir quickly enough to prevent deformation of the motor chamber because of gun gas pressure. In addition, it is evident that the compressibility of the obturation cup walls should be as low as possible to limit motor chamber expansion.

Returning now to the mathematical formulation and assuming that stress transmission is sufficiently rapid to permit the assumption that the fluid system is quasi-static, i.e., close to equilibrium conditions at all times, Eq. 2-7 becomes

$$\rho \bar{g} + \text{div } \bar{S} = 0 \quad (2-10)$$

Furthermore, if it can be assumed that the fluid is sufficiently perfect, i.e., that it can support no shearing stresses, then the stress distribution within it will be isotropic and

$$\text{div } \bar{S} = -\text{grad } p \quad (2-11)$$

Under these conditions,

$$\rho \bar{g} = \text{grad } p \quad (2-12)$$

Now, in general, the hydrostatic pressure p is a function of the density ρ . If the fluid

density changes, for example, because of compressibility, temperature field, impurity content, etc., then it is clear that the pressure distribution will be affected. In general, lines of constant density may or may not coincide with lines of constant pressure. If the former can be assumed, an auxiliary pressure function can be defined

$$\Phi(\rho) = \int^{\rho} \rho^{-1} dp \quad (2-13)$$

which, combined with Eq. 2-12, results in

$$\bar{g} = \text{grad } \Phi \quad (2-14)$$

Now, for the inertial acceleration field g , under consideration here, the following may be written:

$$\bar{g} = -\text{grad } V \quad (2-15)$$

where V is the inertial acceleration field potential. Eqs. 2-14 and 2-15 result in

$$V + \Phi = \text{constant} \quad (2-16)$$

Because the inertial acceleration field V of the projectile can be considered to be spatially uniform, $V = -gx$ may be written where g is the magnitude of the acceleration field, and x is the distance from the fluid-payload interface back toward the aft end of the projectile. Thus,

$$\Phi = gx + \text{constant} \quad (2-17)$$

and for the limit of incompressible behavior

$$\Phi = \frac{p}{\rho} = gx + \frac{p_o}{\rho} \quad (2-18)$$

so

$$p = \rho gx + p_o \quad (2-19)$$

This relation expresses, mathematically, the fact previously mentioned, that the total pressure in the fluid is equal to the sum of a constant value p_o resulting from the inertial reaction of the payload mass plus a component increasing linearly with depth due to inertial reaction of the fluid itself. The accu-

racy of this result is, of course, dependent on the validity of the various simplifying assumptions made during the derivation.

In addition to the previous effects, buoyancy phenomena are certain to play a major role in development of high acceleration systems of the type discussed here. Consider the propellant grain shown schematically in Fig. 2-27, immersed in the pressure transmitting fluid and case-bonded to the chamber wall. The total force F_f acting on the grain by the fluid is

$$F_f = - \iint p d\bar{s} \quad (2-20)$$

where $d\bar{s}$ is a vector surface area element of the grain directed outward from the grain. Now, in general, for a scalar field such as p :

$$\iint p d\bar{s} = \iiint \text{grad } p dV_G \quad (2-21)$$

where V_G is the volume of the propellant grain. Again, assuming the fluid stress distribution to be isotropic, Eq. 2-12 can be used to show that

$$\iint p d\bar{s} = \iiint p \bar{g} dV_G \quad (2-22)$$

Comparison of this result with Eq. 2-20 shows that the total force acting on the grain by the fluid is equal and opposite to the total weight of the displaced fluid given by the right hand side of Eq. 2-22. Observe that only the gradient portion of the total hydrostatic pressure of Eq. 2-19 results in a buoyancy effect on the submerged grain. The relationship expressed by Eq. 2-22 is called Archimedes' principle. The total body force acting on the grain and resulting from the inertial acceleration field \bar{g} is given by

$$F_g = \iiint \rho_G \bar{g} dV_G \quad (2-23)$$

Thus, the total resultant grain force F_G , is

$$F_G = F_g + F_f = \iiint \rho_G \bar{g} dV - \iiint \rho \bar{g} dV_G \quad (2-24)$$

Because the inertial acceleration field is uniform and the fluid and propellant densities

are assumed to be uniform, i.e., independent of position, Eq. 2-24 simplifies to

$$F_G = (\rho_G - \rho) \bar{g} V_G \quad (2-25)$$

A positive resultant force corresponds to a negative buoyancy, i.e., corresponds to a "sinking" tendency. Observe that even though the density difference between the grain and fluid is relatively small, the resultant buoyancy force can be large because of the magnitude of \bar{g} . In the current case, this force results in a shear deformation of the circular port grain.

Up to now, consideration was given only to conditions during travel of the projectile through the gun barrel. Just as the projectile emerges from the muzzle, it is clear that a potentially catastrophic situation is produced. Specifically, the projectile is still being accelerated by the gun gases bearing against the aft of the projectile but the lateral pressure constraint of the gun barrel is removed from the forward portions of the projectile. Clearly, the internal fluid pressure either must be contained by the rocket chamber, relieved by expansion and possible rupture of the chamber, or the acceleration and resultant pressure must be reduced by flow of fluid from the reservoir around the outside of the chamber to the atmosphere. The results of experiments^{4,5} indicate that these muzzle transition effects can be accommodated in high-performance gun-boosted rocket designs launched at practical gun energy levels. Flow properties of the fluid during launch acceleration are clearly of great importance to the success of the rocket launch projection system.

2-5 OBTURATION AND SABOT SEAL DYNAMICS

2-5.1 GENERAL

The combined requirements of efficient gun gas obturation during bore acceleration and of rapid and smooth sabot separation after muzzle exit provide challenging design

problems for sabot projectiles. Poor gun gas obturation leads to augmented gun wear, and degradation of projectile performance because of erosion damage. Solution of the obturation problem often results in sabot separation difficulties with attendant poor ballistic performance. The use of elastomeric seals for obturation of high-performance sabot projectile rounds has become common. These low-modulus materials flow readily under pressure to provide good obturation and excellent sabot discard characteristics.

The general methods used for obturation of sabot projectiles are described qualitatively in this paragraph with reference to the widely diversified applications literature for specific techniques and results. Sabot projectile obturation design principles are not sufficiently well defined or understood at this time to permit a classical "handbook" treatment. Research investigations directed specifically at the detailed motion of practical obturator designs during gun launch are relatively new and few in number.

2-5.2 OBTURATION METHODS

Historically, the sealing of gun gases has been accomplished by forcing a projectile with a rotating band through the gun tube rifling. In small caliber ammunition, the entire cylindrical length of the projectile, which is made from or sheathed in soft metal, is engraved to provide a gun gas seal. Larger caliber ammunition generally utilizes one or more discrete rotating bands that are engraved by the rifling under the action of the accelerating propellant gases. In addition to providing the necessary sliding gas seal, rotating bands generally are required to transmit torque from the rifling to the projectile, thereby providing the spin necessary for gyroscopic stability. Requirements of the obturating device for spin-stabilized sabot projectiles are much the same with the additional complication that the sabot and obturating device be capable of smooth discard at the gun muzzle. Both metal and fiber materials have been used in spin-stabilized sabot projectile develop-

ments (see, for example, Fig. 1-2). As higher projectile velocities are obtained by reducing the projectile mass and diameter, the mass of the sabot becomes a critical performance design constraint as described in par. 2-2. Under these conditions, the use of a relatively dense metal such as copper for the gun gas obturator becomes prohibitive and low-density materials such as plastics and elastomers have become important as sabot obturating devices (see, for example, Figs. 1-3 and 1-4).

Many applications of sabot projectiles fired from rifled and smoothbore guns exist, and the use of plastic or elastomeric seals located at the periphery of the sabot is common (see the abstract bibliography, Appendix D). For deformable sabot materials such as plastics, the obturation means often is incorporated into the sabot structure by making the aft end larger than the gun bore as described in Ref. 2. This procedure also provides an initial resistance to motion resulting in a fixed value of shot start pressure which has certain advantages from an interior ballistic standpoint. In many cases, however, particularly those in which the sabot must be inserted initially forward of the entrance to the gun bore, the use of oversize sabots is not practical and a self-sealing action by the obturator is required. Peripheral undercuts of "flaps" on the base of the sabot often are used to accomplish this self-sealing action by reducing the stiffness of the sabot material at the end of the flap, which allows it to deform easily under the action of low initial gas pressures. Examples of this procedure are illustrated in the sabot designs shown in Figs. 1-3 and 1-4. An investigation of the literature indicates that design of these components is accomplished largely on an empirical basis for each specific application. Par. D-13 of the bibliography (Appendix D) contains a list of references on the subject on static and dynamic seals in general.

2-5.3 SABOT SEAL DYNAMICS

The general motion of the sabot components relative to the projectile during gun

launch acceleration is referred to here as sabot seal dynamics. Control of this motion is a central design problem in many sabot projectile applications.

High-performance kinetic energy penetrator sabot projectiles usually are aerodynamically stabilized and, therefore, it is desirable that the projectile spin remain far below the rate that would be achieved if the projectile were directly coupled to the gun rifling. The use of conventional, rifled tube guns for launch of these projectiles often is dictated by the necessity for firing conventional spin-stabilized projectiles from the same weapon. Thus, it is necessary to decouple the projectile from the rifling through a sliding element incorporated in the sabot obturator. In many cases of interest, the general practice of forcing the obturator into the gun rifling to achieve a tight fit for gas sealing purpose cannot be used; the obturator device must expand under action of the gun accelerating gases to fill the rifling grooves and provide the necessary gas seal with minimum gas leakage.

To accomplish these requirements in high-performance, ring sabot applications, relatively complex sabot configurations have been developed employing sliding plastic obturation rings as indicated in Fig. 2-28⁶. The motion of this ring or combination of rings relative to the sabot projectile body during the launch acceleration cycle is critical to the success of the round. Analytical and experimental procedures have been developed⁶ that can be used in the design and development of sliding plastic obturator rings. Static and dynamic friction between the ring and gun bore and between the ring and sabot projectile, combined with a knowledge of the obturating ring mechanical properties, are critical inputs into the analysis defining the resulting motion and sealing effects.

Another application in which motion of the sabot materials relative to the projectile is critical is the general area of fluid buoyancy support of gun-launched structures discussed in par. 2-4 (see also Fig. 1-5). In this case, a

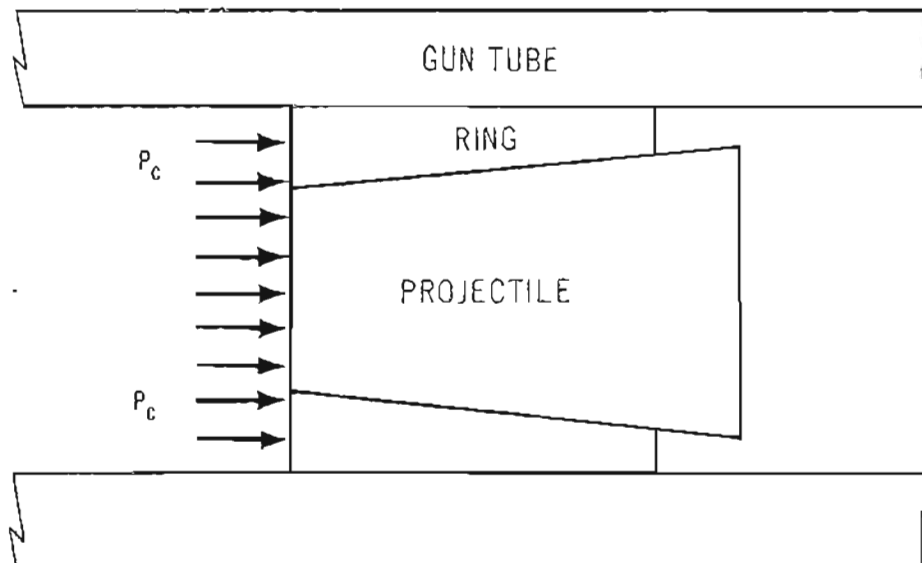


Figure 2-28. Schematic Diagram of Gun Tube, Ring, and Sabot Projectile⁶

component of the "sabot is a pure fluid that distributes the launch acceleration loads uniformly, thereby protecting fragile structures, e.g., rocket motors, from the otherwise destructive effects of the launch acceleration. Flow effects in the fluid relative to the supported structure and the containing device are of critical importance to the utility of this method of structural support for fragile gun-launched structures. Analyses of these effects for specific applications are still being developed at the time of this writing.

REFERENCES

1. C.H. Murphy and G. Taylor, *An Interesting Sabot Design*, BRL Memorandum Report No. 1304, September 1960.
2. G. Taylor, *Sabot-Launching Systems for Experimental Penetrators*, BRL Memorandum Report No. 1505, August 1963.
3. Condon and Odishaw, *Handbook of Physics*, McGraw-Hill Book Co., Inc., N.Y., 1958.
4. D.E. Cantey, *RS-RAP Feasibility Demonstration, Phase I* (U), LPC Report No 953-F, 25 October 1968 (C).
5. D.E. Cantey and F.S. Saam, *F-RAP Feasibility Demonstration, Phase I* (U), LPC Report No. 962-F, December 1968 (C).
6. R.C. Geldmacher, *The Dynamic Behavior of a Sliding Plastic Obturating Ring as Used in the 152-mm XM 578 APFSDS Projectile*, Stevens Institute of Technology, Technical Report No. 3488, September 1967. (AD-820 330) (See also abstract No. 381, Appendix D)

CHAPTER 3

STRUCTURAL DESIGN CONSIDERATIONS

3-0 LIST OF SYMBOLS

a	= acceleration	K	= bulk modulus
A	= area	ℓ	= length
d	= diameter	L	= length
D	= diameter; or, creep compliance	m	= mass; or, reciprocal of Poisson's ratio
e	= coefficient of base thickness sine function	n	= twist rate, turns per caliber
E	= Young's modulus of elasticity	N	= twist rate, turns per unit length
E_c	= effective modulus	p	= buttress groove pitch
E_g	= glassy modulus	P	= pressure
f	= frequency	P_B	= base pressure
F	= force; friction force	P_c	= chamber pressure
G	= shear modulus	R	= radius
h	= rider width	t	= time; or, base plate thickness
H	= thermal pressure	T	= torque; or, temperature
I_c	= moment of inertia of projectile about longitudinal axis	u, v, w	= displacements in x-, y-, z-directions, respectively
I_E	= moment of inertia of projectile cross section about its central axis	v	= velocity
k	= $(L-t)/\ell$ = sabot length, base plate thickness/projectile length	w_d	= distortional energy per unit volume
		W	= weight
		x	= distance from commencement of rifling

x, y, z = Cartesian coordinates

α = thermal expansion coefficient

β = L_w/R_p = length of sabot wall/radius of projectile

γ = t/R_p = baseplate thickness/radius of projectile

δ = percentage of sabot not undercut

δ_{ij} = Kronecker delta

ϵ = strain

$\epsilon_{ij} = \begin{cases} \text{normal strain, } i = j \\ \text{shear strain, } i \neq j \end{cases} \quad i, j = x, y, z$

θ = angle

λ = R_p/R_B = radius of projectile/radius of gun barrel

μ = coefficient of friction

ν = Poisson's ratio

ρ = material density

σ = stress

σ' = critical stress

$\sigma_{ij} = \begin{cases} \text{normal stress, } i = j \\ \text{shear stress, } i \neq j \end{cases} \quad i, j = x, y, z$

σ_o = mean shear or deviatoric stress

σ_{rz} = shear stress

σ_w = working stress

τ = shear stress or shear strength capability of materials

ω = angular velocity

$\dot{\omega} = \frac{d\omega}{dt}$ = angular acceleration

Subscripts:

B = gun bore

c = compressive

cr = critical

f = friction; forward

I = inertial

K = key

max = maximum

N = normal

oct = octahedral

p = projectile

r = radial

R = ring, required

sc = strength of core

ss = strength of sabot

s = sabot; shoulder

str = strength

S = stud

t = tangential

T = torque

w = wall

θ = tangential

μ = friction

3-1 STRUCTURAL DESIGN FUNDAMENTALS

The verification of the structural integrity of a design consists of two phases: (1) a prediction of the stress and strain states induced in the body by various loading conditions and/or combinations of loading conditions, and (2) application of failure criteria to determine if failure will occur, the margin of safety, or the probability of failure^{1*}. Input data required for the stress-strain prediction phase include (1) characterization

*References are located at the end of each chapter.

of the material stress-strain behavior which also is known as the constitutive equation for the material, and (2) the loading conditions to which the body is expected to be subjected or to which the design must be qualified. Inputs to the failure assessment phase include (1) appropriate failure criteria, i.e., a quantitative description of the conditions under which the material will fracture or deform into an unacceptable shape, and (2) a criterion for acceptable behavior for the specific application under consideration. The latter may take the form of an acceptable margin of safety also known as a safety factor, or a permissible probability of failure. The margin of safety is a subjective measure of acceptable structural performance that should account for (1) uncertainties in load predictions, (2) possible errors in structural analysis techniques, (3) statistical variations in material properties, (4) the inability to identify and correct potential failure conditions before catastrophic failure, and (5) the consequences of experiencing a failure.

With the improvement of load prediction and structural techniques, and the development of statistical means for predicting the uncertainties in predicted quantities, it has been possible to predict the effects of Items 1 through 3 relative to margin of safety. The result is a statistical prediction of the probability of failure. The advantage of the statistical approach is that it reduces the level of reliance upon judgment, which may be biased, to a lower level than the margin of safety approach.

The remainder of this chapter is devoted to a general discussion of material characterization, structural analysis, and failure criteria followed by specific analyses pertinent to structural design of sabots, and the presentation of a computerized, finite-element approach to the solution of structural integrity problems with complicated geometry.

3-2 MATERIAL CHARACTERIZATION

Before performing the structural analysis of a sabot or sabot-projectile system, it first is

necessary as well as expedient to establish assumptions of material behavior under which the analysis will be conducted. Notwithstanding glaring deficiencies that will be discussed subsequently, particularly in connection with failure theory, it is proposed to consider the medium as isotropic, homogeneous, and continuous. The practical objections to these assumptions are based upon the fact that if one examines the material on a sufficiently small scale, it can be shown that neither homogeneous, nor perhaps isotropic, media exist. One must only assume that there does exist, on the average macroscale, an equivalent medium of this type. For many analyses, this approximation will be satisfactory, certainly at the current stage, although the assumption can be seriously in error on the microscale, especially at the origin of failure where fracture or tearing begins. Next, the assumption of continuity is not always fulfilled because it implies that there is always a bond between the components of multiphase materials, e.g., Fiberglas. Actually, this assumption may not be correct under excessive tensile stress. On the other hand, the bond still will exist between those surfaces in compression, therefore leading to (noncontinuum) load-induced isotropy. Nevertheless, to conduct present analyses, it is customary, and at least temporarily appropriate, to assume an isotropic, homogeneous continuum.

The second assumption is that the strains will be sufficiently small so that infinitesimal deformations can be assumed. Actually, for the loads and geometries used in current designs, strains of 30 percent frequently are computed from infinitesimal theory, certainly pushing the limit of validity for this assumption. On the other hand, finite strain analysis is complex. Considering the widespread knowledge of infinitesimal deformation theory and its relative ease of application, it is considered appropriate, pending some later qualifications, to begin at this point.

Third, the material stress-strain behavior must be considered. Generally, only three types of stress-strain behavior will be con-

sidered: (1) linear elastic, (2) rigid-plastic, or (3) elastic-plastic (Fig. 3-1). The first is customary and appropriate for most materials. It merely implies that the deformation or recovery of the material from deformation under applied loading will be instantaneous and complete upon application or removal of the load, with no delay or viscoelastic response. On the other hand, some components will be so highly, and intentionally, loaded that the material will yield or permanently deform. Actual behavior usually is somewhere between these two limits, but experience shows that for the majority of situations analyzed herein, a careful assessment of the behavior of these two limits will suffice.

3-2.1 LINEAR ELASTIC BEHAVIOR

The material properties required to perform a stress-strain analysis assuming linear elastic behavior are:

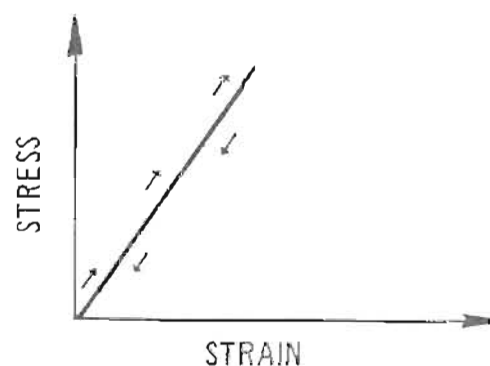
- (1) Material density ρ usually given in units of lbm/in^3
- (2) Modulus of elasticity E usually given in units of psi
- (3) Poisson's ratio ν which is dimensionless
- (4) Coefficient of thermal expansion α usually given in units of $\text{in./in.-}^\circ\text{F}$

Density ρ is the measure of the mass of a unit volume of the material. The modulus of elasticity E and Poisson's ratio are material constants that describe the stress-strain behavior of the material. The coefficient of thermal expansion describes how the dimensions of the material change with changes in temperature. A compilation of the room temperature properties for the materials commonly used for sabots is given in Appendix B.

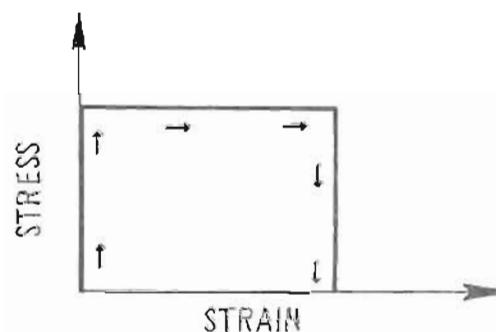
It will be noted that it is also possible to define a shear modulus G and bulk modulus K for the material. In the case of a linear elastic material, however, these properties can be shown to be simple functions of E and ν (Ref. 2):

$$\left. \begin{aligned} G &= \frac{E}{2(1 + \nu)} \\ K &= \frac{E}{3(1 - 2\nu)} \end{aligned} \right\} \quad (3-1)$$

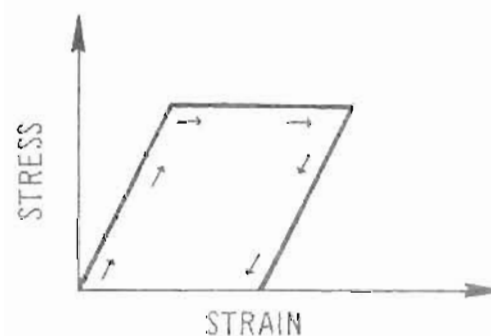
In fact, given the assumption of linear elastic behavior and any two material constants, e.g., E and ν , the other material constants – G , K ,



(A) LINEAR ELASTIC BEHAVIOR



(B) RIGID-PLASTIC BEHAVIOR



(C) ELASTIC-PLASTIC BEHAVIOR

Figure 3-1. Illustration of Possible Stress-strain Behavior

or any other property one might want to define – may be calculated. Furthermore, given the material constants and either the stresses σ or the strains ϵ , the other quantities (strains or stresses) may be calculated using the stress-strain relationships. For a linear, thermomechanically coupled elastic solid, in general, three-dimensional Cartesian coordinates, the stress-strain relationships² are

$$\left. \begin{aligned} \epsilon_{xx} - \alpha T &= \frac{1}{E} [\sigma_{xx} - \nu (\sigma_{yy} + \sigma_{zz})] \\ \epsilon_{yy} - \alpha T &= \frac{1}{E} [\sigma_{yy} - \nu (\sigma_{xx} + \sigma_{zz})] \\ \epsilon_{zz} - \alpha T &= \frac{1}{E} [\sigma_{zz} - \nu (\sigma_{xx} + \sigma_{yy})] \\ \epsilon_{xy} &= \frac{\sigma_{xy}}{G}, \epsilon_{yz} = \frac{\sigma_{yz}}{G}, \epsilon_{xz} = \frac{\sigma_{xz}}{G} \end{aligned} \right\} \quad (3-2)$$

These equations are also known as Hooke's law. The yield strength usually determined in a uniaxial tensile test describes the limit of elastic behavior.

3.2.2 THE FITZGERALD MODIFICATION OF HOOKE'S LAW FOR INCOMPRESSIBLE MEDIA

The deformation characteristics of rubbers and some polymers are found to approach incompressible behavior, i.e., $\nu \rightarrow \frac{1}{2}$ and $K \rightarrow \infty$. Due to the occurrence of a $(1 - 2\nu)$ term in the denominators of certain stress analysis formulas, however, the assumption of incompressible behavior can create serious computational difficulties and may result in oscillations in computer solutions for stresses and strains. One approach to avoiding this difficulty is to assume nearly-incompressible behavior, i.e., $\nu = 0.498, 0.499, \text{ or } 0.4999$. Unfortunately, this is not satisfactory because calculated stresses are sensitive to the value of ν , which is assumed.

An alternate approach growing out of the Grüneisen relationships of polymer physics and because of Fitzgerald*, is the postulate that the quantity $3\alpha K$ is a constant. This quantity, denoted by H , is known as the

thermal pressure and does appear to be a material constant. Furthermore, it appears to be the same constant for polymers in general – approximately 75 psi/°F. Physically, this is the pressure that would develop in the polymer for each degree of temperature change if the polymer were heated under absolute confinement.

To illustrate the effect that this hypothesis will have upon the stress-strain law, it is convenient to begin with the Duhamel-Neuman form³ of the stress-strain relationships for thermomechanically coupled, linear elastic systems. Using tensor notation, these expressions are

$$\left. \begin{aligned} \sigma_{ij} &= \frac{\nu E}{(1 + \nu)(1 - 2\nu)} \epsilon_{kk} \delta_{ij} + 2G\epsilon_{ij} \\ &\quad - \left(\frac{\alpha E T}{1 - 2\nu} \right) \delta_{ij} \\ \text{and} \\ \epsilon_{ij} &= \left(\frac{1 + \nu}{E} \right) \sigma_{ij} - \frac{\nu}{E} \sigma_{kk} \delta_{ij} + \alpha T \delta_{ij} \end{aligned} \right\} \quad (3-3)$$

where the indices i and j take on the values of 1, 2, and 3 (denoting the three Cartesian coordinates x, y, z), repeated subscripts indicate summation, and δ_{ij} is the Kronecker delta defined as

$$\delta_{ij} = \begin{cases} 1, & i = j \\ 0, & i \neq j \end{cases} \quad (3-4)$$

The second of these equations is identically the stress-strain law previously given. For convenience, however, the stresses have been divided into an equivalent system of a pure hydrostatic pressure ($P = -\sigma_{ii} = -\sigma_{xx} - \sigma_{yy} - \sigma_{zz}$) component and pure shear components ($i \neq j$), and tensor notation has been employed to avoid having to explicitly write down all six relationships implied by the tensor expression. The deformations associated with the hydrostatic pressure and shear components of stress are known as the unit dilation (or volume expansion) and the distortional or shear deformations, respectively.

Inserting the assumption that $3\alpha K = \text{constant} = H$ and rewriting yields the result

*Professor of Civil Engineering, University of Utah, Salt Lake City, Utah.

$$\left. \begin{aligned} \sigma_{ij} &= \tilde{\epsilon}_{ij} + \tilde{K} \tilde{\epsilon}_{kk} \delta_{ij} - HT \delta_{ij} \\ \tilde{\epsilon}_{ij} &= \sigma_{ij} - \frac{\sigma_{kk}}{3} \delta_{ij} + \frac{HT}{3\tilde{K}} \delta_{ij} \end{aligned} \right\} \quad (3-5)$$

where $\tilde{\epsilon}_{ij} = 2 G \epsilon_{ij}$, $\tilde{K} = K/(2G)$, and $\nu = 0.5$
and $E = 3\tilde{K} (1 - 2\nu)$ from Eq. 3-1.

The first term on the right-hand side represents shear or distortion. The second term represents pressure loadings or volume change, and the third term represents temperature stress or temperature volume change.

It will be observed that this transformation has replaced the E , ν , and α appearing in the usual stress-strain law for a linear elastic material with the shear modulus G ; a relative bulk stiffness $\tilde{K} = K/(2G)$, which is always finite; and the thermal pressure H , a general material constant almost the same for all polymers.

The important result is that the $(1 - 2\nu)$ factor causing the singularities or oscillations in stress calculations has disappeared from the equations. The choice this gives the structural analyst is that he may continue to use the strictly continuum approach and obtain unbelievable answers (or play with solutions varying greatly as ν goes from 0.499 to 0.498) or accept the fundamental physical reasoning and experimental verification which suggest that $3\alpha K$ is indeed a constant and employ the Fitzgerald modification of the linear elastic stress-strain laws for incompressible or nearly incompressible media. Experience has shown that the latter gives physically acceptable answers while the former gives highly erratic results.

3-2.3 LOADING RATE EFFECTS

At the loading rates normally encountered in engineering practice, the behavior of metals and metallic alloys is adequately described by the linear-elastic material model. Plastics and rubbers generally exhibit viscoelastic behavior, i.e., the mechanical state (stress or strain) depends not only upon the magnitude

of the load but also upon its rate of application and to a lesser degree upon the history of the loading. Under these conditions, the linear-elastic material model, which assumes material properties that at the most may depend upon temperature of the material, is not adequate.

3-2.3.1 LINEAR VISCOELASTICITY

Linear viscoelastic models*, which introduce time-dependency to material behavior in a special fashion, can be used to describe at least the small deformation characteristics of materials whose mechanical response is time dependent^{3,4}. The moduli used to describe the behavior of viscoelastic materials are also dependent upon the rate at which the material is loaded. The following loading modes were found useful in structural analysis of viscoelastic bodies:

- (1) The relaxation modulus, $E(t)$ or $G(t)$, defined as the time-dependent stress resulting from a suddenly (ideally instantaneously) applied strain divided by the magnitude of the strain step.
- (2) The creep compliance $D(t)$ defined as the time-dependent strain resulting from a suddenly (ideally instantaneously) applied stress divided by the magnitude of the stress step.
- (3) The dynamic modulus, $E^*(\omega)$ or $G^*(\omega)$, or compliance $D^*(\omega)$ which is the amplitude of the steady-state stress or strain resulting from a sinusoidally applied strain or stress divided by the amplitude of the applied strain or stress. The dynamic properties are a function of the frequency f of the applied load and can be divided into an

*The assumption of linearity is similar to that in linear elasticity in that stresses are proportional to strains but it must be stated that the "time-dependent stresses" are proportional to the "time-dependent strains".

in-phase or real component, $E'(\omega)$ or $D'(\omega)$, and an out-of-phase or loss component, $E''(\omega)$ or $D''(\omega)$, i.e.,

$$E^*(\omega) = E'(\omega) + iE''(\omega)$$

where

$$i = \sqrt{-1}.$$

The relaxation modulus or creep compliance is used in problems with slowly or monotonically varying loads, and the dynamic properties are used for oscillatory loadings. Fig. 3-2 shows the typical plots of these moduli of a viscoelastic material plotted on log-log scales. It will be observed at very short times or high frequencies that the material behaves like an elastic material while at very long times or low frequencies it also behaves like an elastic material but with a modulus several orders of magnitude (powers of ten) smaller than the short time modulus value. The short- and long-time relaxation modulus are known as the glassy and rubbery or equilibrium moduli, respectively.

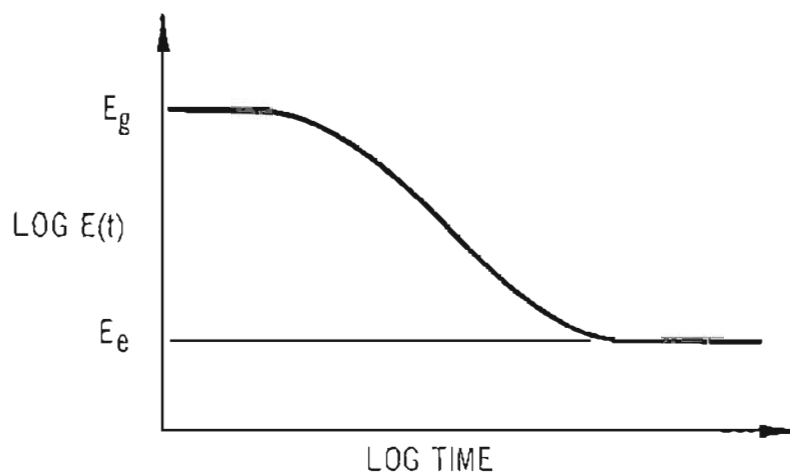
Because of the assumption of linear behavior, the solution of stress problems involving viscoelastic materials is at least philosophically possible. The labor involved, however, is several orders of magnitude greater than an equivalent elastic problem^{5,6} and essentially consists of the following:

- (1) Transformation of material properties, boundary conditions, etc., from time-space into Laplace-transform space
- (2) The solution of a linear elastic problem in transform space for every time period of interest
- (3) Transformation of answer in transform space back into time space.

*The assumption of linearity is similar to that in linear elasticity in that stresses are proportional to strains but it must be stated that the "time-dependent stresses" are proportional to the "time-dependent strains".

A significant decrease in computational detail would be achieved if the assumption of elastic behavior could be justified. If the loading rate were sufficiently high, the modulus of a viscoelastic material would approach the glassy modulus and the material behavior would be elastic. Fortunately, however, even though the sabot strain rates are not high enough to cause the effective modulus to approach the glassy modulus E_g , the range of strain rates and loading rates in most sabot applications is within narrow limits. This makes the assumption of elastic behavior and the resulting simplifications reasonable. For example, consider a cup sabot made of "Lexan", a polycarbonate plastic material. Assuming that the time to maximum local strain of 25 percent is approximately 2 msec, the strain rate then would be 125 in./in./sec. Under these conditions, Ref. 7 indicates that the effective modulus would be $E_e = 300,000$ psi. The maximum modulus for "Lexan" is approximately 320,000 psi and corresponds to strain rates of 700 in./in./sec and above. For all rates below about 0.01 in./in./sec, the effective modulus is approximately 200,000 psi.

The finite element approach to the solution of structural problems discussed in par. 3-5 and the finite element computer program given in Appendix C are capable of handling the bilinear behavior. For example, for the "Lexan" being described in this paragraph, one merely need insert the yield stress (the stress at the bilinear break in the stress-strain curve) of $\sigma = 18,500$ psi and the modulus ratio which for "Lexan" is $6700/320,000 = 0.02$, and the computer will automatically carry out the calculations through the end of the bilinear segment. To determine failure for curves of this sort, assume that the maximum strain of 38 percent governs. Thus, extending the second portion of the bilinear curve out to 38 percent will imply a failure stress of 24,000 psi. The error involved will be approximately the ratio of the neglected area between the bilinear extension and the actual tri-linear section of the stress-strain curve to the total area. In the case of "Lexan", this



(A) RELAXATION MODULUS

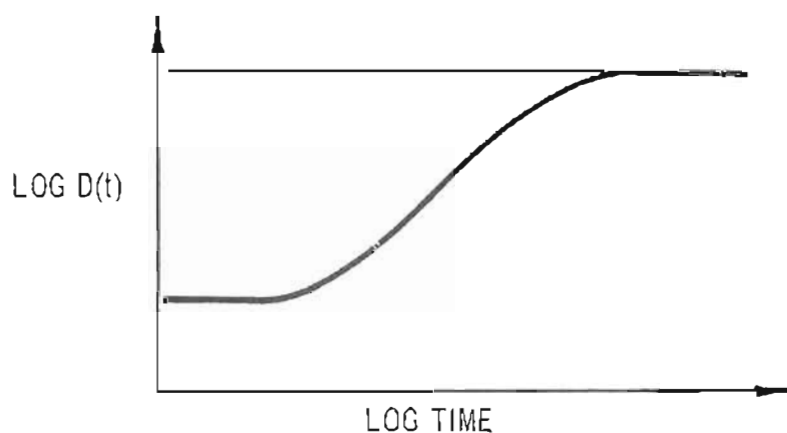
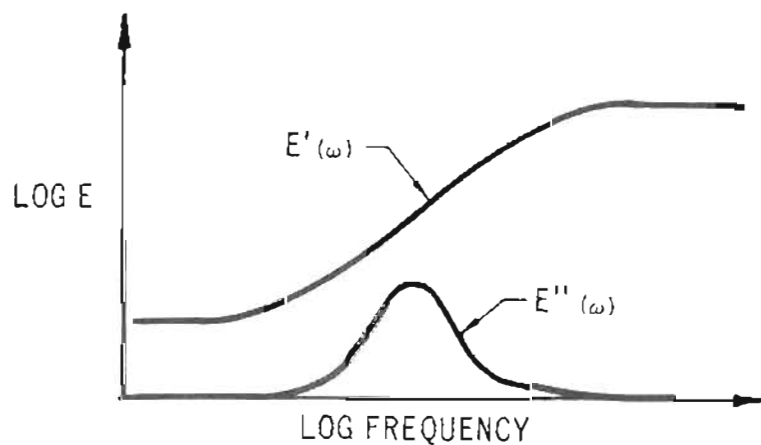
(B) CREEP COMPLIANCE $D(t) = \frac{1}{E(t)}$ (C) DYNAMIC MODULUS $E^* = E' + iE''$

Figure 3-2. Response Characteristics of a Viscoelastic Material

error ratio is approximately 7 percent and on the conservative side.

Thus, it has been shown that the availability of high strain rate data establishing the asymptotic value of the modulus permits one, within acceptable accuracy, to ignore viscoelastic effects in the analysis provided the appropriate modulus is used for the "elastic" analysis.

3.2.3.2 BEHAVIOR OF MATERIALS AT HIGH LOADING RATES

At high loading rates such as those encountered in guns, the behavior of even those materials previously considered elastic become rate dependent. Although increasing the strain rate for viscoelastic materials increases the modulus of the material, the effect of strain rate upon most "elastic" materials is to increase the yield stress and decrease the toughness. The dynamic strength has been found to be 30- to 50-percent higher than the static strength⁸. Available data on dynamic behavior of sabot materials are summarized in the remarks column of the properties tables given in Appendix B. The fact that the dynamic strength of materials is appropriate for the gun launch environment has been adequately demonstrated using gun-launched aerodynamic models^{9,10}. Lockheed Propulsion Company (LPC), using a technique for determining material strength in a gun launch environment, confirms that high rate material properties are appropriate for the structural design of projectiles, models, and sabots. The results of the LPC study are described in Chapter 4 and summarized in Table 3-1. Although the "go-no-go" nature and the limited number of the LPC tests only permit one to establish limits on the strength parameters, the limits are consistent with those predicted from other high rate tests.

In examining the behavior of materials at high strain rate it is further noted that the largest increase in strength occurs at the low strain rates and there appears to be a strain rate above which the material's strength does

not increase. Fig. 3-3 presents dynamic stress-strain curves for "Lexan"⁷. It will be observed that a 32.5 percent increase in strength accompanies the ten-fold increase in strain rate from 0.0125 to 0.125 in./in./sec whereas the further increase in strain rate of approximately one-hundred thousand fold (0.0125 to 1,000 in./in./sec) only increases the strength 88.5 percent, and that there is essentially no change in the material strength for strain rates above 1,000 in./in./sec. A similarity thus is noted between the strength of essentially elastic solids and the moduli of viscoelastic materials.

3.2.3.3 OTHER OBSERVATIONS

Examination of Fig. 3-3 shows that the dynamic stress-strain curves have a definite bilinear form, i.e., the plot points can be approximated by two straight lines. The first line has a relatively high slope or modulus (as much as 320,000 psi) and applies up to 6-percent strain and is followed by a low modulus (6700 psi) portion which holds to 28-percent strain. Actually, there is a third high modulus portion which holds up to the breaking strain of 38 percent but this is usually ignored because available computational techniques are limited to bilinear or "elastic-strain hardening plastic" behavior.

3.2.4 FAILURE CRITERIA

Calculation of the stresses and strains induced in a body by the loads imposed upon it is but an initial step in the structural analysis. To complete the analysis, one must apply criteria to ascertain if the body has failed. Failures fall into two general categories: deformation failures and fractures. In a deformation failure, failure occurs whenever the body deforms to the point that it cannot perform its function. In sabots, a deformation-type failure would occur if during launch the sabot permitted the projectile to carry either to translate or pitch to the point that there would be excessive dispersion at the target. Another possibility is the excessive deformation of sabot parts that result in

TABLE 3-1
RESULTS OF LOCKHEED PROPULSION COMPANY (LPC) TESTS FOR MATERIAL
STRENGTH UNDER GUN LAUNCH CONDITIONS

Material	Measured Static Strength, 10^3 psi	Predicted Dynamic Strength(a), 10^3 psi	Dynamic Strength Limits - LPC Gun Environment Tests(b), 10^3 psi
1. Maraging steel, Grade 300, 18% Ni	269 (yield) 277 (ultimate)	304 313	yield > 242 ultimate < 376
2. Type 4340 steel, R _c 39-41	191 (yield) 192 (ultimate)	206 219	yield > 185 ultimate > 213 (1.54% elongation)
3. Type 7075-T6 Aluminum alloy	83 (yield) 92 (ultimate)	116 127	yield > 117 ultimate < 136
4. Polycarbonate plastic (GE "Lexan")	9.2 - 9.3 (yield)(c) 13.5 - 20.0 (ultimate)(c)	15.7 - 15.9 25.5 - 37.7	yield > 14.0 ultimate > 26 (9.2% elongation)

(a) Based on data reported in the literature

(b) Go/No-go Tests performed in 1.53-in. diameter, smoothbore gun
See par. 4-2 for experimental procedure

(c) 0.05 in./in.-min (Yield strength at 0.5 in./in.-min was 9.5 ksi and ultimate strength was 25.3 ksi.)

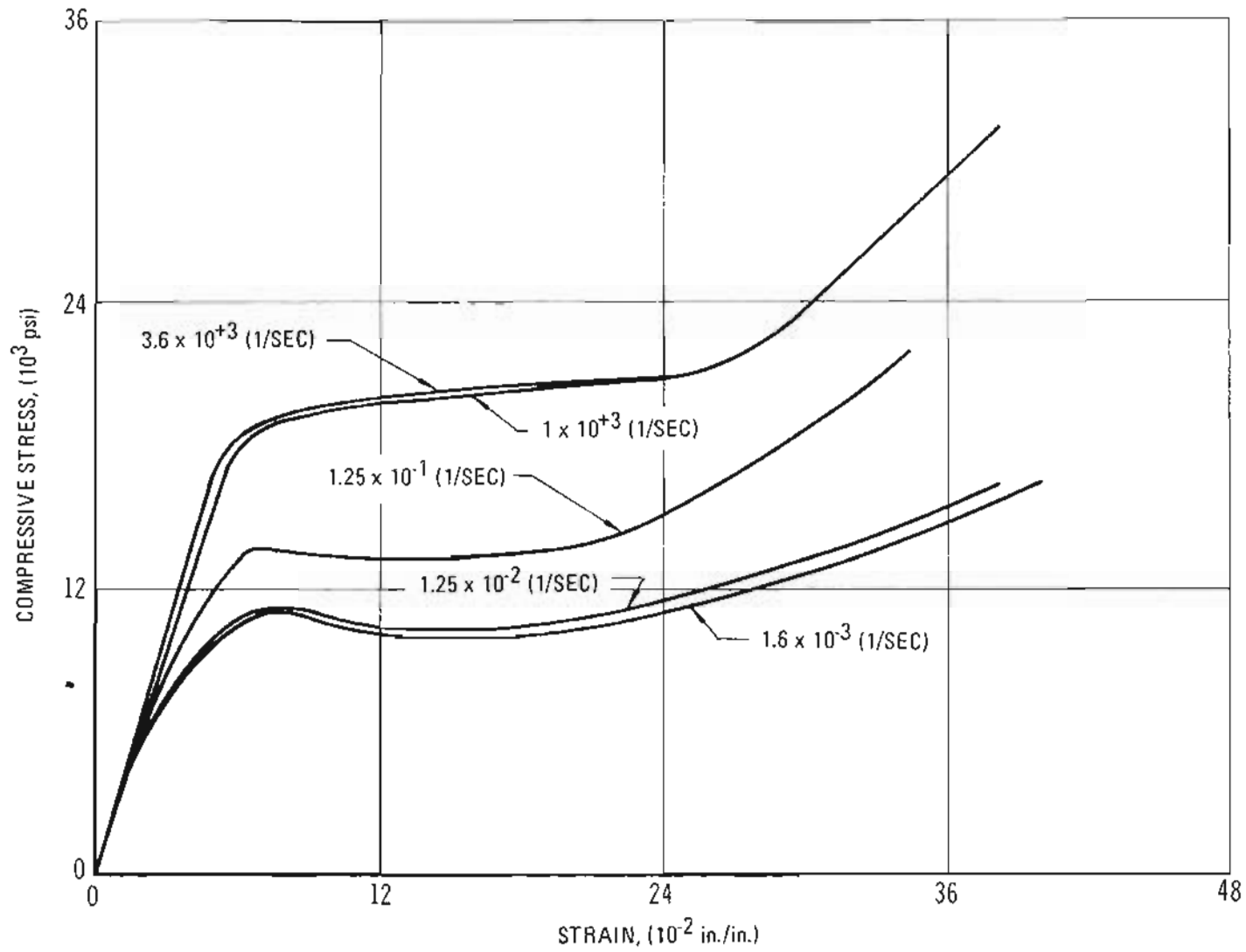


Figure 3-3. Dynamic Stress-strain Relationship for a Polycarbonate Plastic ('Lexan')

separations between the parts and, therefore, gas leakage.

Fracture failure is the condition where the material is incapable of withstanding the stresses or strains imposed upon it and physically yields or separates, creating one or more cracks or fissures. There have been numerous criteria established to predict this type of failure. Five of the criteria commonly used are^{4,11}.

- (1) Maximum principal stress theory
- (2) Maximum principal strain theory
- (3) Maximum shear stress theory
- (4) Maximum strain energy theory
- (5) Maximum distortional strain energy or maximum octahedral shear stress theory.

Each criterion defines a particular functional of the stress or strain field so that if a critical value of the functional is exceeded, the associated yield, rupture, or fracture takes place. The critical value of the functional must be empirically determined for each material of interest. The test most commonly used is the uniaxial tensile test. The limiting value of the functional then may be expressed in terms of the yield or ultimate strength as determined in a simple tensile test.

Criteria (1) and (2) utilize the fact that the maximum stress (strain) at any point in the material is the largest of the three principal stresses (strains), σ_1 , σ_2 , σ_3 (ϵ_1 , ϵ_2 , ϵ_3) at this point. Failure is assumed to occur when the principal stresses (strains) in the body reach the yield or ultimate stress value determined in a uniaxial test.

Criterion (3), also known as the maximum principal stress difference theory, stems from the observation that many materials — particularly those that evidence ductile fracture — do so along a pair of planes or a cone lying in

the direction of greatest shear. The maximum shear stress has the value $(\sigma_1 - \sigma_3)/2$ and is obtained on a plane inclined 45 deg to the direction of the principal normal stresses.

Alternately, Criterion (5) may be used. It is based upon a mean value of the principal stress differences or the strain energy associated with shear deformations, i.e., distortions. The proposed von Mises form is

$$\sqrt{2} \sigma_o = \sqrt{(\sigma_1 - \sigma_2)^2 + (\sigma_2 - \sigma_3)^2 + (\sigma_3 - \sigma_1)^2}$$

and σ_o is termed the mean shear or deviatoric stress. For both simple uniaxial tension and biaxial tension, σ_o is identical with the yield or fracture stress. For pure shear, the yield stress turns out to be $\sigma_o/\sqrt{3}$.

An alternate form of the above is that due to Huber and Hencky. They observe that w_d , the distortional energy per unit volume, is

$$w_d = \frac{\sigma_o^2}{6E} = \frac{(\sigma_1 - \sigma_2)^2 + (\sigma_2 - \sigma_3)^2 + (\sigma_3 - \sigma_1)^2}{12E}$$

This mean deviatoric stress is also $3/\sqrt{2}$ times a quantity known as the octahedral shear stress. The results obtained from the latter two theories usually are similar.

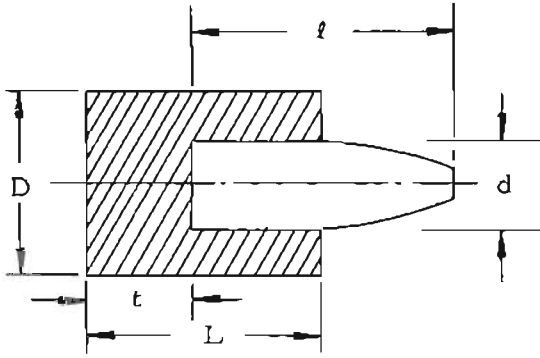
The total strain energy theory was proposed by Baltrami and Haigh. It does not prove satisfactory because there is no correlation between behavior in pure shear and in pure hydrostatic compression.

The important point to observe is that no universal fracture criterion has been established, and that the success of a given fracture hypothesis depends in large measure upon the material with which it is associated.

3-3 ELEMENTARY DESIGN CONSIDERATIONS FOR CUP SABOTS

3-3.1 STANDARD CUP SABOT

The elementary cup sabot and its principal dimensions are shown as follows:



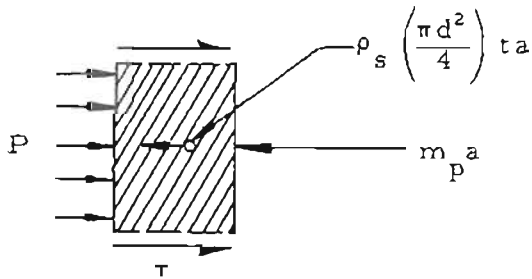
The quantities d , D , and ℓ are inputs to the sabot design as well as the mass of the projectile and a target mass for the sabot and sabot loads. The sabot design problem is to establish the sabot material and the dimensions t and L . For present purposes it may be assumed that the amount of the projectile length which is supported, i.e., $L - t$, is established by launch dynamic considerations and probably lies somewhere between 0.5 to 1.0 of the projectile length. Therefore, let

$$k = \frac{L - t}{\ell} \quad (3-6)$$

where $0.5 \leq k \leq 1.0$

Let it now be assumed that the basic failure mode for the cup sabot will be a shearing out of a piece of the sabot bottom the same diameter as the projectile.

A free body diagram for this piece of the sabot is given as follows:



A summation of the forces yields

$$\Sigma F_x = P \left(\frac{\pi d^2}{4} \right) - m_p a - \rho_s \left(\frac{\pi d^2}{4} \right) t a$$

where P = gas pressure
 τ = shear stress
 m_p = mass of the projectile
 a = acceleration
 ρ_s = density of sabot material

which can be solved for the shear stress

$$\tau = \left[\frac{m_p}{\pi t d} + \left(\frac{\pi d}{4} \right) \rho_s \right] a - \left(\frac{\pi d}{4} \right) P \quad (3-7)$$

which will be maximum whenever the acceleration is maximum (pressure will also be maximum). The maximum shear stress

$$\tau_{max} = \left[\frac{m_p}{\pi t d} + \left(\frac{\pi d}{4} \right) \rho_s \right] a_{max} - \left(\frac{\pi d}{4} \right) P_{max} \quad (3-8)$$

and if the sabot is to be structurally sound the maximum shear stress must be less than the shear strength of the material, i.e.,

$$\tau_{max} < \tau_{sir}$$

Substituting the equation for the maximum shear stress and solving for the thickness of the sabot base yields

$$t > \frac{m_p a_{max} - P_{max} (\pi d^2 / 4)}{\pi d \tau_{sir} - \rho_s a_{max} (\pi d^2 / 4)} \quad (3-9)$$

$$> \frac{m_p a_{max}}{\pi d \tau_{sir}} \left[\frac{1 - \frac{\pi d^2}{4} \left(\frac{P_{max}}{m_p a_{max}} \right)}{1 - \frac{d}{4} \rho_s \left(\frac{a_{max}}{\tau_{sir}} \right)} \right] = \Phi \frac{m_p a_{max}}{\pi d \tau_{sir}}$$

$$\text{where } \Phi = \left[\frac{1 - \frac{\pi d^2}{4} \left(\frac{P_{max}}{m_p a_{max}} \right)}{1 - \frac{d}{4} \rho_s \left(\frac{a_{max}}{\tau_{sir}} \right)} \right]$$

and the expression for the sabot mass becomes

$$m_s = \rho_s \left[\frac{\pi D^2}{4} t + \frac{\pi}{d} (D^2 - d^2) (L - t) \right] \quad (3-10)$$

But $L - t = k\ell$ therefore

$$m_s = \frac{\pi}{4} D^2 \rho_s \left[t + k\ell \left(1 - \frac{d^2}{D^2} \right) \right]$$

or substituting for the thickness and rearranging terms gives

$$\frac{m_s}{m_p} > \frac{\Phi}{4} \left(\frac{\rho_s D a_{max}}{\tau_{str}} \right) \left[\frac{1}{(d/D)} \right] + \frac{\pi k}{4} \left(\frac{D^2 \rho_s \ell}{m_p} \right) \left(1 - \frac{d^2}{D^2} \right)$$

or

$$\frac{m_s}{m_p} > \frac{\Phi}{4} \left(\frac{D \rho_s a_{max}}{\tau_{str}} \right) \left[\frac{1}{(d/D)} \right] + k \left(\frac{\rho_s}{\rho_p} \right) \left[\frac{1}{(d/D)^2} - 1 \right] \quad (3-11)$$

where ρ_p is an effective density of the projectile defined by

$$\rho_p = \frac{4 m_p}{\pi d^2 \ell} \quad (3-12)$$

These equations are adequate for preliminary sizing of cup sabots. Having tentatively established the dimensions of the sabot, it now is possible to consider more complicated loadings.

3-3.1.1 BENDING OF BASE PLATE

Because (1) the stresses imposed on the top of the sabot base plate by the set back of the sabot walls and the projectile will not be equal and (2) frictional forces will be applied around the outer edge of the sabot base plate, bending stresses will be induced into this plate. The bending stresses will be a maximum at the center of the base plate. In addition, the radial and tangential stresses will be equal and are given by the equation

$$\begin{aligned} (\sigma_r)_{max} = (\sigma_t)_{max} = & \frac{3}{8 (t/d)^2 (d/D)} \\ & \left\{ (3 + \nu) \left[k \left(\frac{\ell}{d} \right) + \left(\frac{t}{d} \right) \right] \sigma_\mu \right. \\ & + \frac{a_{max}}{\pi (d/D)} \left[\frac{\pi}{4} \rho_s k \ell \left(\frac{d}{D} \right)^2 - \frac{m_p}{D^2} \right] \\ & \left. \left[(1 - \nu) \left[1 - \left(\frac{d}{D} \right)^2 \right] - 4 (1 + \nu) \log \left(\frac{d}{D} \right) \right] \right\} \quad (3-13) \end{aligned}$$

where $\sigma_\mu = \frac{F_\mu}{\text{contact area}}$

F_μ = friction force = μF_N

F_N = normal force acting on sabot

μ = coefficient of friction

The analysis leading to Eq. 3-13 considers the effects of (1) inertial load because of the projectile, (2) inertial load because of the sabot wall, (3) inertial load because of the base plate, (4) base pressure load, and (5) frictional load between sabot and launch tube walls. Aerodynamic loads such as drag forces arising from compressing air in the barrel in front of the projectile are not considered because they are in the opposite sense of the inertial loads and will subtract from the net loads on the sabot. The exclusion of this load will make the analysis more conservative. Observe that the dependence of the maximum bending stresses on the chamber pressure has been eliminated in favor of expressing the stresses as a function of the acceleration and thickness of the base plate.

The octahedral shear stress is given by

$$\sigma_{oct} = \left[(\sigma_r)^2 - \sigma_r \sigma_\theta + (\sigma_\theta)^2 \right]^{1/2} = \sigma_r$$

thus applying the octahedral shear stress theory of failure the design will be adequate if

$$\sigma_r < \frac{\sqrt{2}}{3} \sigma_y \quad (3-14)$$

where σ_y is the uniaxial tensile yield strength of the sabot material.

Based on the maximum shear stress theory, yielding will occur whenever $\sigma_r = \sigma_y$.

3-3.1.2 CRUSHING OF THE BASE PLATE

Although probably not of serious concern, a check on the compressive stresses induced by inertial forces should be made

$$\sigma_c = \frac{4(m_p + m_s) a_{max}}{\pi D^2} \quad (3-15)$$

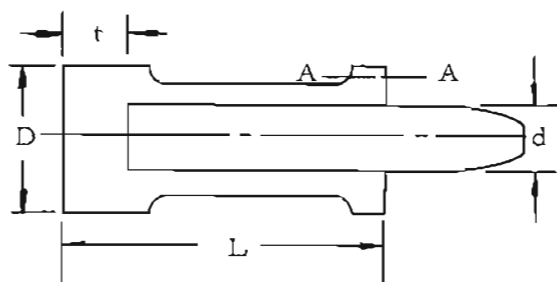
The calculated compressive stress can be compared with the material capabilities or the stress can be set equal to the working stress and an alternate calculation of the thickness can be made.

3.3.1.3 BUCKLING OF THE SABOT WALL

Because for the standard cup sabot there is no room for lateral displacement of the sabot, wall buckling of the sabot is of no concern.

3.3.2 CUP SABOT WITH EXTERNAL UNDERCUT

The previous expressions may be used for calculating stresses with a slight modification of the expression for the frictional stress F_μ and for the mass of the sabot.



now

$$F_\mu = \sigma_\mu \pi D \delta L$$

where σ_μ is the friction force per unit contact area and δ is the percentage of sabot length that is not undercut, i.e., percentage in contact with gun barrel. The bending stresses are thus

$$\begin{aligned} (\sigma_r)_{max} = (\sigma_\theta)_{max} &= \frac{3(3+\nu)(\gamma+\beta\delta)\sigma_\mu}{4\gamma^2\lambda} \\ &+ \frac{3a}{8g\pi(1-\lambda^2)\gamma^2 R_p^2} \left[m_w \lambda^2 \right. \\ &\left. - (1-\lambda^2)m_p \right] \left[(1-\nu)(1-\lambda^2) - 4(1+\nu)\log\lambda \right] \end{aligned} \quad (3-16)$$

where

$$\lambda = \frac{R_p}{R_B}; 0 \leq \lambda \leq 1$$

$$\begin{aligned} L_w &= \text{length of sabot wall} \\ &= \beta R_p \quad (0 \leq \beta \leq \infty) \end{aligned}$$

$$\begin{aligned} t &= \text{base plate thickness} \\ &= \gamma R_p \quad (0 \leq \gamma \leq \infty) \end{aligned}$$

$$R_p = \text{projectile radius}$$

$$R_B = \text{gun bore radius}$$

$$m_w = \text{sabot wall mass}$$

$$m_p = \text{projectile mass}$$

There is the possibility of a shear failure along plate A-A due to frictional forces. However, this is not an expected failure mode. It is more likely that this forward ring will deform plastically. An analysis of friction surfaces is presented in Appendix B of Ref. 12.

With the addition of an undercut, the possibility of lateral displacement is introduced and buckling of the sabot wall becomes a possibility. An approximation for the critical compressive stress is

$$\sigma'_c = \frac{E}{\sqrt{3(1-\nu^2)}} \left[\frac{1}{(d/D)} - 1 \right] \quad (3-17)$$

The approximation is valid whenever the length of the undercut is several times greater than $1.72 D \sqrt{\left(\frac{d}{D}\right)^2 - \left(\frac{d}{D}\right)}$. The latter is the length of a half wave of buckling.

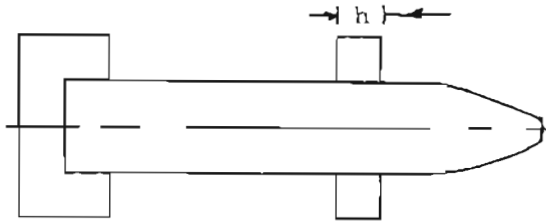
It will be observed that because the compressive load is primarily due to inertial loading, the check should be made at the bottom of the undercut.

3.3.3 CUP SABOT WITH INTERNAL UNDERCUTS

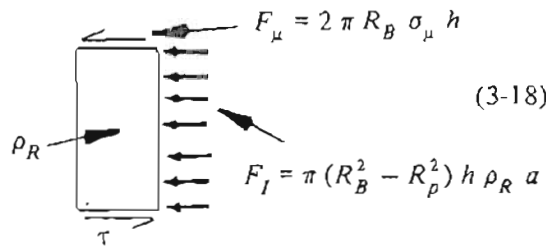
The expressions used for calculating stresses in the cup sabot with external under-

cut (see Fig. 2-9) also apply in this case. In addition, if the cavity is not filled with a hydrostatic liquid, compressive stresses on the sabot walls could cause them to collapse and allow blow-by of the gas.

3-3.4 CUP SABOT WITH RIDER



With the modifications, the expressions generated in pars. 3-3.1.1 and 3-3.1.2 may also be used in obtaining stresses in a cup sabot with a forward rider. Buckling need not be considered. Shearing of the forward ring from the projectile and radial tension failure between the leading edge of the forward ring and the projectile will be considered.



$$\begin{aligned} \sigma_z &= \frac{2R_B \sigma_\mu + (R_B^2 - R_p^2) \rho_R a}{2R_p} \\ &= \frac{2\sigma_\mu R_B + \rho_R a (R_B^2 - R_p^2)}{2R_p} \\ \tau &= \frac{2\sigma_\mu + \rho_R a R_B (1 - \lambda^2)}{2\lambda} \end{aligned} \quad (3-19)$$

The problem of radial tension failure due to bending is given as the sum of solutions for the following two problems:

$$(1) \quad F_\mu = 2 \pi R_B \sigma_\mu h$$

$$(2) \quad F_I = \pi (R_B^2 - R_p^2) h \rho_R a$$

where F_I = inertial reaction force.

The solution to (1) is

$$(\sigma_r)'_{max} = \frac{3 F_\mu}{2 \pi h^2}$$

$$\left[\frac{2R_B^2(m+1) \log(R_B/R_p) + R_B^2(m-1) - R_p^2(m-1)}{R_B^2(m+1) + R_p^2(m-1)} \right]$$

$$= \frac{3 R_B \sigma_\mu}{h}$$

$$\left[\frac{-2(m+1) \log \lambda + (m-1) - \lambda^2(m-1)}{(m+1) + \lambda^2(m-1)} \right]$$

$$= \frac{3 R_B \sigma_\mu}{h}$$

$$\left[\frac{-2(1+\nu) \log \lambda + (1-\nu) - \lambda^2(1-\nu)}{(1+\nu) + \lambda^2(1-\nu)} \right]$$

where

$$m = \frac{1}{\nu} = \text{reciprocal of Poisson's ratio}$$

$$\sigma_r' = \frac{3 R_B \sigma_\mu}{h}$$

$$\left[\frac{-2(1+\nu) \log \lambda + (1-\nu)(1-\lambda^2)}{(1+\nu) + \lambda^2 (1-\nu)} \right]$$

The solution to (2) is

$$(\sigma_r)_{max}'' = \frac{3 \rho_R a}{4h}$$

$$\left[\frac{4 R_B^4 (1+m) \log \frac{R_B}{R_p} - R_B^4 (3+m) + R_p^4 (m-1) + 4 R_B^2 R_p^2}{R_B^2 (1+m) + R_p^2 (m-1)} \right]$$

$$= \frac{3 \rho_R a}{4h}$$

$$\left[\frac{-4(1+m) \log \lambda - (m+3) + \lambda^4 (m-1) + 4\lambda^2}{(1+m) + \lambda^2 (m-1)} \right] R_B^2$$

$$= \frac{3 \rho_R a}{4h}$$

$$\left[\frac{-4(\nu+1) \log \lambda - (3\nu+1) + \lambda^4 (1-\nu) + 4\lambda^2 \nu}{(\nu+1) + \lambda^2 (1-\nu)} \right] R_B^2$$

The combined stress is thus

$$(\sigma_r)_{max} \bigg|_{r=R_p} = \sigma_r' + \sigma_r''$$

$$= \frac{3 R_B \sigma_\mu}{h}$$

$$\left[\frac{-2(1+\nu) \log \lambda + (1-\nu)(1-\lambda^2)}{(1+\nu) + \lambda^2 (1-\nu)} \right]$$

$$+ \frac{3 \rho_R a R_B^2}{4h}$$

$$\left[\frac{-4(1+\nu) \log \lambda - (1+3\nu) + \lambda^4 (1-\nu) + 4\lambda^2 \nu}{(1+\nu) + \lambda^2 (1-\nu)} \right]$$

where ρ_R is the density of the ring material. Note that from this expression it again is possible to calculate the actual stresses or, given a working stress, calculate the required thickness h of the ring.

3-3.5 CUP SABOT WITH BASE PLATE

This design basically provides for an auxiliary base plate or bearing surface multiplier Δ , and its analysis pertains to the configurations shown in Figs. 2-11 and 2-12.



$$R_p \leq \Delta R_p \leq R_B; 1 \leq \Delta \leq 1/\lambda$$

$$\text{where } \lambda = \frac{R_p}{R_B}$$

$$\Delta = \frac{\text{radius of auxiliary base plate}}{\text{radius of projectile base } (R_p)}$$

The same expressions used in par. 3-3.2 in calculating stresses apply, but with ΔR_p substituted for R_p . Thus, for example

$$\begin{aligned} (\sigma_r)_{max} = (\sigma_\theta)_{max} &= \frac{3(3+\nu)(\beta+\gamma)\sigma_\mu}{4\gamma^2\lambda(\Delta)} \\ &+ \frac{3}{8\pi(1-\lambda^2\Delta^2)\gamma^2\Delta^2R_p^2} \\ &\left[m_w \lambda^2(\Delta)^2 - (1-\lambda^2\Delta^2)m_p \right] \cdot \\ &\left[(1-\nu)(1-\lambda^2\Delta^2) - 4(1+\nu) \log(\lambda\Delta) \right] \end{aligned} \quad (3-21)$$

and

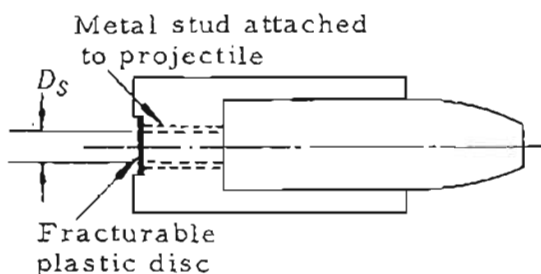
$$\sigma_{rz} = \frac{m_p a}{2\pi g \Delta R_p t} \left[1 - (m_w + m_p) \pi R_B^2 \cdot \right] \quad (3-22)$$

where σ_{rz} is the shear stress (see Eq. 3-27).

Buckling need not be considered for this case since the configuration does not lend itself readily to buckling.

3-3.6 CUP SABOT WITH SHEAR PLATE RESTRAINT

The expressions for the stresses in this case are similar to those used above in Eqs. 3-13 through 3-22. The fracturable plastic disc is included for fragmentation of the sabot once in free flight.



$$D_S = 2R_S = \text{diameter of stud}$$

The bearing area of the projectile is now changed from

$$A_p = \pi R_p^2$$

$$\text{to } A'_p = \pi (R_p^2 - R_S^2).$$

and the maximum tangential stress at $r = R_S$ is given by

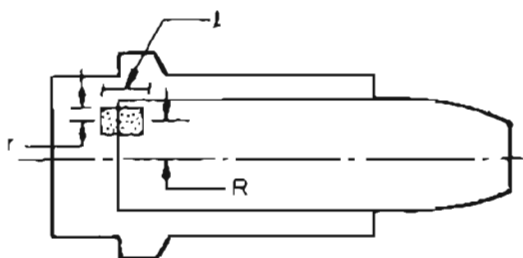
$$\begin{aligned} \sigma_r = \sigma_\theta &= \frac{3\sigma_u (\beta + \gamma)}{2\gamma^2 \lambda (R_B^2 - R_S^2)^2} \left\{ (R_B^2 - R_S^2) \right. \\ &\quad \left[(3+\nu) R_B^2 - (1-\nu) R_S^2 \right] \\ &\quad \left. - 4(1+\nu) R_B^2 R_S^2 \log (R_B/R_S) \right\} \\ &+ \frac{3a}{4\pi g \gamma^2 R_p^2} \left\{ \frac{m_w}{(R_B^2 - R_S^2)^2} \left[(R_B^2 - R_S^2) \right. \right. \\ &\quad \left. \left[(3+\nu) R_B^2 - (1-\nu) R_S^2 \right] \right. \\ &\quad \left. - 4(1+\nu) R_B^2 R_S^2 \log (R_B/R_S) \right] \\ &\quad \left. + 2m_p \left[(1+\nu) - \frac{1}{4}(1-\lambda^2) \right. \right. \\ &\quad \left. \left. \left[(1-\nu) - (1+3\nu) R_S^2/R_p^2 \right] \right] \right\} \quad (3-23) \end{aligned}$$

3-3.7 SPECIAL CONSIDERATIONS FOR SPIN-STABILIZED APPLICATIONS

In addition to the analysis of set-back forces given previously in par. 3-3, if the projectile is to be spin stabilized, a means for transmitting torque between the sabot and the projectile must be provided. Two such means are (1) the use of an eccentrically located pin, and (2) a key located on the aft end of the projectile.

3-3.7.1 ECCENTRICALLY LOCATED PIN

The geometry is assumed to be as follows :



R = distance \mathcal{C} pin to \mathcal{C} projectile

r = radius of pin

The shear force, due to torque, is given by

$$F_T = T/R_p$$

The shear stress due to torque transmission is

$$\tau_T = \frac{T}{R_p} \left(\frac{1}{2\pi R_p t} \right) = \frac{T}{2\pi R_p^2 t} \quad (3-24)$$

This stress is added to the shear stress calculated under conditions of axial acceleration only to give the combined maximum shear stress.

Contact pressure on the sabot base due to torque transmitted through N torque pins :

$$T = F_{pins} R$$

$$\text{Force Transmitted per Pin} = \frac{T}{NR}$$

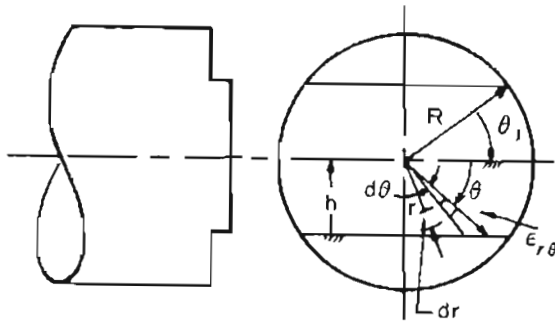
and the contact pressure is

$$\frac{T}{\pi N R r \ell} \quad (3-25)$$

where T = torque
 ℓ = length of pin
 N = turns per unit length
 R = distance center line of pin to center line of projectile
 r = radius of pin

3-3.7.2 TORQUE KEY

The geometry of the key is shown below.



In a complete circular section, the application of a torque T will result in a shear stress distribution given by

$$\sigma_{rz}(\theta) = [r(R)] \frac{r}{R} \quad (3-26)$$

where $\sigma_{rz}(\theta)$ is the shear stress at radius r .

If T is increased to the maximum allowable value, $\tau(R)$ becomes τ_s , the shear strength of the material, and

$$\sigma_{rz}(\theta) = \tau_s \left(\frac{r}{R} \right) \quad (3-27)$$

If the cross section is changed, the stress distribution will change, and distortion of the planes normal to the longitudinal axis will occur. Distortion will also occur in the case shown in the figure in this paragraph where the circular cross section is made up of the key and the mating shoulders, because of the discontinuity in the shear stress. However, in the presence of a high axial compression which keeps the plane sections plane, it is not

unreasonable to assume a distribution of shear stress that is similar to that found with the solid section. The torsional capacity of the split section will, of course, be less than that of the solid, and will be given by the integral of the circular shear distribution over the area of the key or over the area of the shoulder, whichever is less.

Thus, we will assume that the shear stress acting over the cross section of the key at maximum load is given by Eq. 3-27. The torque that can be transmitted is then

$$\begin{aligned} T_K &= \iint r \tau(r) dA \\ &= 4 \int_0^{\pi/2} \int_0^{e_{r\theta}} \tau_s \frac{r}{R} r dr d\theta \\ T_K &= 4 \frac{\tau_s}{R} \left[\int_0^{\theta_1} \int_0^R r^3 dr d\theta + \int_{\theta_1}^{\pi/2} \int_0^{e_{r\theta}} r^3 dr d\theta \right] \quad (3-28) \end{aligned}$$

From the geometry,

$$e_{r\theta} = \frac{h}{\sin \theta} \text{ for } \theta_1 \leq \theta \leq \frac{\pi}{2} \quad (3-29)$$

or

$$T_K = 4 \frac{\tau_s}{R} \left[\int_0^{\theta_1} \frac{R^4}{4} d\theta + \int_{\theta_1}^{\pi/2} \frac{h^4}{4 \sin^4 \theta} d\theta \right]$$

Now

$$\int_{\theta_1}^{\pi/2} \frac{d\theta}{\sin^4 \theta} = - \left[\frac{1}{3} \frac{\cos \theta}{\sin^3 \theta} + \frac{2}{3} \cot \theta \right]_{\theta_1}^{\pi/2}$$

or

$$\int_{\theta_1}^{\pi/2} \frac{d\theta}{\sin^4 \theta} = \frac{1}{3} \frac{\cos \theta_1}{\sin^3 \theta_1} + \frac{2}{3} \cot \theta_1 \quad (3-30)$$

Now

$$\left. \begin{aligned} \cos \theta_1 &= \frac{\sqrt{R^2 - h^2}}{R} \\ \sin \theta_1 &= \frac{h}{R} \\ \cot \theta_1 &= \frac{\sqrt{R^2 - h^2}}{h} \end{aligned} \right\} \quad (3-31)$$

therefore

$$T_K = \tau_s \left\{ R^3 \theta_1 + \frac{h^4}{R} \cdot \left(\frac{1}{3} R^2 \frac{\sqrt{R^2 - h^2}}{h^3} + \frac{2}{3} \frac{\sqrt{R^2 - h^2}}{h} \right) \right\}$$

or

$$T_K = \tau_s R^3 \left\{ \sin^{-1} \frac{h}{R} + \frac{h}{3R} \sqrt{1 - \left(\frac{h}{R}\right)^2} + \frac{2h^3}{3R^3} \sqrt{1 - \left(\frac{h}{R}\right)^2} \right\} \quad (3-32)$$

Then the torque that can be carried by the shoulders is given by:

$$T_s = \frac{\pi R^3 \tau_s}{2} - T_K$$

or

$$T_s = \tau_s R^3 \left\{ \frac{\pi}{2} - \left[\sin^{-1} \frac{h}{R} + \frac{h}{3R} \sqrt{1 - \left(\frac{h}{R}\right)^2} + \frac{2h^3}{3R^3} \sqrt{1 - \left(\frac{h}{R}\right)^2} \right] \right\} \quad (3-33)$$

where h = key or rider width
 R = radius to axis of eccentrically located pin
 T_K = key torque capacity
 T_s = torque capacity of shoulder
 τ_s = shear strength of shoulder

If the core and sabot have shear strengths τ_{sc} and τ_{ss} , respectively, and we wish to make the torque capacities T_K and T_s equal, then

$$\begin{aligned} & \tau_{sc} R^3 \left\{ \sin^{-1} \frac{h}{R} + \frac{h}{3R} \sqrt{1 - \left(\frac{h}{R}\right)^2} + \frac{2h^3}{3R^3} \sqrt{1 - \left(\frac{h}{R}\right)^2} \right\} \\ &= \tau_{ss} R^3 \left\{ \frac{\pi}{2} - \left[\sin^{-1} \frac{h}{R} + \frac{h}{3R} \sqrt{1 - \left(\frac{h}{R}\right)^2} + \frac{2h^3}{R^3} \sqrt{1 - \left(\frac{h}{R}\right)^2} \right] \right\} \end{aligned}$$

If we write

$$\begin{aligned} & \sin^{-1} \frac{h}{R} + \frac{h}{3R} \sqrt{1 - \left(\frac{h}{R}\right)^2} + \frac{2h^3}{3R^3} \sqrt{1 - \left(\frac{h}{R}\right)^2} \\ &= \Phi\left(\frac{h}{R}\right) \end{aligned}$$

then

$$\frac{\tau_{sc}}{\tau_{ss}} = \left[-\frac{\pi}{2 \Phi\left(\frac{h}{R}\right)} - 1 \right] \quad (3-34)$$

The function $\Phi(h/R)$ is shown in Fig. 3-4, and Eq. 3-34 is shown in Fig. 3-5 as τ_{sc}/τ_{ss} versus h/R .

In order to evaluate the torsional capacity of a given key-sabot combination, we first obtain the optimum value of h/R from Eq. 3-34 or Fig. 3-5, and then the corresponding value of Φ from Fig. 3-4. The torque capacity is then simply

$$T_K = \tau_s R^3 \Phi\left(\frac{h}{R}\right) \quad (3-35)$$

It should be noted that for a given shear strength and core size, the variation of T_K with key width is the same as that shown for $\Phi(h/R)$.

Nomenclature

x = distance from commencement of rifling
 $N(x)$ = twist rate, turns per unit length
 $n(x)$ = twist rate, turns per caliber ($2 RN$)
 $v(x)$ = speed of projectile at x
 $\omega(x)$ = angular velocity at x
 $\dot{\omega}(x)$ = angular acceleration at $x = \frac{d\omega(x)}{dt}$
 T_R = required torque
 I_c = moment of inertia of core about its longitudinal axis
 P_B = base pressure
 A_B = area of bore, cross-sectional
 m_p = mass of projectile

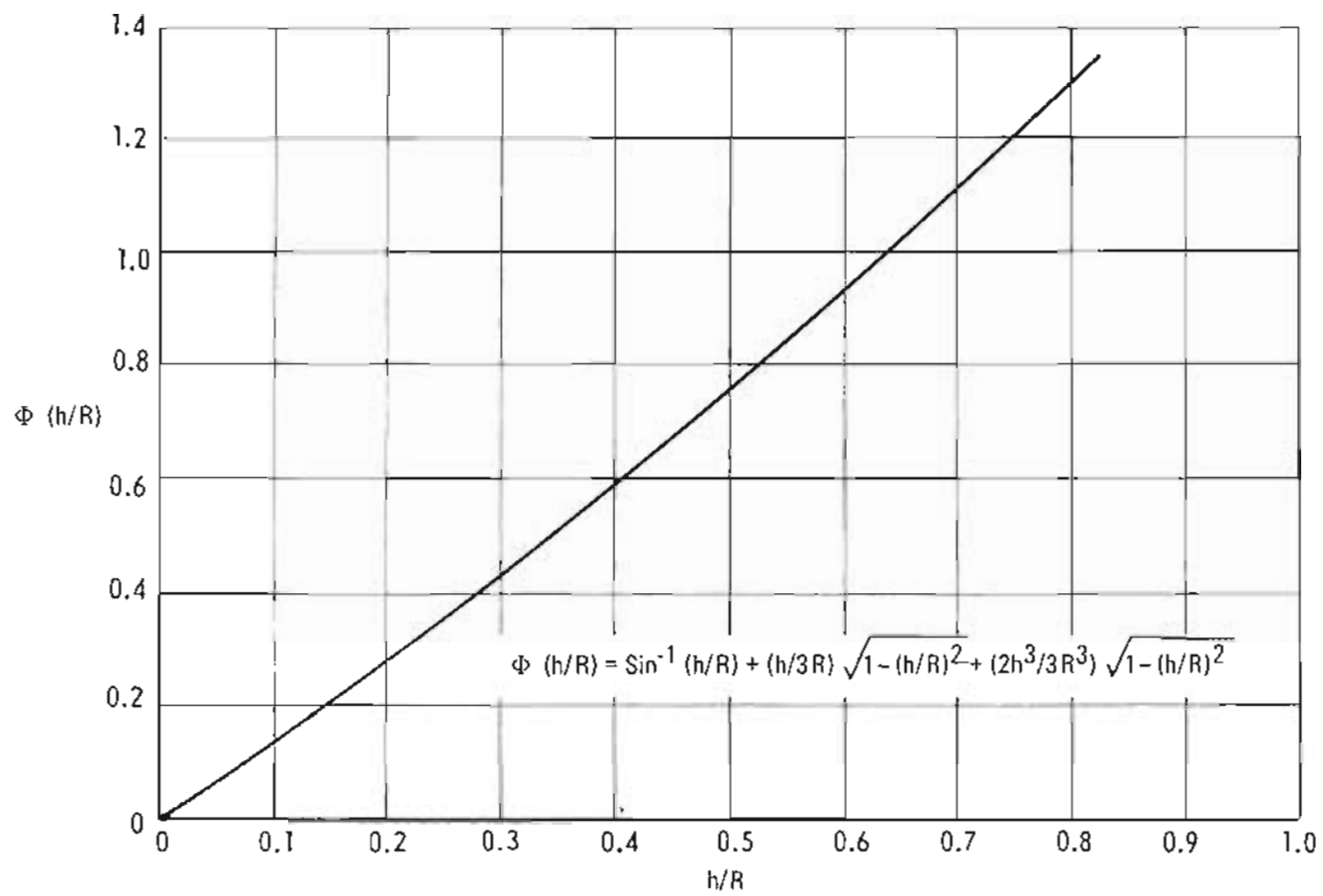


Figure 3-4. Variation of $\Phi (h/R)$ With h/R

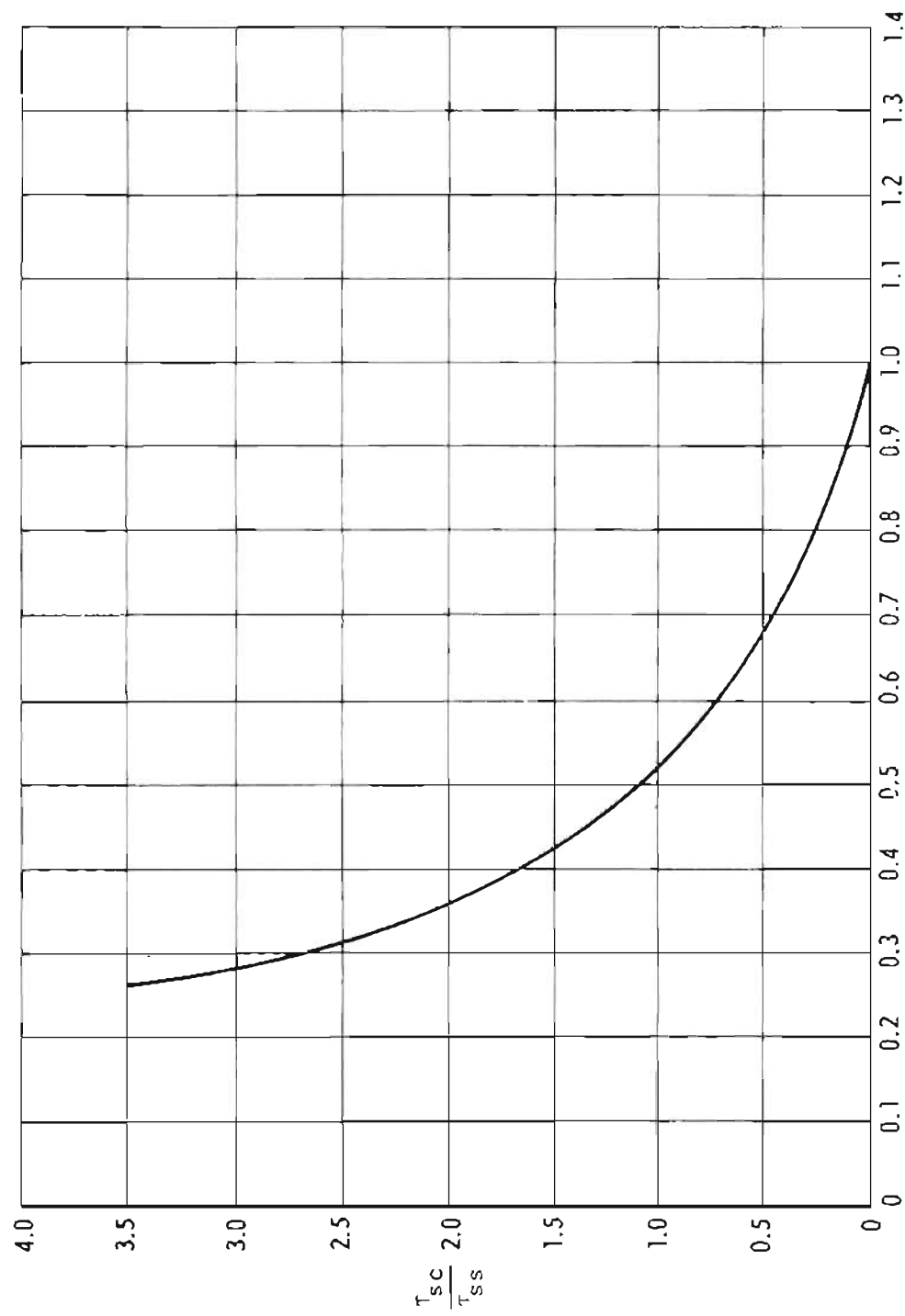


Figure 3-5. Variation of h/R With Stress Ratio τ_{sc}/τ_{ss}

At any point x in the bore, the angular velocity of the projectile will be $\omega(x) = N(x)v(x)$ turns per second, or

$$\omega(x) = 2\pi N(x) \frac{dx}{dt}, \text{ rad/sec} \quad (3-36)$$

and

$$\dot{\omega}(x) = 2\pi \left[\frac{dN(x)}{dt} \frac{dx}{dt} + N(x) \frac{d^2x}{dt^2} \right]$$

i.e.,

$$\dot{\omega}(x) = 2\pi \left[\frac{dN(x)}{dx} \left(\frac{dx}{dt} \right)^2 + N(x) \frac{d^2x}{dt^2} \right] \quad (3-37)$$

Equation of rotary motion for the core,

$$T_R(x) = \frac{d[I_c \omega(x)]}{dt}$$

I_c is a constant therefore

$$T_R(x) = I_c \dot{\omega}(x)$$

or

$$T_R(x) = 2\pi I_c \left[\frac{dN(x)}{dx} \left(\frac{dx}{dt} \right)^2 + N(x) \frac{d^2x}{dt^2} \right] \quad (3-38)$$

$T_R(x)$ is then the torque capacity of the mechanism required to spin the core. The maximum value of $T_R(x)$ can be found easily by differentiating Eq. 3-38 with respect to x and equating the result to zero. However, to do this it is required that the velocity and pressure profiles along the barrel be known or better still, the displacement-time profile.

3-3.7.3 TORQUE KEY FOR CONSTANT TWIST

If the twist is constant along the length of the barrel, then Eq. 3-38 is simplified and the maximum torque requirement only requires a knowledge of the maximum base pressure, i.e.,

$$\frac{dN(x)}{dx} = 0$$

and

$$T_R(x) = 2\pi I_c \left[N(x) \frac{d^2x}{dt^2} \right] \quad (3-39)$$

Now

$$m_p \frac{d^2x}{dt^2} = (P_B)_{max} A_B$$

Then

$$\frac{d^2x}{dt^2} = \frac{(P_B)_{max} A_B}{m_p}$$

and

$$(T_R)_{max} = \frac{2\pi I_c N (P_B)_{max} A_B}{m_p} \quad (3-40)$$

or

$$(T_R)_{max} = \left[\pi I_c n (P_B)_{max} A_B \right] (R m_p) \quad (3-41)$$

$(T_R)_{max}$ must be less than the torque capacity of the mechanism required to spin the core in order to prevent slip.

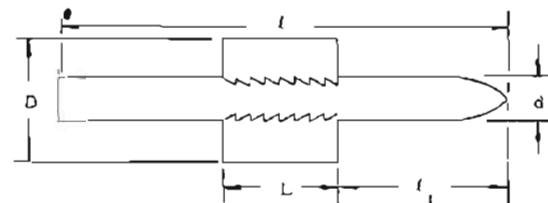
Torsional requirement data are presented in Figs. 3-4 and 3-5.

3-3.8 SPECIAL CUP SABOTS

Several special cup sabot designs have been developed for special purposes such as launching free flight aerodynamic models. One of particular interest is a cup sabot with a hemispherical base [see Figure 1-5(A)]. Equations for the design of this type sabot are not included in this handbook because of the limited applications for which it may be used. Complete and detailed analyses are available in Ref. 13.

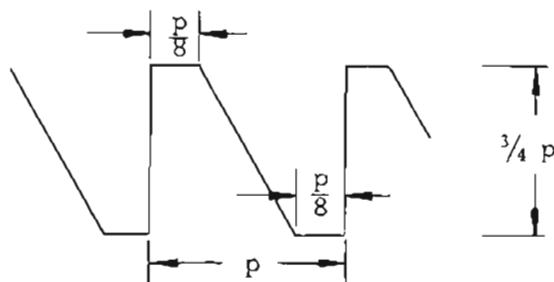
3-4 ELEMENTARY CONSIDERATIONS FOR RING SABOTS

The basic configuration and principal dimensions of a ring sabot are given as follows:



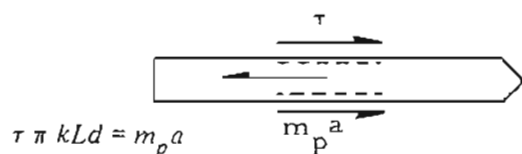
In addition to having to size the sabot (dimension L), it now becomes necessary to decide where on the projectile the sabot shall be located (dimension ℓ_f). It is highly likely that launch dynamic considerations also may play an important role in locating the sabot on the projectile.

The basic failure mode for a ring sabot is shear along the sabot-projectile interface. To ensure a good transfer of shear along this interface, it is conventional to employ a series of buttress-shaped grooves or detents. A typical buttress groove geometry is



where p is the pitch.

The shear stress is determined by summing forces on the projectile in the axial direction, i.e.:



or

$$\tau = \frac{m_p a}{\pi k L d} \quad (3-42)$$

where k is a constant less than one that converts the projected shear area into the effective shear area. If it is noted that the maximum shear stress which must be less than the shear strength of either the sabot or projectile materials corresponds to the maximum acceleration, the following can be written:

$$\tau_{max} = \frac{m_p a_{max}}{\pi k L d} < \tau_{str} \quad (3-43)$$

or

$$L > \frac{1}{\pi k} \left(\frac{m_p a_{max}}{d \tau_{str}} \right) \quad (3-44)$$

and

$$\frac{m_s}{m_p} > \frac{1}{4k} \left(\frac{D \rho_s}{\tau_{str}} \right) \left(\frac{d}{D} \right)^{-1} \left[1 - \left(\frac{d}{D} \right)^2 \right] a_{max} \quad (3-45)$$

3.4.1 BUCKLING OF THE FORWARD PORTION OF THE PROJECTILE

In locating a ring sabot on a projectile, it is important to note the possibility of (1) a buckling of the forward portion of the projectile due to column action, and (2) tensile failure of the aft section of the projectile which is pulled along by the sabot.

Because of the acceleration of the sabot projectile, a body force is generated, part of which serves as a compressive force on the portion of the projectile extending forward of the sabot. The effective weight of this forward section is approximately

$$W_f = \rho_p \frac{\pi}{4} d^2 \ell_f a \quad (3-46)$$

The critical load* for buckling of a fixed free-ended column under load distributed uniformly along its length is

$$(W_f)_{cr} = \frac{\pi^2 E I_E}{(1.122 \ell_f)^2} \quad (3-47)$$

where

I_E = moment of inertia of projectile cross section taken about its central axis

Because the maximum load corresponds to the maximum acceleration condition

*S. Timoshenko, *Theory of Elastic Stability*, Engineering Societies Monograph, McGraw-Hill Book Company, Inc., New York, 1936.

$$(w_f)_{cr} > w_{f_{max}}$$

or

$$\frac{\pi^2 E I_E}{(1.122 \ell_f)^2} > \frac{\pi}{4} d^2 \rho_p \ell_f a_{max}$$

and

$$\ell_f^3 < \frac{4\pi}{(1.122)^2} \frac{E I_E}{d^2 \rho_p a_{max}} \quad (3-48)$$

3-4.2 TENSILE FAILURE IN PROJECTILE AFT SECTION

The forces acting on the aft section of the projectile are (1) the inertial forces, (2) pressure forces, and (3) tensile stresses. Summing these forces requires that

$$(P + \sigma) \frac{\pi}{4} d^2 = \frac{\pi}{4} \rho_p d^2 (\ell - L - \ell_f) a$$

or simplifying and noting that a_{max} ($a = a_{max}$) must be less than σ_y (maximum principal stress theory of failure), requires that

$$\ell_f < \left[\ell - L - \left(\frac{P_{max} - \sigma_y}{\rho_p a_{max}} \right) \right] \quad (3-49)$$

3-5 THE FINITE ELEMENT TECHNIQUE

This paragraph is an introduction to the finite element method of structural analysis. Because of the lengthy and repetitive nature of the calculations involved in the finite element technique, it is most efficiently utilized when programmed for solution on a digital computer. The emphasis of this discussion is on the use of a finite element program, such as the one given in Appendix C, instead of upon the theory of the technique or the mechanics of computer programs. This paragraph thus reflects the attitude of the user instead of the producer. Those persons desiring to pursue the theory in greater detail than presented herein are referred to the many text books and survey articles written on this subject. Refs. 14 and 15 listed at the

end of this chapter are particularly lucid, thorough treatises on the subject.

3-5.1 BACKGROUND

For current purposes, the finite element method is a technique for the stress analysis of solid bodies*. Various geometries, loadings, and types of materials are admissible — depending upon the particular formulation. Limitations are imposed for various reasons. Par. 3-5 discusses generally what can and what cannot be done.

3-5.1.1 GEOMETRY

Analysis is generally restricted to two-dimensional problems; i.e., plane strain (stress), and axisymmetric problems. This is a limitation imposed by current computers. The accurate representation of a body requires a fine subdivision of the body, which generates considerable information to be stored, more than can be economically handled. However, three-dimensional problems have been studied.^{15, 16} This is one of the areas in which one may expect future developments.

3-5.1.2 MATERIALS

Great freedom in material properties is allowed. Materials can be anisotropic, as well as isotropic. Perhaps the most impressive feature concerning materials is the fact that bodies of several materials can be analyzed. In the process of formulating the problem, the type of material in any given portion of the body is specified, and the analysis proceeds without difficulty.

One problem arises with certain materials for which the Poisson ratio approaches 0.5 ($\nu \rightarrow 0.5$), indicating incompressibility in the infinitesimal deformation theory. The difficulty is the fact that the equations become increasingly ill-behaved, due to the

*Actually, the finite element method can be applied far more generally, as will become clear subsequently.

appearance of the term $1-2\nu$ in denominators of the governing equations. This problem has, however, been resolved by use of the so-called "reformulated" approach¹⁷ or by the Fitzgerald modification of Hooke's law (par. 3-2.2). With the reformulated approach, there still is a tendency for stresses to oscillate in problems with high restraint and Poisson's ratio near 0.5.

Finite element analysis generally treats linear elastic materials. Viscoelastic materials have been studied¹⁸, however. Large deformations and plasticity also have been studied. Both these areas require further study to put them on a dependable level. Nonlinear behavior can be handled quite easily, and programs (including the one in Appendix C) are equipped to handle bilinear behavior such as that displayed by "Lexan" (see par. 3-2.3.1).

3-5.1.3 BOUNDARY CONDITIONS

Finite element solutions allow for the boundary conditions which are most common. Typically, the analyst can prescribe either concentrated forces or displacements in either of the coordinate directions at boundary points of the structure. Provision is generally made for application of shears or pressure loads on the boundary by specification of the distributed magnitude, the program internally converting these to concentrated forces as required. Provision is also made, in general, for internal generation of body forces such as centrifugal force or accelerations.

3-5.1.4 DYNAMIC PROBLEM

The majority of finite element work has been devoted to solution of quasi-static problems, i.e., problems in which loads are applied slowly enough that stress waves are not created in the body. The technique has, however, been used to study dynamic phenomena in both elasticity and viscoelasticity media.^{19, 20}

3-5.1.5 MISCELLANEOUS APPLICATIONS

It is worth noting that transient heat conduction problems have been studied by finite element techniques⁸.

Also to be pointed out is the fact that finite element analysis has been applied to plates and shells, which, although they are solid, are of a special geometry. Programs for analysis of specific bodies such as rocket motors frequently include shell elements to represent the motor case²².

3-5.1.6 RELIABILITY AND ACCURACY

As with all approximate techniques, the results obtained are subject to some uncertainty. The reasons for this will become clear in the paragraphs which follow. The reader is cautioned at this point that the finite element method is accurate and reliable in direct proportion to the intelligent use of the method and interpretation of the results. In particular, the user must be careful in the posing of the problem to be solved, and in the modeling of the problem for computer analysis. Properly used and interpreted, the finite element method is as satisfactory an analysis tool as any other and offers a versatility which is recompense for care in use.

3-5.1.7 SUMMARY

Generally, it can be said that the finite element technique is presently in common use for two-dimensional, quasi-static, elastic analysis of solid bodies. However, extension to other type problems, some of which are mentioned previously, is possible.

3-5.2 THEORY OF THE FINITE ELEMENT METHOD

This paragraph outlines the theory upon which the finite element method is based. For a particularly lucid discussion of this theory, the reader is referred to Ref. 14, and for a detailed treatise to Ref. 22. The current development will be limited to the compressible, elastic stress problem for axisymmetric

solids. This will give an idea of the theory without unnecessary complexity.

3-5.2.1 VARIATIONAL PRINCIPLES

Finite element solutions normally begin with the statement of a variational principle. A functional is defined which has as its arguments the relevant physical variables of the problem. It is then shown that the particular functions (among certain admissible types) which minimize the functional are in fact the ones that satisfy the governing differential equations of the problem. For example, the Theorem of Minimum Potential Energy^{2,3} states that the potential energy assumes an absolute minimum for those displacements satisfying the equilibrium equation, provided that classes of admissible functions are limited to those satisfying the boundary conditions.

It is obvious, then, that we could (1) guess an approximate solution to a problem, (2) calculate the potential energy, and (3) compare with another approximate solution. Of the two, we choose the one with the minimum energy as the better. We then search for another approximation to compare. By such a process, we eventually will reach the solution, if it is possible to reach a solution. A more systematic process, akin to the Rayleigh-Ritz method*, is to assume an approximate solution with unknown parameters. We then determine the unknown parameters in such a manner as to minimize the functional. Then, we know that the solution we have is the best of the type with which we started. The finite element method is essentially such a process.

3-5.2.2 FINITE ELEMENTS

The origin of the name of the "finite element" arises from the fact that, to perform the process of minimization previously discussed, the body being analyzed is divided into small subregions, over which expressions

for the displacement are assumed. For example, suppose we wish to analyze the body shown in Fig. 3-6. This body which is axisymmetric, is subjected to axisymmetric loads, e.g., axial acceleration.

We could suppose that this body may be represented by a collection of rings of triangular cross section as in Fig. 3-7.

This is, in fact, the type element used for such problems. However, the triangles usually are combined into quadrilaterals within the program, and we need only concern ourselves with the quadrilateral. Thus, we might break up the body into the subregions such as shown for simplicity only in Fig. 3-8. The right hand section of the body is shown subdivided.

In the axisymmetric case, these elements are each actually rings. If this were a plane problem, they would be prisms with axis perpendicular to the plane of the paper.

The displacement field is now assumed in some form for each element. This introduces several unknown parameters. These parameters can be solved for in terms of the displacements at particular points in the elements, usually the corners which are known as the nodal points. Hence, we have a set of subregions, for each of which we have an assumed displacement shape depending upon the unknown nodal point displacements. The functional for each region now can be calculated and minimized with respect to the unknown displacements. This leads to a system of algebraic equations in the nodal point displacements. Solution of these equations yields the displacement field which minimizes the functional and from which the stresses can be calculated.

In actual practice, this procedure is not carried out as easily as it is described. The handling of the large amount of data and solution of the resulting system of equations are problems which must be solved in an efficient manner. However, this capability has

*For this reason the finite element method is sometimes called the "extended Ritz method".

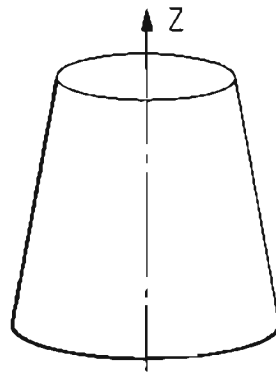


Figure 3-6. Representative Axisymmetric Solid

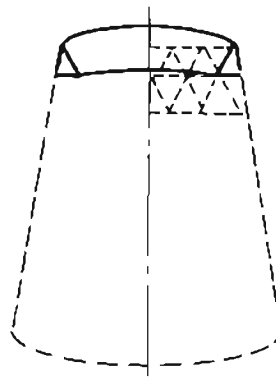


Figure 3-7. Typical Idealization of Axisymmetric Solid

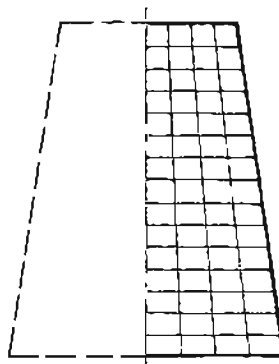


Figure 3-8. Quadrilateral Idealization of Solid

been built into the computer program and as such is not the user's problem.

One point which is significant to a user is the form of the displacement assumption. If the function is linear in each element, then the displacements along the edges of each element will coincide. This appears desirable, and is frequently used. Higher order assumptions will lead to different results. The linear assumption also lends itself to approximation of arbitrary fields as the elements become smaller. The point to be noted is that in areas of bodies where the actual displacement field is linear, a linear approximation is adequate with large elements. In areas where the displacement is more complex, smaller elements will be required to approximate the actual displacements. In addition, errors in the displacement approximation produce even larger errors in stress calculations because stress is related to the derivatives of displacements.

3-5.2.3 SUMMARY

The finite element method requires the approximation of a body by subregions. Displacements are approximated in each element by a form introducing the nodal point displacements as unknown factors. A functional is minimized over each element using these approximations, which yields algebraic equations for the nodal point displacements. The solution of these equations is the displacement field, and stresses are derived therefrom. In areas where displacements are progressively more nonlinear, the elements must be progressively smaller.

3-5.3 APPLICATION OF THE FINITE ELEMENT METHOD

This paragraph and par. 3-5.4 will show in detail the steps involved in using a finite element program and will include some numerical examples. This is undoubtedly the simplest way to discuss the practical use of the finite element method. Because the actual use of a program is dependent on the pro-

gram, one must sacrifice some generality by reference to a particular program. However, we shall assume the available program similar to the one given in Appendix C. Specific details may change from program to program but the general ideas remain the same.

3-5.3.1 INPUT DATA

Broadly speaking, the data that must be input to a computer program can be separated out into several categories: control information, nodal point data, element data, material properties, and load data. These categories are not unique, and some programs may combine one or more into a single category. For example, it is quite natural to lump the last three together because for any element we must associate the material of which it consists and the loads to which it is subjected. We shall discuss the type of data in each category as though they were separate, and indicate the conventions wherever possible.

(1) Control information:

- (a) Title: usually the first item of information required is the title, etc., or any identification the user desires
- (b) Number of nodal points
- (c) Number of rows of nodal points
- (d) Number of materials
- (e) Axisymmetric or plane problem
- (f) Number of cards of same type to be read.

Data of this type refer to the problem in general and/or to the process of input to the computer. Load information that is relevant to the whole problem also may be input to this category. In this case, either Item (1) (b) or (1) (c) information will be required, not both — the program details determine which. Also, Item (1) (e) will not be needed for a

program that is specifically either plane or axisymmetric.

(2) Nodal point data:

- (a) Nodal point number – either a single number or two (I, J) coordinates if the nodal point array is associated with a matrix
- (b) Coordinates of the nodal point
- (c) Indication of whether forces or displacements, or neither, are specified in each coordinate direction
- (d) Specified forces and/or displacement, if any
- (e) Any other relevant information, e.g., temperature, if it is associated with nodal points, or special types of control information.

(3) Element data:

- (a) Element number
- (b) Nodal points to which element is connected
- (c) Material identification.

All this information may be absorbed into other areas. The element number may be associated with a particular nodal point to which the element is connected; this eliminates Item (3)(a) and Item (3)(b); Item (3)(c) can be handled by a request to read the data while reading nodal point information.

(4) Material properties:

- (a) Mechanical properties – modulus, etc.
- (b) Thermal properties – expansion coefficient
- (c) Physical properties – density, etc.

- (d) Identification.

(5) Load data:

- (a) Element to which load is applied
- (b) Magnitude of load – pressure, temperature change, etc.

These data and material properties may be associated with element data, and hence to specific nodal points under some sort of nodal point-element correspondence. It is not necessary to do so, however.

(6) Final comments on the input data:

In general, it is necessary to define the position of every nodal point, the elements connected to that nodal point, the material properties for each element, as well as nodal point and element loads. Because a given problem might involve close to 1000 nodal points, with somewhat fewer elements, the amount of data would be prohibitive if each nodal point and element were treated separately. This is not done, of course. A program will incorporate some sort of self-generating feature. For example, if two nodal points are separated by several for which no data are specified, the program might generate the required intermediate points along a straight line joining the given points, with uniform spacing. Similarly, the elements omitted would be generated.

By this self-generating process, the number of input data are considerably reduced. The only nodal points and elements that require specification are those along the boundary of the object, as well as interior points for which changes from previous data occur. For example, when two different materials are adjacent, the transition from the first to the second must be specified.

3-5.3.2 OUTPUT DATA

At the conclusion of an analysis, a great deal of information has been created –

stresses, displacements, strains, etc. All this information is output. At this point, there is no convenient way to reduce the volume unless the analyst knows that only certain results are needed. In general, the analysis will yield hundreds of pages of results. Provision can be made, however, to write the results on a tape and then to have this information presented graphically in terms of stress and strain contours, etc.

The user must be cautioned against placing total confidence in the results of the analysis. The finite element method is a useful tool, but still is not a panacea for the analyst. Results will be dependent on the ability of the analyst to capture the essential features of the problem by proper layout of the nodal points and elements describing the object of concern. There is no substitute for intelligent engineering consideration of the problem.

3-5.3.3 SUMMARY

Par. 3-5.3 discussed the general type of input to a finite element program and the resulting output. While each specific program incorporates the information differently, the same items are needed in any case. One must, however, exercise a degree of judgment in the use of the results.

3-5.4 EXAMPLE PROBLEMS

This paragraph makes more specific the comments of par. 3-5.3 by presenting a group of examples of finite element analyses, including the whole process of solving the problem. For additional examples, the reader is referred to Refs. 14, 18, 21, 22, and 24.

The program used to solve the examples is the Rohm and Haas AMG032A, suitably modified for use on a UNIVAC 1108 computer. The program in Appendix C is due to Wilson and is similar in operation to the Rohm and Haas program used for these examples.

3-5.4.1 UNIAXIAL COMPRESSION OF A RIGHT CIRCULAR CYLINDER

The first example is the simplest problem that one can formulate — uniaxial compression of a circular cylindrical sample. The setup of the problem is shown in Fig. 3-9. Fig. 3-9(A) shows the physical problem with the necessary defining quantities. As shown in Fig. 3-9(B), it is possible to reduce the problem to one of smaller proportions by taking into account symmetry. This is in a form that can be analyzed by an axisymmetric program, i.e., a body of revolution loaded by axisymmetric forces. We note that points on the axis of the body can only deform in the z -direction, while points on the r -axis can only move in the r -direction, this from the symmetry of the problem. Thus, we have established displacement boundary conditions along the z - and r -axes. On the top surface, the pressure is known, while the side is free. The grid is added and nodal points defined in Fig. 3-9(C). The grid is the simple, obvious one — an array of squares 0.5 in. \times 0.5 in. covering the section of the cylinder, a total of 50 elements and 66 nodal points. The nodal points now have (I, J) coordinates associated with them as shown*. The displacement conditions are indicated by rollers. The nodal points on the two axes can roll along those axes, except that the (1, 1) nodal point cannot move at all.

This figure defines the problem in enough detail to generate the input data, which is shown in Fig. 3-10. For convenience in discussing the data, we have numbered the columns in groups of 10, 1-9 and blank.

The first line of data is simply a title in the required format.

The second line of data gives the number of nodal point cards to be read (34), and number of rows (11).

*Note that I = column number, J = row number.

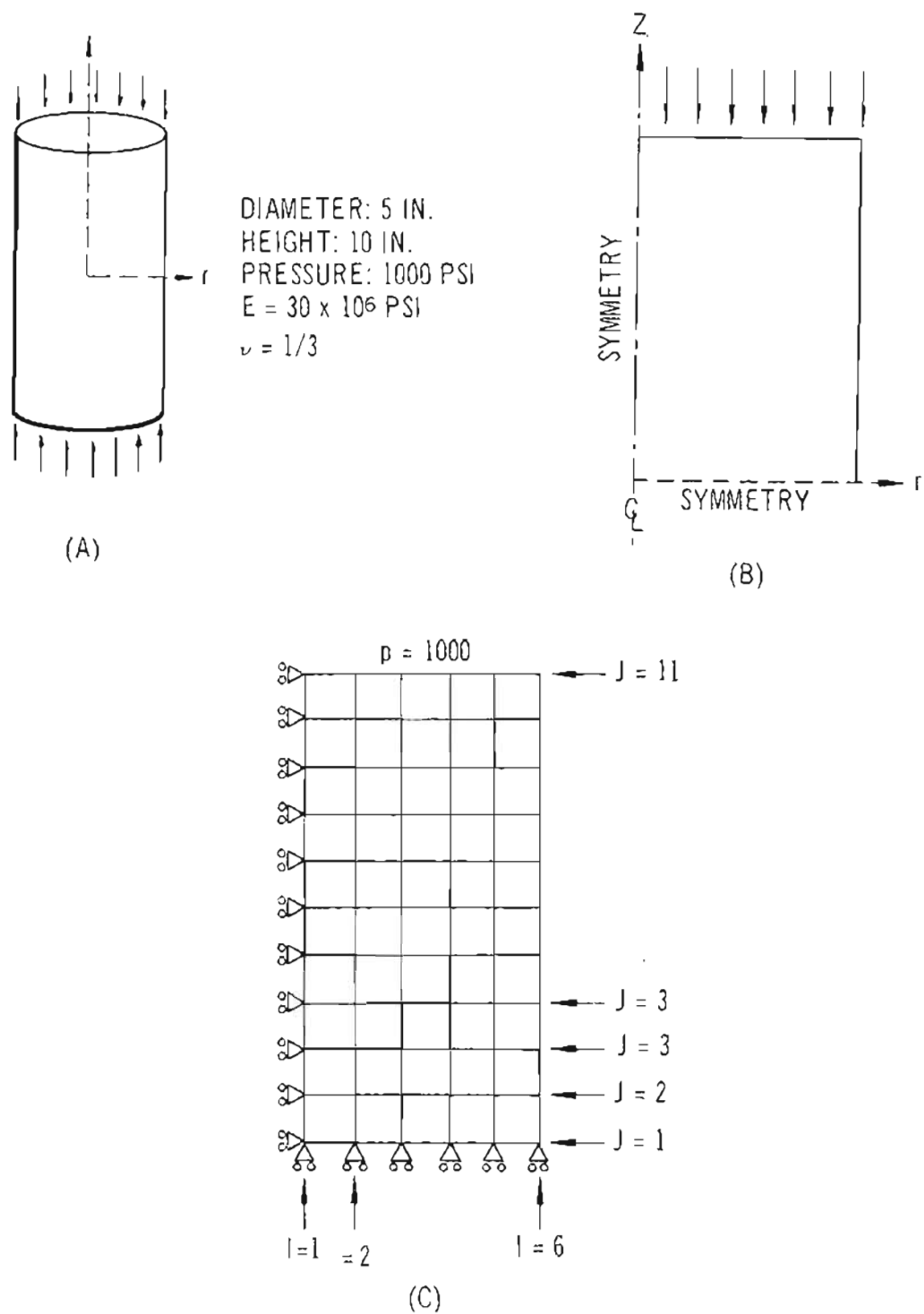


Figure 3-9. Setup of Simple Compression Problem

123456789 123456789 123456789 123456789 123456789 123456789 123456789 123456789

AMC0142A SIMPLE COMPRESSION

[illegible]

Figure 3-10. Input for Simple Compression Problem

The next 34 cards are nodal point cards, followed by 12 cards giving element properties and loads, and finally a card ending the data.

In the system used in the program here, the number of an element is associated with the nodal point of smallest (I, J) connected to it. As nodal points are input, we then specify whether an element is to be associated or not, and what to do about the element properties. This is probably most easily seen by reference to the data. As the computer reads the nodal point cards, the following data is found: I, J , element type, four boundary condition codes, r -coordinate, z -coordinate, four loads and/or displacements. For example, Card 1 reads as follows:

Column	Data	Meaning
5	1	$J = 1$
10	1	$J = 1$
15	1	read element data
16	1	u_r specified
17	1	u_z specified
18	0	no moment or rotation specified
19	0	no slope specified
21-30	0.0	r -coordinate
31-40	0.0	z -coordinate
41-50	0.0	u_r
51-60	0.0	u_z
61-70	0.0	moment/rotation
71-80	0.0	slope

If the number in Column 15 were 0, the program assumes the same data as for the previous element; if it were 5, no element is associated with this point; 2, 3, and 4 also have specific meanings. If the number in Columns 16-18 is zero, no data is specified; if 1, displacement/rotation data; if 2, force/moment data. Column 19 has a 1 if displacement is along a slope, 0 otherwise. Column 20 is blank. The remaining columns, by 10's, contain r, z, u_r, u_z , moment of rotation, and displacement slope. If the data in a given field are zero, it may be left blank.

Thus, the first six cards refer to nodal points (1, 1) to (6, 1), for all of which the z -displacement is zero, the r -displacement specified (as zero) for only (1, 1). Each nodal point has an element associated with it, except (6, 1). The element data is read for (1, 1), and the same for the rest. No slope or moment is specified. Coordinates are given and applied forces or displacements are zero. Note that all the nodal points in Row 1 are specified since it is part of the boundary.

For nodal point (1, 1), element data is to be read, and the same data hold until nodal point (1, 10) because only 1 in Column 15 requests data. The first element card is 27, on which is read, by 10's, the following: E ; ν ; thermal load, $\int \alpha dT$; radial body force; axial body force; pressure; shear; and a number to indicate where the pressure and/or shear acts. Card 28 is also read, and indicates what information is new by a 1 in the appropriate column. For all the elements up to (1, 10), $E = 30 \times 10^6$ psi, $\nu = 1/3$.

Note that all the boundary nodal points are entered as data; and on the left, an element is entered with each nodal point.

Starting with (1, 10), the lower left corner of the left element, we must indicate the pressure load on the top of this element. Thus, we request element data to be read as Cards 29 and 30, where $p = 1000.0$ psi and a 3 indicates the pressure and face on which it acts (according to a standard scheme). Since we don't change E or ν , these values carry on. For element (2, 10) we again read the pressure, since the program does not carry on the pressure from element to element. This process continues to nodal (6, 10), with which no element is associated.

Nodal points (1, 11) through (6, 11) finish the boundary of the regions. No element is associated with these, and only (1, 11) has a specified force or displacement ($u_r = 0$).

While the previous description is somewhat tedious, it gives a detailed illustration of data requirements, both in kind and arrangement.

Output for this problem is shown in Fig. 3-11.

Not all the output is shown; it is too voluminous. It consists of the following:

- (1) Boundary condition information for verifying the boundary conditions
- (2) Coordinates of all nodal points — includes all the interior points for which no coordinates were specified
- (3) Displacements of all nodal points
- (4) Stresses and strains in each element — radial, hoop, axial, and shear stress and strain; and maximum and minimum stresses and strains

Only data for elements (1, 1) through (4, 4) are shown. There is no need to show more, as the values are the same for each row, changing only in r —a phenomenon we should have anticipated, due to symmetry. (We could have saved considerable labor by only using one row of elements). Notice that $\sigma_z = -1000$ psi, $\sigma_r \approx 0$, $\sigma_\theta \approx 0$, as is correct. Also $\epsilon_z = \sigma_z/E = 1/3 \times 10^{-4}$; $\epsilon_r = \epsilon_\theta = -\nu\epsilon_z = 0.111 \times 10^{-4}$, as is correct. In this very simple problem, the displacement field is linear, with consequent good results.

3-5.4.2 THERMAL EXPANSION OF A RIGHT CIRCULAR CYLINDER

This example uses the same shape as Example 1, a circular cylinder, but the loading and boundary conditions are different. In this example we subject the cylinder to a temperature rise of 100°F so that $\int \alpha dT = 6.5 \times 10^{-4}$, and restrain the expansion which would normally occur. This requires removal of the input cards specifying the applied pressure, and addition of a 1 to Column 17 of each card for Row 11 to indicate that $u_r = 0$ for these points. Note that both the nodal point cards for the interior nodes of Row 10, and the material cards corresponding to those nodal points are removed. On the first mate-

rial card the thermal load is then added. The input is shown in Fig. 3-12. The results are shown in Fig. 3-13 in the form of the output for elements (1, 1) — (4, 4). Again the displacement field is linear, and the resulting stresses are exactly correct.

3-5.4.3 CENTRIFUGAL LOADING OF A RIGHT CIRCULAR CYLINDER

Example 3 uses the same data as Example 2, except that the thermal load is replaced by a radial body force, $r\omega^2 = 1000$. This gives the stresses set up by rotation with angular velocity ω . The results for this case are summarized in Fig. 3-14. The stresses σ_r , σ_θ , σ_z , and displacement u_r are shown. The exact solutions are given as solid lines and the results from the finite element program as points. Again, the agreement is excellent.

3-5.4.4 INTERNAL PRESSURIZATION AND ROTATION OF A HOLLOW CYLINDER

In the next two examples the geometry is changed to a hollow cylinder. The inner radius is 0.5 in. and the outer radius 3.0 in. so that the wall thickness is 2.5 in., as was the radius of the original cylinder. In both examples, the longitudinal deformation is restrained, creating a problem in plane strain. For Example 4, an internal pressure of 1000 psi is applied; and for Example 5, radial body force is applied, with $r\omega^2 = 1000$. The results of the analyses are shown in Figs. 3-15 and 3-16.

3-5.4.5 INTERNAL PRESSURIZATION OF A COMPOSITE CYLINDER

To illustrate the ability of the program to handle problems with multiple materials, consider the problem of a composite cylinder subjected to internal pressure. The loading is again an internal pressure of 1000 psi magnitude. The cylinder is now composed of two materials: an inner portion ($r = 0.5$ in. to $r = 1.5$ in.) of copper, and an outer portion ($r = 1.5$ in. to $r = 3.0$ in.) of steel. The result of

I	J/ ANGLE	COORDINATES		RADIAL R	HOOP THETA	S T R E S S E S /		S T R A I N S		MAXIMUM	MINIMUM	MAX SHEAR
		R	Z			AXIAL Z	SHEAR R-Z					
1	1 .00	.250	.250	7.9297-05 1.1111-05	7.9297-05 1.1111-05	-1.0000+03 -3.3333-05	6.2995-06 5.5996-13	6.9065-05 1.1111-05	-1.0000+03 -3.3333-05	5.0000+02 4.4444-05		
2	1 .00	.750	.249	5.8833-05 1.1111-05	8.4412-05 1.1111-05	-1.0000+03 -3.3333-05	3.2093-05 2.8527-12	4.8601-05 1.1111-05	-1.0000+03 -3.3333-05	5.0000+02 4.4444-05		
3	1 .00	1.250	.249	3.3253-05 1.1111-05	7.1623-05 1.1111-05	-1.0000+03 -3.3333-05	3.3352-05 2.9646-12	2.8137-05 1.1111-05	-1.0000+03 -3.3333-05	5.0000+02 4.4444-05		
4	1 .00	1.750	.249	-5.1159-06 1.1111-05	8.6970-05 1.1111-05	-1.0000+03 -3.3333-05	3.8959-05 3.4630-12	-1.2790-05 1.1111-05	-1.0000+03 -3.3333-05	5.0000+02 4.4444-05		
5	1 .00	2.250	.249	-2.8137-05 1.1111-05	2.0464-05 1.1111-05	-1.0000+03 -3.3333-05	3.6304-05 3.2271-12	-3.3253-05 1.1111-05	-1.0000+03 -3.3333-05	5.0000+02 4.4444-05		
1	2 .00	.250	.750	1.0743-04 1.1111-05	9.4644-05 1.1111-05	-1.0000+03 -3.3333-05	1.9691-05 1.7503-12	9.9760-05 1.1111-05	-1.0000+03 -3.3333-05	5.0000+02 4.4444-05		
2	2 .00	.750	.749	7.9297-05 1.1111-05	8.9528-05 1.1111-05	-1.0000+03 -3.3333-05	7.4894-05 6.6572-12	7.4181-05 1.1111-05	-1.0000+03 -3.3333-05	5.0000+02 4.4444-05		
3	2 .00	1.250	.749	1.2790-05 1.1111-05	6.9065-05 1.1111-05	-1.0000+03 -3.3333-05	1.0180-04 9.0488-12	2.5580-06 1.1111-05	-1.0000+03 -3.3333-05	5.0000+02 4.4444-05		
4	2 .00	1.749	.748	-1.5348-05 1.1111-05	7.1623-05 1.1111-05	-1.0000+03 -3.3333-05	8.3951-05 7.4624-12	-2.8137-05 1.1111-05	-1.0000+03 -3.3333-05	5.0000+02 4.4444-05		
5	2 .00	2.249	.749	-3.3253-05 1.1111-05	-5.1159-06 1.1111-05	-1.0000+03 -3.3333-05	4.0564-05 3.6057-12	-4.0927-05 1.1111-05	-1.0000+03 -3.3333-05	5.0000+02 4.4444-05		
1	3 .00	.250	1.250	8.9528-05 1.1111-05	8.4412-05 1.1111-05	-1.0000+03 -3.3333-05	2.8354-05 2.5203-12	8.1855-05 1.1111-05	-1.0000+03 -3.3333-05	5.0000+02 4.4444-05		
2	3 .00	.750	1.249	5.3717-05 1.1111-05	7.1623-05 1.1111-05	-1.0000+03 -3.3333-05	1.0725-04 9.5332-12	4.8601-05 1.1111-05	-1.0000+03 -3.3333-05	5.0000+02 4.4444-05		
3	3 .00	1.249	1.248	-5.1159-06 1.1111-05	7.6739-05 1.1111-05	-1.0000+03 -3.3333-05	1.7516-04 1.5570-11	-1.2790-05 1.1111-05	-1.0000+03 -3.3333-05	5.0000+02 4.4444-05		
4	3 .00	1.749	1.248	-7.6739-06 1.1111-05	7.1623-05 1.1111-05	-1.0000+03 -3.3333-05	1.0758-04 9.5627-12	-1.7906-05 1.1111-05	-1.0000+03 -3.3333-05	5.0000+02 4.4444-05		
5	3 .00	2.250	1.249	3.5811-05 1.1111-05	7.1623-05 1.1111-05	-1.0000+03 -3.3333-05	4.2679-05 3.7937-12	2.8137-05 1.1111-05	-1.0000+03 -3.3333-05	5.0000+02 4.4444-05		
1	4 .00	.250	1.750	8.6970-05 1.1111-05	7.9297-05 1.1111-05	-1.0000+03 -3.3333-05	5.5196-05 4.9063-12	8.1855-05 1.1111-05	-1.0000+03 -3.3333-05	5.0000+02 4.4444-05		
2	4 .00	.750	1.749	2.0464-05 1.1111-05	5.8833-05 1.1111-05	-1.0000+03 -3.3333-05	1.6026-04 1.4246-11	1.0232-05 1.1111-05	-1.0000+03 -3.3333-05	5.0000+02 4.4444-05		
3	4 .00	1.249	1.748	-5.6275-05 1.1111-05	1.7906-05 1.1111-05	-1.0000+03 -3.3333-05	2.5679-04 2.2826-11	-6.9065-05 1.1111-05	-1.0000+03 -3.3333-05	5.0000+02 4.4444-05		
4	4 .00	1.749	1.748	-2.0464-05 1.1111-05	6.9065-05 1.1111-05	-1.0000+03 -3.3333-05	1.0389-04 3.0695-05	-3.0695-05 1.1111-05	-1.0000+03 -3.3333-05	5.0000+02 4.4444-05		

Figure 3-11. Output for Simple Compression Problem

```

123456789 123456789 123456789 123456789 123456789 123456789 123456789 123456789
50 11
AMC012A 851241241 111111111
1 1 11100 0.0 0.0
2 1 00100 0.5 0.0
3 1 00100 1.0 0.0
4 1 00100 1.5 0.0
5 1 00100 2.0 0.0
6 1 50100 2.5 0.0
1 2 01000 0.0 0.5
2 2 50000 2.5 0.5
1 3 01000 0.0 1.0
6 3 50000 2.5 1.0
1 4 01000 0.0 1.5
6 4 50000 2.5 1.5
1 5 01000 0.0 2.0
6 5 50000 2.5 2.0
1 6 01000 0.0 2.5
6 6 50000 2.5 2.5
1 7 01000 0.0 3.0
6 7 50000 2.5 3.0
1 8 01000 0.0 3.5
6 8 50000 2.5 3.5
1 9 01000 0.0 4.0
6 9 50000 2.5 4.0
1 10 01000 0.0 4.5
6 10 50000 2.5 4.5
1 11 51100 0.0 5.0
2 11 50100 0.5 5.0
3 11 50100 1.0 5.0
4 11 50100 1.5 5.0
5 11 50100 2.0 5.0
6 11 50100 2.5 5.0
50000000.00.33333333.00055 0.0
11111111
END OF DATA
0.0 0.0 0.0 0.0 0.0

```

Figure 3-12. Input for Restrained Thermal Expansion Problem

ROHM AND HAAS PROGRAM- INCOMPRESSIBLE						DATE 170768 PAGE 19				
I J ANGLE	COORDINATES		STRESSSES / STRAINS			SHEAR		MAXIMUM	MINIMUM	MAX SHEAR
	R	Z	RADIAL R	HOOP THETA	AXIAL Z	R-Z				
1 1 .00	.250	.250	-1.3097-03 8.6667-04	-1.6371-03 8.6667-04	-1.9500+04 -1.0674-10	3.5384-04 3.1453-11	-1.4734-03 8.6667-04	-1.9500+04 -9.8225-11	9.7500+03 8.6667-04	
2 1 .00	.750	.250	-2.6193-03 8.6667-04	-2.7831-03 8.6667-04	-1.9500+04 -1.5507-10	5.3481-04 4.7539-11	-2.7831-03 8.6667-04	-1.9500+04 -1.4916-10	9.7500+03 8.6667-04	
3 1 .00	1.250	.250	-2.7831-03 8.6667-04	-4.4201-03 8.6667-04	-1.9500+04 -1.8230-10	3.8674-04 3.4377-11	-2.9468-03 8.6667-04	-1.9500+04 -1.7826-10	9.7500+03 8.6667-04	
4 1 .00	1.750	.250	-2.9468-03 8.6667-04	-4.0927-03 8.6667-04	-1.9500+04 -1.6224-10	1.6628-04 1.4780-11	-3.1105-03 8.6667-04	-1.9500+04 -1.5643-10	9.7500+03 8.6667-04	
5 1 .00	2.250	.250	-1.8008-03 8.6667-04	-3.1105-03 8.6667-04	-1.9500+04 -8.3680-11	1.3724-03 1.2199-10	-1.9645-03 8.6667-04	-1.9500+04 -7.6398-11	9.7500+03 8.6667-04	
1 2 -.00	.250	.750	1.6371-04 8.6667-04	-1.6371-04 8.6667-04	-1.9500+04 -1.3930-10	-3.2961-04 -2.9299-11	0.0000 8.6667-04	-1.9500+04 -1.3461-10	9.7500+03 8.6667-04	
2 2 -.00	.750	.750	-2.1282-03 8.6667-04	-1.3097-03 8.6667-04	-1.9500+04 -9.9746-11	-8.4509-04 -7.5119-11	-2.2919-03 8.6667-04	-1.9500+04 -9.0949-11	9.7500+03 8.6667-04	
3 2 -.00	1.250	.750	-3.2742-03 8.6667-04	-4.0927-03 8.6667-04	-1.9500+04 -7.6725-11	-4.0884-04 -3.6341-11	-3.4379-03 8.6667-04	-1.9500+04 -6.9122-11	9.7500+03 8.6667-04	
4 2 -.00	1.750	.750	-4.4201-03 8.6667-04	-4.2564-03 8.6667-04	-1.9500+04 -5.4282-11	-1.0157-03 -9.0283-11	-4.5839-03 8.6667-04	-1.9500+04 -4.7294-11	9.7500+03 8.6667-04	
5 2 -.00	2.250	.750	-2.7831-03 8.6667-04	-4.9113-03 8.6667-04	-1.9500+04 -3.3305-11	-1.2371-03 -1.0997-10	-2.9468-03 8.6667-04	-1.9500+04 -2.5466-11	9.7500+03 8.6667-04	
1 3 -.00	.250	1.250	-4.9113-04 8.6667-04	-8.1855-04 8.6667-04	-1.9500+04 -4.4774-11	-3.6250-04 -3.2222-11	-6.5484-04 8.6667-04	-1.9500+04 -4.0018-11	9.7500+03 8.6667-04	
2 3 -.00	.750	1.250	-2.4556-03 8.6667-04	-2.1282-03 8.6667-04	-1.9500+04 -3.4753-11	-9.5028-04 -8.4469-11	-2.6193-03 8.6667-04	-1.9500+04 -2.5466-11	9.7500+03 8.6667-04	
3 3 -.00	1.250	1.250	-3.6016-03 8.6667-04	-4.5839-03 8.6667-04	-1.9500+04 -2.0663-11	-8.6841-04 -7.7192-11	-3.7653-03 8.6667-04	-1.9500+04 -1.0914-11	9.7500+03 8.6667-04	
4 3 .00	1.750	1.250	-4.7476-03 8.6667-04	-4.4201-03 8.6667-04	-1.9500+04 -1.4734-11	2.5420-04 2.2595-11	-4.9113-03 8.6667-04	-1.9500+04 -1.0914-11	9.7500+03 8.6667-04	
5 3 .00	2.250	1.250	-3.4379-03 8.6667-04	-5.4024-03 8.6667-04	-1.9500+04 -3.2465-11	8.0371-04 7.1441-11	-3.4379-03 8.6667-04	-1.9500+04 -2.9104-11	9.7500+03 8.6667-04	
1 4 -.00	.250	1.750	-1.6371-03 8.6667-04	-1.9645-03 8.6667-04	-1.9500+04 1.3895-11	-1.3184-04 -1.1719-11	-1.8008-03 8.6667-04	-1.9500+04 1.0914-11	9.7500+03 8.6667-04	
2 4 -.00	.750	1.750	-3.4379-03 8.6667-04	-3.1105-03 8.6667-04	-1.9500+04 2.2268-11	-1.9639-04 -1.7457-11	-3.6016-03 8.6667-04	-1.9500+04 2.5466-11	9.7500+03 8.6667-04	
3 4 -.00	1.250	1.750	-4.4201-03 8.6667-04	-5.4024-03 8.6667-04	-1.9500+04 2.3319-11	-2.2414-04 -1.9923-11	-4.5839-03 8.6667-04	-1.9500+04 2.5466-11	9.7500+03 8.6667-04	
4 4 .00	1.750	1.750	-5.4024-03	-5.4024-03	-1.9500+04	-2.6645-04	-5.5661-03	-1.9500+04	9.7500+03	

Figure 3-13. Output for Restrained Thermal Expansion Problem

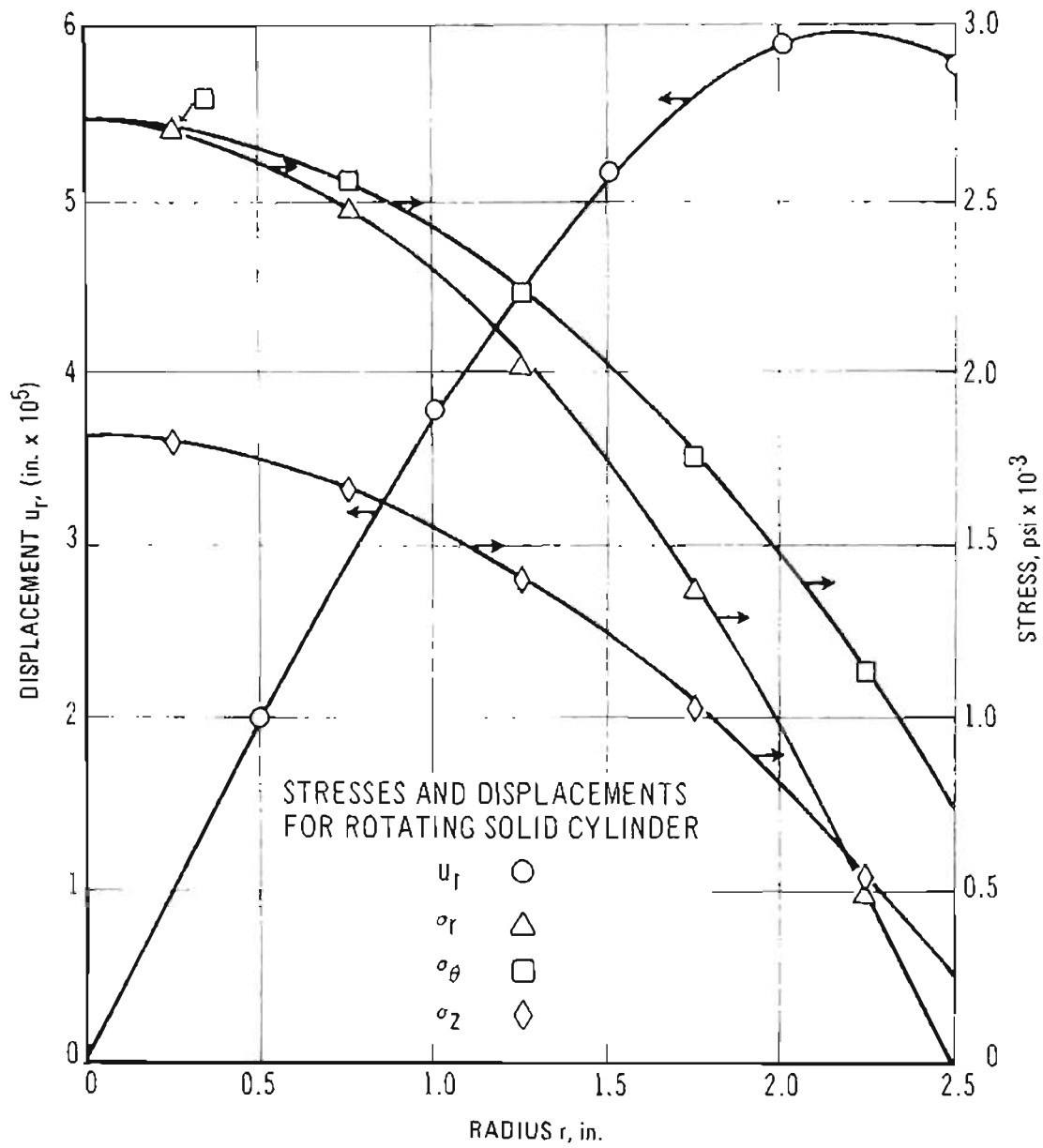


Figure 3-14. Stresses and Displacements for Rotating Solid Cylinder

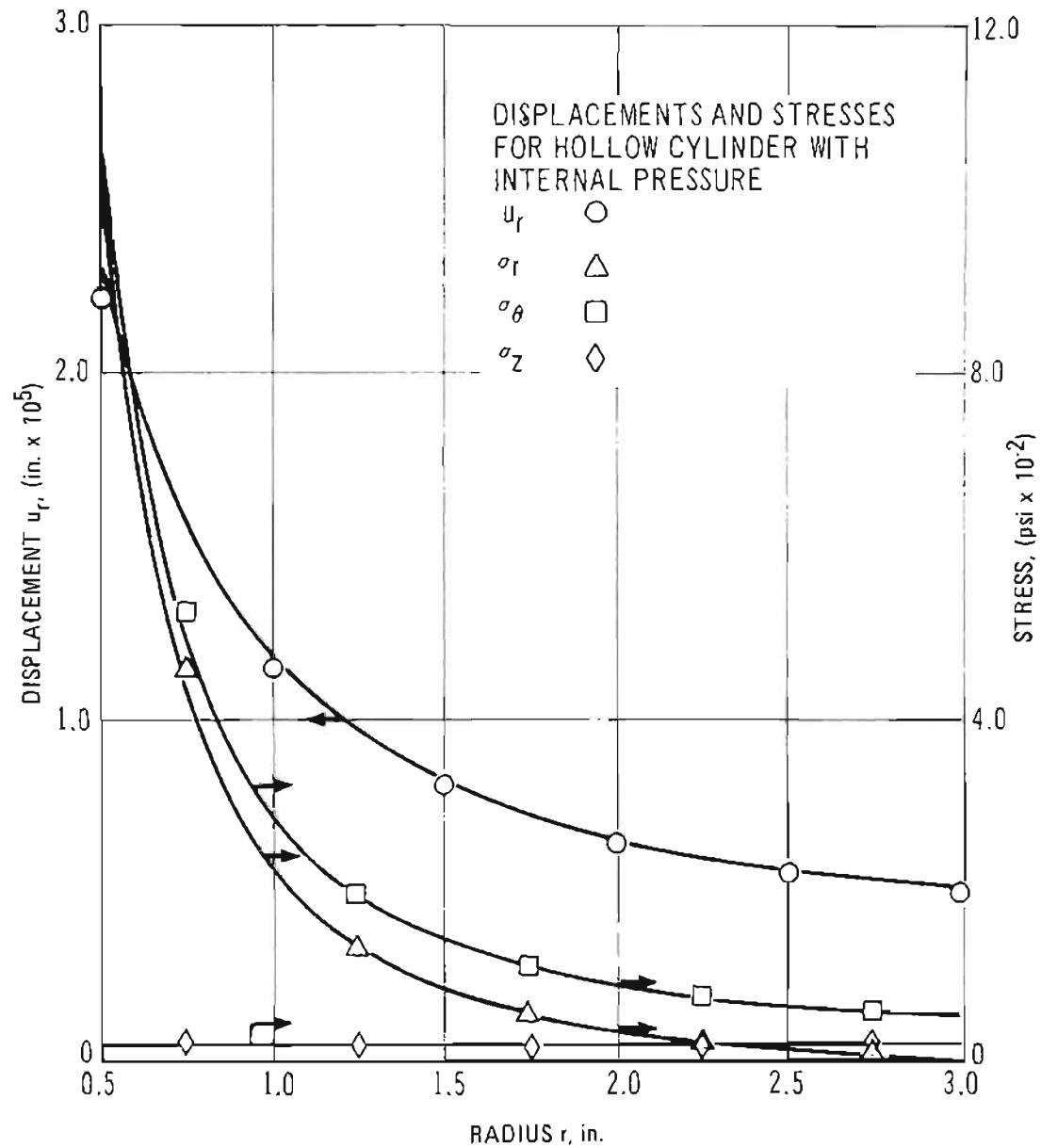


Figure 3-15. Displacements and Stresses for Hollow Cylinder With Internal Pressure

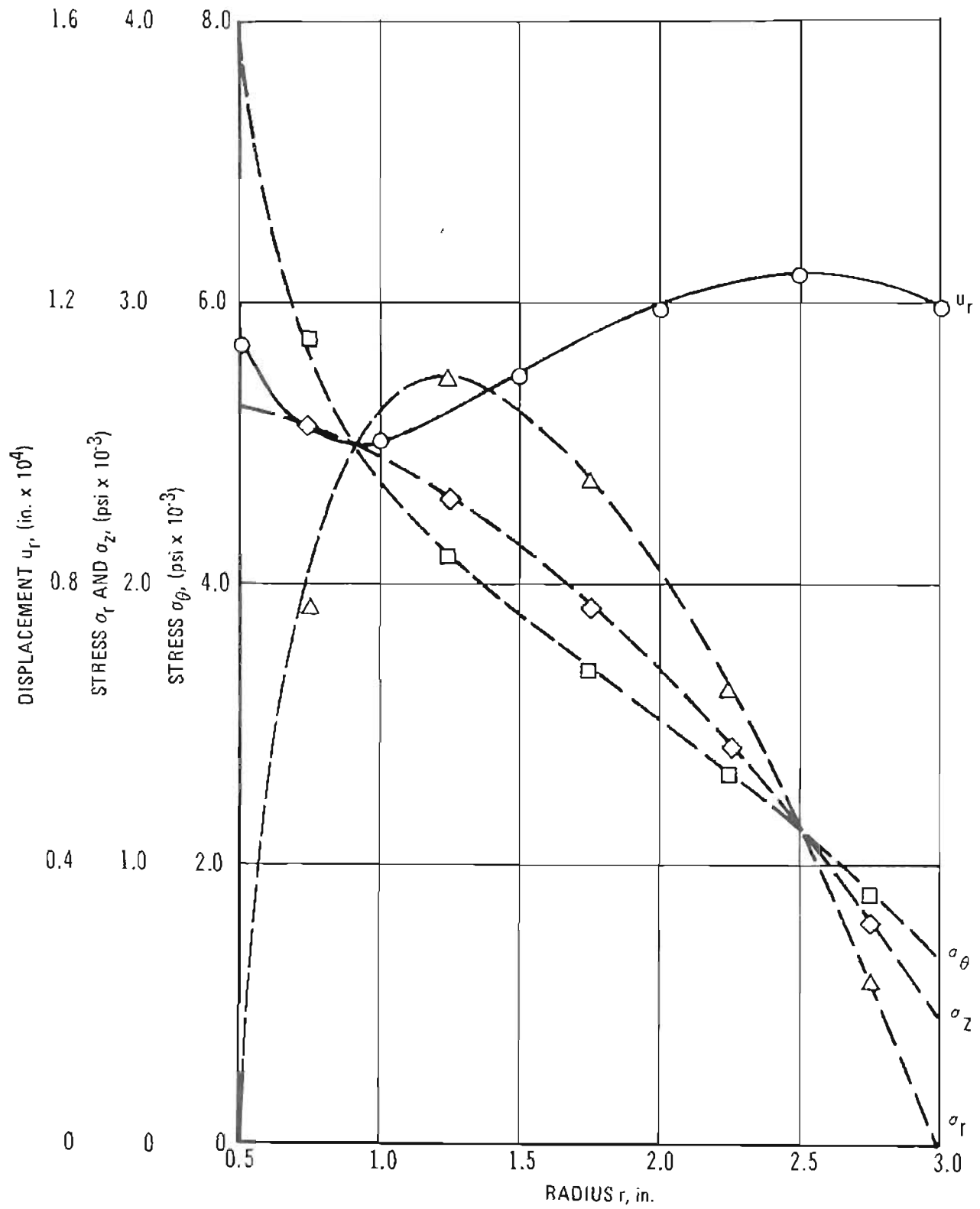


Figure 3-16. Displacements and Stresses in Rotating Hollow Cylinder

the finite element analysis and exact solution are shown in Fig. 3-17. Note that discontinuities exist in the displacement gradient and gradient of σ_r , as well as in σ_θ and σ_z . In this particular example an analysis with a mesh of one-half the original size (0.25 in. compared to 0.5 in.) was performed. The solid points for σ_θ are from the second analysis to demonstrate the accuracy with which the discontinuity is captured.

3-5.4.6 CUP SABOT WITH METAL BASE PLATE

To conclude this discussion of the finite element approach to structural problems, consider the sabot shown in Fig. 3-18. This problem was selected at random to illustrate the application of the finite element technique to more realistic problems. The dimensions, materials, etc., are chosen arbitrarily and thus do not represent a problem of any real situation. It is merely a demonstration of the finite element technique applied to multi-material problems with peculiar shapes. Because this is an idealized problem, only one loading is considered, a unit acceleration, which generates body forces proportional to the densities of the materials.

The sabot-projectile combination is somewhat more than 8 in. long, the projectile diameter is 2 in., and the sabot diameter is 4 in. The projectile is steel. The sabot is plastic and the shock attenuator is a second plastic. Thus, the combination is fairly realistic.

The element layout for the problem is shown in Fig. 3-19. The solid points show prescribed nodes, and the open points the nodes then generated. Observe that the mesh generating routine tends to yield a uniform grid. The points of the grid joining two materials are prescribed, of course. The boundary conditions are indicated, i.e., no radial motion on the centerline or at the gun bore. Observe that the lower left node is fully fixed to remove the possibility of rigid-body motion. As is apparent, no effort has been made to provide a really fine mesh, only to provide one that is realistic.

The input data are given in Fig. 3-20. Observe that the boundaries between materials are given, and that corresponding material properties cards are included.

The results of this analysis again consist of displacements for all the nodal points, and for each element the radial, tangential, axial, and shear stresses and strains, as well as principal stresses and strains. While all these data might be meaningful in a real problem, it certainly is not pertinent here, because the whole problem is so idealized and the mesh so crude.

For this reason the only results presented are those (see Fig. 3-21) for the elements around the junction of the projectile, attenuator, and sabot. Referring to Fig. 3-19, these elements are seen to be those with nodes in Rows 4 through 7. The nodes actually on the line between materials are in Column 4. Thus, the elements of interest (shown shaded in Fig. 3-19 are (3, 4), (4, 4), (3, 5), (4, 5), (3, 6), and (4, 6). Again, it must be emphasized that no inferences are to be drawn from such a crude illustration.

3-5.5 CONCLUSIONS

The purpose of par. 3-5 has been to give a beginner some idea of the finite element technique in stress analysis. To that end a very sketchy description of the basic ideas of finite element analysis has been given, and a more detailed discussion of the mechanics of use of computer programs using finite element methods. Problems have been presented to demonstrate the accuracy of which the method is capable, and a final example was given showing more of the versatility achievable. This by no means can be considered a full treatment of any phase of the topic, nor is it intended as such. If the reader is now aware of the tool at his disposal, however, and has a reasonable idea of how the tool works, the purpose has been fulfilled.

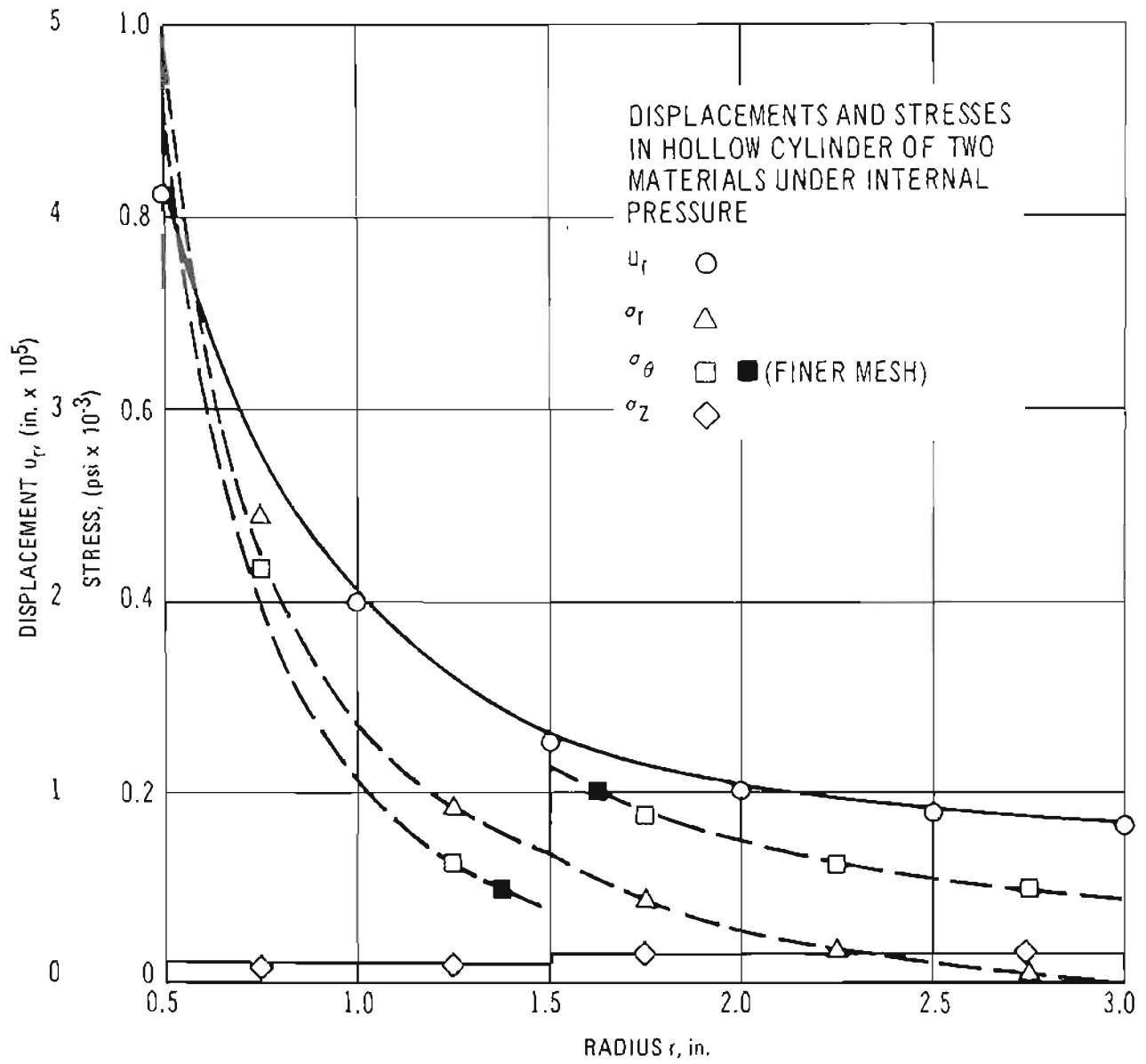


Figure 3-17. Displacements and Stresses in Hollow Cylinder of Two Materials Under Internal Pressure

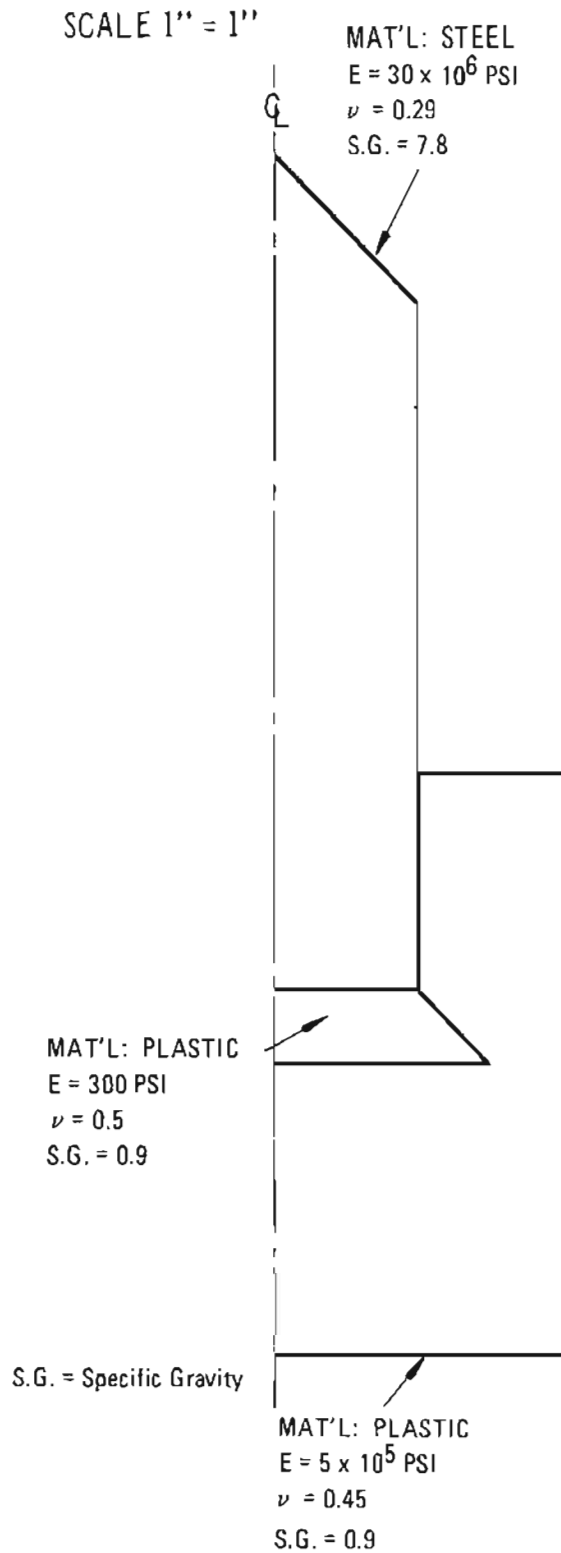


Figure 3-18. Simple Sabot

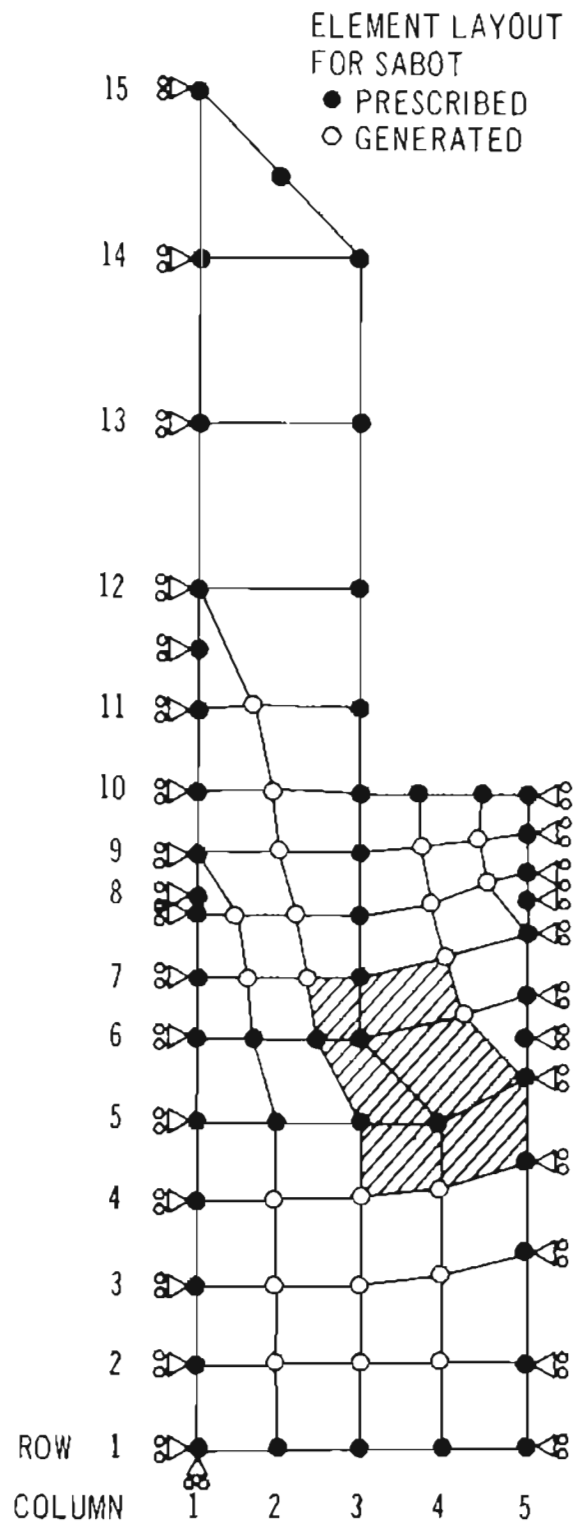


Figure 3-19. Element Layout for Sabot

```

12345678901234567890123456789012345678901
AMG032A SAMPLE SAPOT PROBLEM

40 15
1 1 11100 0.0 0.0 7 10 51000 2.0 4.0
2 1 00000 0.5 0.0 2 11 01000 0.0 4.5
3 1 00000 1.0 0.0 4 11 50000 1.0 4.5
4 1 00000 1.5 0.0 2 12 51000 0.0 4.875
5 1 51000 2.0 0.0 3 12 01000 0.0 5.25
1 2 01000 0.0 0.5 4 12 50000 1.0 5.25
5 2 51000 2.0 0.5 3 13 01000 0.0 6.25
1 3 01000 0.0 1.0 4 13 50000 1.0 6.25
5 3 51000 2.0 1.2 1 14 01000 0.0 7.25
1 4 01000 0.0 1.5 4 14 50000 1.0 7.25
5 4 51000 2.0 1.75 3 15 51000 0.0 8.0
1 5 11000 0.0 2.0 4 15 50000 0.5 7.75
2 5 0.5 2.0 50000.0000.45000000 0.40000000
3 5 1.0 2.0 111111111 0.40000000
4 5 1 1.5 2.0 300.0000000.50000000 0.40000000
5 5 01000 2.0 2.25 111111111 0.40000000
6 5 51000 2.0 2.5 50000.0000.45000000 0.40000000
1 6 11000 0.0 2.5 111111111
2 6 .375 2.5 30000000.00.29 7.8
3 6 .75 2.5 111111111
4 6 1 1.0 2.5 50000.0000.45000000 0.40000000
6 6 51000 2.0 2.75 111111111
1 7 11000 0.0 2.875 30000000.00.29 7.8
4 7 1 1.0 2.875 111111111
6 7 01000 2.0 3.15 50000.0000.45000000 0.40000000
7 7 51000 2.0 3.35 111111111
1 8 11000 0.0 3.25 30000000.00.29 7.8
4 8 1 1.0 3.25 111111111
7 8 51000 2.0 3.5 50000.0000.45000000 0.40000000
1 9 51000 0.0 3.375 111111111
2 9 11000 0.0 3.625 30000000.00.29 7.8
4 9 1 1.0 3.625 111111111
7 9 51000 2.0 3.75 50000.0000.45000000 0.40000000
2 10 11000 0.0 4.0 111111111
4 10 50000 1.0 4.0 30000000.00.29 7.8
5 10 50000 1.375 4.0 111111111
6 10 50000 1.75 4.0 END OF DATA

```

Figure 3-20. Input Data

RQHA AND HAAS PROGRAM- INCOMPRESSIBLE

DATE 020968 PAGE 4

AMG032A SAMPLE SABOT_PROJECT

I ANGLE	J ANGLE	COORDINATES		STRESS		STRAIN		MINIMUM	MAX SHEAR
		1	2	AXIAL	HOOP	AXIAL	HOOP		
3 -32.65	4	1.250	1.703	1.2480+01	6.5884+00	1.2380+01	-1.0842-01	1.2549+01	1.1939+01
				7.8740-06	-9.2096-06	7.5058-06	-6.2283-07	8.0764-06	6.9214-07
4 3.01	6	1.750	1.870	1.4736+01	7.4810+00	4.0605+00	5.1965-01	1.4764+01	4.9621+00
				1.8427-05	-2.6129-06	-1.0195-05	3.0139-06	1.8506-05	2.8780-05
3 65.12	5	1.083	2.259	1.8912+01	1.8911+01	1.8921+01	5.0606-03	1.8923+01	6.6323-03
				-1.00159-06	-1.1601-05	3.0053-05	5.0606-05	4.7740-05	-1.8543-05
4 21.39	6	1.533	2.345	7.4027+00	4.5311+00	5.7669+00	7.8479-01	7.7701+00	1.1554+00
				6.1953-06	-2.3064-06	1.2774-06	4.5518-06	7.0869-06	6.7011-06
3 -85.42	6	1.355	2.688	-1.5282+01	-1.2232+01	3.0336+01	-4.3214+00	3.8682+01	2.7155+01
				-7.4338-07	-6.6222-07	1.5122-06	-3.7164-07	1.5271-06	2.3353-06
4 -47.92	6	1.260	2.751	2.7395+00	2.4985+00	3.1848+00	-2.1774+00	5.1509+00	7.7334-01
				3.0715-07	-3.3102-07	1.6508-06	-1.2629-05	7.3005-06	5.3346-06

Figure 3-21. Selected Element Results for Simple Sabot Program

REFERENCES

1. M. L. Williams, "Systems Approach to Solid Rocket Design", Section VI of *Solid Propellant Structural Test Vehicle, Cumulative Damage and Systems Analysis*, Lockheed Propulsion Co., Tech. Rpt. AFRPL-TR-68-130, October 1968, pp. 307-316.
2. S. Timoshenko and J. N. Goodier, *Theory of Elasticity*, McGraw-Hill Book Co., Inc., New York, 1951.
3. J. E. Fitzgerald, "Solid Propellant Grain Structural Analysis", in *Mechanics and Chemistry of Solid Propellants*, Pergamon Press, New York, 1967.
4. M. L. Williams, P. J. Blatz, and R. A. Schapery, *Fundamental Studies Relating to Systems Analysis of Solid Propellants*, California Institute of Technology, Report No. GALCIT SM 61-5, February 1961.
5. M. L. Williams, "Structural Analysis of Viscoelastic Materials", *AIAA Journal*, May 1964, pp. 785-808.
6. H. H. Hilton, "An Introduction to Viscoelastic Analysis", *Engineering Design for Plastics*, Reinhold Publishing Co., pp. 199-276, 1964.
7. J. L. Rand, J. C. S. Yang, and J. M. Marshall, *Dynamic Compression Testing of a Strain-Rate Material*, U. S. Naval Ordnance Laboratory, Report No. NOLTR 65-10, February 1966.
8. D. P. Kendall and T. E. Davidson, *The Effect of Strain Rate on Yielding in High-Strength Steels*, Watervliet Arsenal, Report No. WVT-6618, May 1966.
9. A. J. Cable, *An Examination of Failing Loads in Model Launching Experiments*, AEDC Report No. AEDC-TR-65-56, March 1965.
10. G. Bertrand and P. Brooks, *Parametric Study for Light Gas Gun Models (U)*, CARDE Report No. TR 411/64, August 1964.
11. S. Timoshenko and G. H. MacCullough, *Elements of Strength of Materials*, 3rd Edition, D. Van Nostrand Co., Inc., N.Y., 1949.
12. P. N. Brooks, *Methods of Transferring Torque to an Armour Piercing Core*, CARDE Report TN 1612/64, February 1964.
13. P. N. Brooks, *On the Design of a Light-Weight Sabot with Hemispherical Base for Launching Aeroballistic Models*, CARDE Report TR 493/64, April 1964.
14. E. L. Wilson, "Structural Analysis of Axisymmetric Solids", *AIAA Journal* 3, No. 12 (1965).
15. Charles H. Parr, "The Application of Numerical Methods to the Solution of Structural Integrity Problems of Solid Propellant Rockets", *Solid Rocket Structural Integrity Abstracts*, 4, No. 1 (1967).
16. F. A. Akyuz and E. Heer, *Stress Analysis of Solid Rocket Motors*, Technical Report 32-1253, Jet Propulsion Laboratory, California Institute of Technology, July 1968.
17. L. R. Herrmann, "Elasticity Equations for Incompressible and Nearly Incompressible Materials by a Variational Theorem", *AIAA Journal* 3, No. 10, (1965).
18. R. L. Taylor and T. Y. Chang, "An Approximate Method for Thermoviscoelastic Stress Analysis", *Nuclear Engineering and Design*, Vol. 4, North Holland Publishing Company, Amsterdam, 1966.

19. E. L. Wilson, *A Computer Program for the Dynamic Stress Analysis of Underground Structures*, University of California Structural Engineering Laboratory Report, No. 68-1, January 1968.
20. R. E. Nickell and J. L. Sackman, *The Extended Ritz Method Applied to Transient, Coupled Thermoelastic Boundary-Value Problems*, University of California Structural Engineering Laboratory Report, No. 61-3, February 1967.
21. E. L. Wilson and R. E. Nickell, "Application of the Finite Element to Heat Conduction Analysis", *Proc. Fifth U. S. National Congress of Applied Mechanics*, ASME, New York, 1966.
22. Eric B. Becker and John J. Brisbane, *Application of the Finite Element Method to Stress Analysis of Solid Propellant Rocket Grains*, Report Number S-76, Rohm and Haas Company, November 1965.
23. I. S. Sokolnikoff, *Mathematical Theory of Elasticity*, McGraw-Hill, N.Y., 1956.
24. O. C. Zienkiewicz and G. S. Hollister, *Stress Analysis*, John Wiley and Sons, N.Y., 1965, Chapter 7.

CHAPTER 4

EXPERIMENTAL METHODS FOR SABOT DEVELOPMENT

4-0 LIST OF SYMBOLS

A	= gun bore cross-sectional area
A_s	= sample cross-sectional area
a	= axial acceleration
F	= force
f	= projectile-gun bore surface frictional force
M	= structural test vehicle mass
M_s	= specimen mass
P_b	= gun shot base pressure
σ	= maximum tensile strength

4-1 INTRODUCTION

The objective of this chapter is to describe specialized techniques for obtaining experimental data on sabots and sabot materials.

In general, the methodology associated with evaluation of sabot projectile performance by gun firing tests is similar to that used in evaluation and development of conventional gun ammunition. Experimental techniques employed in this field have been extensively documented in various publications available in the literature, and the reader is referred to the reference list at the end of this chapter and the bibliography contained in Appendix D for detailed discussions.

Experimental methods used for measurement of gun and projectile performance during travel of the projectile through the gun tube are described in detail in Ref. 1*, *Interior Ballistics of Guns*. Experimental topics in this handbook work include:

- (1) Pressure Measurements
- (2) Measurement of Muzzle Velocity
- (3) Travel-time Measurements
- (4) In-bore Velocity and Acceleration Measurements
- (5) Measurement of Base Pressure
- (6) Measurement of Bore Friction
- (7) Measurement of Barrel Erosion
- (8) Barrel Temperature Measurements
- (9) Motion of the Propellant During Burning.

All of these areas are of importance in the development of sabot projectiles.

A unique feature of most sabot projectile systems is the requirement for uniform and reliable discard of the sabot carrier after transition from the muzzle of the gun. Sabot separation and discard usually are achieved by muzzle blast effects, elastic rebound of the sabot, and aerodynamic forces. During the early critical stages of this discard process, the sabot projectile is enveloped in a cloud of high-velocity propellant gas which for a short time out-runs the projectile after muzzle transition. The gas cloud and blast effectively obscure the sabot and projectile from view during the critical sabot discard period, rendering optical photographic techniques of limited use. Flash X-ray photography is useful

*References are located at the end of each chapter.

for detailed study of the sabot discard process during this period. High resolution shadowgraphs result from this technique, which effectively penetrates the muzzle blast cloud. Sequential and orthogonal exposures are possible, yielding the precise relative motion of projectile and sabot parts during the initial free flight period.

Because of the complex nature of the phenomena associated with high velocity launch of sabot projectiles and the relative difficulty of obtaining detailed experimental information during the gun ballistic cycle, the experimentalist usually is faced with the necessity for conducting a large number of tests to study the detailed effect of design on sabot structural and launch dynamic phenomena. Particularly during the early stages of research and development applications, the use of subscale testing and dynamic similarity analysis^{2, 3, 4} is of significant importance. In many cases, use of subscale modeling techniques permits the acquisition of considerably more information for a given amount of expended effort than could be obtained if the initial experimental research were carried out in full caliber size.

4-2 DYNAMIC FAILURE CHARACTERIZATION OF MATERIALS UNDER GUN LOADING CONDITIONS

Analytical methods for structural design of sabot projectile configurations are described in detail in Chapter 3. It is clear from this treatment that failure characterization of the materials involved is as critical as the accurate determination of loading conditions for the prediction of useful design criteria and limits. The high loading levels and extreme confinement experienced by most practical sabot designs, coupled with the high loading rates involved in gun ballistics, contribute to the questions concerning applicability of conventional static or dynamic material failure property data in sabot design.

A survey of conventional dynamic material property testing methods shows that the

various combined loading effects experienced in guns cannot be duplicated accurately by existing dynamic testing machines. High-rate testing machines can duplicate gun loading rates in direct strain or load application but cannot induce the body forces and resulting stress distributions induced by high acceleration gun launch. Conventional shock testing machines produce the correct type of loading but the acceleration pulse magnitudes and durations experienced by gun projectiles cannot be duplicated readily.

To rectify these deficiencies in material failure property characterization methods for gun projectiles, the experimental technique described in the following paragraphs was developed for dynamic failure characterization of materials by actual gun launch testing.

4-2.1 STRUCTURAL TEST VEHICLE

The sabot projectile designer usually is charged with the responsibility of producing the lightest weight sabot that will function properly and survive the gun launch environment reliably. To utilize the structural engineering design principles described in this handbook, and to avoid the excessive effort required by the purely empirical design and proof testing approach, the sabot and projectile material failure characteristics must be known for the loading conditions to which they will be subjected in the actual design. In general, the yield and failure strength limits must be determined under a variety of known multiaxial stress conditions with inertial loading applied in the rapid pulse form associated with gun projectile acceleration.

The approach utilized here to achieve these results involves high acceleration gun launch of a material sample carrier within which the material under study is subjected to the launch acceleration condition. The Structural Test Vehicle (STV) carrier serves to isolate the material sample from all launch effects except the axial acceleration induced in the STV by the propellant gas expansion. Aerodynamic drag is utilized to decelerate the STV

after muzzle transition to ensure that stresses induced in the sample by impact deceleration are sufficiently small (compared to the gun launch-induced loads) to prevent masking of the launch-induced material response. Systematic variations in geometry of the test samples are made, coupled with multiple gun tests under similar interior ballistic conditions, to determine yield and failure limits for the test material under realistic gun loading conditions.

A typical STV utilized in this experimental method, designed for launch from a 37 mm gun, smoothbored to 1.530-in. diameter, is shown in Fig. 4-1. Interior design details are presented in Fig. 4-2 for uniaxial tensile testing of the test specimen material. The same basic design can be used for a variety of specimen loading conditions by modification of the specimen holder and restraining devices.

Structural loading of the tensile test sample shown in Fig. 4-2 is induced by the inertial reaction of the sample mass to the gun acceleration environment. Maximum stress is induced at the forward end of the narrow cylindrical section by setback acceleration of the mass at the base of the test section and the mass of the aft portion of the test section. Reductions in the diameter of the test section are made until the launch acceleration produces yielding or failure.

4-2.2 LOADING ANALYSIS

The axial acceleration a induced in the structural test vehicle (STV) mass M by the gun shot base pressure P_b is given by

$$a = \frac{P_b A - f}{M} \quad (4-1)$$

where A is the gun bore cross-sectional area and f is the projectile-gun bore surface friction force. The setback force F on the test sample loading mass M_s produced by the launch acceleration is given by

$$F = M_s a \quad (4-2)$$

For the tensile test specimen configuration illustrated in Fig. 4-2, M_s includes all of the specimen mass aft of the section marked A-A. Maximum stress σ in the tensile test specimen occurs at Section A-A and is given by

$$\sigma = \frac{F}{A_s} \quad (4-3)$$

where A_s is the sample cross-sectional area at Section A-A. Combining Eqs. 4-1, 4-2, and 4-3 yields the final result for the maximum material stress as a function of experimentally determined quantities:

$$\sigma = \frac{M_s}{M} \cdot \frac{(P_b A - f)}{A_s} \quad (4-4)$$

Peak stress induced in the sample material during the ballistic cycle occurs when $(P_b A - f)$ is a maximum. In general, the shot base pressure P_b and bore friction f are not directly measured quantities unless sophisticated interior ballistic methods are used¹. In most cases, gun chamber pressure P is directly measured and the shot base pressure P_b is determined by theoretical or experimental means to be some fraction of the measured chamber pressure. Similarly, bore friction f is either neglected or an approximate value is used unless very accurate experimental results are required.

4-2.3 EXPERIMENTAL PROCEDURES

A modified 37 mm smoothbore gun system was used for feasibility study of the structural test vehicle, dynamic failure characterization method. The gun was adjusted to fire the STV's at near zero elevation angle. Final impact point of the aerodynamically unstable projectile is spotted by direct observation for recovery purposes. Smoke-tracer mixes have been used to assist in projectile recovery, if necessary, because of terrain requirements.

Typical flight range of the STV's before initial ground impact was approximately 500

yd. No indication of damage to the structural test samples due to impact deceleration was observed during the firing series. Approximately 80 percent of the projectiles launched in this manner were recovered for examination. Impact deceleration damage to the sample holder assembly was confined to the replaceable end caps and obturation components. Refurbishment and retest of the STV's with new test samples was found to be practical and economical.

The gun was instrumented with quartz piezoelectric pressure gages for measurement of pressure-versus-time in the propellant combustion chamber. An additional pressure gage was located near the gun muzzle to determine travel time and pressure conditions near the gun muzzle. Typical oscilloscope records obtained from firings made during the STV evaluation series are shown in Fig. 4-3. The following are gun loading conditions for the typical upper photo of Fig. 4-3:

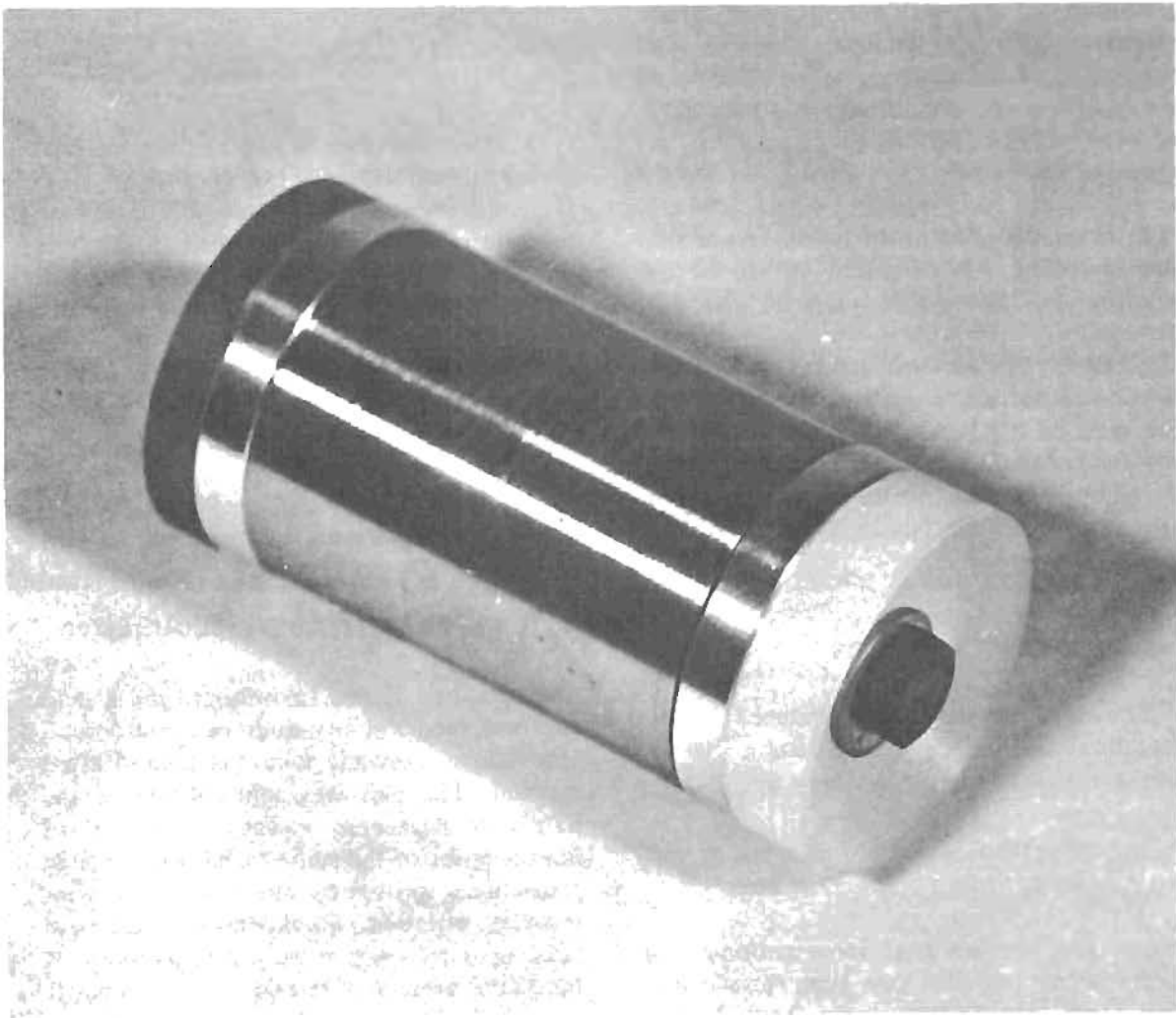
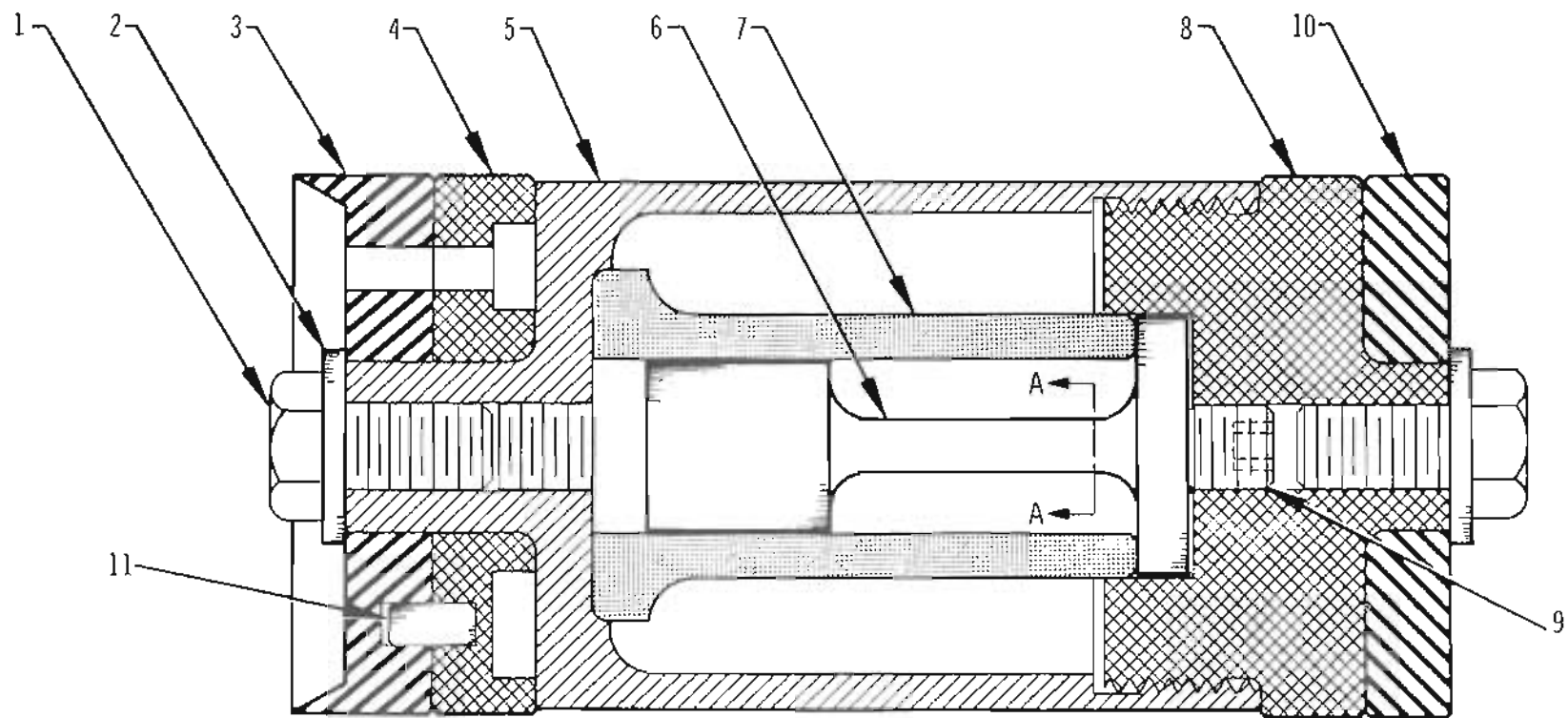


Figure 4-1. Structural Test Vehicle



- | | |
|---------------------------|---------------------------------|
| 1 CAP SCREW, STEEL | 6 TENSILE TEST SPECIMEN |
| 2 WASHER, STEEL | 7 SPECIMEN RETAINER, STEEL |
| 3 OBTURATOR, POLYETHYLENE | 8 HEAD CAP, STEEL |
| 4 BORE RIDER, ALUMINUM | 9 SOCKET SET SCREW, STEEL |
| 5 CHAMBER, STEEL | 10 IMPACT SHIELD, POLYCARBONATE |
| | 11 DOWEL PIN, ALUMINUM |

Figure 4-2. Structural Test Vehicle Schematic

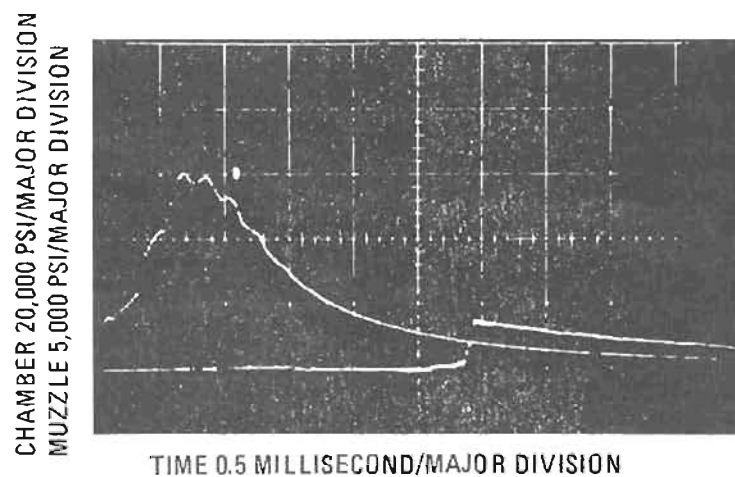
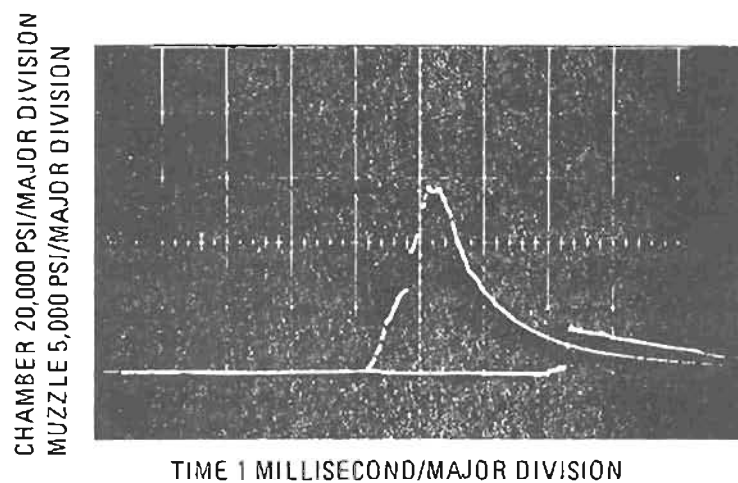


Figure 4.3. Typical Chamber and Muzzle Pressure-time Response

Shot weight	0.713 lb
Gun charge weight	0.540 lb
Propellant type	M2, single perforated

The small oscillations superimposed on the chamber pressure traces were relatively constant from test to test and were not considered objectionable for these research evaluations of material response to gun acceleration conditions. Peak gun chamber pressure values used for computation of projectile peak acceleration were obtained from these photographs and similar high speed oscillograph recordings.

4.2.4 RESULTS OF FEASIBILITY STUDY

Feasibility of the STV procedure for determination of material dynamic fracture properties under actual gun acceleration conditions was confirmed by conducting a limited series of tests on representative projectile structural materials, primarily in the uniaxial tension test mode.

A summary of selected test results is presented in Table 4-1. Static mechanical properties obtained on conventional testing machines are included for comparative purposes. The static test samples were fabricated of the same bar of material used for fabrication of the gun launch test samples. Typical examples of metal and plastic tensile test samples after gun-launch testing are shown in Figs. 4-4 and 4-5, respectively.

The results of this experimental study showed that the gun-launched STV technique described can be used to determine the material failure characteristics needed for detailed engineering design of sabot projectiles. Repetitive testing of specific materials can be expected to produce the dynamic strength values needed to the accuracy required, including determination of statistical variations and lot-to-lot changes in properties. Of significant importance is the fact that the effects of complex geometry, inertial loading, and multiaxial stress fields on failure behavior for specific developmental problems can be directly determined by use of this technique.

REFERENCES

1. AMCP 706-150, Engineering Design Handbook, *Interior Ballistics of Guns*.
2. W. G. Soper, *Scale Modeling*, International Science and Technology, Feb. 1967.
3. Langhaar, *Dimensional Analysis and Theory of Models*, John Wiley & Sons, N.Y., 1951.
4. Sedov, *Similarity and Dimensional Methods in Mechanics*, Academic Press, N.Y., 1959.

TABLE 4-1
EXPERIMENTAL RESULTS

Group No. Test Type	Sample Material	Total Projectile Weight, lb	Gun Propellant Weight, lb	Peak Gun Chamber Pressure, psi	Peak Projectile Acceleration, g	Dynamic Test Results			Measured Static Mechanical Properties				Dynamic / Static Ultimate Strength Ratio		Dynamic / Static Yield Strength Ratio	
						Peak Applied Stress, psi	Test Result	(Results at) Elongation, %	Yield Strength, psi	Ultimate Strength, psi	Elongation, %	Modulus, ksi	Minimum	Maximum	Minimum	Maximum
I	Maraging steel (6 nickel 1300)	0.8134	0.550	59,000	172,000	170,000	Fractured	10.2	268,000	277,000	12.0	R _e 53	0.87	1.36	0.90	---
Tensile		0.8440	0.500	46,000	127,000	242,000	No change	0								
II	Steel	0.754	0.500	46,500	114,000	213,000	Yielded	1.54	181,000	191,000	20.0	R _e 39-41	---	---	1.02	1.18
Tensile	4340	0.737	0.500	54,000	135,000	185,000	No change	0								
III	Aluminum 7057-T6 (extruded)	0.703	0.540	63,000	171,000	136,000	Fractured	1.94	83,000	92,000	11.0	A52	1.27	1.46	1.41	---
Tensile		0.703	0.540	42,000	168,000	117,000	No change	0								
IV	Polycarbonate (injection molded)	0.711	0.540	57,000	153,000	26,000	Yielded	0.2	9,200	13,500					1.46 to 1.52	2.74 to 2.82
Tensile		0.711	0.540	46,000	150,000	27,000	Fractured	0.5	10,500	15,300	12.6	R118	---	---		
V	Polycarbonate (injection molded)	0.750	0.500	52,000	128,000	19,000	Yielded	---								
Compression		0.748	0.500	54,000	131,000	6,000	No change	---	11,500	---	---	R118	---	---	0.52	1.65

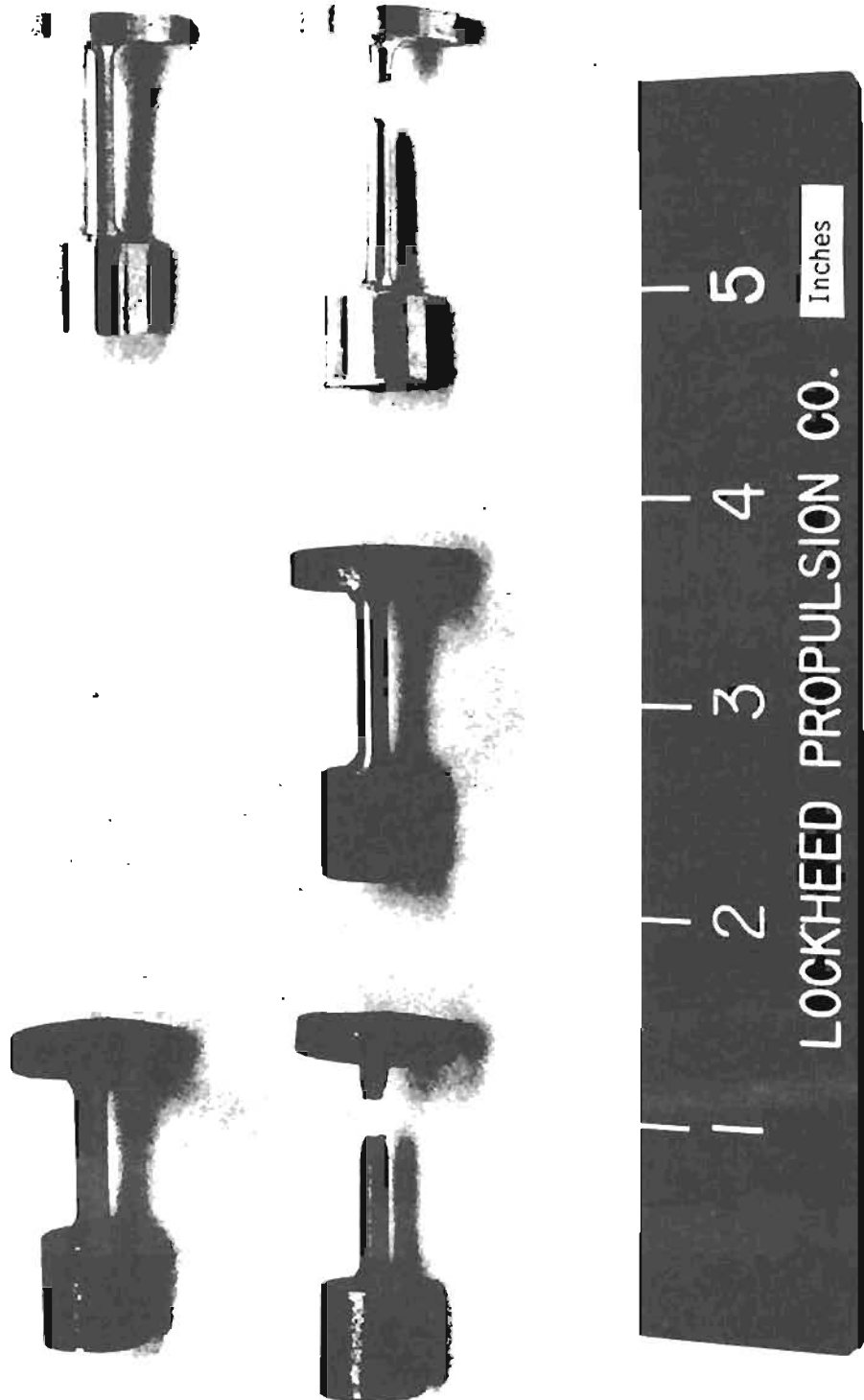


Figure 4-4. Gun Launch Tested Steel and Aluminum Samples

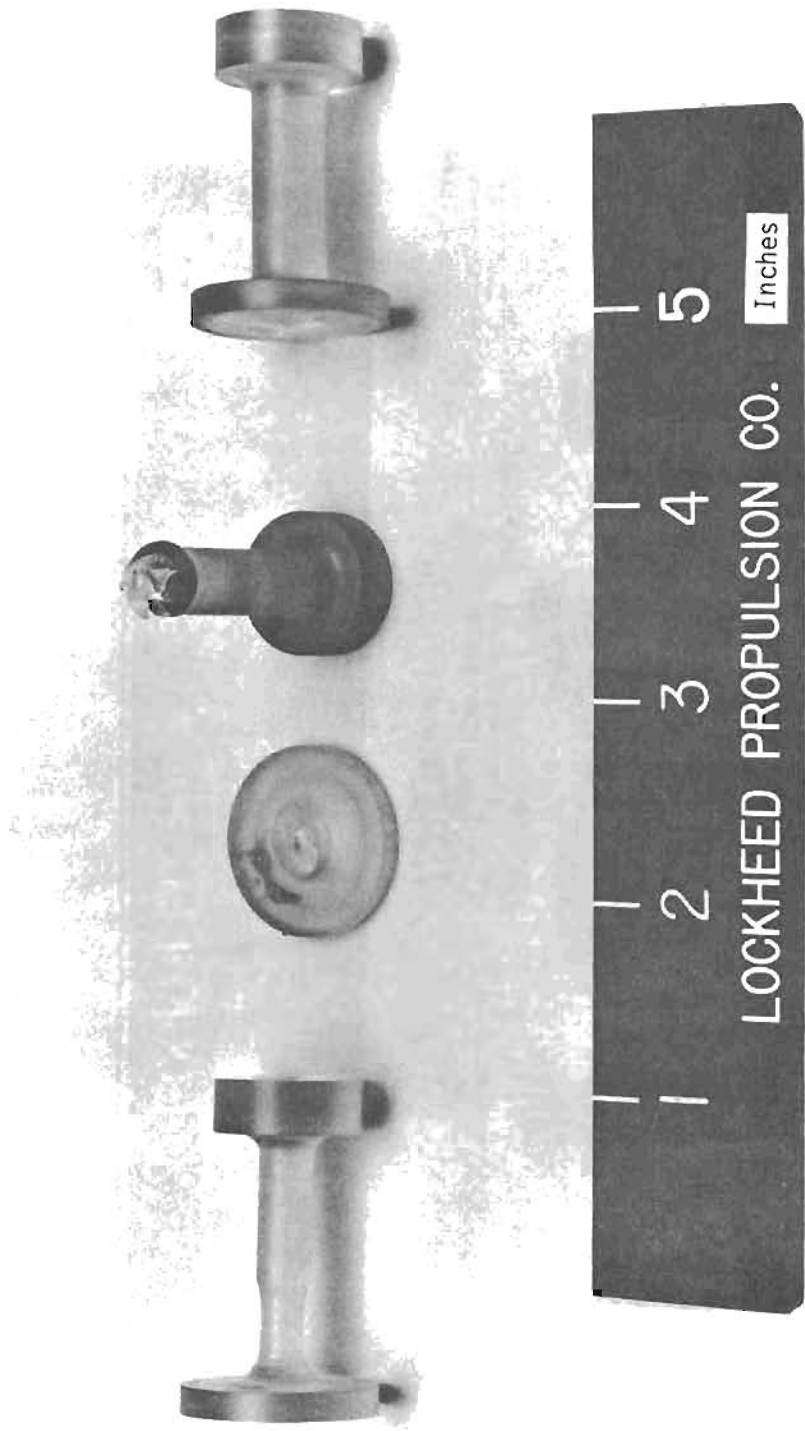


Figure 4-5. Gun Launch Tested Polycarbonate ("Lexan")

Appendix A

**SUMMARY OF SABOT DESIGNS
AND THEIR CHARACTERISTICS**

Item No.	Program	Reference	Projectile Type	Sabot Type	Launch Tube Type	Bore Diameter	Projectile Diameter	Ratio of Bore to Projectile Diameter	Projectile Mass	Sabot Mass	Ratio of Sabot to Projectile Mass	Projectile L/D	Sabot L/D	Sabot Materials	Number of Sabot Segments	Sabot Separation Mechanism	Load Transfer Mechanism	Launch Velocity, Peak Acceleration or Maximum Chamber Pressure	Remarks
4.	T120, 90/40mm APFSDS Shot	152 150	Fin-stabilized	One and two-piece rings with forward bevel and obturator	Smooth bore	90 mm	40 mm	2.25	2.0 lbm	3.78 lbm	0.54	12.2	0.95 Approx.	Aluminum or magnesium with rubber locking rings and obturators	4	Aero-dynamic petalling	Outboard shaped angular grooves	4250 fps 45 500 psi	
9.	T182 or M182, 105mm APFSDS Shot	150 153 171	Spin-stabilized	Cup with internal undercut and fractureable release mechanism	Rifled barrel	105 mm	45 mm Approx.	1.72 Approx.				4.17 Approx.	1.18 Approx.	Magnesium alloy with nylon centering band, fiber rotating band and rubber obturator	3 (petals)	Actual acceleration fractures sabot externally releasing forward portion then upon emerging from launch tube nylon band fractures allowing sabot segments to petals due to centrifugal and aerodynamic loading	Driven on tapered boost tail	5100 fps 55 000 psi	1. Total sabot projectile weight is 12.80 lbm. 2. Maximum spin rate is 480 rpm. 3. Extreme yawing of projectile noted as it emerged from sabot. 4. Rotating band observed to expand and ride up on sabot
16.	Ordnance F100mm AP Shot																		
18a.	Model 1	175	Fin-stabilized	Cup with forward sliding rib - no bolt connected	Smooth bore	90 mm	1.575 in.	2.25	7.725 lbm	3.412 lbm	0.450	8.27 Approx.	2.27 Approx.	Steel base plate with magnesium rider.	6	Aero-dynamic petalling	Base driven	5100 fps 55 700 psi	1. Intended to overcome the heating and obstruction problems inherent in T120 and T146 type designs. 2. Sabot failure noted and believed due to acceleration loading.
18b.	Model 2	176	Fin-stabilized	Cup with forward sliding rib - no bolt connected	Smooth bore	90 mm	1.575 in.	2.25	7.725 lbm	3.015 lbm	0.390	8.27 Approx.	2.27 Approx.	Aluminum base plate with magnesium rider.	6	Aero-dynamic petalling	Base driven		
18c.	Model 3	178 180	Fin-stabilized	Modified cup containing a base plate with four T-shaped radial supports	Smooth bore	87 mm	1.4 in.	2.62	6.23 lbm	4.77 lbm	0.56	9.5 Approx.	2.8 Approx.	Steel base plate with magnesium supports and rubber obturator	4	Aero-dynamic petalling of supports held on base plate with shear pins	Base driven	5640 fps 44 400 psi	

Doc. No.	Model	Proj.	Caliber	Length	Weight	Material	Design	Notes	Remarks
100	Model 4	100	100 mm	100 mm	100 mm	100 mm	100 mm	100 mm	1. A copper short-start band in organized an steel significantly reduced launch velocity and chamber pressure (specimen).
101	Models 11 and 12	101	101 mm	101 mm	101 mm	101 mm	101 mm	101 mm	2. Total shot propulsive mass is 15.00 lbm.
102	Model 13	102	102 mm	102 mm	102 mm	102 mm	102 mm	102 mm	3. Total shot propulsive mass is 16.22 lbm.
103	Model 14	103	103 mm	103 mm	103 mm	103 mm	103 mm	103 mm	4. Total shot propulsive mass is 11.09 lbm.
104	Model 15	104	104 mm	104 mm	104 mm	104 mm	104 mm	104 mm	
105	Model 16	105	105 mm	105 mm	105 mm	105 mm	105 mm	105 mm	
106	Model 17	106	106 mm	106 mm	106 mm	106 mm	106 mm	106 mm	
107	Model 18	107	107 mm	107 mm	107 mm	107 mm	107 mm	107 mm	
108	Model 19	108	108 mm	108 mm	108 mm	108 mm	108 mm	108 mm	
109	Model 20	109	109 mm	109 mm	109 mm	109 mm	109 mm	109 mm	
110	Model 21	110	110 mm	110 mm	110 mm	110 mm	110 mm	110 mm	
111	Model 22	111	111 mm	111 mm	111 mm	111 mm	111 mm	111 mm	
112	Model 23	112	112 mm	112 mm	112 mm	112 mm	112 mm	112 mm	
113	Model 24	113	113 mm	113 mm	113 mm	113 mm	113 mm	113 mm	
114	Model 25	114	114 mm	114 mm	114 mm	114 mm	114 mm	114 mm	
115	Model 26	115	115 mm	115 mm	115 mm	115 mm	115 mm	115 mm	
116	Model 27	116	116 mm	116 mm	116 mm	116 mm	116 mm	116 mm	
117	Model 28	117	117 mm	117 mm	117 mm	117 mm	117 mm	117 mm	
118	Model 29	118	118 mm	118 mm	118 mm	118 mm	118 mm	118 mm	
119	Model 30	119	119 mm	119 mm	119 mm	119 mm	119 mm	119 mm	
120	Model 31	120	120 mm	120 mm	120 mm	120 mm	120 mm	120 mm	
121	Model 32	121	121 mm	121 mm	121 mm	121 mm	121 mm	121 mm	
122	Model 33	122	122 mm	122 mm	122 mm	122 mm	122 mm	122 mm	
123	Model 34	123	123 mm	123 mm	123 mm	123 mm	123 mm	123 mm	
124	Model 35	124	124 mm	124 mm	124 mm	124 mm	124 mm	124 mm	
125	Model 36	125	125 mm	125 mm	125 mm	125 mm	125 mm	125 mm	
126	Model 37	126	126 mm	126 mm	126 mm	126 mm	126 mm	126 mm	
127	Model 38	127	127 mm	127 mm	127 mm	127 mm	127 mm	127 mm	
128	Model 39	128	128 mm	128 mm	128 mm	128 mm	128 mm	128 mm	
129	Model 40	129	129 mm	129 mm	129 mm	129 mm	129 mm	129 mm	
130	Model 41	130	130 mm	130 mm	130 mm	130 mm	130 mm	130 mm	
131	Model 42	131	131 mm	131 mm	131 mm	131 mm	131 mm	131 mm	
132	Model 43	132	132 mm	132 mm	132 mm	132 mm	132 mm	132 mm	
133	Model 44	133	133 mm	133 mm	133 mm	133 mm	133 mm	133 mm	
134	Model 45	134	134 mm	134 mm	134 mm	134 mm	134 mm	134 mm	
135	Model 46	135	135 mm	135 mm	135 mm	135 mm	135 mm	135 mm	
136	Model 47	136	136 mm	136 mm	136 mm	136 mm	136 mm	136 mm	
137	Model 48	137	137 mm	137 mm	137 mm	137 mm	137 mm	137 mm	
138	Model 49	138	138 mm	138 mm	138 mm	138 mm	138 mm	138 mm	
139	Model 50	139	139 mm	139 mm	139 mm	139 mm	139 mm	139 mm	
140	Model 51	140	140 mm	140 mm	140 mm	140 mm	140 mm	140 mm	
141	Model 52	141	141 mm	141 mm	141 mm	141 mm	141 mm	141 mm	
142	Model 53	142	142 mm	142 mm	142 mm	142 mm	142 mm	142 mm	
143	Model 54	143	143 mm	143 mm	143 mm	143 mm	143 mm	143 mm	
144	Model 55	144	144 mm	144 mm	144 mm	144 mm	144 mm	144 mm	
145	Model 56	145	145 mm	145 mm	145 mm	145 mm	145 mm	145 mm	
146	Model 57	146	146 mm	146 mm	146 mm	146 mm	146 mm	146 mm	
147	Model 58	147	147 mm	147 mm	147 mm	147 mm	147 mm	147 mm	
148	Model 59	148	148 mm	148 mm	148 mm	148 mm	148 mm	148 mm	
149	Model 60	149	149 mm	149 mm	149 mm	149 mm	149 mm	149 mm	
150	Model 61	150	150 mm	150 mm	150 mm	150 mm	150 mm	150 mm	
151	Model 62	151	151 mm	151 mm	151 mm	151 mm	151 mm	151 mm	
152	Model 63	152	152 mm	152 mm	152 mm	152 mm	152 mm	152 mm	
153	Model 64	153	153 mm	153 mm	153 mm	153 mm	153 mm	153 mm	
154	Model 65	154	154 mm	154 mm	154 mm	154 mm	154 mm	154 mm	
155	Model 66	155	155 mm	155 mm	155 mm	155 mm	155 mm	155 mm	
156	Model 67	156	156 mm	156 mm	156 mm	156 mm	156 mm	156 mm	
157	Model 68	157	157 mm	157 mm	157 mm	157 mm	157 mm	157 mm	
158	Model 69	158	158 mm	158 mm	158 mm	158 mm	158 mm	158 mm	
159	Model 70	159	159 mm	159 mm	159 mm	159 mm	159 mm	159 mm	
160	Model 71	160	160 mm	160 mm	160 mm	160 mm	160 mm	160 mm	
161	Model 72	161	161 mm	161 mm	161 mm	161 mm	161 mm	161 mm	
162	Model 73	162	162 mm	162 mm	162 mm	162 mm	162 mm	162 mm	
163	Model 74	163	163 mm	163 mm	163 mm	163 mm	163 mm	163 mm	
164	Model 75	164	164 mm	164 mm	164 mm	164 mm	164 mm	164 mm	
165	Model 76	165	165 mm	165 mm	165 mm	165 mm	165 mm	165 mm	
166	Model 77	166	166 mm	166 mm	166 mm	166 mm	166 mm	166 mm	
167	Model 78	167	167 mm	167 mm	167 mm	167 mm	167 mm	167 mm	
168	Model 79	168	168 mm	168 mm	168 mm	168 mm	168 mm	168 mm	
169	Model 80	169	169 mm	169 mm	169 mm	169 mm	169 mm	169 mm	
170	Model 81	170	170 mm	170 mm	170 mm	170 mm	170 mm	170 mm	
171	Model 82	171	171 mm	171 mm	171 mm	171 mm	171 mm	171 mm	
172	Model 83	172	172 mm	172 mm	172 mm	172 mm	172 mm	172 mm	
173	Model 84	173	173 mm	173 mm	173 mm	173 mm	173 mm	173 mm	
174	Model 85	174	174 mm	174 mm	174 mm	174 mm	174 mm	174 mm	
175	Model 86	175	175 mm	175 mm	175 mm	175 mm	175 mm	175 mm	
176	Model 87	176	176 mm	176 mm	176 mm	176 mm	176 mm	176 mm	
177	Model 88	177	177 mm	177 mm	177 mm	177 mm	177 mm	177 mm	
178	Model 89	178	178 mm	178 mm	178 mm	178 mm	178 mm	178 mm	
179	Model 90	179	179 mm	179 mm	179 mm	179 mm	179 mm	179 mm	
180	Model 91	180	180 mm	180 mm	180 mm	180 mm	180 mm	180 mm	
181	Model 92	181	181 mm	181 mm	181 mm	181 mm	181 mm	181 mm	
182	Model 93	182	182 mm	182 mm	182 mm	182 mm	182 mm	182 mm	
183	Model 94	183	183 mm	183 mm	183 mm	183 mm	183 mm	183 mm	
184	Model 95	184	184 mm	184 mm	184 mm	184 mm	184 mm	184 mm	
185	Model 96	185	185 mm	185 mm	185 mm	185 mm	185 mm	185 mm	
186	Model 97	186	186 mm	186 mm	186 mm	186 mm	186 mm	186 mm	
187	Model 98	187	187 mm	187 mm	187 mm	187 mm	187 mm	187 mm	
188	Model 99	188	188 mm	188 mm	188 mm	188 mm	188 mm	188 mm	
189	Model 100	189	189 mm	189 mm	189 mm	189 mm	189 mm	189 mm	
190	Model 101	190	190 mm	190 mm	190 mm	190 mm	190 mm	190 mm	
191	Model 102	191	191 mm	191 mm	191 mm	191 mm	191 mm	191 mm	
192	Model 103	192	192 mm	192 mm	192 mm	192 mm	192 mm	192 mm	
193	Model 104	193	193 mm	193 mm	193 mm	193 mm	193 mm	193 mm	
194	Model 105	194	194 mm	194 mm	194 mm	194 mm	194 mm	194 mm	
195	Model 106	195	195 mm	195 mm	195 mm	195 mm	195 mm	195 mm	
196	Model 107	196	196 mm	196 mm	196 mm	196 mm	196 mm	196 mm	
197	Model 108	197	197 mm	197 mm	197 mm	197 mm	197 mm	197 mm	
198	Model 109	198	198 mm	198 mm	198 mm	198 mm	198 mm	198 mm	
199	Model 110	199	199 mm	199 mm	199 mm	199 mm	199 mm	199 mm	
200	Model 111	200	200 mm	200 mm	200 mm	200 mm	200 mm	200 mm	
201	Model 112	201	201 mm	201 mm	201 mm	201 mm	201 mm	201 mm	
202	Model 113	202	202 mm	202 mm	202 mm	202 mm	202 mm	202 mm	
203	Model 114	203	203 mm	203 mm	203 mm	203 mm	203 mm	203 mm	
204	Model 115	204	204 mm	204 mm	204 mm	204 mm	204 mm	204 mm	
205	Model 116	205	205 mm	205 mm	205 mm	205 mm	205 mm	205 mm	
206	Model 117	206	206 mm	206 mm	206 mm	206 mm	206 mm	206 mm	
207	Model 118	207	207 mm	207 mm	207 mm	207 mm	207 mm	207 mm	
208	Model 119	208	208 mm	208 mm	208 mm	208 mm	208 mm	208 mm	
209	Model 120	209	209 mm	209 mm	209 mm	209 mm	209 mm	209 mm	
210	Model 121	210	210 mm	210 mm	210 mm	210 mm	210 mm	210 mm	
211	Model 122	211	211 mm	211 mm	211 mm	211 mm	211 mm	211 mm	
212	Model 123	212	212 mm	212 mm	212 mm	212 mm	212 mm	212 mm	
213	Model 124	213	213 mm	213 mm	213 mm	213 mm	213 mm	213 mm	
214	Model 125	214	214 mm	214 mm	214 mm	214 mm	214 mm	214 mm	
215	Model 126	215	215 mm	215 mm	215 mm	215 mm	215 mm	215 mm	
216	Model 127	216	216 mm	216 mm	216 mm	216 mm	216 mm	216 mm	
217	Model 128	217	217 mm	217 mm	217 mm	217 mm	217 mm	217 mm	
218	Model 129	218	218 mm	218 mm	218 mm	218 mm	218 mm	218 mm	
219	Model 130	219	219 mm	219 mm	219 mm	219 mm	219 mm	219 mm	
220	Model 131	220	220 mm	220 mm	220 mm	220 mm	220 mm	220 mm	
221	Model 132	221	221 mm	221 mm	221 mm	221 mm	221 mm	221 mm	
222	Model 133	222	222 mm	222 mm	222 mm	222 mm	222 mm	222 mm	
223	Model 134	223	223 mm	223 mm	223 mm	223 mm	223 mm	223 mm	
224	Model 135	224	224 mm	224 mm	224 mm	224 mm	224 mm	224 mm	
225	Model 136	225	225 mm	225 mm	225 mm	225 mm	225 mm	225 mm	
226	Model 137	226	226 mm	226 mm	226 mm	226 mm	226 mm	226 mm	
227	Model 138	227	227 mm	227 mm	227 mm	227 mm	227 mm	227 mm	
228	Model 139	228	228 mm	228 mm	228 mm	228 mm	228 mm	228 mm	
229	Model 140	229	229 mm	229 mm	229 mm	229 mm	229 mm	229 mm	
230	Model 141	230	230 mm	230 mm	230 mm	230 mm	230 mm	230 mm	
231	Model 142	231	231 mm	231 mm	231 mm	231 mm	231 mm	231 mm	
232	Model 143	232	232 mm	232 mm	232 mm	232 mm	232 mm	232 mm	
233	Model 144	233	233 mm	233 mm	233 mm	233 mm	233 mm	233 mm	
234	Model 145	234	234 mm	234 mm	234 mm	234 mm	234 mm	234 mm	
235	Model 146	235	235 mm	235 mm	235 mm	235 mm	235 mm	235 mm	
236	Model 147	236	236 mm	236 mm	236 mm	236 mm	236 mm	236 mm	
237	Model 148	237	237 mm	237 mm	237 mm	237 mm	237 mm	237 mm	
238	Model 149	238	238 mm	238 mm	238 mm	238 mm	238 mm	238 mm	
239	Model 150	239	239 mm	239 mm	239 mm	239 mm	239 mm	239 mm	
240</									

Item No.	Program	Reference	Projectile Type	Sabot Type	Launch Tube Type	Bore Diameter	Projectile Diameter	Ratio of Bore to Projectile Diameter	Projectile Mass	Sabot Mass	Ratio of Sabot to Projectile Mass	Projectile L/D	Sabot L/D	Sabot Materials	Number of Sabot Segments	Sabot Separation Mechanism	Load Transfer Mechanisms	Launch Velocity, Peak Acceleration or Maximum Chamber Pressure	Remarks
12.	Sabot Development for AP7SDS Shots	192	Fin-stabilized	One-piece ring with forward bayonet		22 mm	0.201 in.	6.35	400 grains	400 grains	1.00	27.5	1.3	A214B magnesium with neoprene rubber obturator	5	Aero-dynamic petalling	Friction	4620 fps 310,000 psi 52,000 psi	1. Modified after AA1 small arms design 2. Grip length is 1.42 in.
			Fin-stabilized	Two-piece ring with forward bayonet		22 mm	1.585 in.	6.32	8.2 lbm	10.5 lbm	1.33	13.10	1.48	2K46A-13 magnesium with polyethylene obturator	4	Aero-dynamic petalling	Primarily friction but also small keyed section	4835 fps 40,000 psi	3. Type VI design 4. Gas sealing problems solved
HIGH-EXPLOSIVE, DISCARDING-SABOT PROJECTILES																			
13.	75/40 mm HEDS-AA Projectile	201	Spin-stabilized	Cup with rotating band	Rifled barrel	75 mm	49 mm	1.25	6.81 lbm	1.53 lbm	0.225	5.09	1.90	Glass-filled Epon 828 in nylon or nylon/formica sheath and neoprene or resilient Epon obturator	1	Differential aerodynamic drag	Base driven with spin torque transfer by friction	3022 fps 28,100 psi	1. HEDS stands for High-Explosive Discarding-Sabot 2. Fiberglass materials are too abrasive to be used next to barrel 3. Gas leakage past obturator noted but deemed a solvable problem 4. Designs for 90/70mm, 110/80mm and 120/70 mm projectiles given but not the sabot design
14.	T162, 155/105 mm HEDS Projectile	202	Spin-stabilized	Cup with forward rider	Rifled barrel	155 mm	105 mm	1.46	10.09 lbm	15.47 lbm	0.500	3.84	1.55	Aluminum with steel flame shield, bourrelet, and rotating band	3	Tensile failure of rivet holding segments together (sometimes epoxied)	Base driven with shear pins for torque transfer and rider circumferentially keyed to projectile	3800 fps 40,000 psi 26,200 psi	
15.	T163, 155/105 mm HEDS Projectile	202	Spin-stabilized	Cup with forward rider	Rifled barrel	155 mm	105 mm	1.48	12.20 lbm	11.38 lbm	0.415	3.84	1.56	Same as above	3	Same as above	Same as above	3800 fps 40,000 psi 25,500 psi	
16.	T164, 155/105 mm HEDS Projectile	202	Spin-stabilized	Cup with forward rider	Rifled barrel	155 mm	105 mm	1.48	11.18 lbm	13.45 lbm	0.429	3.84	1.56	Same as above	3	Same as above	Same as above		
17.	T121, 280/203 mm HEDS Projectile	203	Spin-stabilized	Cup with external undercut and rotating band	Rifled barrel	280 mm	203 mm	1.38	201.0 lbm	84.6 lbm	0.47	3.93	1.69	Aluminum with steel flame shield, bourrelet and rotating band	3	Tensile failure of rivet holding segments together	Base driven with shear pins for torque transmission and rider circumferentially keyed to projectile	3900 fps 38,000 psi	1. Friction on tapered surfaces also considered for spin torque transfer 2. Maximum spin rate is 12,768 rpm

Item No.	Project	Reference	Proposed Design	Notes	Launch Tube Length	Item Diameter	Projectile Diameter	Ratio of Shot to Projectile Diameter	Projectile Mass	Shot Mass	Ratio of Shot to Projectile Mass	Projectile L/D	Shot L/D	Shot Diameter	Number of Shot Segments	Shot Segment Mechanism	Shot Transfer Mechanism	Launch Velocity, Peak Acceleration or Maximum Chamber Pressure	Remarks
18.	T100 127/60 mm HSDS - AA Projectile	206	Spin-stabilized	Two-piece ring + 16. D-ring and small obturator	Smooth bore	127 mm	60 mm	2.12	17.18 lbsm	1.70 lbsm	0.097	16.7	0.12	Aluminum with "Super-Alex" hard rubber or nylon backing ring and rubber obturator	4 10 180	Differential aerodynamic ring drag and aerodynamic preloading	Differential shaped shock bell groove	4000 fps 29,500 psi	1. The relatively long effective L/D for shot and ring by using lock on projectile as rear guide. 2. Shot parts connected together
OTHER SABOT PROJECTILES																			
19.	4.2-in. x 75-mm. SSDB Projectile	218	Spin-stabilized with tapered boat tail	Cup with external obturator, rotating band with shock plate restraint	Boat-tail (1.45)	4.20 in.	1.70 in.	1.14	19.00 lbsm	0.18 lbsm	0.004	1.17	1.45	Aluminum with molded-on nylon rotating band and phenolic shock plate	1	Differential aerodynamic ring drag after free fall of shock plate and instant spring assisted separation	Both axial and spin loads transferred through tapered boat tail	9700 fps 14,500 psi	1. Shot stands for spin-stabilized, descending shot. 2. Two steel skins introduced between aluminum skin and projectile because of possible galling between the two parts
20.	4.8-in. FSDS Projectile	222	Spin-stabilized	Ring	Boat-tail	4.80 in.	1.5 in.	2.00	16.7 lbsm	0.2 lbsm	0.011	12.8	0.88	Four steel alloy segments with nylon obturating band	4	Nylon band is fastened for centering and complete blast loads from segments are dynamically equal	Segment-shaped shock groove	3800 fps 10,000 psi	1. Preliminary design study for anti-aircraft weapon. FSDS stands for Horizontal, Descending Sabot.
			Spin-stabilized	Cup with external obturator and shock diaphragm restraint	Boat-tail	4.80 in.	1.5 in.	1.49	11.8 lbsm	10.4 lbsm	0.882	8.91	1.92	Cup pressure from shock plate restraint then shot aerodynamically preloaded	1	Cup pressure from shock plate restraint then shot aerodynamically preloaded		2600 fps	1. Shot and projectile held together by shock stud and flexible diaphragm
21.	GAAB	229	Spin-stabilized	Cup with forward (nose) external obturator and obturator	Smooth bore	16.0 in.	6.1 in.	2.64	110 lbsm	170 lbsm	1.45	8.79	1.10	Aerodynamic preloading		Aerodynamic preloading	Shock driven	10,000 psi 15,000 psi	1. Feasibility study - GAAB stands for Gun-Launched, Anti-Missile Defense System. 2. Scale-up of 5.0 in. AAP
			Spin-stabilized	Boat-tail plate	Smooth bore	16.0 in.	6.0 in.	2.66	110 lbsm	170 lbsm	0.429	8.0	1.10				Shock driven	10,000 psi 28,000 psi	

Item No.	Program	Reference	Projectile Type	Sabot Type	Launch Tube Type	Bore Diameter	Projectile Diameter	Ratio of Bore to Projectile Diameter	Projectile Mass	Sabot Mass	Ratio of Sabot to Projectile Mass	Projectile L/D	Sabot L/D	Sabot Materials	Number of Sabot Segments	Sabot Separation Mechanism	Load Transfer Mechanisms	Launch Velocity, Peak Acceleration or Maximum Chamber Pressure	Remarks
SMALL CALIBER SABOT PROJECTILES																			
22.	Caj 22 Single Flashed	141 242 243 244 250	Fla-stabilized	Ring located around projectile nose and conical cavity in sabot nose	Smooth-bore except at the muzzle end	0.72 in.	0.072 in.	3.06	10.0 grains	9.0 grains	0.900	20.8	1.59 Approx.	Magnesium segments with rubber obturator and rubber cement to seal all cracks exposed to gas pressure	6	Centrifugal force created by rifling at end of barrel	Friction	6400 fps 20,000 psi	1. Abundant grooves on one of the axial configurations caused excess drag and decreased range
			Fla-stabilized	Ring located around projectile nose and small hole in sabot nose	Smooth-bore except at the muzzle end	0.22 in.	0.070 in.	3.14	10.0 grains	4.2 grains	0.62	21.2	1.20 Approx.	Four Teflon coated magnesium segments with rubber obturator	4	Same as above	Friction	6400 fps 60,000 psi	
			Fla-stabilized	Same as above	Same as above	0.22 in.	0.070 in.	3.14	-	-	-	25.4	1.13 Approx.	"Glass-metallic" Fiberglass rod with longitudinal glass fibers and silicone rubber obturator	16	Same as above	Friction	6170 fps	1. Excessive spin transmitted to projectile during sabot stripping process deemed responsible for shot dispersion
GUN-LAUNCHED ROCKETS, PROBES AND SPACE VEHICLES																			
23.	GASP	140	Space vehicle	Cylindrical piston with axial explosion in duct	Smooth-bore	14 in.	14 in.	1.00	95 tons	95 tons	1.00	3 in.	1.57	-	1	-	Base driven	60,000 psi	1. Feasibility Study. GASP made for Ground Accelerated Space Program 2. Proposed launcher is a mass-restrained, automatic-operated cannon 3. Sabot must attenuate shock created by initial explosion
TERMINAL BALLISTICS STUDIES																			
24.	SAL Experimental Penetration Studies	191	High density rod	Cup and ring type (see remarks)	Smooth-bore	96 to 109 mm	0.6 and 1.3 in. or greater (see remarks)	See remarks	-	-	-	0.15 to 25.0	-	Cup Design: Plastic ("Lexan" polycarbonate, "Ethocel" ethyl cellulose) with 7015-T6 aluminum and steel base plate	-	Forward	Base driven for cup design and buttress-shaped, multi-piece construction	70,000 psi maximum	1. For projectiles L/D > 1, dia. < 0.4 in. W L/D > 1, diameter > 1.5 in. 2. One-piece cup sabots used if D _B /D _P > 2.5. For D _B /D _P > 2.5 and L/D > 10 a multi-base plate is added. Shock absorber added for brittle materials. Ring-type sabots used for L/D > 10. 3. Obturation means incorporated into sabot structure by making aft end larger than bore
			Steel rod	Cup	Smooth-bore	105 mm	See above	See remarks	1.30 lbm	5.27 lbm	2.52	0.15	-	Ring Design: Aluminum with plastic axial ring	-	-	-	8200 fps 63,400 psi	
			Tungsten rod	Cup	Smooth-bore	105 mm	See above	See remarks	2.05 lbm	4.25 lbm	4.02	10.0	-	See above	-	See above	See above	7820 fps 68,150 psi	
			Uranium 238 rod with steel sheath	Ring	Smooth-bore	96 mm	See above	See remarks	1.30 lbm	5.13 lbm	2.40	25.0	-	See above	-	See above	See above	8400 fps 19,100 psi	$D_{aft} = 1.024 D_B$

Item No.	Program	Reference	Projectile Type	Ring	Smooth-bore	Diameter	Propellant Diameter	Barrel Bore Diameter	Propellant Mass	Subcal Mass	Ratio of Subcal to Propellant Mass	Propagable L/D	Subcal L/D	Nature Material	Number of Segments	Subcal Segment Mechanism	Load Type and Mechanism	Limiting Acceleration or Displacement or Other Parameter
25.	APL Experimental Penetration Study (Continued)		Two-piece aluminum sheath	Ring	Smooth-bore	90 mm	See above	See remarks	2.32	4.18 lbm	2.32	25.0	See above	See above	See above	See above	See above	1. Static sabot failure mode assumed by compressive stress 2. Lateral vibration due to friction force assumed to be negligible 3. Under stress of projectile assumed to be sabot failure 4. Shear failure of ballistics copper core 5. Spallation of long projectile, mode of brittle material limited
26.	Experimental Penetration Study	385	Two-piece steel sheath	Two-piece ring	Smooth-bore	90 mm	0.578 in.	3.07	1.60	2.80 lbm	1.60	16.9	See above	Steel with brass push ring	4	Active dynamic jetting	Ballistic shear and abrasion	1000 g's to 1000 psi
27.	APL Experimental Penetration Study	451	Two-piece steel sheath	Two-piece ring	Smooth-bore	120 mm	0.618 in.	5.03	2.20	3.5 lbm	2.20	18.4	See above	Steel with brass push ring	4	Active dynamic jetting	Ballistic shear and abrasion	1000 g's to 1000 psi
28.	NRL Terminal Ballistics Study	594	Two-piece steel sheath	Two-piece ring	Smooth-bore	120 mm	0.618 in.	5.03	2.20	3.5 lbm	2.20	18.4	See above	Steel with brass push ring	4	Active dynamic jetting	Ballistic shear and abrasion	1000 g's to 1000 psi

Item No.	Program	Reference	Projectile Type	Sabot Type	Launch Tube Type	Bore Diameter	Projectile Diameter	Ratio of Bore to Projectile Diameter	Projectile Mass	Sabot Mass	Ratio of Sabot to Projectile Mass	Projectile L/D	Notes	Sabot Materials	Number of Sabot Specimens	Sabot Description	Notes	Velocity (ft/sec)	Notes
20	CARDE Free-Flight Testing	401 430 501	Conical shell	Cup with hemispherical base	Smooth-bore	1. Analytical study of stresses in "spine" sabot design. No indication of sabot being disturbed after impact.	...
			Conical and spherical shells	Cup	Smooth-bore	4 in.	2 in.	2.0	1.09 lbm	0.93 lbm	0.85	2.55	...	70-75 Aluminum alloy with styro-foam support wedges	...	Aero-dynamic peeling of sabot weakened by longitudinal slots	...	19.4 g/s	1. Parametric analytical study. Data used as design example given to illustrate use of results.
			Sphere	Cup with hemispherical base	Smooth-bore	1.125 in.	2.966 in.	1.955	0.400 lbm	0.254 lbm	0.635	1.0	21.0	Aluminum	4 (petals)	Aero-dynamic peeling of sabot weakened by longitudinal slots	Base driven	12,500 psi	1. Parametric study 2. Risk and regular cup-type sabots also included
			Conical shell	Cup with forward bevel	Smooth-bore	2.10 in.	1.75 in.	1.18	2.35	1.85	"Incess" with aluminum base plate	4 (petals)	Same as above	Base driven	1700 psi, 16K101, etc.	Numerous model failures noted but none attributable to sabot

Appendix B

**SUMMARY OF STRUCTURAL PROPERTIES
FOR MATERIALS USED IN SABOTS**

Material	Density, lbm/cu. in.	Modulus of Elasticity E, 10 ⁶ psi	Poisson's Ratio ν	Shear Modulus G, 10 ⁶ psi	Tensile Yield Strength, 10 ³ psi	Ultimate Tensile Strength, 10 ³ psi	Elonga- tion, %	Reduction of area, %	Shear Strength, 10 ³ psi	Coefficient of Linear Thermal Expansion 10 ⁻⁶ in./in.-°F	Remarks
<i>Aluminum and Aluminum Alloys</i>											
Pure Al	0.096-0.104	9.9-11.4	0.32-0.34	3.7-3.85	--	--	--	--	--	11.1-13.4	Specific Heat = 0.214 Btu/lbm-°F.
A356-T6	--	--	--	--	5.0	13.0	40.0	--	--	--	Str at 2660 in./in.-sec is 2.1 static strength
2000 Series	0.100	10.3-10.9	--	--	30.2-36.7	40.9-41.6	11-8.8	6-10	25.5-30.0	--	Notched str = 1.26-1.70 unnotched str
6061-T6	--	9.7-10.3	--	--	42.0-70.0	47-75.0	10-14.6	31.0	35.0-41.0	12.3	Comp. str = 43-50 ksi. Specific Heat = 0.23 Btu/lbm °F. Thermal Conductivity = 90 Btu/(hr) (ft ²) (°F/ft).
6062-T6	--	--	--	--	43.5-44.5	45.0-47.4	11.0	--	26.7	--	Str at 10,800 in/in.sec = 1.28 static str Notched str = 1.05 unnotched str.
7039-T6	--	--	--	--	40.0	45.0	17.0	--	--	--	
7075-T6	--	--	--	--	25.6-50.1	46.0-60.8	16-15.0	--	--	--	Notched str = 0.96-0.97 unnotched str.
7079-T6	--	10.4	--	4.0	56.0-78.0	68.0-87.4	16-16.0	--	52.5	--	Str at 1.0 in./in.-sec = 1.06 static str. Str at 6600 in/in.sec = 1.70 static str. Notched str = 1.36-1.47 unnotched str.
7178-T6	--	--	--	--	51.7-63.0	66.7-83.0	18-13.8	10.7-23.9	--	--	K _{1c} = 27.0-37.7 ksi √in.
7178-T6	--	--	--	--	78	88	10	--	--	--	
<i>Copper and Copper Alloys</i>											
Pure Cu	0.323-0.324	17.0-18.0	0.33-0.36	5.8-6.7	10.0-40.0	32.0-45.0	10-45.0	--	--	9.2-9.4	Str at $\dot{\epsilon} > 100$ in/in-sec = 1.23-1.33 static str.
Cartridge Brass	0.302-0.307	14.5-15.9	0.33-0.36	5.3-6.0	30.0-75.0	48.0-100.0	10-55.0	--	--	11.0-11.6	
Beryllium Copper	--	17.0-18.0	--	6.9-7.1	--	70.0-200.0	10-4.5	--	100.0	--	Comp. str = 128-206 ksi
<i>Lead</i>											
Pure Pb	0.385-0.406	2.0	--	--	1.9	2.5	50.0	--	--	14.4-16.0	Specific Heat = 0.031-0.032 Btu/lbm-°F. Thermal conductivity = 16-19 Btu/(hr) (ft ²) (°F/ft).
<i>Magnesium Alloys</i>											
Pure Mg	0.0635-0.066	--	--	--	--	--	--	--	--	14.0	
Cast	--	6.5	--	--	20.0-22.0	30.0-33.0	10-3.0	--	--	--	
Extruded	--	6.5	--	--	27.0-38.0	40.0-50.0	10-16.0	--	20.0-22.0	--	Str at $\dot{\epsilon} > 100$ in/in-sec = 1.17-1.44 static str.
Forged	--	--	--	--	19.0-25.0	33.0-41.0	10-9.0	--	16.0-21.0	--	
Mg-99-0.5 3r	--	--	--	--	46.0-52.0	59.0-61.0	10-8.0	--	--	--	Comp. str = 48.0-52.0 ksi. Notched str = 0.40-0.47 unnotched str.
Mg-14Li-0.35Li	--	--	--	--	9.5	15.0	10-35	--	--	--	
Mg-14Li-0.95Li	--	--	--	--	13.3	18.2	6.0	--	--	--	
<i>Nickel Alloy 718</i>											
Pure Ni	0.296	30.7-31.0	--	--	89.9-165.9	174-275	10-30.0	23.0-48.0	--	9.3	Thermal conductivity = 11.2 Btu/(hr) (ft ²) (°F/ft).
<i>Steels</i>											
Carbon and Low Alloy	0.279-0.284	28.0-32.0	0.26-0.29	11.0-11.9	34.0-130.0	36.0-188	--	--	41.0-120	5.5-7.1	Specific Heat = 0.107 Btu/lbm-°F.
AISI 1040	--	--	--	--	58.0-88.0	91.0-113	10-27.0	42.0-62.0	--	--	
AISI 4130	--	--	--	--	52.0-158.0	81.0-167.0	10-28.0	54.0-56.0	--	--	Str at 1.0 in./in-sec = 1.04 static str.
AISI 4140	--	30.0	--	12.0	100.0-177.0	134.0-195.0	10-25.0	--	90.0-150.0	--	Charpy V-notch energy absorption = 14.0 ft-lbf @ 32°F. Str at $\dot{\epsilon} > 100$ in/in-sec = 1.06-1.13 static str.
AISI 4340	--	--	--	--	225.1	230.0-264.4	10.3	43.0	--	--	Str at 2 in./in-sec = 1.14 static str. K _{1c} = 62.7 ksi √in.
Gun Steel	--	--	--	--	178-185	194-200	11-13.2	29.6-36.4	--	--	Std Charpy energy absorption = 16-20 ft-lbf.
SAE 6145	--	30.0	--	12.0	98-210	105-230	10-25.0	--	75-180	--	
HY-80	--	--	--	--	89.6	109	26.1	78.2	--	--	
HY 130/150 (5Ni-Cr-Mo-V)	--	--	--	--	131-149	140-182	16-22	56-68	--	--	Charpy V-notch energy absorption = 53-113 ft-lbf @ RT.
H-17	--	--	--	--	190-250	225-305	5-15	52	--	--	K _{1c} = 25-25.3 ksi √in.
H-19 (Tool Steel)	--	--	--	--	178-183	204-215	5.4	12.0	--	--	
9Ni-4Co-0.25C	0.28	27.3-27.8	--	--	175-250	185-295	9-18.5	40.0-68.0	128.0	6.2-6.4	Comp. str = 188-201 ksi. Charpy V-notch energy absorption = 35-60 ft-lbf @ 0°F. Notched str = 1.05-1.48 unnotched str.
<i>Martensitic Steel</i>											
18Ni, 250 grade	--	--	--	--	110-290	150-300	10-18.0	51.0-72.0	--	--	Str at 10 in./in-sec = 1.13 static str. Charpy V-notch energy absorption = 28-99 ft-lbf @ 30°F.
18Ni, 350 grade	--	--	--	--	174-290	283-300	--	--	--	--	
18Ni, 350 grade	--	--	--	--	233-335	339-346	4-14.5	19-39	--	--	Charpy V-notch energy absorption = 5.5-12.1 ft-lbf @ -40°F.
<i>Stainless Steel</i>											
18%Cr, 8%Ni	0.276-0.286	28.0-30.0	0.30	10.6-12.0	35-175	90-215	5-60	--	60-160	8.3-8.4	Specific Heat = 0.115 Btu/lbm-°F. Thermal conductivity = 8 Btu/(hr) (ft ²) (°F/ft). Str at $\dot{\epsilon} > 100$ in/in-sec = 1.19 static str.
AISI 301	--	25.3-26.8	--	--	143-233	200-253	10-5.4	--	--	--	Str at 1.0 in./in-sec = 1.15 static str. Notched strength = 0.94-1.05 unnotched str.
AISI 321	0.285-0.29	--	--	--	33.6-36.6	85.1-85.3	35-40	--	--	8.15	Specific Heat = 0.12 Btu/lbm-°F. Thermal conductivity = 8.75 Btu/(hr) (ft ²) (°F/ft).

	Modulus of Elasticity E, 10 ⁶ psi	Poisson's Ratio ν	Shear Modulus G, 10 ⁶ psi	Tensile Yield Strength, 10 ³ psi	Ultimate Tensile Strength, 10 ³ psi	Elonga- tion, %	Reduction of area, %	Shear Strength, 10 ³ psi	Coefficient of Linear Thermal Expansion, 10 ⁻⁶ in./in. ^o F	Remarks
	15.4-16.6	0.34	6.0	92.0-154	123-197	5.0-15.0	10.0-43.0	--	4.9	Charpy V-notch energy absorption = 17-28.5 ft-lbf @ 32 ^o F. Str at ε̇ = 1.0 in./in.-sec = 1.15-1.53 uniaxial str.
	16.2-16.5	--	--	100-105	110-122.5	15-24.8	40.6-43.2	86.1	--	Notched str = 1.135 unnotched str. Biaxial str = 1.37 uniaxial str.
	15.5-15.9	--	--	106-141.2	115-156	8.0-16.2	3.8-36.0	--	--	K _{IC} = 104-106 ksi √in. Charpy V-notch energy absorption = 15-30 ft @ RT, No
	16.5-16.7	--	--	146-195	150-202	3.6-13.6	3.8-44.7	--	--	K _{IC} = 32-95 ksi √in.
	53.9-54.7	0.286-0.288	20.9-21.2	--	15.5 (4350 ^o F)	--	--	--	--	Bulk modulus = 42.3-42.6 × 10 ⁶ psi.
	--	--	--	--	75.0 (3800 ^o F)	--	--	--	--	
	--	--	--	--	65.0 (3000 ^o F)	--	--	--	--	
	30.0	--	--	190-215	190-216	0	--	--	--	
	0.30-1.0	--	--	--	2.0-12.0	2.0-6.0	--	--	16.7-50.0	
043	0.35-0.50	--	--	--	10.0	--	--	--	50.0	Specific Heat = 0.33 Btu/lbm ^o F. Str @ 1200 in./in-sec = 2.12 static str.
	0.16-0.28	---	--	--	12.0	50-300	--	--	27-29	
0475	0.32-0.37	--	--	8.0-11.0	8.2-16.4	60-110	--	--	39-61.2	Comp. str = 11.0-11.8 ksi. Specific Heat = 0.30 Btu/lbm ^o F. Thermal conduct Izod V-notched energy absorption = 10-16 ft-lbf. Str @ 700 in/in/sec = 31.
	0.014-0.055	--	--	--	1.5-2.4	400-700	--	2.35	83-167	Specific Heat = 0.55 Btu/lbm ^o F.
0346	0.025-0.090	--	--	--	2.5-5.5	100-300	--	3.10	83-167	Unnotched izod energy absorption = 32 ft-lbf. Notched izod energy absorption
5	0.17	--	--	--	5.0	7220	--	--	3.4	
0386	0.40-0.60	--	--	--	5.5-8.0	1.0-3.0	--	--	33-45	Comp. str = 11.5-13.5 ksi. Specific Heat = 0.33 Btu/lbm ^o F. Izod energy abs
	0.20-0.60	--	--	--	6.0-9.0	5.0-25	--	--	28-33	Comp. str = 12.0 ksi.
049	0.00011-0.00060	0.50	0.00004- 0.00020	--	0.525-0.60	--	--	--	36-110	Specific Heat = 0.42 Btu/lbm ^o F.
	0.0002-0.0020	--	--	--	0.80-2.5	50-850	--	--	105-172	
	0.00015-0.0060	--	--	--	0.8-4.5	80-510	--	--	117	
047	0.0004-0.0026	--	--	--	> 5.0	40-750	--	--	55-110	

REFERENCES

1. "Materials Selector Issue", *Materials Engineering*, Vol. 66, No. 5, Mid-October 1967.
2. F.A. McClintock and A.S. Argon, Eds., *Mechanical Behavior of Materials*, Addison-Wesley Publishing Co., Inc., Reading, Mass., 1966.
3. J.E. Campbell, *Mechanical Properties of Metals*, Defense Metals Information Center, Battelle Memorial Institute, DMIC Review of Recent Developments, 13 May 1966; 5 August 1966; 23 November 1966; 3 February 1967; 24 May 1967; 22 August 1967; 8 November 1967; 16 February 1968; 10 May 1968; 19 July 1968.
4. J.B. Hallowell, *Aluminum and Magnesium*, Defense Metals Information Center, Battelle Memorial Institute, DMIC Review of Recent Developments, 17 October 1967; 26 April 1968; 13 November 1968.
5. D.P. Kendall and T.E. Davidson, *The Effect of Strain Rate on Yielding in High Strength Steels*, Benet Laboratories, Watervliet Arsenal, Technical Report WVT-6618, May 1966 (AD-637 217).
6. A. Vallance and V.L. Doughtie, *Design of Machine Elements*, McGraw-Hill Book Co., Inc., New York, 1951.
7. R.S. DeFries, *An Evaluation of Elevated Temperature Materials for the 81 mm Mortar Tube*, Benet R E Laboratories, Watervliet Arsenal, Technical Report WVT-6629, November 1966 (AD-807 425).
8. P.P. Puzak, et al., *Metallurgical Characteristics of High Strength Structural Materials*, U.S. Naval Research Laboratory, Report No. 6364 (8th Quarterly Report), August 1965 (AD-625 374).
9. W.H. Asche and M.R. Gross, *Effect of Tempering on the Strength, Hardness, and Notch Toughness of HY-130/150, 5Ni-Cr-Mo-V Steel*, U.S. Navy Marine Engineering Laboratory, Report No. 72/66, March 1966 (AD-630 464).
10. T.P. Groeneveld, *High-Strength Steels*, Defense Metals Information Center, Battelle Memorial Institute, DMIC Review of Recent Developments, 16 December 1966; 22 March 1967; 1 September 1967; 20 December 1967; 20 March 1968; 27 September 1968.
11. *Mechanical-Property Data HP 9Ni-4Co-25C Steel: Tempered Plate*, AF Materials Laboratory, October 1966 (AD-803 546).
12. J.G. Sessler and V. Weiss, Eds., "Ferrous Alloys", Suppl. 4, *Aerospace Structural Metals Handbook*, Vol. 4, AF Materials Laboratory, AF Systems Command, Report No. ASD-TDR-63-741, March 1967 (AD-819 736).
13. R.A. Wood and D.J. Maykuth, *Titanium and Titanium Alloys*, Defense Metals Information Center, Battelle Memorial Institute, DMIC Review of Recent Developments, 16 November 1966; 24 February, 1967; 24 August 1967; 5 December 1967; 29 May 1968; 23 August 1968.
14. J. Van Orsdel, E.S. Bartlett, and V.D. Barth, *Refractory Metals (Cb, Ta, Mo, W)*, Defense Metals Information Center, Battelle Memorial Institute, DMIC Review of Recent Developments, 19 January 1968; 28 July 1967; 27 July 1966.
15. F. St. Germain, *Evaluation of RMSRP Tungsten Sheet*, Solar: A Division of International Harvester Co., Report No. ER 1399-6, 9 July 1965 (AD-617 733).
16. "Plastics: Sheet, Rod, Tube, Film", Cadillac Plastics and Chemical Co., 1966 *Catalog and Price List*.

17. J.L. Rand and W. Hinckley, *Dynamic Compression Testing of Shock Mitigating Materials*. U.S. Naval Ordnance Laboratory, Report No. NOLTR 66-39, 9 January 1966 (AD-639 062).
18. J.L. Rand, J.C.S. Yang, and J.M. Marshall, *Dynamic Compression Testing of a Strain-Rate Material*, U.S. Naval Ordnance Laboratory, Report No. NOLTR 65-10, 1 October 1965 (AD-477 279).
19. E.P. Stiles, *Extruding High Density Polyethylene for Quality and Savings*, Paper presented at the 11th Annual Wire and Cable Symposium held in Asbury Park, N.J., 28-30 November 1962 (AD-656 065).
20. G.H. Sollenberger, *General Properties of the New Super-Polyethylenes*, Paper presented at the 4th Annual Wire and Cable Symposium held December 1955 (AD-656 389).

Appendix C

**A FINITE ELEMENT PROGRAM FOR DETERMINING
THE STRESSES AND STRAINS IN
AXISYMMETRIC, ELASTIC BODIES**

Part A: Program Listing (UNIVAC 1108, FORTRAN IV)

Part B: Input Data

Part C: Additional Remarks and Output Data

PART A - PROGRAM LISTING (UNIVAC 1108, FORTRAN IV)

```

ON FOR WILSON
C   ARBITRARY AXISYMMETRIC SOLIDS
COMMON NUMNP,NUMEL,NUMMAT,NUMPC,ACELZ,ANGFO, RAND,TEMP,MTYPE,Q,NP,
1  HED(12),E(8,8,12),RO(12),XXNH(12),R(900),Z(900),UR(900),UZ(900),
2  CODE(900),T(900),IPC(200),JBC(200),PR(200),ANGLE(4)
COMMON /ARG/ PRR(5),ZTZ(5),S(10,10),C(10),TT(4),LM(4),OD(3,3),
1  HH(6,10),RR(4),ZZ(4),C(4,4),H(6,10),D(6,6),F(6,10),TP(6),XI(10)
2  ,EE(7),IX(800,5),EPS(800)
COMMON /BANARG/ MRAND,NUMRLK,R(104),A(108,54)
COMMON /PLANE/ NPP
C   READ AND PRINT OF CONTROL INFORMATION AND MATERIAL PROPERTIES
50 READ (5,1000) HED,NUMNP,NUMEL,NUMMAT,NUMPC,ACELZ,ANGFO,Q,NP,NPP
WRITE (6,2000) HED,NUMNP,NUMEL,NUMMAT,NUMPC,ACELZ,ANGFO,Q,NP
IF (NPP) 54,56,54
54 WRITE (6,2008)
56 DO 50 M=1,NUMMAT
  READ (5,1001) MTYPE,NUMTC,PO(MTYPE),XXNH(MTYPE)
  WRITE (6,2011) MTYPE,NUMTC,PO(MTYPE),XXNH(MTYPE)
  READ (5,1005) (IE(I,J,MTYPE),J=1,8),I=1,NUMTC)
  WRITE (6,2010) (IE(I,J,MTYPE),J=1,8),I=1,NUMTC)
  DO 50 I= NUMTC,6
  DO 50 J=1,8
50 IE(I,J,MTYPE)=F(NUMTC,J,MTYPE)
50 CONTINUE
C   READ AND PRINT OF MODAL POINT DATA
WRITE (6,2004)
L=0
60 READ(5,1002) N, CODE(N),R(N),Z(N),UR(N),UZ(N),T(N)
NL=L+1
ZY=N-L
DR=(R(N)-R(L))/ZY
DZ=(Z(N)-Z(L))/ZX
DT=(T(N)-T(L))/ZX
70 L=L+1
IF(N-L) 100,90,80
80 CODE(L)=0.0
R(L)=R(L-1)+DR
Z(L)=Z(L-1)+DZ
UR(L)=0.0
UZ(L)=0.0
T(L)=T(L-1)+DT
GO TO 70
90 WRITE(6,2002)(KK, CODE(KK),R(KK),Z(KK),UR(KK),UZ(KK),T(KK),KK=NL,N)
IF(NUMNP-N) 100,110,60
100 WRITE (6,2009) N
CALL EXIT
110 CONTINUE
C   READ AND PRINT OF ELEMENT PROPERTIES
WRITE (6,2001)
N=0
130 READ (5,1003) M,(IX(M,I),I=1,5)
140 N=N+1
IF (N-N) 170,170,150
150 IX(N,1)=IX(N-1,1)+1
IX(N,2)=IX(N-1,2)+1
IX(N,3)=IX(N-1,3)+1
IX(N,4)=IX(N-1,4)+1
IX(N,5)=IX(N-1,5)

```

PART A - PROGRAM LISTING (Continued)

```

177 WRITE (6,2003) N, (IX(I,I), I=1,5)
   IF (M=N) 180,180,140
180 IF (NUMEL=N) 190,190,130
190 CONTINUE
C   READ AND PRINT OF PRESSURE BOUNDARY CONDITIONS
   IF (NUMPC) 290,310,290
290 WRITE (6,2005)
   DO 300 L=1,NUMPC
     READ (5,1004) IRC(L),JRC(L),PP(L)
300 WRITE (6,2007) IRC(L),JRC(L),PP(L)
310 CONTINUE
C   DETERMINE BAND WIDTH
   J=0
   DO 340 N=1,NUMEL
     DO 340 I=1,4
       DO 325 L=1,4
         KK=IAPS(IX(N,I)-IX(I,L))
         IF (KK-J) 325,325,320
320 J=KK
325 CONTINUE
340 CONTINUE
   MRAND=2*J+2
C   SOLVE NON-LINEAR STRUCTURE BY SUCCESSIVE APPROXIMATIONS
   DO 350 N=1,NUMEL
350 EPS(N)=0.0
   DO 500 NNN=1,NP
C   FORM STIFFNESS MATRIX
     CALL STIFF
C   SOLVE FOR DISPLACEMENTS
     CALL RANSOL
     WRITE (6,2006) (N,B(2*N-1),B(2*N),N=1,NUMNP)
C   COMPUTE STRESSES
     CALL STRESS
500 CONTINUE
   GO TO 50
1000 FORMAT (12A6/4I5,3F10.2,2I5)
1001 FORMAT (2I5,2F10.0)
1002 FORMAT (I5,F5.0,5F10.0)
1003 FORMAT (6I5)
1004 FORMAT (2I5,F10.0)
1005 FORMAT (8F10.0)
2000 FORMAT (1H1,12A6/
1 30H0 NUMBER OF NODAL POINTS----- I3 /
2 30H0 NUMBER OF ELEMENTS----- I3 /
3 30H0 NUMBER OF DIFF. MATERIALS--- I3 /
4 30H0 NUMBER OF PRESSURE CARDS---- I3 /
5 30H0 AXIAL ACCELERATION----- E12.4/
6 30H0 ANGULAR VELOCITY----- E12.4/
7 30H0 REFERENCE TEMPERATURE----- E12.4/
8 30H0 NUMBER OF APPROXIMATIONS--- I3)
2001 FORMAT (49H1ELEMENT NO.      I      J      K      L      MATERIAL )
2002 FORMAT (1I12,F12.2,2F12.3,2E24.7,F12.3)
2003 FORMAT (1I13,4I6,1I12)
2004 FORMAT (108H1NODAL POINT      TYPE  R-ORDINATE  Z-ORDINATE  R LO
1AD OP DISPLACEMENT  Z LOAD OR DISPLACEMENT TEMPERATURE )
2005 FORMAT (29H0PRESSURE BOUNDARY CONDITIONS/ 24H      I      J      PRESS
1URE )
2006 FORMAT (12H1N.P. NUMBER 18X 2HUR 18X 2HUR / (1I12,2E20.7))

```

PART A — PROGRAM LISTING (Continued)

```

2007 FORMAT (2I6,F12.3)
2008 FORMAT (23H0PLANE STRESS STRUCTURE )
2009 FORMAT (26H0MODAL POINT CARD ERROR N= 15)
2010 FORMAT (15H0 TEMPERATURE 10X SHE(RZ) 9X ANNU(RZ) 11X UHE(T)
      1 10X SNUU(T) 6X PHALPHA(RZ) 7X BHALPHA(T) 15H YIELD STRESS /
      2 (F15.2,7E15.5))
2011 FORMAT (17H0TEMPERIAL NUMBER= 13, 30H, NUMBER OF TEMPERATURE CARDS=
      1 13, 15H, MASS DENSITY= E12.4 ,16H,MODULUS RATIO= E12.4 )
C
      END
      QN FOR STIFF
      SUBROUTINE STIFF
      COMMON NUMNP,NUMEL,JOUMAT,NUMPC,ACELZ,NGFC, RAND,TEMP,MTYPE,Q,NP,
      1 HED(12),E(8,9,12),RO(12),YXINI(12),R(900),Z(900),UR(900),UZ(900),
      2 COF(900),T(900),TC(200),JRC(200),OP(200),ANGLE(4)
      COMMON /ARG/ RRF(15),ZZZ(5),S(10,10),P(10),TT(4),LM(4),DD(3,3),
      1 WH(6,10),RR(4),ZZ(4),C(4,4),H(6,10),D(6,6),F(6,10),TP(6),XI(10)
      2 ,EE(7),IX(800,5),EPS(400)
      COMMON /BANARG/ IPAND,NUMBLK,R(100),J(108,54)
      COMMON /PLANE/ NPP
C
      INITIALIZATION
      REWIND 11
      NR=27
      NC=2*NR
      NC2=2*NC
      STOP=0.0
      NUMBLK=0
      DO 50 N=1,NC2
      R(N)=0.0
      DO 50 V=1,NC
      A(N,V)=0.0
50
C
      FORM STIFFNESS MATRIX IN BLOCKS
      60 NUMBLK=NUMBLK+1
      NH=NP*(NUMBLK+1)
      NM=NH-NB
      NL=NM-NP+1
      KSHIFT=2*NL-2
      DO 210 N=1,NUMEL
      IF ((IX(N,5)) 210,210,65
      65 DO 80 I=1,4
      IF ((IX(N,I)-NL) 80,70,70
      70 IF ((IX(N,I)-NM) 90,90,90
      80 CONTINUE
      GO TO 210
      90 CALL QUAD(N,VOL)
      IF (VOL) 142,142,144
      142 W=ITF (6,2003) *
      STCF=1.0
      144 IF ((IX(N,3)-IX(N,4)) 145,145,145
      145 DO 150 II=1,9
      CC=S(II,10)/S(10,10)
      P(II)=P(II)-CC*P(10)
      DO 160 JJ=1,9
      150 S(II,JJ)=S(II,JJ)-CC*S(10,JJ)
      DO 160 II=1,8
      CC=S(II,9)/S(9,9)
      P(II)=P(II)-CC*P(9)
      DO 160 JJ=1,6

```

PART A - PROGRAM LISTING (Continued)

```

160 S(II,JJ)=S(II,JJ)-CC*S(9,JJ)
C
C      ADD ELEMENT STIFFNESS TO TOTAL STIFFNESS
165 DO 166 I=1,4
164 L=(I)=2+IX(N,I)-2
      DO 200 I=1,4
      DO 200 K=1,2
      II=L*(I)+K-KSHIFT
      KK=2*I-2+K
      B(II)=B(II)+P(KK)
      DO 200 J=1,4
      DO 200 L=1,2
      JJ=L*(J)+L-II+1-KSHIFT
      LL=2*J-2+L
      IF (JJ) 200,200,175
175 IF (N=JJ) 180,195,195
180 WRITE (6,2004) N
      STOP=1.0
      GO TO 210
195 A(II,JJ)=A(II,JJ)+S(KK,LL)
200 CONTINUE
210 CONTINUE
C      ADD CONCENTRATED FORCES WITHIN BLOCK
DO 250 N=NL,NM
      K=2*N-KSHIFT
      B(K)=B(K)+UZ(N)
250 B(K-1)=B(K-1)+UR(N)
C      BOUNDARY CONDITIONS
C      1. PRESSURE B.C.
      IF (IUMPC) 260,310,260
260 DO 300 L=1,NUMPC
      I=IJC(L)
      J=JJC(L)
      PP=PP(L)/6.
      DZ=(Z(I)-Z(J))*PP
      DR=(R(J)-R(I))*PP
      RX=2.0*R(I)+R(J)
      ZX=R(I)+2.0*R(J)
      IF (NPP) 262,264,262
262 RX=3.0
      ZX=3.0
264 II=2*I-KSHIFT
      JJ=2*J-KSHIFT
      IF (II) 280,280,265
265 IF (II=ND) 270,270,280
270 SINA=0.0
      COSA=1.0
      IF (CODE(I)) 271,272,272
271 SINA=SIN(CODE(I))
      COSA=COS(CODE(I))
272 B(II-1)=B(II-1)+RX*(COSA*DZ+SINA*DR)
      B(II)=B(II)-RX*(SINA*DZ-COSA*DR)
280 IF (JJ) 300,300,285
285 IF (JJ=ND) 290,290,300
290 SINA=0.0
      COSA=1.0
      IF (CODE(J)) 291,292,292
291 SINA=SIN(CODE(J))

```

PART A - PROGRAM LISTING (Continued)

```

      COSA=COS(CODE(J))
292 R(JJ-1)=R(JJ-1)+ZX*(COSA*ND+SINA*NP)
      R(JJ)=R(JJ)-ZX*(SINA*ND-COSA*NP)
300 CONTINUE
C      2. DISPLACEMENT P.C.
310 DO 400 M=NL,NH
      IF (M-NUMLP) 315,315,400
315 U=UR(M)
      N=2*M-1-KSHIFT
      IF (CODE(M)) 390,400,316
316 IF (CODE(M)-1.) 317,370,317
317 IF (CODE(M)-2.) 318,390,318
318 IF (CODE(M)-3.) 390,390,390
370 CALL MODIFY(A,R,ND2,MRAND,M,U)
      GO TO 400
380 CALL MODIFY(A,B,ND2,MRAND,M,U)
390 U=UZ(M)
      N=N+1
      CALL MODIFY(A,B,ND2,MRAND,M,U)
400 CONTINUE
C      WRITE BLOCK OF EQUATIONS ON TAPE AND SHIFT UP LOWER BLOCK
      WRITE (11) (B(N), (A(N,M), M=1,MRAND), N=1,ND)
      DO 420 N=1,NC
      K=N+ND
      R(N)=B(K)
      B(K)=0.0
      DO 420 M=1,ND
      A(N,M)=A(K,M)
420 A(K,M)=0.0
C      CHECK FOR LAST BLOCK
      IF (M-NUMLP) 60,490,490
490 CONTINUE
      END FILE 11
      IF (STOP) 490,500,490
500 CALL EXIT
500 RETURN
2003 FORMAT (26H0NEGATIVE AREA ELEMENT NO. 14)
2004 FORMAT (29H0PARAM WIDTH EXCEEDS ALLOWABLE 14)
      END
END FOR QUAD
      SUBROUTINE QUAD(N,VOL)
      COMMON NUMNP,NUMEL,NUMMAT,NUMPC,ACELZ,ANGF0,MRAND,TEMP,MTYPE,Q,NP,
1 HED(12),E(B,A,12),RO(12),XXNH(12),R(900),Z(900),UR(900),UZ(900),
2 CODE(900),T(900),IPC(200),JBC(200),PR(200),ANGLE(4)
      COMMON /ARG/ PRR(5),ZZZ(5),S(10,10),P(10),TT(4),LM(4),DD(3,3),
1 HH(6,10),RR(4),ZZ(4),C(4,4),H(6,10),D(6,6),F(6,10),TP(6),XI(10)
2 ,EE(7),IX(900,5),EPS(600)
      COMMON /BANDPG/ ND,IMPLK,R(108),A(108,54)
      COMMON /PLANE/ NPP
90 I=IX(N,1)
      J=IX(N,2)
      K=IX(N,3)
      L=IX(N,4)
      MTYPE=IX(N,5)
      IX(N,5)=-IX(N,5)
C      FORM STRESS-STRAIN RELATIONSHIP
      TEMP=(T(I)+T(J)+T(K)+T(L))/4.0
      DO 103 M=2,8

```

PART A - PROGRAM LISTING (Continued)

```

      IF (E(M,1,MTYPE)-TEMP) 103,104,104
103 CONTINUE
104 RATIO=0.0
      DEN=E(M,1,MTYPE)-E(M-1,1,MTYPE)
      IF (DEN) 70,71,70
      RATIO=(TEMP-E(M-1,1,MTYPE))/DEN
71 DO 105 KK=1,7
105 EF(KK)=E(M-1,KK+1,MTYPE)+RATIO*(E(M,KK+1,MTYPE)-E(M-1,KK+1,MTYPE))
      TEMP=TEMP-0
      EPSR=EF(7)/EE(1)
      IF (EPSR-EPS(N)) 106,108,108
106 RATIO=(EE(7)/(EPS(N)*EF(1)))*(1.0-XX/N(MTYPE))+XX/N(MTYPE)
      EF(1)=EE(1)*RATIO
      EE(3)=EE(3)*RATIO
108 CONTINUE
      IF (NPP) 84,86,84
84 XY=EF(1)/EE(3)
      COMM=EF(1)/(XX-EF(2)*2)
      C(1,1)=COMM*XX
      C(1,2)=COMM*EF(2)
      C(1,3)=0.0
      C(2,1)=C(1,2)
      C(2,2)=COMM
      C(2,3)=0.0
      C(3,1)=0.0
      C(3,2)=0.0
      C(3,3)=0.0
      C(4,4)=.5*EE(1)/(XX+EE(2))
      GO TO 88
86 C(1,1)=1.0/EE(1)
      C(1,2)=-EE(2)/EE(1)
      C(1,3)=-EE(4)/EE(3)
      C(2,1)=C(1,2)
      C(2,2)=C(1,1)
      C(2,3)=C(1,3)
      C(3,1)=C(1,3)
      C(3,2)=C(2,3)
      C(3,3)=1.0/EE(3)
      CALL SYMINV(C,3)
      C(4,4)=EE(1)/(2.0+2.0*EE(2))
88 DO 110 M=1,3
110 TT(M)=(C(M,1)+C(M,2))*EE(5)+C(M,3)*EE(6))*TEMP
C      FORM QUADRILATERAL STIFFNESS MATRIX
      RRR(5)=(R(I)+R(J)+R(K)+R(L))/4.0
      ZZZ(5)=(Z(I)+Z(J)+Z(K)+Z(L))/4.0
      DO 94 M=1,4
      MM=JX(N,M)
      IF (NPP) 93,89,93
89 IF (S(MM)) 93,91,93
91 R(MM)=.01*RRR(5)
      IF (CODE(MM)) 93,92,93
92 CODE(MM)=1.0
93 RRR(M)=R(MM)
94 ZZZ(M)=Z(MM)
      DO 100 II=1,10
      P(II)=0.0
      DO 95 JJ=1,6
95 HH(JJ,II)=0.0

```

PART A — PROGRAM LISTING (Continued)

```

      DO 100 JJ=1,10
100  S(II,JJ)=0.0
      DO 110 II=1,4
      JJ=IY(N,II)
110  ANGLEN(II)=COEFF(JJ)/0.7,3
      IF (K=1) 125,120,125
120  CALL TRISTF(1,2,3)
      RPR(5)=(RPR(1)+RPR(2)+RPR(3))/3.0
      ZZZ(5)=(ZZZ(1)+ZZZ(2)+ZZZ(3))/3.0
      VOL=YI(1)
      GO TO 130
125  VOL=0.0
      CALL TRISTF(4,1,5)
      VOL=VOL+YI(1)
      CALL TRISTF(1,2,5)
      VOL=VOL+YI(1)
      CALL TRISTF(2,3,5)
      VOL=VOL+YI(1)
      CALL TRISTF(3,4,5)
      VOL=VOL+YI(1)
      DO 140 II=1,6
      DO 140 JJ=1,10
140  HX(II,JJ)=HX(II,JJ)/0.0
130  RETURN
      END
      SUBROUTINE TRISTF(II,JJ,KK)
      COMMON NUMNP,NUMEL,NUMMAT,NUMPC,ACELZ,ANGFO,MBAND,TEMP,MTYPE,Q,NP,
1  PED(12),E(9,9,12),RO(12),XXMIN(12),R(900),Z(900),UR(900),U7(900),
2  CDF(900),T(900),JJC(200),JJC(200),JPC(200),JPC(200),ANGLE(4)
      COMMON /ARG/ RPR(5),ZZZ(5),S(10,10),P(10),T(4),LM(4),OD(3,3),
1  PH(6,10),RR(4),ZT(4),C(4,4),H(6,10),D(6,6),F(6,10),TP(6),XI(10)
2  EE(7),IX(800,5),EPS(900)
      COMMON /PLANE/ NPP
      C      1. INITIALIZATION
      LV(1)=II
      LV(2)=JJ
      LV(3)=KK
      RP(1)=RPR(II)
      RP(2)=RPR(JJ)
      RP(3)=RPR(KK)
      RP(4)=RPR(II)
      ZZ(1)=ZZZ(II)
      ZZ(2)=ZZZ(JJ)
      ZZ(3)=ZZZ(KK)
      ZZ(4)=ZZZ(II)
      R5 DO 90 I=1,6
      DO 90 J=1,10
      F(I,J)=0.0
      90 H(I,J)=0.0
      DO 100 J=1,6
100  D(I,J)=0.0
      C      3. FORM INTEGRAL(C)*T*(C)*(G)
      CALL INTER(XI,RP,ZT)
      D(2,6)=XI(1)*(C(1,2)+C(2,3))
      D(3,5)=XI(1)*C(4,4)
      D(5,5)=XI(1)*C(4,4)
      D(6,6)=XI(1)*C(2,2)

```

PART A - PROGRAM LISTING (Continued)

```

      IF (I/PP) 104,106,104
104  D(2,2)=XI(1)*C(1,1)
      D(3,3)=XI(1)*C(4,4)
      GO TO 108
106  D(1,1)=XI(3)*C(3,3)
      D(1,2)=XI(2)*C(1,3)+C(3,3)
      D(1,3)=XI(5)*C(3,3)
      D(1,6)=XI(2)*C(2,3)
      D(2,2)=XI(1)*C(1,1)+2.0*C(1,3)+C(3,3)
      D(2,3)=XI(4)*C(1,3)+C(3,3)
      D(3,3)=XI(6)*C(3,3)+XI(1)*C(4,4)
      D(3,6)=XI(4)*C(2,3)
108  DO 110 I=1,6
      DO 110 J=1,6
110  D(I,J)=D(I,J)
C      4. FORM COEFFICIENT-DISPLACEMENT TRANSFORMATION MATRIX
      COMM=PP(2)*(ZZ(3)-ZZ(1))+PP(1)*(ZZ(2)-ZZ(3))+RR(3)*(ZZ(1)-ZZ(2))
      DD(1,1)=(RR(2)*ZZ(3)-RR(3)*ZZ(2))/COMM
      DD(1,2)=(RR(3)*ZZ(1)-RR(1)*ZZ(3))/COMM
      DD(1,3)=(RR(1)*ZZ(2)-RR(2)*ZZ(1))/COMM
      DD(2,1)=(ZZ(2)-ZZ(3))/COMM
      DD(2,2)=(ZZ(3)-ZZ(1))/COMM
      DD(2,3)=(ZZ(1)-ZZ(2))/COMM
      DD(3,1)=(RR(3)-RR(2))/COMM
      DD(3,2)=(RR(1)-RR(3))/COMM
      DD(3,3)=(RR(2)-RR(1))/COMM
      DO 120 I=1,3
      J=2*LM(I)-1
      H(1,J)=DD(1,I)
      H(2,J)=DD(2,I)
      H(3,J)=DD(3,I)
      H(4,J+1)=DD(1,I)
      H(5,J+1)=DD(2,I)
120  H(6,J+1)=DD(3,I)
C      ROTATE UNKNOWN'S IF REQUIRED
      DO 125 J=1,2
      I=LM(J)
      IF (ANGLE(I)) 122,125,125
122  SINA=SIN(ANGLE(I))
      COSA=COS(ANGLE(I))
      IJ=2*I
      DO 124 K=1,6
      TEM=H(K,IJ-1)
      H(K,IJ-1)=TEM*COSA+H(K,IJ)*SINA
124  H(K,IJ)= -TEM*SINA+H(K,IJ)*COSA
125  CONTINUE
C      5. FORM ELEMENT STIFFNESS MATRIX (H)*T*(C)*(H)
      DO 130 J=1,10
      DO 130 K=1,6
      IF (H(K,J)) 128,130,128
128  DO 129 I=1,6
129  F(I,J)=F(I,J)+D(I,K)*H(K,J)
130  CONTINUE
      DO 140 I=1,10
      DO 140 K=1,6
      IF (H(K,I)) 138,140,138
138  DO 139 J=1,10
139  S(I,J)=S(I,J)+H(K,I)*F(K,J)

```

PART A — PROGRAM LISTING (Continued)

```

140 CONTINUE
C      6. FORM THERMAL LOAD MATRIX
      IF (NPP) 145,150,145
145 TT(3)=0.0
      COMM=XI(1)*EE(4)
      S(9,9)=S(9,9)+COMM
      S(10,10)=S(10,10)+COMM
150 COMM=RO(MTYPE)*ANGF(.*2
      TP(1)=COMM*XI(7) + XI(2)*TT(3)
      TP(2)=COMM*XI(9) + XI(1)*TT(1)+TT(3))
      TP(3)=COMM*XI(10)+ XI(4)*TT(3)
      COMM=-RO(MTYPE)*ACFLZ
      TP(4)=COMM*XI(1)
      TP(5)=COMM*XI(7)
      TP(6)=COMM*XI(8) +XI(1)*TT(2)
      DO 160 I=1,10
      DO 160 K=1,6
160 P(I)=P(I)+H(K,I)*TP(K)
C      FORM STRAIN TRANSFORMATION MATRIX
400 DO 410 I=1,6
      DO 410 J=1,10
410 HH(I,J)=HH(I,J)+H(I,J)
      RETURN
      END
QN FOR SYMINV
      SUBROUTINE SYMINV(A,NMAX)
      DIMENSION A(4,4)
      DO 200 N=1,NMAX
      D=A(N,N)
      DO 100 J=1,NMAX
100 A(N,J)=-A(N,J)/D
      DO 150 I=1,NMAX
      IF(N-I) 110,150,110
110 DO 140 J=1,NMAX
      IF(N-J) 120,140,120
120 A(I,J)=A(I,J)+A(I,N)*A(N,J)
140 CONTINUE
150 A(I,N)=A(I,N)/D
      A(N,N)=1.0/D
200 CONTINUE
      RETURN
      END
QN FOR INTER
      SUBROUTINE INTER(XI,RP,ZZ)
      DIMENSION RR(1),ZZ(1),XI(1),XM(6),R(6),Z(6),XX(6)
      COMMON /PLANE/ NPP
      DATA (XX(I),I=1,6)/3*1.0,3*3.0/
      COMM=RR(2)*(ZZ(3)-ZZ(1))+PR(1)*(ZZ(2)-ZZ(3))+RR(3)*(ZZ(1)-ZZ(2))
      COMM=COMM/24.0
      R(1)=RR(1)
      R(2)=RR(2)
      R(3)=RR(3)
      R(4)=(R(1)+R(2))/2.
      R(5)=(R(2)+R(3))/2.
      R(6)=(R(3)+R(1))/2.
      Z(1)=ZZ(1)
      Z(2)=ZZ(2)
      Z(3)=ZZ(3)

```

PART A — PROGRAM LISTING (Continued)

```

      Z(4)=(Z(1)+Z(7))/2.
      Z(5)=(Z(2)+Z(3))/2.
      Z(6)=(Z(3)+Z(1))/2.
      IF (MPP) 10,30,10
10  DO 20 I=1,6
20  XM(I)=XX(I)
      GO TO 40
30  DO 35 I=1,6
35  XM(I)=XX(I)*R(I)
40  DO 50 I=1,10
50  YI(I)=0.0
      DO 100 I=1,6
      XI(1)=XI(1)+YM(I)
      XI(7)=XI(7)+XM(I)*P(I)
      XI(8)=XI(8)+XM(I)*Z(I)
      XI(9)=XI(9)+XM(I)*R(I)**2
      XI(10)=XI(10)+XM(I)*P(I)*7(I)
      IF (R(I).LT.1.E-10) GO TO 100
      XI(2)=XI(2)+YM(I)/S(I)
      XI(3)=XI(3)+XM(I)/(R(I)**2)
      XI(4)=XI(4)+YM(I)*2(I)/R(I)
      XI(5)=XI(5)+XM(I)*Z(I)/(R(I)**2)
      XI(6)=XI(6)+XM(I)*2(I)**2/(R(I)**2)
100 CONTINUE
      DO 150 I=1,10
150 XI(I)=XI(I)*COMM
      RETURN
      END
ON FOR MODIFY
      SUBROUTINE MODIFY(A,B,NEG,MBAND,N,U)
      DIMENSION A(108,54),B(108)
      DO 250 M=2,MBAND
      K=N-M+1
      IF (K) 235,235,230
230 B(K)=B(K)-A(K,M)*U
      A(K,M)=0.0
235 K=N+M-1
      IF (NEG-K) 250,240,240
240 B(K)=B(K)-A(N,M)*U
      A(N,M)=0.0
250 CONTINUE
      A(N,1)=1.0
      B(N)=U
      RETURN
      END
ON FOR BANSOL
      SUBROUTINE BANSOL
      COMMON /BANARG/ MM,SUPBLK,P(108),A(108,54)
      NN=54
      NL=NN+1
      NH=NN+NN
      REWIND 11
      REWIND 12
      NF=0
      GO TO 150
C      REDUCE EQUATIONS BY BLOCKS
C      1. SHIFT BLOCK OF EQUATIONS
100 NF=NF+1

```

PART A - PROGRAM LISTING (Continued)

```

      DO 125 N=1,NN
      NN=NN+1
      B(N)=R(NM)
      R(NM)=0.0
      DO 125 M=1,MM
      A(N,M)=A(NM,M)
125  A(NM,M)=0.0
C    2. READ NEXT BLOCK OF EQUATIONS INTO CORE
      IF (NUMBLK-NB) 150,200,150
150  READ (11) (B(N), (A(N,M), M=1,MM), N=NL,NH)
      IF (NB) 200,100,200
C    3. REDUCE BLOCK OF EQUATIONS
200  DO 300 N=1,NB
      IF (A(N,1)) 225,300,225
225  B(N)=B(N)/A(N,1)
      DO 275 L=2,MM
      IF (A(N,L)) 230,275,230
230  C=A(N,L)/A(N,1)
      I=N+L-1
      J=0
      DO 250 K=L,MM
      J=J+1
250  A(I,J)=A(I,J)-C*A(N,K)
      B(I)=B(I)-A(N,L)*B(N)
      A(N,L)=C
275  CONTINUE
300  CONTINUE
C    4. WRITE BLOCK OF REDUCED EQUATIONS ON TAPE 2
      IF (NUMBLK-NB) 375,400,375
375  WRITE (12) (B(N), (A(N,M), M=2,MM), N=1,NB)
      GO TO 100
C    BACK-SUBSTITUTION
400  DO 450 M=1,NN
      NN=NN+1-M
      DO 425 K=2,MM
      L=N+K-1
425  B(N)=B(N)-A(N,K)*B(L)
      NM=N+NN
      B(NM)=B(N)
450  A(NM,NB)=B(N)
      NB=NB-1
      IF (NB) 475,500,475
475  BACKSPACE 12
      READ (12) (B(N), (A(N,M), M=2,MM), N=1,NB)
      BACKSPACE 12
      GO TO 400
C    ORDER UNKNOWN IN C ARRAY
500  K=0
      DO 600 N9=1,NUMBLK
      DO 600 N=1,NN
      NM=N+NN
      K=K+1
600  B(K)=A(NM,NB)
      RETURN
      END
END FOR STRESS
SUBROUTINE STRESS
COMMON NUMNP,NUMEL,NUMMAT,NUMPC,ACELZ,ANGFO,MBAND,TEMP,MTYPE,0,NP,

```

PART A — PROGRAM LISTING (Continued)

```

1 FEO(12),E(8,8,12),PC(12),XXMIN(12),R(900),Z(900),UP(900),UJZ(900),
2 CODE(900),T(900),TBC(200),JBC(200),PR(200),ANGLE(4),SIG(10)
COMMON /ARG/ RRP(5),Z77(5),S(10,10),P(10),TT(4),LM(4),RD(3,3),
1 HH(6,10),RR(4),Z2(4),C(4,4),H(6,10),D(6,6),F(6,10),TP(6),XI(10)
2 ,EF(7),IX(800,5),FES(800)
COMMON /BANAPG/ ND,NUMEL,R(108),A(108,54)
COMMON /PLANE/ HPP
C COMPUTE ELEMENT STRESSES
XKE=0.0
XFE=0.0
MPRTIT=0
DO 300 M=1,NUMEL
N=V
IX(N,5)=IABS(IX(N,5))
MTYPE=IX(N,5)
CALL QUAO(N,VOL)
IX(N,5)=MTYPE
DO 120 I=1,4
II=2*I
JJ=2*IX(N,I)
P(II-1)=B(JJ-1)
120 P(II)=B(JJ)
DO 150 I=1,2
RP(I)=P(I+8)
DO 150 K=1,8
150 RP(I)=PR(I)-S(I+8,K)*P(K)
COMM=S(9,9)*S(10,10)-S(9,10)*S(10,9)
IF (COMM) 155,160,155
155 P(9)=(S(10,10)*RR(1)-S(9,10)*RR(2))/COMM
P(10)=(-S(10,9)*RP(1)+S(9,9)*RR(2))/COMM
GO TO 165
160 P(9)=0.0
P(10)=0.0
165 DO 170 I=1,6
TP(I)=0.0
DO 170 K=1,10
170 TP(I)=TP(I)+HH(I,K)*P(K)
RP(1)=TP(2)
RP(2)=TP(6)
RP(3)=(TP(1)+TP(2)*RRR(5)+TP(3)*Z72(5))/RRR(5)
RP(4)=TP(3)+TP(5)
175 DO 180 I=1,3
SIG(I)=-TT(I)
DO 180 K=1,3
180 SIG(I)=SIG(I)+C(I,K)*RP(K)
SIG(4)=C(4,4)*RP(4)
C CALCULATE ENERGY TERMS
DO 250 I=1,10
COMM=C.0
DO 200 K=1,10
200 COMM=COMM+S(I,K)*P(K)
250 XPE=XPE+COMM*P(I)
XKE=XKE+VOL*PO(MTYPE)*(P(9)**2+P(10)**2)
C
C CALCULATE EFFECTIVE STRAIN
IF (NPP) 251,252,251
251 RP(3)=- (SIG(1)+SIG(2))*EF(2)/EF(1)
252 CC=(PR(1)+RR(2))/2.0

```

PART A - PROGRAM LISTING (Continued)

```

CR=SQRT( ((RP(2)-RP(1))/2.0)**2 + (RP(4)/2.0)**2 )
RF(1)=CC+CR
RR(2)=CC-CR
EPS(1)=SQRT((RR(1)-RR(2))**2+(RR(1)-RR(3))**2+(RR(2)-RR(3))**2)
1 * .707/(1.0+EPS(2))
C OUTPUT STRESSES
C CALCULATE PRINCIPAL STRESSES
CC=(SIG(1)+SIG(2))/2.0
CR=SQRT(((SIG(2)-SIG(1))/2.0)**2 + SIG(4)**2 )
SIG(5)=CC+CR
SIG(6)=CC-CR
SIG(7)=28.648*ATAN2(2.*SIG(4),(SIG(1)-SIG(2)))
C STRESSES PARALLEL TO LINE I-J
I=IX(N,1)
J=IX(N,2)
ANG=2.*ATAN2(Z(J)-Z(I),R(J)-R(I))
COS2A=COS(ANG)
SIN2A=SIN(ANG)
CX=.5*(SIG(1)-SIG(2))
SIG(A)=CX*COS2A+SIG(4)*SIN2A+CC
SIG(9)=2.*CC-SIG(8)
SIG(10)=-CX*SIN2A+SIG(4)*COS2A
IF (MPP) 103,104,103
103 SIG(9)=EE(4)*P(9)
SIG(10)=EE(4)*P(10)
104 IF (MPRINT) 110,105,110
105 WRITE (6,2000)
MPPINT=50
110 MPPINT=MPPINT-1
305 WRITE (6,2001) N,RR(5),ZZZ(5),(SIG(I),I=1,10)
300 CONTINUE
IF (YKE) 310,320,310
310 W=SQRT(XPE/XKE)
WRITE (6,2006) W
320 RETURN
2000 FORMAT (7H1EL.NO. 7X 1HR 7X 1HZ 4X AHR-STRESS 4X BHZ-STRESS 4X
1 AHT-STRESS 3X 9HR7-STRESS 2X 10HMAX-STRESS 2X 10HMIN-STRESS
2 37H ANGLE 1J-STRESS JK-STRESS SHEAR )
2001 FORMAT (I7,2F8.2,1P6E12.4,0P1F7.2,1P3E10.2)
2006 FORMAT (36H0APPROXIMATE FUNDAMENTAL FREQUENCY = E12.5)
END

```

PART B – INPUT DATA

The following is a description of the input data used to describe the problem to the computer:

A. IDENTIFICATION CARD – (72H)

Columns 1 to 72 of this card contain information to be printed with results.

B. CONTROL CARD – (415, 3F10.2, 215)

Columns 1 – 5 Number of nodal points (900 maximum)

6 – 10 Number of elements (800 maximum)

11 – 15 Number of different materials (12 maximum)

16 – 20 Number of boundary pressure cards (200 maximum)

21 – 30 Axial acceleration in the Z-direction

31 – 40 Angular velocity

41 – 50 Reference temperature (stress free temperature)

51 – 55 Number of approximations

56 – 60 = 0 Axisymmetric analysis

= 1 Plane stress analysis

C. MATERIAL PROPERTY INFORMATION

The following group of cards must be supplied for each different material:

First Card – (215, 2F10.0)

Columns 1 – 5 Materials identification – any number from 1 to 12.

6 – 10 Number of different temperatures for which properties are given – 8 maximum

11 – 20 Mass density of material

21 – 30 Ratio of plastic modulus to elastic modulus

Following Cards – (8F10.0) One card for each temperature

Columns 1 – 10 Temperature

11 – 20 Modulus of elasticity – E_r and E_z

21 – 30 Poisson's ratio – ν_{rz}

31 – 40 Modulus of elasticity – E_θ

41 – 50 Poisson's ratio – $\nu_{\theta r}$ and $\nu_{\theta z}$

51 – 60 Coefficient of thermal expansion – α_r and α_z

61 – 70 Coefficient of thermal expansion – α_θ

71 – 80 Yield stress – σ_y

D. NODAL POINT CARDS – (215, F5.0, 5F10.0)

One of the first steps in the structural analysis of a two-dimensional solid is to select a finite element representation of the cross section of the body. Elements and nodal

points are then numbered in two numerical sequences each starting with one. The following group of punched cards numerically define the two-dimensional structure to be analyzed. There is a card for each nodal point and each card contains the following information:

Columns 1 – 5 Nodal point number

5 – 10 Number which indicates if displacements or forces are to be specified

11 – 20 R -ordinate

21 – 30 z -ordinate

31 – 40 XR

41 – 50 XZ

51 – 60 Temperature

If the number in column 10 is

0 – XR is the specified R -load and
 XZ is the specified Z -load.

1 – XR is the specified R -displacement and
 XZ is the specified Z -load.

2 – XR is the specified R -load and
 XZ is the specified Z -displacement.

3 – XR is the specified R -displacement and
 XZ is the specified Z -displacement.

All loads are considered to be total forces acting on a one radian segment (or unit thickness in the case of plane stress analysis). Nodal point cards *must be in numerical sequence*. If cards are omitted, the omitted nodal points are generated at equal intervals along a straight line between the defined

nodal points; the necessary temperatures are determined by linear interpolation; the boundary code (column 10), XR and XZ are set equal to *zero*.

E. ELEMENT CARDS – (615)

1. Order nodal points counterclockwise around element.

2. Maximum difference between nodal point ID must be less than 27.

One card for each element

Columns 1 – 5 Element number

6 – 10 Nodal Point I

11 – 15 Nodal Point J

16 – 20 Nodal Point K

21 – 25 Nodal Point L

26 – 30 Material Identification

Element cards must be in element number sequence. If element cards are omitted, the program automatically generates the omitted information by incrementing by one the preceding I , J , K , and L . The material identification code for the generated cards is set equal to the value given on the last card. The last element card must always be supplied.

Triangular elements are also permissible, they are identified by repeating the last nodal point number (i.e., I , J , K , L).

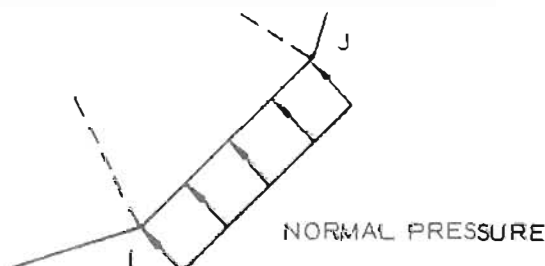
F. PRESSURE CARDS – (215, 1F10.0)

One card for each boundary element which is subjected to a normal pressure.

Columns 1 – 5 Nodal Point I

6 – 10 Nodal Point J

11 – 20 Normal Pressure



As shown above, the boundary element must be on the left as one progresses from I to J . Surface tensile force is input as a negative pressure.

INPUT FOR A TYPICAL PROBLEM

SAMPLE	SABOT	END	PPRESSURE
45A	390	3	31
1	10.0007289	1.0	
0.0	30000000.0	0.29	30000000.0 0.29 1. 1. 100000000.
2	10.000253261	1.0	
0.0	10000000.0	0.33	10000000.0 0.33 1. 1. 100000000.
3	10.000084111	1.0	
0.0	170000.0	0.49	170000.0 0.49 1. 1. 100000000.
1	10.0	0.0	
4	.625	0.0	
5	10.0	0.15	
8	.625	0.15	
9	10.0	0.35	
12	.625	0.35	
13	10.0	0.55	
16	.625	0.55	
17	10.0	0.75	
20	.625	0.75	
21	10.0	0.95	
24	.625	0.95	
25	10.0	1.15	
29	.625	1.15	
20	10.0	1.35	
32	.625	1.35	
33	10.0	1.55	
36	.625	1.55	
37	10.0	1.75	
40	.625	1.75	
41	10.0	1.95	
44	.625	1.95	
45	10.0	2.15	
48	.625	2.15	
49	10.0	2.35	
52	.625	2.35	
53	10.0	2.55	
56	.625	2.55	
57	10.0	2.75	
60	.625	2.75	
61	10.0	2.95	
64	.625	2.95	
65	10.0	3.15	
68	.625	3.15	
69	10.0	3.35	
72	.625	3.35	
74	.875	3.35	
76	1.2	3.35	
83	12.5	3.35	
84	10.0	3.55	
87	.625	3.55	
89	0.94375	3.55	
90	1.2	3.55	
97	12.5	3.55	
98	10.0	3.75	
101	.625	3.75	
103	1.0125	3.75	
104	1.2	3.75	
111	12.5	3.75	
112	10.0	3.95	

INPUT FOR A TYPICAL PROBLEM (Continued)

115	.625	3.05	255	12.5	5.75
116	0.4	3.95	256	10.0	5.95
118	1.08125	3.95	258	.625	5.95
120	1.4	3.95	264	1.6	5.95
126	12.5	3.05	265	1.76875	5.05
127	10.0	4.15	266	2.0	5.95
130	.625	4.15	268	1.2.5	5.95
132	1.0	4.15	270	10.0	6.15
133	1.15	4.15	273	.625	6.15
134	1.40	4.15	278	1.6	6.15
140	12.5	4.15	278	1.8375	6.15
141	10.0	4.35	280	2.0	6.15
144	.625	4.35	283	12.5	6.15
146	1.0	4.35	284	10.0	6.35
147	1.21875	4.35	287	.625	6.35
148	1.4	4.35	292	1.6	6.35
154	12.5	4.35	294	1.90625	6.35
155	10.0	4.55	295	2.2	6.35
157	.625	4.55	297	12.5	6.35
161	1.0	4.55	298	10.0	6.55
162	1.2875	4.55	302	.625	6.55
164	1.6	4.55	308	1.8	6.55
166	12.5	4.55	308	1.975	6.55
170	10.0	4.75	310	2.2	6.55
171	.625	4.75	312	12.5	6.55
175	1.2	4.75	313	10.0	6.75
177	1.35625	4.75	316	.625	6.75
178	1.6	4.75	322	1.8	6.75
183	12.5	4.75	323	2.04375	6.75
184	10.0	4.95	324	2.2	6.75
187	.625	4.95	326	12.5	6.75
190	1.2	4.95	327	10.0	6.95
191	1.425	4.95	330	.625	6.95
192	1.6	4.95	334	1.8	6.95
197	12.5	4.95	338	2.1125	6.95
198	10.0	5.15	340	12.5	6.95
201	.625	5.15	341	10.0	7.15
204	1.2	5.15	344	0.625	7.15
206	1.49375	5.15	351	2.0	7.15
208	1.8	5.15	352	2.18125	7.15
212	12.5	5.15	354	12.5	7.15
213	10.0	5.35	355	10.0	7.35
216	.625	5.35	359	.625	7.35
220	1.4	5.35	365	2.0	7.35
221	1.5625	5.35	366	2.25	7.35
222	1.8	5.35	368	12.5	7.35
224	12.5	5.35	368	10.0	7.55
227	10.0	5.55	372	.625	7.55
230	.625	5.55	373	10.0	7.75
234	1.4	5.55	376	.625	7.75
235	1.63125	5.55	377	10.0	7.95
236	1.8	5.55	380	.625	7.95
240	12.5	5.55	381	10.0	8.15
241	10.0	5.75	384	.625	8.15
244	.625	5.75	385	10.0	8.35
248	1.4	5.75	388	.625	8.35
250	1.7	5.75	388	10.0	8.55
252	2.0	5.75	392	.625	8.55

INPUT FOR A TYPICAL PROBLEM (Continued)

393	10.0	8.75	57	74	75	89	89	3		
396	.625	8.75	58	75	76	90	89	3		
397	10.0	8.95	66	84	85	99	98	1		
400	.625	8.95	69	87	88	102	101	2		
401	10.0	9.15	71	89	90	104	103	3		
404	.625	9.15	70	98	99	113	112	1		
405	10.0	9.35	82	101	102	116	115	2		
408	.625	9.35	84	103	118	117	117	2		
409	10.0	9.55	85	103	104	119	118	3		
412	.625	9.55	93	112	113	128	127	1		
413	10.0	9.75	96	115	116	131	130	2		
416	.625	9.75	99	118	119	133	133	3		
417	10.0	9.95	100	117	120	134	133	3		
420	.625	9.95	107	127	128	142	141	1		
421	10.0	10.15	110	130	131	145	144	2		
424	.625	10.15	113	133	134	148	147	3		
425	10.0	10.35	120	141	142	156	155	1		
428	.625	10.35	123	144	145	159	158	2		
429	10.0	10.50	126	147	162	161	161	2		
432	.625	10.50	127	147	148	163	162	3		
433	10.0	10.70	134	155	156	171	170	1		
436	0.5625	10.70	137	158	159	174	173	2		
437	10.0	10.90	141	162	163	177	177	3		
440	0.5	10.90	143	163	164	178	177	3		
441	10.0	11.1	147	170	171	185	184	1		
443	0.4375	11.1	151	173	174	188	187	2		
444	10.0	11.3	155	177	178	192	191	3		
446	.375	11.3	161	184	185	199	198	1		
447	10.0	11.5	164	187	188	202	201	2		
449	0.3125	11.5	169	191	206	205	205	2		
451	10.0	11.7	160	191	192	207	206	3		
451	0.25	11.7	175	198	199	214	213	1		
452	10.0	11.9	178	201	202	217	216	2		
453	0.1875	11.9	183	206	207	221	221	3		
454	10.0	12.1	184	207	208	222	221	3		
455	.125	12.1	180	213	214	228	227	1		
456	10.0	12.3	192	216	217	231	230	2		
457	0.0625	12.3	197	221	222	236	235	3		
458	30.0	12.5	202	227	228	242	241	1		
1	1	2	6	5				1		
4	5	6	10	9				1		
7	9	10	14	13				1		
12	13	14	18	17				1		
13	17	18	22	21				1		
16	21	22	26	25				1		
19	25	26	30	29				1		
22	29	30	34	33				1		
25	33	34	38	37				1		
28	37	38	42	41				1		
31	41	42	46	45				1		
34	45	46	50	49				1		
37	49	50	54	53				1		
40	53	54	58	57				1		
43	57	58	62	61				1		
46	61	62	66	65				1		
49	65	66	70	69				1		
52	69	70	85	84				1		
55	72	73	88	87				2		
					57	74	75	89	89	3
					58	75	76	90	89	3
					66	84	85	99	98	1
					69	87	88	102	101	2
					71	89	90	104	103	3
					70	98	99	113	112	1
					82	101	102	116	115	2
					84	103	118	117	117	2
					85	103	104	119	118	3
					93	112	113	128	127	1
					96	115	116	131	130	2
					99	118	119	133	133	3
					100	117	120	134	133	3
					107	127	128	142	141	1
					110	130	131	145	144	2
					113	133	134	148	147	3
					120	141	142	156	155	1
					123	144	145	159	158	2
					126	147	162	161	161	2
					127	147	148	163	162	3
					134	155	156	171	170	1
					137	158	159	174	173	2
					141	162	163	177	177	3
					143	163	164	178	177	3
					147	170	171	185	184	1
					151	173	174	188	187	2
					155	177	178	192	191	3
					161	184	185	199	198	1
					164	187	188	202	201	2
					169	191	206	205	205	2
					160	191	192	207	206	3
					175	198	199	214	213	1
					178	201	202	217	216	2
					183	206	207	221	221	3
					184	207	208	222	221	3
					180	213	214	228	227	1
					192	216	217	231	230	2
					197	221	222	236	235	3
					202	227	228	242	241	1
					205	230	231	245	244	2
					210	235	250	249	249	2
					211	235	236	251	250	3
					216	241	242	257	256	1
					217	244	245	260	259	2
					225	250	251	265	265	3
					226	251	252	266	265	3
					231	256	257	271	270	1
					233	259	260	274	273	2
					230	265	266	280	279	3
					243	270	271	285	284	1
					246	273	274	289	287	2
					252	279	294	293	293	2
					253	279	280	295	294	3
					257	284	285	300	299	1
					260	297	288	303	302	2
					267	294	295	309	309	3
					268	295	296	310	309	3
					271	299	300	314	313	1

INPUT FOR A TYPICAL PROBLEM (Continued)

274	302	303	317	316	2
281	309	310	324	322	3
284	313	314	328	327	1
287	316	317	331	330	2
294	323	324	337	337	2
296	323	324	338	339	3
296	324	325	339	338	3
299	327	328	342	341	1
301	330	331	345	344	2
307	338	339	353	352	3
311	341	342	356	355	1
314	344	345	359	358	2
322	352	353	367	366	3
324	355	356	370	369	1
327	369	370	374	373	1
330	373	374	378	377	1
333	377	378	382	381	1
336	381	382	386	385	1
337	385	386	390	389	1
342	389	390	394	393	1
345	393	394	398	397	1
348	397	398	402	401	1
351	401	402	406	405	1
354	405	406	410	409	1
357	409	410	414	413	1
360	413	414	418	417	1
363	417	418	422	421	1
366	421	422	426	425	1
369	425	426	430	429	1
372	429	430	434	433	1
375	433	434	438	437	1
378	437	438	442	441	1
381	439	440	443	442	1
384	441	442	445	444	1
387	444	445	449	447	1
389	447	448	451	450	1
386	448	449	451	451	1
387	450	451	453	452	1
389	452	453	455	454	1
389	454	455	457	456	1
390	456	457	458	459	1
1	2	1000.0			
2	3	1000.0			
3	4	1000.0			
4	8	1000.0			
8	12	1000.0			
12	16	1000.0			
16	20	1000.0			
20	24	1000.0			
24	28	1000.0			
28	32	1000.0			
32	36	1000.0			
36	40	1000.0			
40	44	1000.0			
44	48	1000.0			
48	52	1000.0			
52	56	1000.0			
56	60	1000.0			

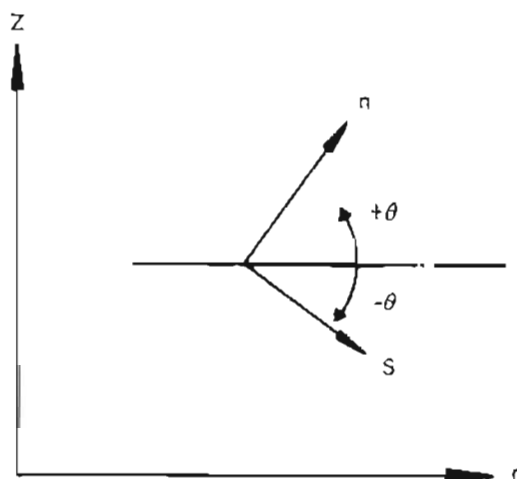
PART C — ADDITIONAL REMARKS AND OUTPUT DATA

A. MATERIAL PROPERTIES

Material properties vs temperature are input for each material in tabular form. The properties for each element in the system are then evaluated by interpolation. The mass density of the material is required only if acceleration loads are specified or if the approximate frequency is desired. Listing of the coefficients of thermal expansion are necessary only for thermal stress analysis. The plastic modulus ratio and the yield stress are specified only if nonlinear materials are used.

B. SKEW BOUNDARIES

If the number in columns 5-10 of the nodal point cards is other than 0, 1, 2 or 3, it is interpreted as the magnitude of an angle in degrees. This angle is shown below.



The terms in columns 31-50 of the nodal point card are then interpreted as follows:

XR is the specified load in the s -direction
 XZ is the specified displacement in the n -direction

The angle θ must always be input as a negative angle and may range from -0.001 to -180 deg. Hence, $+1.0$ deg is the same as -179.0 deg. The displacements of these nodal points which are printed by the program are:

u_r = displacement in the s -direction

u_z = displacement in the n -direction

C. USE OF THE PLANE STRESS OPTION

A one punch in column 60 of the control card indicates the body is a plane stress structure of unit thickness. In the case of plane stress analysis, the material property cards are interpreted as follows:

Columns 11 – 20	Modulus of elasticity – E_r
21 – 30	Poisson's ratio – ν
31 – 40	Modulus of elasticity – E_z

The corresponding stress-strain relationship used in the analysis is:

$$\begin{bmatrix} \sigma_r \\ \sigma_z \\ \tau_{rz} \end{bmatrix} = \frac{E_r}{\mu - \nu^2} \begin{bmatrix} \mu & \nu & 0 \\ \nu & 1 & 0 \\ 0 & 0 & \frac{\mu - \nu^2}{2(\mu + \nu)} \end{bmatrix} \begin{bmatrix} \epsilon_r \\ \epsilon_z \\ \gamma_{rz} \end{bmatrix}$$

where $\mu = \frac{E_r}{E_z}$

D. OUTPUT DATA

The following information is developed and printed by the program:

1. Reprint of input data
2. Nodal point displacements
3. Stresses at the center of each element

4. An approximate fundamental frequency. (The displacements for the given load condition are used as an approximate mode shape in the calculation of a frequency by Rayleigh's procedure. A considerable amount of engineering judgment must be used in the interpretation of this frequency.)

E. PLOT OF FINITE ELEMENT MESH

The program automatically develops a plot of the outline of each element in the

system. This serves as an excellent check on the input data. In order to obtain the plot from AGC's computer operation, an additional charge card must be submitted with the job. If only a plot of the mesh is desired, the calculation of displacements and stresses may be eliminated by specifying more pressure cards than actually exist. The first 30 columns of the identification card are used as a title for the plot.

Appendix D

**ABSTRACT
BIBLIOGRAPHY OF SABOT TECHNOLOGY**

PREFACE

This is the second edition of an abstract bibliography of publications related to sabot technology. The first edition of this bibliography appeared in Sabot Technology Engineering Handbook, Lockheed Propulsion Co. Report No. 800-F, Rev. 0, 15 November 1967. All references contained in the first edition are included in this second edition.

Each of the publications abstracted was reviewed and deemed appropriate to sabot technology. The first edition of the bibliography emphasized projectiles and other shots which incorporated sabots in their design. It therefore included a summary of pertinent data for each different sabot design. This summary of sabot designs and their characteristics is included in this second handbook edition as Appendix A. The number of different sabot designs uncovered during preparation of the second edition was significantly decreased and therefore the sabot summary was not materially revised. The entries added in the second edition of the bibliography emphasizes sabot materials and their properties.

The major subject headings used are the same as those in the first bibliography edition with the exception of two new categories, i. e. a general category and one on obturators. Author and corporate author indexes covering the entire bibliography are included in this issue. Reference entries are numbered sequentially throughout the entire bibliography.

Unclassified references and unclassified abstracts of classified literature have been included in the bibliography. Information concerning classified subjects may be obtained directly from the Defense Documentation Center or from the originating source by authorized users.

BIBLIOGRAPHY

TABLE OF CONTENTS

<u>Section No.</u>	<u>Title</u>	<u>Page</u>
D-1	GENERAL	D-6
D-2	ARMOR-PIERCING, DISCARDING-SABOT (APDS) PROJECTILES	D-7
D-2.1	Canadian 20-PR APDS Shot	D-7
D-2.2	T89 or M331, 76/50 mm HVAPDS Shot	D-8
D-2.3	T102, 120/75-MM HVAPDS Shot	D-11
D-2.4	T137, 90/60-MM HVAPDS Shot	D-12
D-2.5	APFSDS Projectile for 90-105 MM Guns	D-16
D-2.6	CARDE "Minnow" Project	D-16
D-2.7	AMF Optimum Sabot Ammunition Study	D-16
D-2.8	T320 90/40-MM APFSDS Shot	D-19
D-2.9	T382 or M392, 150-MM APDS Shot	D-20
D-2.10	Other APFSDS Shots (371, T346, etc.)	D-25
D-2.11	Delta-Finned, Armor Piercing Shot	D-27
D-2.12	152 mm APFSDS Shot	D-30
D-2.13	Sabot Development for APFSDS Projectiles	D-30
D-2.14	Miscellaneous	D-31
D-3	HIGH EXPLOSIVE, DISCARDING-SABOT (HEDS) PROJECTILES	D-32
D-3.1	75/60-mm HEDS-AA Shell	D-32
D-3.2	75-mm, 90-mm, 120-mm HEDS-AA Shells	D-32
D-3.3	T162, T163 or T164, 155/105-mm HEDS-Shell	D-33

<u>Section No.</u>	<u>Title</u>	<u>Page</u>
D-3.4	T121, 280/203-mm HEDS Shell	D-33
D-3.5	T144, 127/60-mm HEDS-AA Shell	D-35
D-3.6	Other HEDS Shell	D-35
D-4	OTHER SABOT PROJECTILES	D-37
D-4.1	"5/3.75" Spin Stabilized Discarding-Sabot Projectile	D-37
D-4.2	Gun-Launched Anti-Missile Defense (GADS)	D-38
D-4.3	Miscellaneous Sabot Projectiles	D-38
D-5	SMALL-CALIBER SABOT PROJECTILES	D-40
D-5.1	General	D-40
D-5.2	0.22 Caliber Flechette	D-43
D-5.3	Multiple Projectile Shots	D-46
D-5.4	Miscellaneous	D-49
D-6	ROCKET-ASSISTED PROJECTILE (RAP)	D-50
D-7	GUN-LAUNCHED ROCKETS, PROBES, AND SPACE VEHICLES	D-52
D-7.1	High Altitude Research Probes (HARP)	D-54
D-7.2	HARP Instrumentation	D-61
D-7.3	Target Placement System	D-63
D-7.4	Gun-Launched Antimissile System (GLAM)	D-63
D-7.5	Martlet System	D-63
D-7.6	Related Systems	D-63
D-7.7	Ground-Accelerated Space Platform (GASP)	D-64
D-7.8	HIBEX Program	D-65
D-8	TERMINAL BALLISTICS STUDIES	D-66
D-9	FREE FLIGHT AERODYNAMIC TESTING	D-92

<u>Section No.</u>	<u>Title</u>	<u>Page</u>
D-10	GUN DEVELOPMENT STUDIES	D-101
D-11	MUZZLE BLAST EFFECTS	D-108
D-12	MATERIAL PROPERTIES	D-111
D-12.1	Experimental Techniques	D-121
D-12.2	Steels and Refractory Metals	D-123
D-12.3	Lead	D-132
D-12.4	Light Alloys	D-132
D-12.5	Plastics and Rubbers	D-134
D-13	SEALS AND OBTURATORS	D-138
D-14	UNCLASSIFIED ABSTRACTS FROM CLASSIFIED DOCUMENTS	D-139
	AUTHOR INDEX	D-148
	AGENCY INDEX	D-158

ABSTRACTS

D-1 GENERAL

- 1 Dardick, David; Green, Stanley; Rush, Stanley; Fedowitz, Frank, Jr.; "GUN/PROJECTILE SYSTEMS," Space/Aeronautics, Vol. 47, No. 3, March 1967, pp. 92-99.

Gun system analysis starts with the mission goal, target defeat, and works back through inflight ballistics to the weapon itself, making tradeoffs all the way: impact velocity vs. projectile shape, fragment dispersion near the target vs. at the muzzle, peak chamber pressure vs. bore size, etc.

- 2 Doherty, Stephen J.; "SABOT MATERIALS AND DESIGNS FOR HIGH VELOCITY KINETIC-ENERGY ARTILLERY AMMUNITION," U. S. Army Materials Research Agency, Technical Report AMRA TR 67-11, April 1967, Confidential. (AD 382 260)

Experimental ballistic studies were conducted in which fin-stabilized, kinetic-energy artillery projectiles equipped with plastic sabots were launched at high velocity to: (1) determine the feasibility of a three-segment sabot with two incorporated steel load-bearing inserts. (2) evaluate the durability of the plastic coating on the sabot and aluminum fin surfaces to heat and friction developed during inbore travel. Discarding characteristics of the sabot material and their relationship to terminal accuracy were also observed and evaluated. An optimum pressure-velocity level was determined for the sabot material and gun tube. Plastic sabot material molding techniques, procedures, and properties were also presented. The feasibility of internal load-bearing inserts in a sabot to launch fin-stabilized kinetic-energy projectiles was established. Finally, the long-term storage capability of the experimental rounds at temperatures of 40 to 90°F was also noted.

- 3 Geldmacher, R. C.; "THE DYNAMIC BEHAVIOR OF A SLIDING PLASTIC OBTURATING RING AS USED IN THE 152 MM XM578 APFSDS PROJECTILE," Stevens Institute of Technology, Technical Report No. 3488, September 1967. (AD 820 330)

The purpose of this investigation has been to develop analytical and experimental procedures which can be used by ordnance engineers in the design and development of a sliding plastic obturation ring. The analytical formulation defines the parameters to be measured and the analytical solution brings forward the relative importance of each parameter.

- 3 Two sets of measurable quantities, based on the theoretical
(Cont'd) analysis, are given. From these quantities the magnitudes
of the critical parameters of the system can be obtained under
quasi-dynamic and dynamic conditions.

Examples have been calculated which illustrate the effects of
changing critical parameters. Recommendations for design
procedures are given.

- 4 Marshall, Melvin R.; "STRESS ANALYSIS OF FIVE-INCH
ANTI-PERSONNEL PROJECTILES," U. S. Naval Weapons
Laboratory, Technical Memorandum No. T-35/65, December
1965. (AD 370 496)
- 5 Symonds, P. S.; "SURVEY OF METHODS OF ANALYSIS FOR
PLASTIC DEFORMATION OF STRUCTURES UNDER DYNAMIC
LOADING," Brown University, Final Report, NSRDC 1-67,
June 1967. (AD 659 972)

This survey provides a critical study of methods for the analysis
of metal structures under dynamic loads leading to large plastic
deformation. Relevant material behavior and analytical and
numerical methods are summarized. Emphasis is put on criti-
cal study of experiments, particularly on beams, with consider-
ation of strain rate sensitive plastic behavior.

D-2 ARMOR-PIERCING, DISCARDING-SABOT (APDS) PROJECTILES

D-2.1 Canadian 20-PR APDS Shot

- 6 Permuter, L.; Goode, J. B.: "Principles of A. P. Shot Design,
Part II, Experimental Study and Application of New Principles in
the Development of New Sub-Projectiles for the 20 Pr. A. P. D. S.
Shot (U)"; (Confidential Report), Armament Research Establish-
ment, Report 45/54, 1954, AD 71 766.

(Unclassified Abstract) This report forms part of a series dealing with the
principles of design of A. P. shot. A. P. shot design has two objects: The
best penetration for a given gun energy and adequate accuracy. This part
reports research aimed at improving the penetrative performance of A. P.
shot.

- 7 Permuter, L.; Goode, J. B.: "Principles of A. P. Shot Design,
Part III, Sabot Design: Accuracy Trials with Experimental and
Service Designs for the Q. F. 20 Pr Gun (U)"; (Confidential
Report), Armament Research Establishment, Report 46/54,
December 1954, AD 71 765.

Page D-8 Missing

- 12 Ritner, F. C.: "Malfunction Investigation of Shot, HVAPDS-T, 76/50-MM, M331A2, Improvement of Shot, HVAPDS-T, 76/50-MM, M331A2"; (Unclassified Report), General Electric MPR No. 2, 9 December 1954, AD 57 549.
- 13 Ritner, F. C.: "Malfunction Investigation of Shot, HVAPDS-T, 70/50-MM, M331A2, Improvement of Shot, HVAPDS-T, 70/50-MM, M331A2"; (Unclassified Report), General Electric MPR No. 3, 9 January 1955, AD 57 248.
- 14 Ritner, F. C.: "Malfunction Investigation of Shot, HVAPDS-T, 76/50-MM, M331A2, Improvement of Shot, HVAPDS-T, 76/50-MM, M331A2"; (Unclassified Report), General Electric MPR No. 4, 9 February 1955, AD 58 990.
- 15 Ritner, F. C.: "Malfunction Investigation of Shot, HVAPDS-T, 76/50-MM, M331A2, Improvement of Shot, HVAPDS-T, 76/50-MM, M331A2"; (Confidential Report), General Electric MPR No. 5, 9 March 1955, AD 57 250.
- 16 Ritner, F. C.: "Malfunction Investigation of Shot, HVAPDS-T, 76/50-MM, M331A2, Improvement of Shot, HVAPDS-T, 76/50-MM, M331A2"; (Confidential Report), General Electric MPR No. 6, 9 April 1955, AD 72 743.
- 17 Ritner, F. C.: "Malfunction Investigation of Shot, HVAPDS-T, 76/50-MM, M331A2, Improvement of Shot, HVAPDS-T, 76/50-MM, M331A2"; (Confidential Report), General Electric MPR No. 7, 9 May 1955, AD 69 998.
- 18 Ritner, F. C.: "Malfunction Investigation of Shot, HVAPDS-T, 76/50-MM, M331A2, Improvement of Shot, HVAPDS-T, 76/50-MM, M331A2"; (Confidential Report), General Electric MPR No. 8, 9 June 1955, AD 69 999.
- 19 Ritner, F. C.: "Malfunction Investigation of Shot, HVAPDS-T, 76/50-MM, M331A2, Improvement of Shot, HVAPDS-T, 76/50-MM, M331A2"; (Confidential Report), General Electric MPR No. 10, 9 August 1955, AD 74 208.
- 20 "Test of Cartridge, HVAPDS-T, 76-MM, M331A2 for Guns, M32 and T124 (U)"; (Confidential Report), Continental Army Command Report Number 1689-10, 17 August 1955, AD 68 824.
- 21 Ritner, F. C.: "Malfunction Investigation of Shot, HVAPDS-T, 76/50-MM, M331A2, Improvement of Shot, HVAPDS-T, 76/50-MM, M331A2"; (Confidential Report), General Electric MPR No. 11, 9 September 1955, AD 75 694.

- 22 McGregor, J. M.: "Cartridge, 76/50-MM, HVAPDS-T, M331A2"; (Unclassified Report), Aberdeen Proving Ground Report No. DPS/OAC-I-59/3, June 1959, AD 217 548.

(Unclassified Abstract) The following group of reports concerns development of the T89, 76/50MM HVAPDS shot. The study includes armor-piercing ability, accuracy studies, pressure-velocity level, and design and development tests of the plastic-discarding sabot (including one completely moldable model).

Included in the study are design drawings, pictorial representations, and in-flight photographs.

- 23 "Development of Shot, HVAPDS, 76/50-MM, T89E3 for 76-MM Gun, T91, Investigation of Flight Characteristics"; (Unclassified Report), Aberdeen Proving Ground No. P-57205, 13 August 1953, AD 31 204.
- 24 "Development of Shot, HVAPDS, 76/50-MM, T89E3"; (Unclassified Report), Aberdeen Proving Ground No. P-58336, 19 January 1954, AD 31 205.
- 25 Peters, J. D.: "Investigation of Launching and Flight Characteristics of Shot, HVAPDS, 76-MM T89 Series, Models E3 and E5 (U)"; (Confidential Report), Aberdeen Proving Ground, TA1-1302-25, 2 October 1957, AD 146 464.
- 26 Peters, J. D.: "Development Test of Plastic Discarding Sabot Shot for 76-MM Gun, T91 (U)"; (Confidential Report), Aberdeen Proving Ground TA1-5002-8, 22 January 1958, AD 155 206.
- 27 Nelson, J. G.: "Development Tests of Plastic, Discarding Sabot, Shot, T89, for the 76-MM Gun (U)"; (Confidential Report), Aberdeen Proving Ground No. TA1-5002-9, 19 June 1958, AD 300 465.
- 28 Rosan, S. P.; Barnet, F. Robert: "Plastics Sabot Development, 76/50-MM: Report III (U)"; (Confidential Report), NAVORD Report 6195, 24 September 1958, AD 306 933.
- 29 Nelson, J. G.: "Pressure and Velocity Limits and Accuracy of Shot, HVAPDS, 76/50-MM, T89E3, Plastic Sabot (C)"; (Confidential Report), Aberdeen Proving Ground No. TA1-5008-6, 27 October 1958, AD 303 563.
- 30 Bertrand, Guy: "Development of Shot HVAPDS/T, 76-MM (U)"; (Confidential Report), CARDE Report No. 311/59, January 1959, AD 305 806.

- 31 Struve, J. R. : "Test of Shot, HVAPDS, 76/50-MM, Plastic Sabot, T89 (U)"; (Confidential Report), Aberdeen Proving Ground Report No. DPS/TW-426/9, September 1959, AD 312 693.
- 32 Prosen, S. P.; Johnson, Walter T. : "Plastics Sabot Development, 76/50-MM; Report IV (U)"; (Confidential Report), NAVORD Report 6757, 15 December 1959, AD 315 727.
- 33 "Development of 76-MM Hypervelocity Armor-Piercing Discarding-Sabot Shot, T89 Series (U)"; (Confidential Report), University of Pittsburgh TIR 6-6-4A1(3), February 1960, AD 351 778, for U. S. Army Materiel Command.

D-2.3 T102, 120/75-MM HVAPDS Shot

- 34 Huchital, E. : "Design and Development of Shot, HVAPDS-T, 120/75-MM, T102E2 and Shot, HVTP, 120-MM, T106E1"; (Unclassified Report), Electro-Mechanical Research Co., Progress Report Project TA1-1602, 31 March 1953, AD 18 159.

(Unclassified Abstract) Work being performed under the subject contract is the continuation of design and development of shot, T102E2 and T106E1 initiated under the contract and is referred to as Phase II of the project.

Data calculations are started to fix the weight of the T106E1 so that its trajectory crosses that of the sub-projectile of the T106E2 at 1500 yards. Magnesium alloy for experimentation and prototypes of the sabot base and sabot ring is being used. The tooling and machining of a prototype of the shot T102E2 is in progress.

- 35 Bushey, B. W. : "Development of Shot, HVAPDS, 120-MM, T102 (U)"; (Confidential Report), Frankford Arsenal Report No. R-1417, November 1957, AD 157 411.
- 36 Bailey, E. W. : "Accuracy, Armor Plate Penetration and General Evaluation of Shot, HVAPDS-T, 120/75MM, T102E4 for 120-MM Gun, T123 (U)"; (Confidential Report), Aberdeen Proving Ground Report No. TA1-1602-14, 8 March 1957, AD 131 417.
- 37 Thompson, E. W. : "Functioning and Accuracy of Q. F. 120 MM TK Experimental DS/T Practice Shot (C)"; (Confidential Report), Armament Research and Development Establishment Memorandum (P)2/59, January 1959, AD 305 735.

D-2.4 T137, 90/60-MM HVAPDS Shot

(Unclassified Abstract) The first group of reports are General Electric Monthly Progress Reports concerning development and fabrication of HVAPDS-T Shot 90/60-MM, T137 Series.

The second group are Monthly Progress Reports made by General Electric to Picatinny Arsenal for a product engineering study of shot HVAPDS-T, 90-MM, T137E1. There is some detail concerning the design of the sabot and its parts.

The other reports recorded progress in the development of the HVAPDS shot for the 90-MM, tank gun T119 and other related designs. Flight characteristics, terminal ballistics, accuracy, parts security, plate penetration at various obliquities, and general functioning characteristics are studied.

Several inflight photographs of sabot separation, firing records, and pictorial representations are included.

- 38 Hittenberger, O. K.: "Development of HVAPDS-T Shot 90/60-MM, T137 Series"; (Unclassified Report), General Electric MPR No. 1, 9 November 1953, AD 31 948.
- 39 Hittenberger, O. K.: "Development of HVAPDS-T Shot 90/60-MM, T137 Series"; (Unclassified Report), General Electric MPR No. 2, 9 December 1953, AD 31 947.
- 40 Hittenberger, O. K.: "Development of HVAPDS-T Shot 90/60-MM, T137 Series"; (Unclassified Report), General Electric MPR No. 3, 9 January 1954, AD 26 126.
- 41 Hittenberger, O. K.: "Development of HVAPDS-T Shot 90/60-MM, T137 Series"; (Unclassified Report), General Electric MPR No. 4, 9 February 1954, AD 31 946.
- 42 Hittenberger, O. K.: "Development of HVAPDS-T Shot 90/60-MM, T137 Series"; (Unclassified Report), General Electric MPR No. 5, 9 March 1954, AD 31 945.
- 43 Hittenberger, O. K.: "Development and Fabrication of Shot, HVAPDS-T, 90/60-MM, T137 Series"; (Unclassified Report), General Electric MPR No. 6, 9 April 1954, AD 31 944.
- 44 Hittenberger, O. K.: "Development of HVAPDS-T Shot, 90/60-MM, T137 Series"; (Unclassified Report), General Electric MPR No. 7, 9 May 1954, AD 61 433.

- 45 Hittenberger, O. K. : "Development and Fabrication of Shot, HVAPDS-T, 90/60-MM, T137 Series (U)"; (Confidential Report), General Electric MPR No. 10, 9 August 1954, AD 47 965.
- 46 Ritner, F. C. : "Development and Fabrication of Shot, HVAPDS-T, 90/60-MM, T137 Series"; (Unclassified Report), General Electric MPR No. 11, 9 September 1954, AD 47 964.
- 47 Ritner, F. C. : "Development and Fabrication of Shot, HVAPDS-T, 90/60-MM, T137 Series (U)"; (Confidential Report), General Electric MPR No. 12, 9 October 1954, AD 47 963.
- 48 Ritner, F. C. : "Development and Fabrication of Shot, HVAPDS-T, 90/60-MM, T137 Series"; (Unclassified Report), General Electric MPR No. 13, 9 November 1954, AD 56 396.
- 49 Ritner, F. C. : "Development and Fabrication of Shot, HVAPDS-T, 90/60-MM, T137 Series"; (Unclassified Report), General Electric MPR No. 14, 9 December 1954, AD 56 395.
- 50 Ritner, F. C. : "Development and Fabrication of Shot, HVAPDS-T, 90/60-MM, T137 Series (U)"; (Confidential Report), General Electric MPR No. 17, 9 March 1955, AD 68 023.
- 51 Ritner, F. C. : "Development and Fabrication of Shot, HVAPDS-T, 90/60-MM, T137 Series (U)"; (Confidential Report), General Electric MPR No. 18, 9 April 1955, AD 68 022.
- 52 Ritner, F. C. : "Development and Fabrication of Shot, HVAPDS-T, 90/60-MM, T137 Series (U)"; (Confidential Report), General Electric MPR No. 19, 9 May 1955, AD 68 021.
- 53 Ritner, F. C. : "Development and Fabrication of Shot, HVAPDS-T, 90/60-MM, T137 Series (U)"; (Confidential Report), General Electric MPR No. 20, June 1955, AD 68 661.
- 54 Ritner, F. C. : "Development and Fabrication of Shot, HVAPDS-T, 90/60-MM, T137 Series (U)"; (Confidential Report), General Electric MPR No. 21, July 1955, AD 82 324.
- 55 Ritner, F. C. : "Development and Fabrication of Shot, HVAPDS-T, 90/60-MM, T137 Series (U)"; (Confidential Report), General Electric MPR No. 22, 9 August 1955, AD 75 693.
- 56 Ritner, F. C. : "Development and Fabrication of Shot, HVAPDS-T, 90/60-MM, T137 Series (U)"; (Confidential Report), General Electric MPR No. 28, 9 February 1956, AD 101 334.

- 57 Ritner, F. C.: "Shot, HVAPDS-T, 90-MM, T137E1, Product Engineering Study (U)"; (Confidential Report), General Electric MPR No. 2, November 1955, AD 91 746.
- 58 Ritner, F. C.: "Shot, HVAPDS-T, 90-MM, T137E1, Product Engineering Study (U)"; (Confidential Report), General Electric MPR No. 3, December 1955, AD 87 975.
- 59 Ritner, F. C.: "Shot, HVAPDS-T, 90-MM, T137E1, Product Engineering Study"; (Unclassified Report), General Electric MPR No. 4, January 1956, AD 91 610.
- 60 Ritner, F. C.: "Shot, HVAPDS-T, 90-MM, T137E1, Product Engineering Study (U)"; (Confidential Report), General Electric MPR No. 7, April 1956, AD 99 912.
- 61 Ritner, F. C.: "Shot, HVAPDS-T, 90-MM, T137E1, Product Engineering Study (U)"; (Confidential Report), General Electric MPR No. 8, May 1956, AD 105 768.
- 62 Ritner, F. C.: "Shot, HVAPDS-T, 90-MM, T137E1, Product Engineering Study (U)"; (Confidential Report), General Electric MPR No. 9, June 1956, AD 105 769.
- 63 Ritner, F. C.: "Shot, HVAPDS-T, 90-MM, T137E1, Product Engineering Study (U)"; (Confidential Report), General Electric MPR No. 10, July 1956, AD 112 026.
- 64 Ritner, F. C.: "Shot, HVAPDS-T, 90-MM, T137E1, Product Engineering Study (U)"; (Confidential Report), General Electric MPR No. 11, August 1956, AD 112 027.
- 65 Ritner, F. C.: "Shot, HVAPDS-T, 90-MM, T137E1, Product Engineering Study (U)"; (Confidential Report), General Electric MPR No. 12, September 1956, AD 112 581.
- 66 Ritner, F. C.: "Shot, HVAPDS-T, 90-MM, T137E1, Product Engineering Study (U)"; (Confidential Report), General Electric MPR No. 18, March 1957, AD 134 953.
- 67 Ritner, F. C.: "Shot, HVAPDS-T, 90-MM, T137E1, Product Engineering Study (U)"; (Confidential Report), General Electric MPR No. 19, April 1957, AD 139 241.
- 68 Ritner, F. C.: "Shot, HVAPDS-T, 90-MM, T137E1, Product Engineering Study (U)"; (Confidential Report), General Electric MPR No. 20, May 1957, AD 142 937.

- 69 Ritner, F. C.: "Shot, HVAPDS-T, 90-MM, T137E1, Product Engineering Study (U)"; (Confidential Report), General Electric MPR No. 21, June 1957, AD 142 938.
- 70 Ritner, F. C.: "Shot, HVAPDS-T, 90-MM, T137E1, Product Engineering Study (U)"; (Confidential Report), General Electric MPR No. 22, July 1957, AD 142 939.
- 71 Ritner, F. C.: "Shot, HVAPDS-T, 90-MM, T137E1, Product Engineering Study (U)"; (Confidential Report), General Electric MPR No. 23, August 1957, AD 154 476.
- 72 Ritner, F. C.: "Shot, HVAPDS-T, 90-MM, T137E1, Product Engineering Study (U)"; (Confidential Report), General Electric MPR No. 24, September 1957, AD 159 246.
- 73 Ritner, F. C.: "Shot, HVAPDS-T, 90-MM, T137E1, Product Engineering Study (U)"; (Confidential Report), General Electric MPR No. 25, October 1957, AD 159 247.
- 74 Sheffer, Bruce M.: "Shot, HVAPDS-T, 90-MM, T137E1, Product Engineering Study (U)"; (Confidential Report), General Electric MPR No. 26, November 1957, AD 157 226.
- 75 Sheffer, Bruce M.: "Shot, HVAPDS-T, 90-MM, T137E1, Product Engineering Study (U)"; (Confidential Report), General Electric MPR No. 27, December 1957, AD 157 227.
- 76 Sheffer, Bruce M.: "Shot, HVAPDS-T, 90-MM, T137E1, Product Engineering Study (U)"; (Confidential Report), General Electric MPR No. 30, March 1958, AD 159 881.
- 77 Crater, R. E.: "Production Engineering Study of Shot, HVAPDS-T, 90/60-MM, T137E1 (U)"; (Confidential Report), Picatinny Arsenal Technical Report DC-TR: 12-58, December 1958, AD 304 890.
- 78 Sleeper, J. C. Jr.: "Final Engineering Tests of Shot, HVAPDS-T, 90/60-MM, T137E1 Mod 3, for 90-MM Gun, M36 (T119) (U)"; (Confidential Report), Aberdeen Proving Ground Report No. TA1-1460-38, 29 January 1959, AD 305 259.
- 79 Riel, R. H.: "Firing Trials of Shot, HVAPDS-T, 90-MM, T137 (U)"; (Confidential Report), Aberdeen Proving Ground Report No. TA1-1460-23, 18 October 1955, AD 85 041.

- 80 Sleeper, J. C. Jr.: "Development of Shot, HVAPDS-T, 90/60-MM, T137E1, Model 9, for 90-MM Gun, M36, (T119) (U)"; (Confidential Report), Aberdeen Proving Ground Report No. TA1-1460-40, 29 January 1959, AD 305 260.
- 81 Rieden, William J.: "Test of Shot HVAPDS 90-MM T137 Mod 1, with Swivel-Cap Penetrator for Determination of Ballistic Limits Against Armor Plate at Various Obliquities (U)"; (Confidential Report), Aberdeen Proving Ground Report No. DPS/TW-426/6, July 1959, AD 309 709.
- 82 Sleeper, Joseph C. Jr.: "Development of Shot, HVAPDS-T, T137 for 90-MM Gun, M41 (T119 and T139) (U)"; (Confidential Report), Aberdeen Proving Ground Report No. TA1-1460-30, 9 August 1965, AD 149 230.
- 83 Jacobson, Sidney: "Development of the 90-MM T137E1 Mod 3 HVAPDS-T Cartridge for the M36(T119, M41(T139), and T125 Guns (U)"; (Confidential Report), Picatinny Arsenal Technical Report 2443, November 1957, AD 149 394.
- 84 Peters, J. D.: "Development Test of Shot, HVAPDS, 90-MM, T137 (U)"; (Confidential Report), Aberdeen Proving Ground Report No. TA1-1460-35, 6 February 1958, AD 155 211.

D-2.5 APFSDS Projectile for 90-105 MM Guns

- 85 Riel, R.H.: "Development of Armor Piercing, Fin Stabilized, Discarding Sabot, "Arrow" Projectiles for 90 MM and 105 MM Tank Guns"; (Unclassified Report), Aberdeen Proving Ground, No. TA1-1475-1, 21 February 1955, AD 78 795.

D-2.6 CARDE "Minnow" Project

- 86 Hubbard, F. T.: "A Summary of Development on the Minnow Project from February 1956 to March 1957 (U)"; (Secret Report) 13, Technical Memorandum No. 144/57, April 1957, AD 300 017.
- 87 Hubbard, F. T.: "A Summary of Development of the Minnow Project from April 1957 to March 1958 (U)"; (Secret Report) 14, CARDE Technical Memorandum 187/58, April 1958, AD 302 575.

D-2.7 AMF Optimum Sabot Ammunition Study

(Unclassified Abstract) The following list of progress reports contains a theoretical study leading to the design of sabot ammunition of optimum performance, to be used in various conventional guns in the 75 to 280-MM calibre range. Actual design was carried out for the 90-MM T-119 gun, but the procedure is applicable to the other guns mentioned.

The scope of the project is confined to the HVAPDS (Hypervelocity Armor Piercing Discarding Sabot) shot.

A detailed analysis of performance optimization, carried out numerically for an actual 90-MM gun (T-119), plus the development test of the shot, is presented in the above mentioned monthly progress reports of this project.

The final report summarizes the optimization theory developed to date. The theory is presented in dimensionless form to be applicable to a gun of arbitrary calibre. Results of tests of the 90-MM AMF sabot round, as well as the subsequently analyzed spin-cone stabilization procedure, are taken into account in the final report.

- 88 "Design and Development of Optimum Sabot Ammunition for Artillery Weapons"; (Unclassified Report), American Machine and Foundry Report No. PR-1, 29 November 1954, AD 50 201.
- 89 "Design and Development of Optimum Sabot Ammunition for Artillery Weapons"; (Unclassified Report), American Machine and Foundry Report No. PR-2, 30 December 1954, AD 57 850.
- 90 "Design and Development of Optimum Sabot Ammunition for Artillery Weapons"; (Unclassified Report), American Machine and Foundry Report No. PR-3, 31 January 1955, AD 57 849.
- 91 "Design and Development of Optimum Sabot Ammunition for Artillery Weapons"; (Unclassified Report), American Machine and Foundry Report No. PR-4, 28 February 1955, AD 62 912.
- 92 "Design and Development of Optimum Sabot Ammunition for Artillery Weapons"; (Confidential Report), American Machine and Foundry Report No. PR-5, 31 March 1955, AD 65 515.
- 93 "Design and Development of Optimum Sabot Ammunition for Artillery Weapons"; (Confidential Report), American Machine and Foundry Report No. PR-6, 30 April 1955, AD 64 869.
- 94 "Design and Development of Optimum Sabot Ammunition for Artillery Weapons"; (Confidential Report), American Machine and Foundry Report No. PR-7, 31 May 1955, AD 68 033.
- 95 "Design and Development of Optimum Sabot Ammunition for Artillery Weapons"; (Confidential Report), American Machine and Foundry Report No. PR-8, 30 June 1955, AD 67 948.

- 96 "Design and Development of Optimum Sabot Ammunition for Artillery Weapons"; (Confidential Report), American Machine and Foundry Report No. PR-9, 31 July 1955, AD 70 961.
- 97 "Design and Development of Optimum Sabot Ammunition for Artillery Weapons"; (Confidential Report), American Machine and Foundry Report No. PR-10, 31 August 1955, AD 71 295.
- 98 "Design and Development of Optimum Sabot Ammunition for Artillery Weapons"; (Confidential Report), American Machine and Foundry Report No. PR-11, 30 September 1955, AD 76 951.
- 99 "Design and Development of Optimum Sabot Ammunition for Artillery Weapons"; (Confidential Report), American Machine and Foundry Report No. PR-13, 30 November 1955, AD 82 732.
- 100 "Design and Development of Optimum Sabot Ammunition for Artillery Weapons"; (Confidential Report), American Machine and Foundry Report No. PR-14, 30 December 1955, AD 84 548.
- 101 "Design and Development of Optimum Sabot Ammunition for Artillery Weapons"; (Confidential Report), American Machine and Foundry Report No. PR-15, 31 January 1956, AD 88 042.
- 102 "Design and Development of Optimum Sabot Ammunition for Artillery Weapons"; (Confidential Report), American Machine and Foundry Report No. PR-17, 30 March 1956, AD 95 641.
- 103 Finch, H. Lt.: "Development Test of Shot, HVAPDS-T, 90/54-MM T-, Optimum Sabot (Accuracy and Plate Phase)"; (Confidential Report), Aberdeen Proving Ground TAI-5002-5, March 1956, AD 107 744.
- 104 "Design and Development of Optimum Sabot Ammunition for Artillery Weapons"; (Confidential Report), American Machine and Foundry, Final Report, 30 September 1956, AD 127 567.
- 105 "Design and Development of Optimum Sabot Ammunition for Artillery Weapons"; (Confidential Report), American Machine and Foundry Report No. PR-18, 15 June 1956, AD 108 876.

D-2.8 T320 90/40-MM APFSDS Shot

(Unclassified Abstract) The following list of reports covers development of the APFSDS, 90-MM, T320 shot for the 90-MM smoothbore gun.

During development, problems arose concerning cartridge extraction and fin damage. The cartridge case of the T320 was bulging at the side walls near the base flange because of firing pressure. The fins were damaged because of excessive aerodynamic heating, causing some accuracy loss. Both situations were overcome satisfactorily after a number of changes in procedure and design.

After evaluation of various materials, the lightest possible sabot was developed for the launch. The sabot consisted of four segments and was discarded shortly after it left the muzzle. Many in-flight photographs, firing records, accuracy reports, and drawings are included in the reports.

- 106 Bailey, E. W.: "Development of Shot, APFSDS, 90/40-MM T320 for 90-MM Smoothbore Guns"; (Confidential Report), Aberdeen Proving Ground TA1-1475, 21 November 1957, AD 151 245.
- 107 Carothers, H. E. W.: "Development of Lightweight Sabot for Shot, APFSDS, 90/40-MM T320"; (Confidential Report), Aberdeen Proving Ground TA1-1475-7, 27 January 1958, AD 155 273.
- 108 Miller, O. G.: "Development of Shot, 90/40-MM, APFSDS, T320"; (Confidential Report), Aberdeen Proving Ground TA1-1475-19, May 1958, AD 300 425.
- 109 Miller, O. G.: "Development of Shot, 90/40-MM, APFSDS, T320"; (Confidential Report), Aberdeen Proving Ground TA1-1475-18, 4 June 1958, AD 300 486.
- 110 Miller, O. G.: "Development of Shot, 90/40-MM, APFSDS, T320"; (Confidential Report), Aberdeen Proving Ground TW-418-1, 25 June 1958, AD 300 426.
- 111 Allen, Ralph H.: "Test of Cartridge, 90/40-MM, APFSDS, T320E60, and Cartridge, 90-MM, HEFS, T340E14"; (Confidential Report), Aberdeen Proving Ground TA1-1475-15, 12 August 1958, AD 301 629.
- 112 Miller, O. G.: "Development of Shot, 90/40-MM, APFSDS, T320"; (Confidential Report), Aberdeen Proving Ground TW 418-3, 4 September 1958, AD 301 967.
- 113 Miller, O. G.: "Development of Shot, 90/40-MM, APFSDS, T320"; (Confidential Report), Aberdeen Proving Ground TW-418-4, 15 September 1958, AD 302 188.

- 114 Miller, O.G.: "Development of Shot, 90/40-MM, APFSDS, T320"; (Confidential Report), Aberdeen Proving Ground TW-418-5, 15 May 1958, AD 300 428.
- 115 Miller, O.G.: "Development of Shot, 90/40-MM, APFSDS, T320"; (Confidential Report), Aberdeen Proving Ground TW-418-10, 22 September 1958, AD 304 717.
- 116 Miller, O.G.: "Development of Shot, 90/40-MM, APFSDS, T320"; (Confidential Report), Aberdeen Proving Ground TW-418-11, 7 November 1958, AD 303 744.
- 117 Miller, O.G.: "Development of Shot, 90/40-MM, APFSDS, T320"; (Confidential Report), Aberdeen Proving Ground TW-418-12, 12 November 1958, AD 303 745.
- 118 Miller, O.G.: "Development of Shot, 90/40-MM, APFSDS, T320"; (Confidential Report), Aberdeen Proving Ground TW-418-13, 20 January 1959, AD 304 882.
- 119 Miller, O.G.: "Development of Shot, 90/40-MM, APFSDS, T320"; (Confidential Report), Aberdeen Proving Ground TW-418-15, 11 February 1959, AD 305 569.
- 120 Miller, O.G.: "Development of Shot, 90/40-MM, APFSDS, T320"; (Confidential Report), Aberdeen Proving Ground TW-418-16, 12 February 1959, AD 305 626.
- 121 Miller, O.G.: "Development of Shot, APFSDS, 90/40-MM, T320 Series"; (Confidential Report), Aberdeen Proving Ground TW-418-17, 22 April 1959, AD 307 410.

D-2.9 T382 or M392, 150-MM APDS Shot

(Unclassified Abstract) The following group of reports deals with studies on or related to the M392. The studies include:

- (1) Comparison studies of U.K. and U.S. rounds
- (2) Propellant studies
- (3) Emergency zero studies
- (4) Ballistic tests (interior, exterior and terminal)
- (5) Temperature tests
- (6) Design analyses
- (7) Jump evaluation

- (8) Cartridge tests
- (9) Tube wear studies
- (10) Dispersion tests
- (11) Accuracy tests
- (12) Penetration capabilities

Several photographs, charts, graphs, etc., are included concerning all aspects of the testing. Very little detailed sabot information is included, however. The majority of the information relates firing test results.

- 122 Allen, Ralph H.: "Test of Cartridge, 105-MM, APDS, T382"; (Confidential Report), Aberdeen Proving Ground Report No. DPS/DSCLOG 517-FY58/1, April 1959, AD 306 683.
- 123 Allen, Ralph H.: "Test of U.S. Propellant-Ignition and Shot, APDS, M392A1 for 105-MM Gun, M68"; (Confidential Report), Aberdeen Proving Ground Report No. DPS/DCSLOG-517-FY58/2, February 1960, AD 315 352.
- 124 Allen, R.H.: "Evaluation of Preproduction Shot, APDS, 105-MM M392A1 for M68 Gun "; (Secret Report) 4, Aberdeen Proving Ground Report No. DPS/OAC-I/60/2, June 1960, AD 317 307.
- 125 Heinemann, Robert W.; Schimmel, Robert T.: "Development of a Bridgewire Initiator for the 105-MM Tripartite Round "; (Secret Report) 7, Picatinny Arsenal Technical Memorandum ORDBB-TE9-31, August 1960, AD 319 754.
- 126 Lamon, H.J.; Elsner, J.W.: "Determination of Emergency Zero for M60 Tank (105-MM Gun, M68, Firing 105-MM Shot, HVAP-DS-T, M392E1)"; (Confidential Report), Aberdeen Proving Ground Report No. DPS-102, November 1960, AD 319 945.
- 127 Allen, Ralph H.: "Test of UK Gun, 105-MM TK X15E8, APDS and HESH Ammunition, and Related Components"; (Confidential Report), Aberdeen Proving Ground Report No. DPS-127, January 1961, AD 321 189.
- 128 Yuen, Jason G.: "Desert Summer Environmental Test of Cartridge, 105-MM, APDS, M392 and M392A1"; (Confidential Report), Aberdeen Proving Ground Report No. DPS/OTA-48, March 1961, AD 322 266.

- 129 Allen, Ralph H.: "Production Evaluation of Cartridge, 105-MM, APDS-T, M392E1"; (Confidential Report), Aberdeen Proving Ground Report No. DPS-153, March 1961, AD 322 267.
- 130 Rieden, W.J.: "Preliminary Evaluation of T36 and T28 Propellants with Projectile, APDS, M392A1 for 105-MM Guns, M68 (US) and S7A1 (UK)"; (Confidential Report), Aberdeen Proving Ground Report No. DPS-207, May 1961, AD 323 049.
- 131 Angstadt, R.P.: "Granulation Test of T36 Propellant for Cartridge, 105-MM, APDS-T, M392E1"; (Confidential Report), Aberdeen Proving Ground Report No. DPS-257, June 1961, AD 323 961.
- 132 Callis, Ben: "Evaluation of Shot, APDS-T, 105-MM, M392E1 (Modified Forward Sheath) with T36 Propellant"; (Confidential Report), Aberdeen Proving Ground Report No. DPS-279, July 1961, AD 324 305.
- 133 Elsnor, James: "Jump Firings and Tube-Wear-Effect Studies of APDS-T, M392E1, and HESH, M393 (UK), 105-MM Cartridges for the M60 Tank"; (Confidential Report), Aberdeen Proving Ground Report No. DPS-311, August 1961, AD 324 918.
- 134 "Report of Project No. 2167 Service Test of Cartridge, 105-MM, APDS-T, M392E1 "; (Secret Report)8, U.S. Army Armor Board, Fort Knox, Kentucky, 14 December 1961, AD 326 862.
- 135 Lindsey, W.L.: "Production Engineering Test of M115B1 Steel Cartridge Case for 105-MM, M68 Gun"; (Unclassified Report), Aberdeen Proving Ground Report No. DPS-428, January 1962, AD 270 162.
- 136 Allen, Ralph H.: "Test of Laminar Coolant in Cartridge, 105-MM, APDS-T, M392E1, for 105-MM Gun, M68"; (Confidential Report), Aberdeen Proving Ground Report No. DPS-412, February 1962, AD 327 736.
- 137 Reynolds, M.A.: "Test of 105-MM Gun Tank, M60E1, Pilot No. 1 (Turret Phase)"; (Confidential Report), Aberdeen Proving Ground Report No. DPS-438, February 1962, AD 327 737.
- 138 Dempsey, R.N.: "Safety Certification Test of T36 Propellant with Projectile, APDS-T, M392E1 for Gun, 105-MM, M68"; (Confidential Report), Aberdeen Proving Ground Report No. DPS-449, February 1962, AD 328 041.

- 139 Lindsey, W.L.: "Granulation Test of MP, T36 Propellant with 105-MM Shot, APDS-T, M392E1 for Gun, M68"; (Confidential Report), Aberdeen Proving Ground Report No. DPS-460, February 1962, AD 327 739.
- 140 Dempsey, R.N., "Production Engineering of Armor-Penetrating Capabilities of Projectile, 105-MM, APDS-T, M392 "; (Secret Report) 5, Aberdeen Proving Ground Report No. DPS-492, March 1962, AD 328 882L.
- 141 Ages, J.A. Jr.: "Accuracy Test of 105-MM, M68 Gun Tube No. 978"; (Confidential Report), Aberdeen Proving Ground Report No. DPS-499, AD 328 570.
- 142 "Service Test of Cartridge, 105-MM, APDS-T, M392E1"; (Confidential Report), U.S. Army Artic Test Board Report No. 2-22, 9 May 1962, AD 329 523.
- 143 Wagner, E.W.: "Artic Winter Environmental Tests, 1961-62, of Breech Operating Cam for Gun, 105-MM, M68; Cartridge, 105-MM, APDS, M392E1; Cartridge, 105-MM, HEP-T, M393E1; and Cartridge, 105-MM, HEAT-T, T384E4"; (Confidential Report), Aberdeen Proving Ground Report No. DPS/OTA-148, July 1962, AD 330 176.
- 144 Echtenkamp, A.: "Metal-Parts Security of Projectile, 105-MM, APDS-T, M392E3, Special Lot FA-5-MPC-15"; (Confidential Report), Aberdeen Proving Ground Report No. DPS-602, July 1962, AD 331 499.
- 145 Allen, Ralph H.: "Preliminary Evaluation of Projectile 105-MM, APDS-T M392E3, Assembled with Uranium Alloy Nose Pad Component"; (Confidential Report), Aberdeen Proving Ground Report No. DPS-606, July 1962, AD 331 125.
- 146 Dempsey, R.N.: "Production Engineering Test to Investigate Accuracy Dispersion of Projectile, 105-MM, APDS-T, M392"; (Confidential Report), Aberdeen Proving Ground Report No. DPS-515, August 1962, AD 331 593.
- 147 Allen, Ralph H.: "Second Evaluation of Projectile, 105-MM, APDS-T, M392E3, Assembled with D38 Alloy Nose-Pad Component"; (Confidential Report), Aberdeen Proving Ground Report No. DPS-667, September 1962, AD 332 154.
- 148 Zeller, G.A.; Kirby, R.L.; Bolte, P.L.: "Report of the Group Appointed to Evaluate the 105-MM APDS, M392A1, and Heat, M456, Projectiles "; (Secret Report), USA Armor Board BRL Memorandum Report No. 1446, January 1963, AD 334 411.

- 149 "Report of USATECOM Test Project No. 1C-3651-60 (23-OBX), Check Test of Cartridge, 105-MM, APDS-T, M392A2"; (Confidential Report), U.S. Army Arctic Test, 25 April 1963, AD 335 917L.
- 150 Crisman, W.N.: "Comparison Test of Projectile, 105-MM, APDS-T, M392A1"; (Confidential Report), Aberdeen Proving Ground Report No. DPS-986, June 1963, AD 337 950.
- 151 "Development of Ammunition for M68 105-MM Gun Cannon "; (Secret Report), U.S. Army Materiel Command Technical Information Report 1-1-2J5 Supplement I, October 1963, AD 347 105.
- 152 "Minutes of the Meeting of Working Group "A" - Tanks - of the Trilateral Military Subcommittee"; (Confidential Report), Military Assistance Advisory Group, Bonn, Germany, Report No. WGA-MM, November 1963, AD 350 145.
- 153 Dempsey, R.N.: "Final Report of Product Improvement Test of Projectile, 105-MM, APDS-T, M392 (Lubrication of Sabot Groove)"; (Confidential Report), Aberdeen Proving Ground Report No. DPS-1332, May 1964, AD 349 915.
- 154 Scudder, Russell W.: "Final Report of Engineer Design Test of Armor Plate, Steel, Cast and Rolled, versus Projectile, 105-MM, APDS-T (Ballistic Penetration Data)"; (Confidential Report), Aberdeen Proving Ground Report No. DPS-1616, April 1965, AD 359 701.
- 155 Demaree, C.L.: "Final Report of Engineer Design Test of Ribbed Cast Armor (Ballistic Evaluation)"; (Confidential Report), Aberdeen Proving Ground Report No. DPS-1643, April 1965, AD 360 016L.

(Unclassified Abstract) Cast homogeneous steel armor ribbed plates with three different rib designs were tested with 105-mm ADPS-T, M392 and AP-T, T182E1 projectiles during the period 21 January to 28 February 1965. The V-50 ballistic limits (protection) were determined at 60 degrees obliquity with both projectile types. The ribbed plate designs were compared with each other and rated against flat cast armor on a weight-to-weight basis.

Photographs of plate damage are included along with round-by-round firing data.

- 156 "Development of Ammunition for M68 105-MM Gun Cannon "; (Secret Report), U.S. Army Materiel Command Technical Information Report 27.3.3.1, January 1966, AD 369 753.

D-2.10 Other APFSDS Shots (371, T346, etc.)

(Unclassified Abstract) The following list of reports deals with development of several different APFSDS shots. The following aspects of development are included:

- (1) A limited range target-practice round simulating the T320, APFSDS
 - (2) A new fin design to resist in-gun and aerodynamic heating damage
 - (3) Accuracy and flight performance of T346E17 and T346E17 Mod. 1; spaced-armor plate penetration of the T346E17 Mod. V
 - (4) Results of U. S. antitank lethality trials in which KE projectiles were used
 - (5) Development of a smoke tracer as the trajectory-sensing device to be incorporated in the delta-wing shot
- 157 "Development of 105-mm Hypervelocity Armor-Piercing Discarding Sabot Shot, T279 (U)"; (Confidential Report, U.S. Army Material Command, Technical Information Report 6-9-4A1(3). December 1957, AD 311 633.
 - 158 Allen, R.: "Development Test of Shot, HVAPDS-T, 105/60 mm, T279 (C); (Confidential Report), Aberdeen Proving Ground Report No. TA1-1503-4, 28 January 1957, AD 122 068.
 - 159 Allen, R. H.: "Test of Shot, Quasi, APFSDS, for 90-mm Gun T208E4 (U)"; (Confidential Report), Aberdeen Proving Ground Report No. TW-424-1, 11 August 1958, AD 301 446.
 - 160 "Report on XM60 Weapon System Evaluation (U) "; (Secret Report)⁹, Aberdeen Proving Ground First Report on Project TW-419, October 1958, AD 327 007.
 - 161 Miller, D. G.: "Development of Shot, 90/40-mm, APFSDS, Quasi, T371 (U)"; (Confidential Report), Aberdeen Proving Ground Report No. DPS/TW-424-2, March 1959, AD 306 432.
 - 162 Miller, D. G.: "Evaluation of Cartridge, APFSDS, 90/40 mm, T342, in T139 Gun (U)"; (Confidential Report), Aberdeen Proving Ground Report No. DPS/TW-426/5, June 1959, AD 308 615.
 - 163 Jacobson, Sidney; Barrieres, Elie L.: "A Proposed Armament System for Medium Tanks (U)"; (Confidential Report), Feldman Research and Engineering Laboratories, Technical Memorandum Report No. ORDBB-TE 5-9, July 1959, AD 312 751

(Unclassified Abstract) This report describes an armament system designed to provide increased firepower for existing medium tanks and to provide a weapon system for future generation tanks. The system consists of a 105-mm smoothbore gun designed to minimize turret intrusion and gun length. It fires a discarding-sabot, kinetic-energy projectile capable of penetrating more than five inches of armor plate at 60° obliquity at a range of 2000 yards or six inches at 60° at ranges up to 500 yards. The ammunition complement of this system will include HEAT, HE, and WP cartridges.

The system proposed in this report is designed to incorporate discarding-sabot and heat ammunition of minimum size and weight for ease of handling and rapid loading to minimize time to hit.

- 164 Sleeper, J. C.: "Development of Shot, APFSDS, 105/40-mm, T346E17 and T346E17 Mod I, for 105-mm Gun, T210 (U)"; (Confidential Report), Aberdeen Proving Ground Report No. DPS/TW-426/7, November 1959, AD 313 368.
- 165 Sleeper, J. C.: "Development of Shot, APFSDS, 105/40-mm, T346E17, for 105-mm Gun T210 (U)"; (Confidential Report), Aberdeen Proving Ground Report DPS/TW-420/1, April 1959, AD 306 685.
- 166 Herring, J. L.: "Development and Fabrication of T384 Ammunition for Gun, 105-mm, M68 (U)"; (Confidential Report), The Budd Company Report PR-15, December 1961, AD 327 686.

(Unclassified Abstract) This is the fifteenth and final progress report for Part L of this contract.

All T384 rounds were delivered. Final engineering and safety tests were satisfactory. User tests are complete and are being evaluated. The round exhibited superior performance in all tests made to date. The probable error characteristics are about 0.08 at 1000 meters, 0.10 at 1200 meters and 0.20 at 2000 meters. The first-round hit probability is excellent. Gun crews can sense a hit or miss when using the round, thus providing valuable time for obtaining a second shot at a target.

Firing tests for the heat, APDS, and HEP rounds using the M60 tank are included.

- 167 "Development of 105-mm Armor-Piercing Fin-Stabilized Discarding-Sabot Shot, T346 (U)"; (Confidential Report, US Army Material Command Technical Information Report 6-9-1A2(1) TIR 6-9-1A2(1), September 1959, AD 311 639.

(Unclassified Abstract) This report covers development of the T223 105-mm smoothbore tank gun designed to provide a special weapon for continuing the test program for armor-piercing fin-stabilized discarding sabot projectiles.

The 40-mm penetrator and the windshield of the T320E10 90-mm APFSDS shot were adopted for the T346 shot tested in the T223 gun.

- 168 Benjamin, William C. Jr.; Gholstron, William; "Compilation of Results Obtained from Some U.S. Firings of Kinetic Energy Projectiles Against Tanks (U)"; (Confidential Report), BRL Memorandum Report No. 1295, August 1960, AD 320 090.
- 169 Sissom, B.; Lamon, Lt. H.; Anderson, H. B.: "Visit to Fort Hood, Texas Regarding Inaccuracy of the M60 Tank-Gun-Ammunition System (U) "; (Secret Report)¹⁰, Aberdeen Proving Ground Report No. DPS-64, September 1960, AD 319 077.
- 170 Erwin, T. W.: "Development of Smoke Tracer for APDS Shot (U)"; (Confidential Report), Aberdeen Proving Ground Report No. DPS-483, March 1962, AD 328 420.
- 171 Permutter, L.; Temple, E. P.; James, S. M.: "Uranium Alloy and Tungsten Alloy Cores for A.P.D.S. Shot, Comparative Plating Trials in 105-mm and 120-mm Calibres (U) "; (Secret Report)¹⁵, Royal Armament Research and Development Establishment Memorandum (P)13/63, February 1963, AD 337 629.
- 172 Nadin, V.: "Antitank Projectile"; (Unclassified Report), Foreign Technology Division Translation FTD-IT-63-643, 23 August 1963, AD 428 312.

(Unclassified Abstract) General discussion and brief history of armor piercing, subcalibre sabot projectiles.

- 173 Bertrand, G.; Hansen, Capt. P.: "Improved APDS Shot for Tank Guns (U) "; (Secret Report)¹², CARDE T. N. 1601/64, July 1964, AD 357 466.

(Unclassified Abstract) This article includes a brief discussion of the development of armor protection and of antitank projectiles designed to defeat such armor. Three types of projectiles - armor piercing, sub-calibre, and shaped charge - are described.

- 174 Dempsey, Robert N.: "Research Test of Cartridges, 105-mm, UK, APDS-T, L52A1 and US, Heat-T, M456 Series for BRL Study (U) "; (Secret Report)¹¹, Aberdeen Proving Ground Report No. DPS-1983, April 1966, AD 371 829.

D-2.11 Delta-Finned, Armor Piercing Shot

- 175 Huchital, Eugene; "Development of Delta Wing Armor Penetrating Shot (U)"; (Confidential Report), Electro Mechanical Research Co. Report No. 2, September 1958, AD 302 242.

(Unclassified Abstract) This and following EMRC reports include a portion of the design and development of a delta-wing armor-penetrating shot. Aside from the normal studies of tube wear, accuracy, penetration capabilities, etc. some history of previous work and some stress analysis of the carrier are included. Detailed description of the sabot is given.

- 176 Jacobson, Sidney; Barrieres, Elie L.: "Design and Testing of a Delta-Finned, Discarding Sabot, Armor-Penetrating Projectile for Use in the Smoothbore 90mm Gun, T208E4 (U)"; (Confidential Report), Feltman Research and Engineering Laboratories Technical Memorandum Report Nr. ORDBB-TE5-10, June 1959, AD 312 180.

(Unclassified Abstract) Two designs of delta-finned, discarding-sabot, armor-penetrating shot were made and tested. These designs showed that fin deterioration from in-gun and aerodynamic heating common to other hypervelocity, fin-stabilized ammunition had been eliminated. Propellant gas obturation was excellent even at the fiftieth round level in the 90-mm smoothbore gun T208E4. Deficiencies were noted, however, in the launching of the sub-projectile; launching imparted excessive yaw to the sub-projectile and caused erratic flight. Retardation of the flight projectile was lower than that of the arrow design; this was anticipated from experimental wind tunnel data.

Several in-flight photographs, pictorial representations, and drawings of the projectile and sabot are included.

- 177 Huchital, Eugene: "Development of Delta Wing Armor Penetrating Shot (U)"; (Confidential Report), EMRC Report No. 11, March 1960, AD 315 893.

(Unclassified Abstract) Nine rounds of shot, F.S., 105-mm, Mod 3, were proof-tested at the Aberdeen Proving Ground for general flight performance and security of parts. Velocities were of the order of 5550 feet per second, with chamber pressures at about 52,000 psi. Several sabot "T" sections were recovered and examined.

- 178 Crox, J. F. Jr., ; "Development of Shot, 105/40-mm APFSDS, Mod. 3 (U)"; (Confidential Report), Aberdeen Proving Ground Report No. DPS/TW-426/13, April 1960, AD 315 926.

(Unclassified Abstract) Ten rounds of 105-mm, FS, Mod. 3 ammunition for the T210 gun were test-fired on a 1000-yard range. It was concluded that the stability and drag characteristics of the Model 3 design are good over a range of 1000 yards, and that the sabot-discarding mechanism is workable, though too lightly joined to the obturator.

Mention is made of the failure of the sabot used on Models 1 and 2 during launch. Obturation photographs are shown. Study drawings of the sabot and delta shot are included.

- 179 Huchital, Eugene: "Design and Development of Low-Drag, High-Energy, Armor-Penetrating Projectiles (U)"; (Confidential Report), EMRC Report No. 16, 31 March 1961, AD 322 620.
- 180 Callis, Ben: "Development of Shot, 105-mm FS (Delta Wing) (U); (Confidential Report), Aberdeen Proving Ground Report No. DPS-386, December 1961, AD 327 233.

(Unclassified Abstract) Testing was conducted during the period July 1960 to May 1961 to evaluate the 105-/4C-mm shot, APFSDS. During July 1960, a Model 4 design was evaluated. Because of several sabot failures, accuracy data were not obtained at any range, nor was it possible to determine the protection ballistic limits (PBL) of the shot against armor plate at 1000 yards, because so many rounds missed the plate. In a firing against 6-inch plate at a range of 2000 yards 30 July 1960, a PBL could not be established because of an inability to obtain a complete penetration. Also, breaking of the sabot occurred during this firing. In May of 1961 a Model 8 design was evaluated against 5- and 6-inch armor plate and also against the tripartite triple-spaced armor target. A PBL of 4648 fps was obtained on the 5-inch plate, 5131 fps on the 6-inch plate, and 5105 on the tripartite plate. Results indicate that there was no complete breakup of any sabot assembly. However, some of the sleeves collapsed inward. Photographs show that fins began to separate from the shell.

- 181 Erwin, T. W.: "Development of Shot, 120/40-mm, APFSDS, Model 6 and 7 (U)"; (Confidential Report), Aberdeen Proving Ground Report No. DPS-472, March 1962, AD 328 571.

(Unclassified Abstract) The "Delta" projectile was developed as a kinetic-energy penetrator to replace the "Arrow" projectile. The Delta incorporates the Arrow penetrator and a pusher-type sabot instead of the pull-type used with the Arrow.

Complete study drawings of both Delta models and the sabot are included. The function and performance of the sabot and obturator are given with recommendations. Obturation and flight photographs are shown. Overall performance of both models is discussed.

- 182 Huchital, Eugene: "Design and Development of Low-Drag, High-Energy, Armor-Penetrating Projectiles (U)"; (Confidential Report, EMRC Report No. 30 (Final), 31 October 1962, AD 333 623.
- 183 Holmes, Rolf F.: "Feasibility Test of the APFSDS Delta Program (1962 Progress Report) (U)"; (Confidential Report), Aberdeen Proving Ground Report No. DPS-816, March 1963, AD 335 255.

(Unclassified Abstract) This program is an experimental effort to gain increased knowledge of kinetic energy antitank projectiles. Deficiencies in velocity dispersion and projectile launch were previously encountered.

A shot-start band, incorporated into the base of the sabot, ended the velocity-dispersion problem. No solution for the launch problem was found. A low-order detonation of the propellant severely damaged the weapon after a propellant-assessment and granulation study was complete. Protection ballistic limits of 5169 and 5175 fps for 6-inch, 60°, rolled homogeneous armor were determined for Delta shot, Mod 9 and 10, respectively. A PBL of 4750 fps for the Delta Mod 9 shot was determined against a modified medium triple tripartite armor. However, the Mod 10 could not effect a complete penetration of this target. Loss of fins because of setback loads prevented the Mod 9 shot from obtaining a PBL against the heavy triple tripartite armor target.

- 184 "Research Test of Shot, APFSDS, Delta, Models 11 and 12 (Armor Penetration Phase) (U) "; (Secret Report), Aberdeen Proving Ground Report No. DPS-1109, November 1963, AD 344 980L.
- 185 "Research Test of 120-mm Delta System (with Prototype Gun) (U) "; (Secret Report), Aberdeen Proving Ground, Report No. DPS-1326, June 1964, AD 351 586.
- 186 Barrièrès, Elie L.: "First Report on Ammunition Development for the US/FRG Main Battle Tank - Feasibility Study of the 120mm Delta Shot (U) "; (Secret Report), Picatinny Arsenal Technical Report 3249, July 1965, AD 364 536.

D-2.12 152 mm APFSDS Shot

- 187 "152-mm Gun/Launcher Full-Track Combat Tank, XM70 (MBT-70) (U) "; (Secret Report), US Army Materiel Command Technical Information Report 27.3.1.1, August 1966, AD 376 323.
- 188 "152-mm Gun-Launcher Cannon, XM150 Series (U) "; (Secret Report), University of Pittsburgh Technical Information Report 27.3.2.1, February 1967, AD 380 824.

D-2.13 Sabot Development for APFSDS Projectiles

- 189 Hollmann, Alfred: "Analysis of Scope of Work and Report of Results for Development of Plastic Sabots (U)"; (Confidential Report), Universal Match Corp. Report, 9 June 1958, AD 300 685.

(Unclassified Abstract) The scope of work under the subject contract originally was based upon the exclusive use of anti-aircraft projectiles. However, this requirement was changed to the use of an A.P. shot tank projectile, using the 76-mm tank gun in lieu of the original 75-mm sky-sweeper gun.

This report briefly summarizes the results of the sabot testing at UMC between March of 1953 and December of 1957, and provides recommendations for additional development of the sabot for use in 90- and 120-mm guns.

- 190 Miller, O. G. : "Evaluation of Friction Sabot Round for 90-mm, T208 Gun (U)"; Aberdeen Proving Ground (Confidential Report), APG. Report No. DPS/TW-426/3, May 1959, AD 307 407.
- 191 Brooks, P. N. : "Methods of Transferring Torque to an Armour Piercing Core"; (Unclassified Report), CARDE T. N. 1612/64, February 1964, AD 422 304.

(Unclassified Abstract) A theoretical analysis of two methods of transferring torque to an armor-piercing core is given, i. e., sabot spin torques: the torsion key, and the friction surfaces. The torsional capacities of both methods are determined and compared with the estimated torsional requirement for spin stabilization.

- 192 Black, W. L. : "Design and Fabrication of APDS Shot (U)"; (Confidential Report), Aircraft Armaments, Inc. Final Report No. ER-4341, March 1966, AD 372 916, for Picatinny Arsenal.

(Unclassified Abstract) The feasibility of adapting a friction technique to the design of a large-calibre, armor-piercing, discarding-sabot round was investigated. The program was conducted in three phases. Phase I was a theoretical study establishing the expected performance of a 152-mm round employing a 8.2-pound projectile. Calculations were made to establish the characteristics of a subscale (22-mm) round possessing performance characteristic equivalent to the full-scale unit. Phase II was an experimental program that determined the character and several of the features desirable in the full-scale design. The information developed during this phase guided the design of the full-scale round. Phase III was a design, fabrication, and test program for the development of a full-scale, large-calibre round. Closeup still photographs of recovered sabots, plus several pictorial representations, are shown.

D-2.14 Miscellaneous

- 193 Galagher, W. J. : "ELEMENTS WHICH HAVE CONTRIBUTED TO THE DISPERSION OF THE 90/40 PROJECTILE," Ballistic Research Laboratories, Report No. R-1013, March 1957. (AD 135 306)
- 194 MacAllister, L. C. ; "DRAG PROPERTIES AND GUN LAUNCHING LONG ARROW PROJECTILES," Ballistic Research Laboratories, Memorandum Report No. MR-600, April 1952. (AD 802 165)
- 195 Rottenberg, Mark; Settles, Charles; "DEVELOPMENT OF 20MM ARMOR-PIERCING CARTRIDGE TYPE MLU-36/C," AAI Corporation, ATL-TR-67-94, August 1967. (AD 387 167)

- 196 "DESIGN AND TESTING OF A DELTA-FINNEED, DISCARDING SABOT, ARMOR-PENETRATING PROJECTILE FOR USE IN THE SMOOTHBORE 90MM GUN, T208E4, "Picatinny Arsenal, Report No. ORD BB-TE5-10.
- 197 "DEVELOPMENT OF 105-MM HYPERVELOCITY ARMOR-PIERCING DISCARDING SABOT SHOT, T279, " University of Pittsburgh, Technical Information Report 6-9-4A1(3), December 1957. (AD 311 633)

D-3 HIGH EXPLOSIVE, DISCARDING-SABOT (HEDS) PROJECTILES

D-3.1 75/60-mm HEDS-AA Shell

(Unclassified Abstract) The three reports listed below are progress reports dealing with the design and development of the sabot used on the 75-mm high-explosive discarding-sabot (HEDS) shell. This work was done in conjunction with the UMC contract described in the next abstract.

Through the use of many firing records, yaw cards, drawings, pictorial representations, still photographs, and in-flight photographs, the reports follow the development of the sabot through many design changes and tests.

- 198 Lombard, E. Maj.: "Test of Shell, HEDS, 75/60-mm (U)"; (Confidential Report), Aberdeen Proving Ground Report No. TA1-5008-2, 26 October 1955, AD 99 767.
- 199 Roberts, E. A.: "Test of Shell, HEDS, 75/60-mm (U)"; (Confidential Report), Aberdeen Proving Ground Report No. TA1-5008-3, 10 January 1956, AD 99 765.
- 200 Burns, Benjamin Jr.: "Development of Shell, HEDS, 75/60-mm (U)"; (Confidential Report), Aberdeen Proving Ground Report No. TA1-5008-5, 23 August 1957, AD 144 083.

D-3.2 75-mm, 90-mm, 120-mm HEDS-AA Shells

(Unclassified Abstract) The following monthly progress reports from the Universal Match Corporation, covering the period July 1953 through February 1956, deal with various stages in the design and development of:

HEDS 75/60-mm T-(for 75-mm gun T83E6) shell.
HEDS 90/72-mm T-(for 90-mm gun M1 and M2) shell.
HEDS 120/80-mm T-(for 120-mm gun M1) shell.

Of prime interest was the design and development of sabots to fit the above configurations best. Several different materials ranging from fortisan, reinforced plastic, to a mixture of nylon, chopped glass, and epon-thiokol resin were used and tested during the progress of these reports.

The test procedures involved static testing of all components fabricated, static testing of the complete round, proof firing of the complete round, and evaluating the results. Included in the series of reports are many pictorial representations of both sabot and shell. Stress analysis of the shell and of the sabot also are given.

- 201 "HEDS AA Shells, 75-mm, 90-mm, 120-mm (U)"; (Unclassified and Confidential Reports), Universal Match Corporation, Monthly Progress Reports, 23 July 1953, AD 19 585; 5 October 1953, AD 25 513; 4 November 1953, AD 25 512; 3 December 1953, AD 25 511; 24 December 1953, AD 26 662; 2 February 1954, AD 28 263; 23 February 1954, AD 31 406; 24 March 1954, AD 31 405; 27 April 1954, AD 31 403; May 1954, AD 33 554; 25 June 1954, AD 35 408; 30 July 1954, AD 38 692; 25 August 1954, AD 40 047; 20 September 1954, AD 43 097; 22 November 1954, AD 50 910; 20 December 1954, AD 50 908; 24 January 1955, AD 54 096; 20 February 1955, AD 56 865; 20 March 1955, AD 58 862; 25 April 1955, AD 62 673; 19 May 1955, AD 66 552; 10 June 1955, AD 69 688; 22 October 1955, AD 75 641; 22 November 1955, AD 81 603; 21 February 1956, AD 92 575.

D-3.3 T162, T163 or T164, 155/105-mm HEDS Shell

- 202 Detaranto, J.: "Continued Design & Development of 155/105-mm (Discarding Sabot) H. E. Shell (U)"; (Unclassified Report), Marotta Engineering Company, Report No. 245P9, October 1953, AD 22 997, for Picatinny Arsenal.

(Unclassified Abstract) The aim of this contract was to ensure the manufacturing services of this facility in producing and evaluating twenty-five each experimental models of seven different proposed configurations of discarding sabot ammunition in the 155/105-mm calibre combination.

Sabot and shell stress analysis are included, as well as detailed drawings of both the shell and sabot with dimensions and weights. Drop test results of the sabot are also included.

D-3.4 T121, 280/203-mm HEDS Shell

- 203 Detaranto, J.: "Design & Development of 280/203-mm HEDS Shell"; (Unclassified Report), Marotta Engineering Company, Report No. 226P11, 30 September 1954, AD 47 264.

(Unclassified Abstract) This report discusses the designing and developing of a 280/203-mm HEDS shell. Calculations of stability factors and dynamical constants, along with stress analyses of torque pins, shells, and sabots, are given.

- 204 Tag, Donald K.: "Development of Shell, HEDS, 280/203-mm, T121 Type (U)"; (Confidential Report), Aberdeen Proving Ground, Report No. TA1-2040-8, May 1956, AD 151 463.

(Unclassified Abstract) Increased range potential of standard artillery weapons has been of continuing interest to the Ordnance Corps, and various means of accomplishing this end have been investigated and developed through the years. This report outlines the development progress to date using the sabot principle in the 280-mm gun, T131. One type of sabot, employing an 8-inch shell, HE, M106 (sub-projectile), held in a 280-mm, rear-driving "pot sabot", was tested and is reported herein. The sabot principle adapts a subcalibre projectile to a larger bore weapon, and the attendant reduction in weight permits substantially higher velocities and ranges than can be reached normally. This feature in turn necessitates a change of the propelling charges used. Accordingly, a limited charge establishment was conducted using T161 proof slugs to simulate the weight of the prototype round.

- 205 "Development of 280-mm High-Explosive Discarding Sabot Shell, T121 Series (U)"; (Confidential Report), U. S. Army Materiel Command, Technical Information Report 6-19-7A2(2), December 1958, AD 311 659.

(Unclassified Abstract) This report covers the development of large-calibre field artillery weapons able to cover large areas under all weather conditions.

In May of 1950 the Ordnance Technical Committee (OTC) approved development of the T131 280-mm gun and two rounds of ammunition for it, the T122 high-explosive (HE) shell and the T121 HEDS shell. It was estimated that a shell with a sabot would enable the T131 gun to fire to a range of between 45,000 and 49,000 yards, as compared to 35,000 yards for the larger and more lethal conventional projectile.

Because work was to begin immediately, it was necessary to use existing weapons as prototypes wherever possible. Consequently, shells of the T163 series, with 155-mm sabots and 105-mm projectiles, were designed and employed to evaluate proposed designs for 280/203-mm projectiles.

As the result of the T163 development, two designs for aluminum sabots were accepted. The first was a pot-type sabot with a square base, a short forward bourrelet with a single steel band, and a relatively long rear bourrelet with two gilding-metal bands. The second design called for a two-piece assembly consisting of a pot-type, square-base, sabot with three gilding-metal bands and a steel cap, and a forward multipiece sabot ring banded with a steel ring. Cutaways of the sabot and shell are shown.

D-3.5 T144, 127/60-mm HEDS-AA Shell

The following reports are part of a series of engineering progress reports dealing with the development and testing of the HEDS 127/60-mm T144 projectile. Complete firing data on each round, plus detailed drawings, are included in each report.

- 206 Falvey, D. R. and Shober, G. B.: "Research and Development of 127/60-mm Non-Lethal Discarding Sabot"; (Unclassified Report), The Budd Company, Engineering Progress Reports, 15 February 1953, AD 32 157; 15 March 1953, AD 32 158; 15 April 1953, AD 32 157; 15 May 1953, AD 32 160.
- 207 Dunne, S. G.: "The Development of a Procedure to Fabricate Shell HEDS 127/60-mm"; (Unclassified Report), Murray Tube Works, Final Report, 29 June 1954, AD 35 269.
- 208 Falvey, D. R.: "Engineering Progress Report on the 127/60-mm T144 and 90-mm T82 Shell (U)"; (Confidential Report), The Budd Company, MPR-24, 30 June 1955, AD 70 285, for Frankford.

(Unclassified Abstract) A brief report is given on the evaluation of the performance of an aluminum, four-segment, discarding sabot design for the 90/40-mm T320 projectile.

- 209 Falvey, D. R.: "Engineering Progress Report on the 127/60-mm T144 & 90/40-mm T320 Shell (U)"; (Confidential Report), The Budd Company, MPR-25, 31 July 1955, AD 70 286, for Frankford.

(Unclassified Abstract) The purpose of this test was to determine suitability of preloaded coil springs in aiding the separation in flight of sabot segments from the T320 projectile.

D-3.6 Other HEDS Shell

- 210 Nicolaidis, J. D.: "On The Development of a Low-Spin, Anti-Tank Projectile (U)"; (Unclassified Report), BRL Memorandum Report No. 527, November 1950, AD 805 133

(Unclassified Abstract) The data obtained from the supersonic wind tunnel at $M = 1.72$ and from the transonic range at $M = 1.5$ to 1.1 furnished a basis for estimating the center of pressure variation with Mach number for the E-20 shell configuration. With these data and the assumption that the normal force coefficient is constant over the range of flight Mach numbers, the missile velocity, spin, stability factor, precession rate, and drift as a function of distance down range may be estimated for the Standard E-20 model. An analysis of the results furnishes a partial explanation of the results obtained from accuracy firings at 1000 yards for the Standard E-20 model.

Calculations also are carried out for other center of gravity locations for the E-20 configuration, upon which new model designs were based. The results obtained from accuracy firings of these new designs are given herein and briefly discussed.

It is shown both theoretically and experimentally that the performance of the E-20 shell can be substantially improved by locating the center of gravity in a particular rear position.

- 211 Rosenberg, M.: "The Selections of Optimum Sabots for HE, Spin-Stabilized Ammunition to Obtain Maximum Range"; (Unclassified Report), Picatinny Arsenal Report No. RDL-6, January 1955, AD 75 813, Theoretical Discussion

(Unclassified Abstract) A brief theoretical discussion of the sabot is given, including a definition of the sabot.

- 212 "Concerning the Development of the Spin Stabilized Non-Rotating Hollow Charge 105mm Shell (U)"; (Confidential Report), LABORATOIRE D'Etudes BALISTIQUES, de Saint-Louis, France Progress Report, December 1962, AD 336 530.

(Unclassified Abstract) The report gives a short discussion of the possibility of adapting the British or American design of APDS round to French applications.

- 213 Labuwi, L. R.: "Engineer Design Test of Cartridge, 90-mm, with 81-mm, HE warhead"; (Unclassified Report), Lewis R. Labuwi, APG Report No. DPS-1949, March 1966, AD 478 820L.

(Unclassified Abstract) The performance of the 90-mm, M371E1, HEAT-FS, cartridge (anti-personnel) was evaluated. Data were collected from concept-feasibility, propellant charge establishment, fuze arming and fuze reverse functioning, vertical target dispersion, range firings, evaluation of sabot design, and sight reticle verification firings.

Complete detailed sabot design drawings are included. Five sabot designs were tested. The basic sabot design is discussed.

- 214 "DESIGN AND DEVELOPMENT OF SET-BACK MECHANISM FOR FUZE, T-265, FOR 127/60MM DISCARDING SABOT SHELL," Hesse-Eastern Corporation, Progress Report 19-553, May 1953 (AD 31 624); Progress Report 20-653-6A, June 1953 (AD 31 625); Progress Report 21-753-6A, June 1953.

D-4 OTHER SABOT PROJECTILES

D-4.1 5"/3.75" Spin Stabilized Discarding-Sabot Projectile

(Unclassified Abstract) The following reports describe the 5.0"/3.75" spin-stabilized discarding sabot projectile developed by the Naval Ordnance Laboratory. This projectile, designated the NOL XS-1B projectile, uses torque drive pins and gas-pressure actuated shear release studs for sabot attachment to the sub-projectile. The torque pin drive is a positive drive in which a pair of truncated conical pins are threaded to the sabot base and match corresponding conical recesses in the base of the sub-projectile. The shear release stud is a conventional stud with a 45° silver-brazed joint at mid-length. Severance is accomplished by using powder pressure to load the stud in compression by a flexible diaphragm, thus shearing the stud at the silver-brazed joint. The pot-type sabot is aluminum with a nylon rotating band and a soft-iron front bourrelet. A group of twenty rounds fired from a special high twist 5"/38 gun barrel averaged a 3,800-ft/sec muzzle velocity. Sabot separation was complete for all rounds and the performance generally was satisfactory. It has been concluded that the XS-1B projectile, although capable of further refinements and improvements, is an operable round.

The five reports listed below deal with this development. Included in these reports are many drawings, pictorial representations, still photographs, and in-flight photographs of the projectile and sabot.

- 215 Butler, Rex B.: "Ballistic Test of 5"/3.75" Spin-Stabilized Discarding Sabot Projectile Design XS-1A"; (Unclassified Report), NPG Report No. 1253, 15 March 1954, AD 310 058.
- 216 Butler, R. B.: deGaetano, Felix P.: "Ballistic Test of 5"/3.75" Spin-Stabilized Discarding-Sabot Projectile Design XS-1B"; (Unclassified Report), NPG Report No. 1294, AD 41 103.
- 217 Butler, R. B.: deGaetano, Felix P.: "Development of a 5"/3.75" Spin-Stabilized Discarding-Sabot Projectile"; (Unclassified Report), NPG Report No. 1300, 25 October 1954, AD 45 659.
- 218 Butler, R. B.: deGaetano, Felix P.: "Development and Evaluation of a 5"/3.75" Spin-Stabilized Discarding-Sabot Projectile"; (Unclassified Report), NPG Report No. 1310, 26 November 1954, AD 47 701.
- 219 Nardis, L.: "Development of the 5.0"/3.75" Spin-Stabilized Discarding Sabot Projectile"; (Confidential Report), NAVORD Report 3987, 19 September 1955, AD 82 450.

D-4.2 Gun-Launched Anti-Missile Defense (GADS)

- 220 "Parametric Study of Gun-Launched Anti-Missile Defense System (GADS) (U)"; (Secret Report)²⁹ Naval Ordnance Laboratory Report No. NOLTR 62-56, 3 Sept, 1963, AD 350 416.

D-4.3 Miscellaneous Sabot Projectiles

- 221 Rossbacher, R. I.: "A Summary of Firing Results in Angled Arrow Projectile Propellant Development Through 1953 (U)"; (Confidential Report), NPG Report No. 1378, 24 May 1955, AD 70 790.

(Unclassified Abstract) A summary is given of the firing results in the propellant development for the angled Arrow projectile. The material covers the period from 1951-1953. Test rounds weighed approximately 105 pounds and were supported by a discarding sabot and base plate.

- 222 Naylor, P. W.: "A Preliminary Design Study of the Adaptability of Fin Stabilized Discarding Sabot Projectiles to the 5"/38 Gun (U)"; (Confidential Report), NAVORD Report 4245, 21 August 1956, AD 130 644.

(Unclassified Abstract) A study has been made of the adaptability of fin-stabilized, discarding sabot projectiles to the 5"/38 gun. Such a projectile has a definite time-to-target and range advantage over spin-stabilized projectiles. Preliminary design details of fixed and semifixed 5-inch rounds incorporating an FSDS projectile are presented. These projectiles could be fired through rifled barrels interchangeably with standard spin-stabilized ammunition, but modifications to ammunition handling and fire control equipment would be required for compatibility with the FSDS round. The magnitude of the alterations involved would depend upon the efficiency desired in the overall system. The fixed-round, one-piece ammunition offers several advantages in respect to stowing, handling, and increased cyclic rate. Relative merits of using the British 127/59-mm round in the 5"/38 gun also are discussed. Pictorial representations are given.

- 223 McCallum, F. L.; Miller, R. J.; McMurtry, W. M.; Jones, W. A.: "An Adaptation of the Shock Tube to Smoke Trail Production (U)"; (Unclassified Report), Suffield Experimental Station Technical Note No. 48, 25 November 1964, AD 454 983.

(Unclassified Abstract) This note is an evaluation of an air-fired smoke "mortar" developed at the S.E.S. shock tube laboratory. The device basically is a small shock tube fired by a standard shock wave valve and using commercially available smoke-producing chemicals to give well defined white smoke trails extending from the tube "muzzle" to heights exceeding fifty feet.

A simple plastic cylinder sabot is used for launching. Photographs and functional drawings are included.

- 224 Quinn, R. B.: "Round Requirement for Area Bombardment with a Proposed Long Range Gun (U)"; (Confidential Report), Bureau of Naval Weapons Report No. TM-R-58-66-2/1, January 1966, AD 370 647.

(Unclassified Abstract) Need for longer range effectiveness of gunfire has led to a proposal for a smoothbore sabot gun. The proposal of "Operation Gunfighter" envisions a range of 50 miles. One version of such a gun would use a bored-out 6"/47 barrel and a 3" sabot projectile. The HARP program has encouraged a renewed interest in the possibilities for sub-calibre projectiles. This memorandum estimates the number of rounds required for an expected 0.3 coverage of a soft target as a measure of the effectiveness of the proposed weapon.

- 225 Giraud, M.; "EXPERIMENTAL STUDY OF A SWEPT-BACK PROJECTILE," Institut Franco-Allemand de Recherches, Report No. ISL-T-26/67, July 21, 1967 (in French).

Development and construction of a four-part thrust ring for firing projectiles at 1000 m/s velocity in a 30 mm caliber smooth barrel is described. Comparison between molded and machine formed thrust rings established the latter as the better propelling device.

- 226 Giraud, M.; "SWEPT-BACK TYPE PROJECTILES. MANUFACTURE AND PRELIMINARY TESTS," Institut Franco-Allemand de Recherches, Report No. ISL-T-25/67, July 21, 1967 (in French).

The test evaluation of an 18.5 mm long fin-stabilized projectile in a free flight test range showed a medium velocity decrease of 0.13 m/s per meter flight distance. At an initial velocity of 1000 m/s, the projectile stability remained high with a maximal deflection angle of less than 2° at 130 m distance from the gun muzzle.

- 227 Michaels, J. V.; Burnett, W. M.; Lindemann, M. J.; Goldberg, M. I.; Duda, J. L.; "OPERATIONAL EFFECTIVENESS OF THE 8-INCH, 55-SUBCALIBER FIN-STABILIZED GUNFIGHTER PROJECTILE," Naval Ordnance Station, Report No. NOS-IHTR-264. (AD 389 632L)

- 228 Nicolarder, J. D.; "A TRANSONIC RANGE STUDY OF THE FREE FLIGHT PERFORMANCE OF THE 127/60 ANTI-AIRCRAFT MISSILE T-144E2," Ballistic Research Laboratories, Memorandum Report No. MR-746, December 1953. (AD 30 118)

D-5 SMALL-CALIBER SABOT PROJECTILES

D-5.1 General

- 229 Oliver, Alfred G. ; Merkler, Jules M. ; Brown, Bernard J. : "Wound Ballistics of the 7.2-Grain Steel Flechette (U)" (Secret Report)²², Edgewood Arsenal, Army Chemical Research and Development Laboratories Technical Report CRDLR 3066, April 1961, AD 323 113.
- 230 Little, Arthur D. Inc. : "Feasibility Study of Caliber Diameter Finned Flechettes (U)"; (Confidential Report), Report No. C63851, May 1962, AD 367 114.

(Unclassified Abstract) The equation governing the energy decay of flechettes is examined theoretically in this report and the basic performance feasibility of small calibre diameter flechettes is established. Several designs are presented. Methods of testing small diameter projectiles are discussed. Full-calibre diameter finned flechettes requiring no sabot are investigated to determine if they can compete, (from a performance standpoint), with the sabot-type flechette.

- 231 Kymer, J. R. ; Reagan, R. : "Special Ammunition for Calibre .50 M2 and M85 Machine Guns (U)"; (Confidential Report), No. M64-10-1, September 1963, AD 345 372.

(Unclassified Abstract) A study was conducted to determine the feasibility of developing, for the calibre .50 M2 and M85 machine guns, a flechette round capable of defeating armored personnel carriers at ranges greater than 600 yards. Based on an empirical formula and using the combined sabot-flechette weight, the limit velocities required by the proposed flechettes to defeat various targets at 600 and 1000 yards, were calculated. From known interior and exterior ballistic performance of various flechettes, the calculated velocity of the proposed flechette was determined both at the muzzle and at the 600 and 1000-yard ranges.

- 232 Scanlon, John J. ; Stevenson, Thomas : "Sabotless Flechette in Caseless ammunition (C) Investigation of Special Projectiles in Caseless Ammunition (U)"; (Confidential Report), Technical Report R-1696, September 1963, AD 348 833.

(Unclassified Abstract) A study was conducted to develop a sabotless flechette with solid propellant caseless ammunition. A calibre diameter (sabotless) finned flechette with terminal effects, exterior ballistics, accuracy, and physical properties comparable to the Special Purpose Infantry Weapon (SPIW) 10-grain super calibre finned flechette, was demonstrated and a molded 17.0-grain caseless charge of IMR 4895 granular propellant was developed for firing the sabotless flechette. Drawings of various rounds and flechette types are included.

- 233 Katlin, J. M. ; Kymer, J. R. ; Baldini, L. F. : "Effect of Projectile Hardness and Plate Composition on Penetration of Spin Projectiles (U)"; (Confidential Report) Frankford Arsenal Technical Report R-1711, March 1964, AD 349 745, for Ordnance Corps.

(Unclassified Abstract) Calibre 5.6-mm flechette-type projectiles of Rock 11 C60, C45, and B90 hardnesses were fired against steel and 2024-T4 and 5083 aluminum armor. Protection ballistic limits were determined for several conditions of attack by the various projectiles against plates of equivalent areal densities.

Two types of sabots were used for launching the flechettes: A four piece magnesium sabot held together by a silicone rubber ring, and a fiber glass sabot slotted to form 16 partial segments.

- 234 MacMillan, J. T. : "Final Summary Report - To Develop and Supply Experimental Shotgun Ammunition" ; (Secret Report)²⁴, Remington Arms, Report No. AB 64-19, October 1964, AD 354 449.
- 235 "Sabot, Flechette & Tracer Flechette Investigations"; (Confidential Report), Technik Incorporated, Report No. TR #65-14, June 1965, AD 366 463.

(Unclassified Abstract) Report summarizes the flechette investigations performed by Technik, Inc. under the SPIW program. It is an edited compilation of the progress reports issued during the course of this program.

The work consisted of sabot and flechette analyses, including flechette tracer studies. The program as summarized herein, was designed to investigate problem areas and make necessary recommendations.

The sabot investigations consist of those given below:

A. Sabot Gripping

1. Sabot pulling force requirements
2. Sabot edge sensitivity
3. Sabot slot effect
4. Sabot contact gap

B. Sabot Strength

C. Sabot Types

1. Straight cylinder type sabot
2. Adhesive-type sabot

- 236 Dziemian, Arthur J.; Olivier, Alfred G.; McDonald, Walter C.: "Wound Ballistics of SPIW Flechettes (U)" ; (Secret Report), Edgewood Arsenal Army Chemical R & D Lab., Report No. CRDLR 3308, July 1965, AD 364 425.
- 237 Nusbaum, M. S.: "Small Arms Ammunition Supporting Research Defeat of Armor (U)"; (Confidential Report), ITT Research Institute, Final Report DA-36-038-AMC-1685(A), September 1965, AD 368 026, for Frankford Arsenal.

(Unclassified Abstract) This report describes studies conducted to develop a 20-mm discarding sabot for a 4. 17-mm-diameter tungsten carbide penetrator having a length-to-diameter ratio of 25. The successful design permitted launching a stable penetrator at the required velocity. Dynamic strength evaluations made for the components used.

- 238 Hebert, J. R.; Settles, C. P.; Hartlove, C. F.: "Study and Development of 20-mm Armor Piercing Ammunition (U)"; (Confidential Report), Aircraft Armaments Inc. Report No. ATL-TR-66-37, May 1966, AD 373 665.

(Unclassified Abstract) The objective for this program was the feasibility investigation and preliminary development of 20-mm armor piercing ammunition using the sub calibre flechette and discarding sabot principle successfully developed for .22 calibre ammunition. The various configurations tested under this program are illustrated.

Design studies and experimental investigation on the 20-mm ammunition established that a 370-grain sabot was adequate for a 420-grain projectile and that this assembly could be launched at a muzzle velocity of approximately 4670 ft/sec. The maximum projectile length that was compatible with the M103 cartridge case was 6 inches. This resulted a projectile diameter of 0.221 in. for steel and 0.159 in. for tungsten alloy. Penetration of rolled homogeneous armor plate (250 Brinell) at 60° obliquity at 1000 yards was originally computed to be 0.8 and 1.2 inch thick plate for steel and tungsten respectively (based on BRL MR1442). Test results conformed the computed performance for steel, however, tungsten carbide resulted in penetrations that were 59 percent in excess of the computed performance. The above performance figures are predicated on the stated muzzle velocity, projectile mass to sabot mass ratio, and projectile drag coefficient of 0.3.

Extrapolation of experimental test data and analytical studies indicated that a refined tungsten carbide round should penetrate approximately 1.9 inches of armor plate at 60° obliquity or 3.8 at 0° obliquity at 1000 yard range from a ground mounted weapon. This means that this round is capable of defeating light tanks from the sides and back in low level attack modes and all tanks, heavy and light from the top in 30° dive angle attack modes.

The report is saturated with charts, graphs and pictorial representations of the test procedures and results.

- 239 Cavell, Winston W. ; Dietsch, Frank W. ; Caven, James J. ; DiGirolamo, Ronald D. : "Tracer Projectile for SPIW Point Target Ammunition (U)"; (Confidential Report), June 1966, AD 374 357.

(Unclassified Abstract) Of all the small arms tracer ammunition, the SPIW tracer projectile possesses the highest muzzle velocity (4600 fps), the lightest projectile weight (14.5 grains), the smallest tracer cavity and tracer charge (0.060 in. diameter cavity and one grain tracer charge), and is the only sabot-launched small arms tracer projectile, thus making it the most unconventional tracer ever designed and developed. To illustrate the important differences in design features between special purpose individual weapon (SPIW) tracers and conventional tracers, a comparison first is presented of the arrangement of the major components of the SPIW tracer and of the smallest standard military tracer of conventional design, namely, 7.62 mm M62 NATO tracer.

This presentation describes the SPIW tracer cartridge design features, ballistic and pyrotechnic functioning characteristics, and some of the problems encountered during developmental studies and tests.

- 240 "Special Purpose Individual Weapon (U)"; (Confidential Report) Aircraft Armaments, Inc., Report No. ER-4681, December 1966, AD 378 554.

(Unclassified Abstract) The primary objectives were as follows:

- a. To continue the design, development, test, and fabrication of an improved model weapon system leading to a final prototype rifle, 5.6-mm; with grenade launcher, 40-mm.
- b. To develop a 5.6-mm cartridge and associated accessory types of point target cartridges.
- c. To design and fabricate simulated production processes for fabricating and assembling the point target cartridge.
- d. To manufacture 130,000 cartridges by a method simulating the mass production processes to be delivered to the Government.

A special section describing the operation of the sabot injection molding machine is included, as also are drawings of the sabot assembly.

D-5.2 0.22 Caliber Flechette

- 241 LaCosta, N. J. : "Small Arms Cartridge (U)"; (Confidential Report), Aircraft Armaments, Inc. Report No. ER-1026, March 1957, AD 126 947.

(Unclassified Abstract) During the performance of this contract, the objective was to establish the feasibility of launching a fin-stabilized projectile at an approximate velocity of 4000 feet per second. Various projectiles and sabot configurations were launched successfully at this velocity. All of the rounds were launched from a calibre .22 smoothbore Mann barrel.

Several pictorial representations of different sabot types and rounds are given.

- 242 "Development of a Special Type Small Arms Cartridge (Sabot-Supported) (U)"; (Confidential Report) Aircraft Armaments, Inc., Report No. ER-1414, July 1958, AD 300 912.

(Unclassified Abstract) The feasibility of a new lightweight weapon system is established. Short, lightweight rounds producible by mass production techniques are developed. The major objective of the work was development of a special type small arms cartridge using a fin-stabilized projectile that could be launched at a muzzle velocity of 4000 feet per second and could achieve terminal velocities high enough to be lethal at reasonable ranges.

The development of a .22 calibre projectile puller type sabot configuration that would use a smooth surface projectile is discussed in considerable detail.

- 243 "Development of a Special Type Small Arms Cartridge (U)"; Aircraft Armaments, Inc., (Confidential Report), Report No. ER-1725, June 1959, AD 309 272.

(Unclassified Abstract) Continuation of the development of a special type small arms cartridge, .22 calibre, employing a fin-stabilized projectile.

A considerable improvement in round performance was achieved, and the feasibility of satisfying the down range velocity and accuracy objectives was proven. A gun mechanism was fabricated and tested. An extensive section on sabot projectile development, including down range velocity problems, pulling problems, accuracy problems and manufacturing problems is presented.

- 244 "Evaluation of Single Flechette (U)" ; (Secret Report), Army Infantry Board, Fort Benning, Georgia, Report of Project Nr. 2876, 18 March 1960, AD 316 128.

- 245 "Small Calibre Demonstration Guns (U)"; (Confidential Report), Aircraft Armaments, Inc. Report No. ER-2059, June 1960, AD 317 351.

(Unclassified Abstract) The design and firing capabilities of a fivebarrel .22 calibre demonstration-gun are given. The gun was developed to demonstrate a new .22 calibre fin-stabilized sabot ammunition.

Mention is made of a sabot stripper threaded to the muzzle of each barrel to disperse the sabot pieces from the projectile.

Muzzle velocity was 4,400 feet per second and the peak primer pressure was 3,540 psi.

Photographs of the gun, assembled and disassembled, are shown.

- 246 Sober, John: "Test of Flechette Flight Characteristics (C)"; (Confidential Report), Picatinny Arsenal Report No. ET 182-60, 25 May 1960, AD 371267.

(Unclassified Abstract) A firing range was set up and a special smooth bore .220 swift high-velocity gun was used to fire the individual flechette projectiles over a distance of 150 feet. Most of the tests conducted involved firings of the flechette with the front or pointed end in the rearmost position at the time of firing. The purpose here was to check stabilizing characteristics under the most adverse condition. This factor gave rise to a problem in how to sabot the projectile properly. The sabots used were aluminum and soft enough for a deep penetration of the flechette point into the butt-plate when firing flechettes backward. On a few occasions, this penetration was deep enough to cause the butt-plate to stick to the flechette over the full range of travel.

- 247 Ricchiazzi, Antonio J.; Herr, E. Louis; Grabarek, Chester L.: "An Experimental Study of the Characteristics and Effectiveness of Particles Ejected Behind Armor Plate Attached by Flechettes (U)"; (Confidential Report), BRL Memorandum Report No. 1311, November 1960, AD 321 770.

(Unclassified Abstract) Experimental data are given on the velocity and mass distribution of particles ejected from the backside of a steel target attacked by a flechette. The experimental method is described. The capability of the particles to incapacitate personnel is computed for a few cases.

The flechettes were sabot-launched by pusher type fiber sabots from a smoothbore gun.

- 248 Lentz, S. S.: "An Investigation of the Characteristics of Flechette Rounds When Fired from a Multi-Barreled Test Gun (U)"; (Confidential Report), BRL Technical Note No. 1379, February 1961, AD 355 191.

(Unclassified Abstract) Experimental firings were conducted with a five-barreled test gun firing cal. 0.22, single flechette rounds in single shots, in salvos, and in a burst at a rate of fire of 2680 rds/min. Measurements were made of action time and velocity; dispersions were obtained of the flechettes and sabots at several locations down range and photographs were taken of the flechettes and sabots at two positions along their trajectories.

- 249 Martin, Luther S.: "Effectiveness of Flechettes Against the 90-mm T108 HEAT Shell (U)", (Confidential Report) Picatinny Arsenal Technical Memorandum 1246, January 1964, AD 347954.

(Unclassified Abstract) Several organizations conducted programs to investigate the vulnerability of simulated HEAT-type warheads to high velocity flechettes. Results of these tests were promising since the flechettes were able to detonate the explosive filler, but this did not establish the capabilities of flechettes against actual HEAT projectiles. Thus, a program was initiated at Picatinny Arsenal to study the possibility of using flechettes fired from a special 0.220 calibre smoothbore gun, to defeat HEAT projectiles.

The 90-mm T108 HEAT round was chosen as the test vehicle. Angles of attack from 0 to 90° were used for these tests.

Best results were obtained by using a sabot consisting of an aluminum butt-plate with paper wadding packed around the flechette inside the cartridge.

- 250 "Research and Development on .22-Calibre Arrow Ammunition (U)"; (Confidential Report) Aircraft Armaments, Inc. Report No. ER-3361, February 1964, AD 363 368.

(Unclassified Abstract) Section II of this report gives a summary of the status of each of the following as of 30 June 1960: 1) sabot-projectile configuration, 2) cartridge case configuration, 3) stripper development, 4) propellant charge development, 5) projectile accuracy investigation, and 6) sabot lethality investigation.

The remainder of the report covers the research and development activities conducted by AAI on calibre .22 arrow ammunition during the period 1 July 1960 through the end of the R&D program, approximately 31 January 1963. The effort involved the sabot, projectile, and cartridge.

Investigation of multipiece sabots and sabot materials and configurations to reduce manufacturing costs, improve accuracy, and decrease short range sabot lethality is presented with emphasis on plastic-type sabots.

- 251 "Design, Development and Manufacture of Interim Tooling for Fabrication and Assembly of .22-Calibre Ammunition (U); Aircraft Armaments, Inc. (Confidential Report), Report No. ER-3491, May 1964, AD 350 673.

(Unclassified Abstract) This report is a description of the tooling processes for fabricating the sabot and projectile for the XM110 cartridge. Included is a description of the machines used for assembling the cartridge automatically.

D-5.3 Multiple Projectile Shots

- 252 Long, J. E.: "Photographic Study of Separation of Shotgun 'Scatter' Projectile Clusters," (Unclassified Report), Remington Arms, Aeroballistic Research Report 207, 4 November 1953, AD 49 699.

(Unclassified Abstract) The purpose of this study was to find the causes of the excessive dispersion of the shotgun "scatter" projectile clusters. Separation characteristics of the shotgun clusters have been obtained. Results are presented in the form of photographs taken near the gun muzzle of the cluster in free flight.

Investigation of sabot separation on launching the 20-mm cluster is briefly included.

- 253 McDonough, John P.: "Preliminary Study of the Application of Plastic Discarding Carriers and Missile Binders for Canister Shot (C)," (Confidential Report), Watertown Arsenal Laboratory Report No. WAL 763/885-1, 3 June 1955, AD 68995.

(Unclassified Abstract) This report describes the preliminary study of the use of WAL Type Discarding Carriers in establishing the range-velocity characteristics of steel spheres and cylinders at velocities ranging from 700 to 4000 ft/sec. This was accomplished by mounting a single missile separately in a plastic discarding carrier and firing it from a small arms barrel.

- 254 McDonough, John P.: "Development of Plastic Discarding Type Carriers as Casings for 40-mm Canister Shot, T229E3 (C)," (Confidential Report), Watertown Arsenal Laboratory Report No. WAL 763/885-2, 3 June 1955, AD No. 69132.

(Unclassified Abstract) This report describes the ballistic performance of standard and special plastic compounds tested in the development of the WAL Type 40-mm Canister Shot, T229E3, considering the range-velocity performance of the canister missile spheres, the significance of the missile binder, molding techniques, and preparation of the experimental canister shot.

- 255 Weistling, L.: "Air-to-Ground Effectiveness Study of Scatter Projectiles (U);" (Confidential Report), Aircraft Armaments, Inc., Report No. ER-703, 9 January 1956, AD 84 048.

(Unclassified Abstract) This study investigates the air-to-ground effectiveness of scatter projectile weapons, determines an optimum weapon of this type, and compares it with standard and developmental weapons of a more conventional nature. A number of scatter projectile weapons are evaluated and compared with conventional guns and a rocket installation relative to a variety of targets and tactical situations. A scatter projectile weapon is defined as a gun installation that fires rounds containing a number of fin-stabilized sub-projectiles which are constrained by a sabot while in the gun bore, but which are released as distinct projectiles at the muzzle.

- 256 Calhoun, J. D.: "Final Summary Report," Remington Arms Co. Inc., Report No. A13-62-1, 31 January 1962, AD 327 683.

(Unclassified Abstract) This report outlines in detail the design and development work conducted by Remington Arms Co., Inc. from 22 March to 31 December 1961 to develop the cartridge, 5.6 mm XM-110. The component designs which were developed are delineated, as well as the tools and processes used to carry out this development. Complete results and recommendations are detailed and test procedures are outlined.

A sabot of minimum weight was developed of such a design and material as to reduce sabot lethality and increase projectile accuracy. Detailed drawings of these are given.

- 257 Long, J. E.: "Photographic Study of Sabot Separation of Scatter Projectile Clusters" (C); (Confidential Report), NAVORD Report 2893, 9 June 1963, AD 58 813.

(Unclassified Abstract) The Naval Ordnance Laboratory was requested by Aircraft Armaments, Incorporated, through the Office of Naval Research, to investigate the sabot separation characteristics of the 20-mm scatter projectile clusters and the shotgun clusters. Photographs taken in the Aerodynamics Range are shown, and a detailed description of the sabots used is given.

- 258 Anderson, H. K.; Chadwick, G.; Degan, M.: "Ballistic Range Testing of Self-Dispersing Shapes," (Unclassified Report), Aberdeen Proving Ground, Report No. AVMSD-0154-66-RR, May 1966, AD 486 505.

(Unclassified Abstract) An experimental test program was conducted at the Ballistic Research Laboratories' 1000-foot transonic free flight range to determine feasibility of using this type of ground test facility to obtain measurements of the aerodynamic performance and structural survivability of self-dispersing configurations in unrestrained flight.

Test results are discussed, test models are discussed and shown, and sabots are shown in detail and briefly discussed.

Spherical bomblets and fluttner rotors were the two models launched from a smoothbore conventional gun. Velocities up to 3200 ft/sec were attained.

- 259 Weg, H. W.; Flesher, F. E.; Sweeney, Patrick E.: "Antiaircraft Feasibility Study Scatter Projectile All-Arms Weapon (U)"; (Confidential Report), Aircraft Armaments, Inc., Report No. ER-1287, January 1958, AD 161 411.

(Unclassified Abstract) This report discusses briefly the history of the Aircraft Armaments, Inc., scatter projectile for use in an antiaircraft weapon system. It contains a narrative summary of all the work performed during the contractual period, 1 July 1957 to 24 January 1958. Primary objective of this contract was the preliminary design of an integrated, all-arms antiaircraft weapon system based on the scatter projectile concept.

The report discusses the housing of multi-projectiles in a sabot to facilitate higher muzzle velocities, better ballistics, and greater efficiency. The ammunition is a 40-mm round containing six (6) finned sub-projectiles in a plastic sabot.

- 260 Haag, C.W.; Clarke, C.C.: "Design, Manufacture and Testing of Canister Fillers (C);" (Confidential Report), Whirlpool Corp. Monthly Progress Report No. 2, 10 July 1958, AD 302 826.

(Unclassified Abstract) This report summarizes previous work done under the contract and is a continuation of the design and development of canister and other anti-personnel ammunition fillers. Sabot carriers for the three sizes of flechette were designed and released to shop for fabrication in trial quantities. These designs varied in dimensional size to match the flechette and were made either of balsa wood, hard maple wood, or magnesium. Detailed drawings, as well as photographs of the sabot and projectile, are included.

- 261 "Summary Report Volume I - Design, Manufacturing and Testing of Canister Fillers (U)"; (Secret Report) Whirlpool Corporation, October 1959, AD 315 434.

- 262 Moore, David J.: "Evaluation of Special Flechette for Beehive Ammunition (U)"; (Confidential Report), Remington Arms Co., Inc., Report No. MPR No. 1, 13 December 1961, AD 327437.

(Unclassified Abstract) This is the first monthly report under this contract and it states that tools have been designed and are being fabricated for the manufacture of a flechette fragment composed of an incendiary-pyrophoric alloy mixture. Test facilities include a calibre .222 barrel with the flechette driven by a plastic sabot which will strip upon exit. Projectiles are to be used for mine detonation and will be fired against a "D60" steel plate target.

D-5.4 Miscellaneous

- 263 Hegge, Edward N.; McDonough, John P.; "SUBCALIBER PROJECTILE AND SABOT FOR HIGH VELOCITY FIREARMS" (ARMY), "U. S. Patent Office, No. 3, 148, 472, September 15, 1964.

The plastic sabot is for use with a projectile. A portion of the mating surfaces between the sabot and projectile is contoured to form a shear area which is capable of resisting relative movement between the sabot and the projectile during passage through the bore of the gun. The sabot disintegrates after leaving the barrel of the gun.

- 264 Kimura, William S.; "ANTI-PERSONNEL RECOILLESS RIFLE AMMUNITION (BEEHIVE), Army Concept Team in Vietnam, Final Report, covering period July-December 1967, March 1968. (AD 388 467)
- 265 McNeill, Joseph W.; "AN EVALUATION OF A PROPOSED SCATTER PROJECTILE FOR USE IN THE ALL-ARMS ANTI-AIRCRAFT WEAPON," Ballistic Research Laboratories, Report No. TN 1053, November 1955. (AD 384 615)
- 266 Moore, David J.; "EVALUATION OF SPECIAL FLECHETTE FOR BEEHIVE AMMUNITION," Remington Arms Company, Inc., Monthly Progress Report No. 2, MPR-2, January 1962. (AD 327 925)
- 267 Watt, R. M.; "FREE-FLIGHT RANGE TESTS OF FLECHETTE-TYPE PROJECTILES AT NOMINAL MACH NUMBERS OF 4 AND 5," ARNO, Inc., Arnold Engineering Development Center, Final Report AEDC-TR-67-259, January 1968. (AD 386 279)
- 268 Wheeler, R. E.; "DEVELOPMENT OF WDU-4A/A FLECHETTE WARHEAD," Northronics, Division of Northrop Corp., Final Report, No. 67y161, November 1967. (AD 388 328)
- 269 "BLU-26 B BOMBLET: LIGHT/RIFLE LAUNCHED WEAPONS: ATAW AND LAW," Lockheed Missiles & Space Company, Report No. A373656, February 1967.
- 270 "PHOTOGRAPHIC STUDY OF SEPARATION OF SHOT-GUN "SCATTER" PROJECTILE CLUSTERS," Naval Ordnance Laboratory, Aero-ballistic Research Report No. ARR-207, November 1953, (AD 49 699)

D-6 ROCKET-ASSISTED PROJECTILE (RAP)

- 271 "Feasibility of Field-Artillery-Boosted Rockets"; (Confidential Report), Arthur D. Little, Inc. Progress Report, May 1961, AD 324 928.

(Unclassified Abstract) A series of trajectory calculations for a 155-mm, 40-pound projectile was described in the progress report for April. These calculations have been analyzed with the aid of an IBM 7090 Computer. The results of the analysis are discussed. Curves are presented that show the effect of the following:

- (1) Sustainer thrust level and burning time on range
- (2) Sustainer thrust level on Mach number and drag of the projectile
- (3) Quadrant elevation on projectile drag

- (4) Sustainer action on maximum range
- (5) Delayed thrust on maximum range

Curves that show the quadrant elevation for maximum range, the projectile Mach number versus horizontal distance, and the characteristics of optimum boost sustainer systems also are included. A brief evaluation of the performance of subcalibre (sabot) projectiles is presented. A section is included on the hazards from sabot fragments.

- 272 "Feasibility of Field-Artillery-Boosted Rockets"; (Confidential Report), Arthur D. Little, Inc. Report No. C-63625, September 1961, AD 327 571.

(Unclassified Abstract) This report summarizes work carried out in a program comprised primarily of theoretical design studies of field artillery-boosted rocket systems. An evaluation of weapon systems based on the first-order criteria of propulsion efficiency, launcher weight, accuracy, lethality, and cost is presented. Trajectories for 115-mm and 155-mm gun-boosted rockets were computed and an analysis of the trajectories is included. The merits of spin stabilization and fin stabilization are compared. Methods for improving the effectiveness of the XM54 projectile are described. The use of sabots, ramjets, and ducted rockets for increasing the range of gun-fired projectiles is briefly assessed. The possibility is explored of improving projectile performance by the addition of a guidance system.

It is concluded that the use of a sabot with subcalibre ammunition can result in considerable range increase. Hazards presented by the sabot to friendly troops and materials can be eliminated by suitable design.

- 273 Barnett, F. Q.; King, F. G.; "COMPARISON OF T-212 ROCKET-ASSIST GUN WITH CONVENTIONAL GUNS," Ballistic Research Laboratories, Memorandum Report No. MR-562, August 1951. (AD 377 331)
- 274 Bastress, E. K.; Allan, D. S.; "THEORETICAL EVALUATION OF PROPULSION PARAMETERS FOR ZONED ROCKET-ASSISTED ARTILLERY PROJECTILE," Arthur D. Little, Incl, Bulletin of 20th ISP Meeting, Vol. IV, July 1964, pp. 329-343, Confidential.
- 275 Chadwick, W. R. et al; "DYNAMIC STABILITY OF THE 5-INCH/54 ROCKET ASSISTED PROJECTILE (THE INFLUENCE OF A NON-LINEAR MAGNUS MOMENT)," Naval Weapons Laboratory, Report No. 2059, October 1966. (AD 802 001)
- 276 Chadwick, W. R.; Sylvester, J. F.; "DYNAMIC STABILITY OF THE 5-INCH/38 ROCKET ASSISTED PROJECTILE," Naval Weapons Laboratory, Technical Memorandum No. TM K-63/66, November 1966. (AD 803 358)

- 277 Harnett, Stephen J. et al; "ED REVIEW POINT NOTES FOR THE 105MM, XM548 HE ROCKET ASSISTED CARTRIDGE," Picatinny Arsenal, Technical Report No. TR-3347, November 1966. (AD 378 269)
- 278 Marshall, Melvin R.; "FIVE-INCH ROCKET ASSISTED PROJECTILE (RAP) WARHEAD DEVELOPMENT TEST PROGRAM OUTLINE," Naval Weapons Laboratory, Technical Memorandum No. T-31/65, October 1965. (AD 368 204)
- 279 Remington, Richard D.; Barnett, Fred Q.; "RAM-JET ASSISTED SHELL COMPARED WITH ARROW SHELL FOR USE AS UNGUIDED AA MISSILES," Ballistic Research Laboratories, Technical Note No. TN 728, September 1952. (AD 384 622)
- 280 Scharf, R. W.; Watson, J. G.; "CLOSED TUBE LAUNCHED SOLID ROCKET ORDNANCE SYSTEM," Bulletin of 20th ISP Meeting, Vol. IV, July 1964, pp. 383-400, Confidential.
- 281 "SOLID ROCKET PROPULSION SYSTEMS FOR THE 105 MM HOWITZER AND THE 107 MM MORTAR BOOSTED SPIGOT PROJECTILES," Picatinny Arsenal, Technical Report No. TR 3741, March 1968, Confidential.

A program was undertaken by the Ammunition Engineering Directorate's Solid Rocket Propulsion Laboratory which demonstrated the feasibility of achieving an extended range for a heavy weight supercaliber projectile when launched from the 107 mm XM95 mortar with the aid of a rocket assist. The program culminated in successful maximum range flight firings within an extended temperature range. Additionally, range zoning by thrust termination was successfully demonstrated by several different techniques.

Initially, a termination device was designed that caused the rocket motor to separate from the warhead section at any predetermined velocity or time. A requirement was subsequently established to accomplish thrust termination without in-flight separation. This was done in two different ways; in one design the rocket motor action was terminated by suddenly venting the gases and dropping the pressure; in the other approach, liquid quenching of the rocket motor caused the motor to stop burning. Additional studies in the 107 mm system demonstrated the feasibility of delivering an even heavier warhead to full range.

D-7 GUN LAUNCHED ROCKETS, PROBES, AND SPACE VEHICLES

- 282 Bull, G. V.; Lyster, D.; Parkinson, G. V.; "ORBITAL AND HIGH ALTITUDE PROBING POTENTIAL OF GUN-LAUNCHED

- ROCKETS, " Space Research Institute, McGill University, SRI-H-R-13, October 1966. (AD 807 731)
- 283 Cox, R. N.; "THE CASE FOR GUN-LAUNCHED SPACE PROBES," New York Scientist, Vol. 36, November 9, 1967, pp. 337-340.
 - 284 Eyre, F. W.; "THE DEVELOPMENT OF LARGE BORE GUN LAUNCHED ROCKETS," Canadian Aeronautics and Space Journal, Vol. 12, April 1966, pp. 143-149.
 - 285 Groundwater, F. M.; "THE DEVELOPMENT OF GUN LAUNCHED ROCKETS," Space Research Institute, McGill University, SRI-H-R-6, February 1968.
 - 286 Hurst, N. J.; Burleson, W. G.; "ANALYSIS, DESIGN, AND COGENT FLIGHTS OF THE FIRST LARGE DIAMETER GUN LAUNCHED TEST BODIES - LAHIVE," U. S. Army Missile Command, Report No. RS-TR-67-4, April 1967. (AD 818 372)
 - 287 Kardos, G.; "NOTES ON MECHANICAL DESIGN OF GUN LAUNCHED VEHICLES," Report No. TN-62-5, July 1962. (AD 450 668)
 - 288 McCluney, Eugene L.; "THEORETICAL TRAJECTORY PERFORMANCE OF 5" GUN PROBE SYSTEM," ECOM 5015, ERDA, WSMR, October 1965. (AD 473 271)
 - 289 McKee, R. M.; "A PARAMETRIC STUDY OF MULTI-STAGE GUN LAUNCHED ROCKETS," Space Research Institute, McGill University, SRI-H-R-2, March 1965; see also "CONTINUATION OF GUN-LAUNCHED ROCKET PARAMETRIC STUDY," SRI-H-R-5, May 1965.
 - 290 Parkinson, G. V.; "SIMPLIFIED FORMS OF PRELIMINARY TRAJECTORY CALCULATION FOR GUN-LAUNCHED VEHICLES," Space Research Institute, McGill University, SRI-R-19, August 1967.
 - 291 Raymond, H. A.; "ORBIT INJECTION CONTROL FOR HARP," Canadian Aeronautics and Space Journal, Vol. 11, May 1965, pp. 154-159.
 - 292 "AN EVALUATION OF PAYLOAD DELIVERY SYSTEMS FOR NIKE-X," Brown Engineering, Report No. TN AS-214, September 15, 1966.
 - 293 "GUN LAUNCHED VEHICLES COST EFFECTIVENESS STUDY," Lockheed Missiles and Space Company, Report No. LMSC-688043, September 29, 1967. (AD 826 497)

D-7.1 High Altitude Research Probes (HARP)

- 294 MacAllister, L.C.; Bradley, J.W.: "Comments on the Use of Guns to Launch High-Altitude Probes"; (Unclassified Report), BRL Memorandum Report No. 1252, March 1960, AD 237 038.

(Unclassified Abstract) The capability of current conventional and light-gas guns to launch altitude probes is reviewed. Peak altitudes from 200,000 to 1,000,000 feet appear possible depending on the size of the gun launcher and on the amount of effort put into design, or redesign, of the gun and projectile to optimize the system for upper atmosphere probes.

Weight penalty for using sabots is discussed.

- 295 Marks, Spence T.; MacAllister, Leonard C.; Gehring, J. William; Vitagliano, H. Douglas; Bentley, Bedford T.: "Feasibility Test of an Upper Atmosphere Gun Probe System"; (Unclassified Report), BRL Memorandum Report No. 1368, October 1961, AD 267 354.

(Unclassified Abstract) The feasibility test of an upper atmosphere gun probe system, employing a smoothbore 120-mm gun, and a fin stabilized (non-spinning) 60-mm probe, is described. Results obtained from the first and second vertical test series are given (a total of twelve rounds). The present gun probe system is evaluated, and the future prospects for such a system are discussed. Major parts of the sabot used are briefly discussed and photographs of sabot separation are included. Pictorial representations and photographs of probe vehicles and sabots are given.

- 296 Boyer, Eugene D.: "Five-Inch HARP Tests at Wallops Island, September 1963;" (Unclassified Report), BRL Memorandum Report No. 1532, January 1964, AD 430 232.

(Unclassified Abstract) The results of vertical firing tests of the five-inch HARP system are presented. The tests were conducted at the NASA facility, Wallops Island, with successful radar tracks of both projectile and payloads.

Package function and exact altitude were the prime concern.

In-flight photographs of sabot separation, plus a still photograph of the actual projectile and sabot, are shown. Sabot diameter and weight are given.

- 297 "Project HARP, Report on the First Twelve Firings and Status as of July 30, 1963;" (Unclassified Report), McGill University, Report No. 63-5, November 1963, AD 428 795.

(Unclassified Abstract) Project HARP is the code name covering a program of research and development into the capabilities of vertically fired gun probes. A 16.4" vertical firing gun facility has been established in Barbados for the following purposes: 1) studies of the potential of vertical firing guns launching sabot vehicles, 2) determine the economic and engineering feasibility of placing significant payloads at altitudes of interest, 3) demonstrate the ability of these vehicles to perform studies of scientific interest, and 4) application of the technique for preparation in various scientific studies of the earth's atmosphere.

This report describes both the current range status and the results of test firings as of 30 July 1963. Several pictorial representations of different Martlet vehicles and sabots are given.

- 298 Wasserman, S.; Lattal, G.; Smolnik, J.: "Parametrics Studies on use of Boosted Artillery Projectiles for High Altitude Research Probes, Project HARP;" (Unclassified Report), Picatinny Arsenal Report No. 3147, January 1964, AD 601 409.

(Unclassified Abstract) This Report contains a general parametric and preliminary design study of rocket-boosted artillery projectiles for high altitude probes when fired from existing gun systems. The following systems were studied:

- 5" diameter boosted projectile fired from a 5" gun
- 4.5" diameter boosted projectile fired from a 7" gun
- 7" diameter boosted projectile fired from a 7" gun
- 8.4" diameter boosted projectile fired from a 16.4" gun
- 13.8" diameter boosted projectile fired from a 16.4" gun
- 16.4" diameter boosted projectile fired from a 16.4" gun

The rocket is supported about the periphery of the base of each compartment by the sabot. The sabot also envelopes the base of the projectile, including the nozzle and folding flare stabilizer. The rocket igniter assembly is located within the nozzle. A sabot drag device is housed within the hemispherical base of the sabot.

- 299 Eyle, F.W.: "Outline Aerodynamics and Performance of the Martlet 2C;" (Unclassified Report), McGill University Tech Note S.R.I. -H. TN-1, November 1964, AD 454 878.

(Unclassified Abstract) This note gives the predicted basic aerodynamic data pertinent to the vehicle, and presents performance as a function of the major parameters. The combination of weight and muzzle velocity necessary to meet the 125 KM specification are presented together with center of gravity tolerance.

Trajectory studies have been run for a range of parameters on the McGill I. B. M. 7040 computer. The dominant variable -- muzzle velocity -- is the object of continuous improvement. Currently feasible is 6000 ft/sec for the sabotated Martlet 2C at 400 lbs. assembled weight, 6500 ft/sec should soon be achieved. Results are summarized.

- 300 "Shells into Orbit"; (Unclassified Article), Machine Design, Vol. 37, No. 1, January 7, 1965, pp. 115-17.

(Unclassified Abstract) A general interest article on the activities of the HARP program. The purposes of the Wallops Island 7-inch, 58 ft gun and the Barbados Island 16-inch, 80 ft gun are discussed briefly. One of the goals of the HARP program is to be able to put a gun-launched vehicle into earth orbit. To accomplish this, sabots are necessary. Clear photographs of the guns and photographs of the sabot separation are shown. A typical projectile has an aluminum sabot and four fins slightly canted to induce a roll of about 9 rev/sec.

- 301 Luckeot, H. J.: "Report of March 1965, Test Firing Series. Project HARP;" (Unclassified Report), McGill University Report No. SRI-H-R-9, July 1965, AD 475 146.

(Unclassified Abstract) The purpose of the series was to demonstrate the mechanical and ballistic performance of the 16.4" gun at Barbados with the new 51-foot extension, and secondly, to conduct engineering reliability and proving tests of vehicles and payloads, with scientific data gathering where possible. The series were successful in both aspects.

Five Martlet series vehicles were tested: 2A, 2C, 2D, 3B fiberglass and 3B steel. Cross sections of vehicles and sabots are shown. Sabot and launch system component weights are given. In-flight sabot separation photographs are given. Fiberglass sabot and gun-busted rocket system, Martlet 3B series, was successfully launched at 3600 g's.

- 302 Marks, Spence T.; Pilcher, James O. II; Brandon, Fred J.: "The Development of a High Acceleration Testing Technique for the Electronic Instrumentation of HARP Projectile Systems;" (Unclassified Report), BRL Memorandum Report No. 1738, March 1966 AD 635 782.

(Unclassified Abstract) A brief description of Project HARP (High Altitude Research Project) which uses smoothbore 5-inch, 7-inch, and 16-inch guns to launch sub-calibre sabotated projectiles for upper atmospheric research, is given. Acceleration testing requirements for the electronic instrumentation of the projectiles are stated. The acceleration testing methods employed previously are reviewed. A BRL project for the development of a satisfactory acceleration testing technique for this purpose is described. Test results are given. Test results are analyzed, and test criteria are established and evaluated. A detailed photographic coverage of the test is given.

- 303 Braun, Walter F.: "An Inbore Velocity Measuring Probe System for Large Calibre Guns;" (Unclassified Report), BRL Technical Note No. 1610, April 1966, AD 637 280.

(Unclassified Abstract) Of prime interest is the description of an inbore velocity measuring technique using contact switches. Reliability and accuracy requirements are discussed and typical field results are given.

Inflight photographs of the 16-inch sabot and projectile are given.

Shock waves at velocities above 6000 fps and leakage of powder gases past the sabot cause transient and undefinable contact switch operation. Success in measuring velocity depends chiefly on the proper functioning of the sabot.

- 304 Murphy, C. H.; Bull, G. V.: "Review of the High Altitude Research Program (HARP);" (Unclassified Report), BRL Report No. 1327, July 1966, AD 645 284

(Unclassified Abstract) Project High Altitude Research Program (HARP) is directed toward the use of guns for scientific probing of the upper atmosphere. The attractive features of guns for this purpose include the basic economy of such a system and the high inherent accuracy of guns for placement at altitude, as well as accuracy in ground impact. The basic liability for such an approach lies in the very high accelerations experienced by gun-launched payloads.

The guns used in Project HARP vary in size from 5-inch and 7-inch extended guns on mobile mounts to transportable fixed 16-inch guns. Altitude performance varies from 20-pound, 5-inch projectile reaching 240,000 feet to 185-pound, 16-inch projectiles reaching 470,000 feet. Single and multiple stage rockets launched from the 16-inch gun possess promising predicted performance and are under development.

Scientific results to date are primarily wind profiles measured by radar chaff, aluminized balloons and parachutes, and tri-methyl-aluminum trails, although a number of successful 250 MHz and 1750 MHz telemetry flights have been made. Sun sensors, magnetometers, and temperature sensors have been flown and an electron density sensor was fired earlier. Development of other active sensors is continuing.

The role of the sabot in the HARP is discussed briefly. Photographs of the gun and sites are included.

- 305 Boyer, Eugene D.: "Five-Inch HARP Tests at Barbados, West Indies, January-February 1966;" (Unclassified Report), BRL Memorandum Report No. 1771, July 1966, AD 640 438.

(Unclassified Abstract) The installation of a 5-inch HARP gun system at Barbados, West Indies, is presented. Primary interest is in carrying a

low-cost wind sensor to 200,000 feet. Secondary interest is in the firing data, pay-load acquisition, vehicle altitude, charge weight, gun pressure, and vehicle and sabot weight. A sectioned view of the HARP 5-1 probe projectile and sabot is shown.

- 306 Billings, R. G.; Atmore, R. F.; "A STUDY TO GUIDE RESEARCH AND DEVELOPMENT TOWARD AN OPERATIONAL METEOROLOGICAL SOUNDING ROCKET SYSTEM," Thiokol Chemical Corporation, NASA CR-91057, April 1967.
- 307 Boyer, Eugene D.; "FIVE-INCH GUN METEOROLOGICAL SOUNDING SITE, HIGHWATER, QUEBEC," Ballistic Research Laboratories, Report No. MR-1929, July 1968. (AD 673 712)

The use of a meteorological gun-probe in a confined area has been demonstrated. A program utilizing the 5 in. HARP system at Highwater, Province of Quebec, near the Vermont state border, is described. Wind soundings were made to altitudes of 230,000 ft with a ground impact area limitation of 1 sq mi for the spent projectile.
- 308 Boyer, E. D.; MacAllister, L. C.; "SEVEN-INCH HARP GUN LAUNCHED VERTICAL PROBE SYSTEM: INITIAL DEVELOPMENT," Ballistic Research Laboratories, Report No. MR-1770, July 1966. (AD 640 825)
- 309 Boyer, E. D.; Williamson, L. E.; "FIVE-INCH HARP SYSTEM--INITIAL TEST SERIES -- FORT GREELEY, ALASKA," Ballistic Research Laboratories, Technical Note 1657, May 1967. (AD 655 267)
- 310 Braithwaite, K.; Luckert, H. J.; "REPORT OF THE AUGUST/-SEPTEMBER 1965 TEST FIRING SERIES PROJECT HARP," Space Research Institute, McGill University, Report No. SRI-R-17, December 1967. (AD 825 694)
- 311 Brown, J. A.; Marks, S. T.; "FEASIBILITY TEST OF A POTENTIAL METEOROLOGICAL SHELL FOR THE STANDARD 175 MM GUN," Ballistic Research Laboratories, Technical Note 1584, February 1966. (AD 631 245)
- 312 Brown, J. A.; Marks, S. T.; "HIGH ALTITUDE GUN PROBE SYSTEMS FOR METEOROLOGICAL MEASUREMENTS," The Meteorological Rocket Network, IRIG Document 111-64, February 1965, pp. 211-221. (AD 464 583)
- 313 Bull, G. V., "DEVELOPMENT OF GUN LAUNCHED VERTICAL PROBES FOR UPPER ATMOSPHERE STUDIES," Canadian Aeronautics and Space Journal, Vol. 10, October 1964, pp. 236-247.

- 314 Bull, G. V., "PROJECT HARP," Ordnance, Vol. LII, March - April 1968, pp. 482-486.
- 315 Bull, G. V.; Murphy, C. H.; "GUN BOOSTED ROCKETS FOR HIGH PERFORMANCE SOUNDING MISSIONS," AIAA Sounding Rocket Vehicle Technology Specialist Conference Proceedings, February 1967, pp. 581-593.
- 316 Bull, G. V.; Murphy, C. H.; "GUN LAUNCHED MISSILES FOR UPPER ATMOSPHERE RESEARCH, AIAA Preprint, No. 64-18, January 1964.
- 317 Edwards, J. W.; Kirk, B. P.; Temchin, J. R.; Carsey, J. N.; "SURVEY OF DEVELOPMENTS IN GUN-LAUNCHED HIGH ALTITUDE PROBES," U. S. Naval Propellant Plant, Report No. NPP/RP 66-7, September 1966.
- 318 Lathrop, Wayne; "STUDY OF 280-MM GUN AS A TOOL FOR UPPER ATMOSPHERIC RESEARCH," Sandia Corporation, Report No. SC-RR-66-149, November 1966.

An estimate of the capability of the 280-mm gun as a research tool to perform upper atmospheric studies for Sandia's Aerospace Nuclear Safety Program is presented. Performance characteristics of the 280-mm gun are compared with those of the 16-inch and 7-inch guns presently used for upper atmospheric studies by the Ballistic Research Laboratory, Aberdeen Proving Ground, and McGill University, Montreal.
- 319 Lorimor, George; "7-INCH HARP (NAVY MODEL) FINAL REPORT," Rock Island Arsenal, Technical Report 67-296, January 1967. (AD 808 813L)
- 320 Lorimor, George; "7-INCH HARP FINAL REPORT," Rock Island Arsenal, Technical Report 66-3411, November 1966. (AD 808 327L)
- 321 Luckert, H. J.; "REPORT OF THE MAY/JUNE 1965 TEST FIRING SERIES PROJECT HARP," Space Research Institute, McGill University, Report No. SRI-H-R-10, September 1966. (AD 649 116)
- 322 Luckert, H. J.; "REPORT OF THE NOVEMBER 1965 TEST FIRING SERIES PROJECT HARP," Space Research Institute, McGill University, Report No. SRI-R-20, January 1968. (AD 666 744)
- 323 Marks, S. T.; Boyer, E. D.; "A SECOND TEST OF AN UPPER ATMOSPHERE GUN PROBE SYSTEM," Ballistic Research Laboratories, Memorandum Report 1464, April 1963. (AD 405 889)

- 324 Millman, P. M.; "BIG GUN ON BARBADOS," Sky and Telescope, Vol. 32, August 1966, pp. 64-67.
- 325 Murphy, Charles H.; Bull, Gerald V.; "AEROSPACE APPLICATION OF GUN LAUNCHED PROJECTILES AND ROCKETS," Space Research Institute, McGill University, Report No. SRI-R-24, February 1968. (AD 666 746)

Project High Altitude Research Program (HARP) is directed toward the use of guns for scientific probing of the upper atmosphere. The attractive features of guns for this purpose are the basic economy of such a system and the high inherent accuracy of guns for placement at altitude as well as accuracy in ground impact. The basic liability for such an approach lies in the very high accelerations experienced by gun-launched payloads. The guns used in Project HARP vary in size from 5-inch and 7-inch extended guns on mobile mounts to transportable fixed 16-inch guns. Altitude performance varies from 20 pound, 5-inch projectiles reaching 240,000 feet to 185-pound, 16-inch projectiles reaching 590,000 feet. Scientific results to date are primarily wind profiles measured by radar chaff, aluminized balloons and parachutes, and tri-methyl-aluminum trails, although a number of successful 250 MHz and 1750 MHz telemetry flights have been made.

- 326 Murphy, C. H.; Bull, G. V.; "GUN-LAUNCHED PROBES OVER BARBADOS," Bulletin of the American Meteorological Society, Vol. 49, June 1968, pp. 640-644.
- 327 Murphy, C. H.; Bull, G. V.; "REVIEW OF THE HIGH ALTITUDE RESEARCH PROGRAM," The Fluid Dynamic Aspects of Ballistics, AGARD CP 10, September 1966, pp. 403-437. (AD 803 753)
- 328 Murphy, C. H.; Bull, Gerald V.; Edwards, H. D.; "UPPER ATMOSPHERE WINDS MEASURED BY GUN-LAUNCHED PROJECTILES," Ballistic Research Laboratories, Memorandum Report 1747, May 1966. (AD 637 850)
- 329 Rossmiller, R.; Salsbury, M.; "16-INCH HARP WORK AT ROCK ISLAND ARSENAL -- SUMMARY REPORT," Rock Island Arsenal, Technical Report 66-1493, April 1966. (AD 482 573)
- 330 Wasserman, S.; Bull, G. V.; Murphy, C. H.; "ROCKET ASSIST PROJECTILES FOR HIGH ALTITUDE RESEARCH PROBES (PROJECT HARP)," Bulletin of the 20th Interagency Solid Propulsion Meeting, Vol. IV, Chemical Propulsion Information Agency Publication No. 49B, October 1964, pp. 371-382. (AD 355 356)

- 331 Webster, R. C.; Dunfee, D. D.; Peterson, J. S.; "A CLOSED TUBE LAUNCHED SOUNDING ROCKET," Bulletin of the 20th ISP Meeting, Vol. IV, July 1964, pp. 401-412, Confidential.
- 332 Williamson, L. E.; "GUN-LAUNCHED VERTICAL PROBES AT WHITE SANDS MISSILE RANGE," Atmospheric Sciences Office, Report No. ECOM-5030, February 1966. (AD 482 330)
- 333 Williamson, L. Edwin; Boyer, E. D.; "THE GUN-LAUNCHED METEOROLOGICAL SOUNDING SYSTEM," AMS/AIAA Paper, No. 66-382, March 1966.
- 334 Williamson, L. Edwin; Kennedy, Bruce; "METEOROLOGICAL SHELL FOR STANDARD ARTILLERY PIECES. A FEASIBILITY STUDY," Atmospheric Sciences Lab., White Sands Missile Range, Report No. ECOM-5161, October 1967. (AD 667 914)

A feasibility study has been performed which considered the applicability of an instrumented shell for a standard rifled gun as a means of obtaining meteorological data for tactical Army applications. The conclusions have shown that the technical feasibility of a meteorological shell is within the state-of-the-art of engineering practices.

- 335 "REPORT OF THE NOVEMBER 1965 TEST FIRING SERIES PROJECT HARP," Space Research Institute, McGill University, Report No. SRI-R-20, November 1966.
- 336 "REPORT OF THE AUGUST/SEPTEMBER 1965 TEST FIRING SERIES PROJECT HARP," Space Research Institute, McGill University, Report No. SRI-R-17, September 1965.

-7.2 HARP Instrumentation

- 337 Cruickshank, W. J.; "A FEASIBILITY TEST OF A 1750 Mc/s TELEMETRY AND TRACKING SYSTEM FOR FIVE-INCH HARP PROJECTILES," Ballistic Research Laboratories, Memorandum Report No. 1651, May 1965. (AD 469 653)
- 338 Cruickshank, W. J.; "HIGH 'G' UHF TELEMETRY FOR GUN-LAUNCHED SOUNDING PROBES," Ballistic Research Laboratories, Memorandum Report No. 1632, January 1965. (AD 463 928)
- 339 Cruickshank, W. J.; "1750 MHz TELEMETRY/SENSOR RESULTS FROM HARP FIRINGS AT BARBADOS AND WALLOPS ISLAND, 1965," Ballistic Research Laboratories, Memorandum Report No. 1824, February 1967. (AD 815 761)

- 340 Evans, J. W.; "DEVELOPMENT OF GUN PROBE PAYLOADS AND A 1750 Mc/s TELEMETRY SYSTEM," Ballistic Research Laboratories, Memorandum Report No. 1749, May 1966. (AD 637 747)
- 341 Evans, J. W.; "EVALUATION OF A TUNNEL-DIODE OSCILLATOR FOR USE IN GUN PROBE TELEMETRY," Ballistic Research Laboratories, Memorandum Report No. 1711, November 1965. (AD 631 514)
- 342 Marks, S. T.; "HIGH-G COMPONENT TEST," Ordnance, Vol. LII, January 1968, pp. 386-388.
- 343 Mermagen, W. H.; "HARP 250 MC TELEMETRY EXPERIMENTS, JUNE/-OCTOBER 1964," Ballistic Research Laboratories, Memorandum Report No. 1614, November 1964. (AD 459 576)
- 344 Mermagen, W. H.; "HARP 250 Mc/s TELEMETRY EXPERIMENTS, WALLOPS ISLAND, March 1965," Ballistic Research Laboratories, Memorandum Report No. 1694, September 1965, (AD 631 268)
- 345 Mermagen, W. H.; "HIGH 'G' TELEMETRY FOR BALLISTIC RANGE INSTRUMENTATION," Ballistic Research Laboratories, Memorandum Report No. 1566, April 1964. (AD 444 246)
- 346 Mermagen, W. H.; "TELEMETRY EXPERIMENTS CONDUCTED ON THE HARP PROJECT IN BRITISH WEST INDIES AND WALL-OPS ISLAND, VIRGINIA, DURING THE PERIOD JAN-MAR 1964," Ballistic Research Laboratories, Memorandum Report No. 1578, July 1964. (AD 449 867)
- 347 Mermagen, W. H.; Cruickshank, W. J.; Vratovic, F.; "VHF AND UHF HIGH-G TELEMETRY FOR HARP VEHICLES," The Fluid Dynamic Aspects of Ballistics, AGARD CP 10, September 1966, pp. 439-464. (AD 805 753)
- 348 Mermagen, W. H.; Cruickshank, W. J.; Vratovic, F.; "VHF AND UHF HIGH-G TELEMETRY INSTRUMENTATION FOR HARP VEHICLES," Ballistic Research Laboratories, Memorandum Report No. 1768, May 1966. (AD 640 596)
- 349 Northcote, D. L. S.; "HARP 1/4 SCALE MODELS -- GENERAL DESCRIPTION OF INSTRUMENTATION," Inspection Services, Canadian DND, TN 5/64, December 1964.
- 350 Pulfer, J. K.; "TELEMETRY SYSTEMS FOR GUN-LAUNCHED UPPER ATMOSPHERE PROBES," National Research Council of Canada, Report No. ERB-742, June 1966. (AD 655 874)

- 351 Wilkin, N. D.; "TM RESEARCH PROGRAM -- HIGH-G TESTS OF COMPONENTS," Harry Diamond Laboratory, Report No. TM-65-33, July 1965. (AD 622 405)

D-7.3 Target Placement System

- 352 Bull, G. V.; Aikenhead, B.; Palacio, L.; Lyster, D.; "A GUN LAUNCH TARGET PLACEMENT SYSTEM," Space Research Institute, McGill University, Report No. SRI-2-TN-4, August 1966. (AD 475 146).

D-7.4 Gun-Launched Antimissile System (GLAM)

- 353 Galati, L.; Marheska, A.; "CONCEPT STUDY OF A GUN-LAUNCHED ANTIMISSILE SYSTEM GLAM," Picatinny Arsenal, Report No. SMUPA-TK-900, July 1964.

D-7.5 Martlet System

- 354 Delfour, M. C.; Galiana, F. D.; Aikenhead, B. A.; "THE EFFECT OF DISPERSION IN TRAJECTORY PARAMETERS ON A NOMINAL MARTLET IV TYPE ORBIT," Space Research Institute, McGill University, Report No. SRI-R-26, September 1967.
- 355 Eyre, F. W.; "THE MARTLET 2A BALLISTIC VEHICLE -- SUMMARIZED PERFORMANCE DATA," TN 64-4, May 1964.

D-7.6 Related Systems

- 356 Kumar, S.; Murray, J. J.; Rajan, J. R. N.; "VACUUM-AIR MISSILE BOOST SYSTEM," Journal of Spacecraft and Rockets, Vol. 1, September-October 1964, pp. 464-470.

The vacuum-air missile boost system consists of a partially evacuated vertical launching tube with a breakable seal at the top and with the lower end sealed by a missile on a held-down sabot. When the sabot is released, atmospheric pressure from air entering the base of the tube accelerates the missile. A "muzzle chamber" near the top of the tube reduces the velocity loss due to compression of the residual air above it, and the

tube length beyond the muzzle chamber serves as an "atmospheric shock reducer." The system is considered suitable for small- and medium-sized missiles. Advantages compared to the usual surface-launching technique are a significant fuel saving or an increase in payload, less sensitivity to surface gusts, and a shelter prior to firing. The motion of the missile is analyzed by assuming incompressible, quasi-steady air flow; effects of muzzle chamber size, viscous loss, and turbulence are included. Theoretical curves of muzzle velocity vs vehicle weight are given for various tube lengths for maximum accelerations of 8 and 15 g's. Muzzle velocities of 600 to 800 fps appear to be feasible at these acceleration levels. Results obtained in experiments in 3- and 1.25 in. - i. d. by 20-ft tubes show good agreement with theory.

- 357 Valenti, A. M.; Molder, S.; Salter, G. R.; "GUN LAUNCHING SUPERSONIC COMBUSTION RAMJETS," *Astronautics and Aerospace Engineering*, Vol. 1, December 1963, pp. 24-29.
- 358 "SELF EJECT SYSTEM LAUNCH-TESTED IN UTAH," *Aerospace Facts* (published by Thiokol Chemical Corp.), April-June 1968.

Announcement of a test to demonstrate that chamber pressure below a missile can be regulated to allow use of the motor exhaust gases to eject the missile from a launch tube. The test vehicle was launched from a 90-foot long steel tube to an altitude of 1,200 feet. Flight duration was 18 seconds. A 15.5-inch diameter rocket motor with a short duration solid propellant grain was utilized for the demonstration.

- 359 "A FEASIBILITY STUDY OF THE SCRAMJET IN-TUBE CONCEPT," General Applied Science Laboratories, Technical Report No. TR 669, AFAPL-TR-67-131, November 1967. (AD 388 535)

D-7.7 Ground-Accelerated Space Platform (GASP)

- 360 "Feasibility Study of a GASP Launch Payload Vehicle;" (Confidential Report), AVCO Corp., Research and Advanced Development Division, Report RAD-SR-26-60-54, 5 July 1960, AD 319 583.

(Unclassified Abstract) The feasibility of launching payload-vehicles into space by the use of a mass-restrained, atomic-powered cannon is discussed. This is part of the ground accelerated space platform (GASP) program.

The primary objectives of the study was the establishment of a GASP-launched payload-vehicle design. Two other objectives are included: (1) Design of a sabot to guide the payload-vehicle in the tube and to protect it from the expanding high-temperature propellant gases, and (2) determination of the extent of erosion in the launch tube caused by high-temperature and high-velocity gases sweeping over the launch tube walls and by mechanical contact of the sabot with the tube walls.

A good general discussion of the sabot and the problems to be concerned with is presented. The following phases are discussed under sabot design: (1) general requirements, (2) initial shock, and (3) acceleration phase. Some comments on the basic problems dealing with high-strain rate loading are included under the topic initial shock.

- 361 Brogan, J. L.: "Arbalist Progress Report;" (Confidential Report), Douglas Aircraft Company Report No. E250-AN-3022, 17 July 1964, AD 366 574, for U. S. Army Missile Command.

(Unclassified Abstract) In this 21st progress report, the general status of the program is given. Launching techniques and tests are discussed. Drawings of the arbalist rocket and forward supporting damping sabot are shown.

- 362 Barakauskas, E. J.; Small, D. A; Murphy, J. J.: "Final Report Large Cold Launch Missile (LCLM) Feasibility Demonstration;" (Confidential Report), Westinghouse Electric Corporation Report No. R501, September 1965, AD 365 487L.

(Unclassified Abstract) The objectives of the LCLM program were to: (1) demonstrate the feasibility of eject launch of large 300,000-pound class missiles (2) demonstrate the feasibility of an air-supported elevator for elevation of a missile or missile segments in inaccessible launch tubes, and (3) develop a sabot and seals for eject launch. A launch tube was installed at Edwards Air Force Base to conduct eject launch and air-elevator feasibility tests. The 327,000-pound, water-filled dummy missile and sabot were ejected from the silo using off-the-shelf rocket motors as gas generators. The launch demonstrated that eject launching could provide an acceptable launch velocity at a low acceleration level. The air elevator concept was demonstrated by the assembly of the segmented dummy missile upon the sabot and by adjusting air pressure to raise and lower the dummy missile within the launch tube. The air elevator could be remotely controlled, precisely positioned, and held in a fixed position. Elevating and lowering rates of approximately 4 feet per minute were achieved. These tests, summarized in this final report, accomplished all program objectives and proved the feasibility of eject launch of large missiles. The tests demonstrated that the air elevator is a practical device for the assembly and maintenance of large missiles.

D-7.8 HIBEX Program

- 363 "ARPA Project HIBEX Flight Test Report Vehicle D-2;" (Confidential Report), The Boeing Co. Report No. D2-99579-5, 10 December 1965, AD 367 882L.

(Unclassified Abstract) This report presents the results of the fifth test of a HIBEX (High-g Boost Experiment) vehicle. The vehicle, designated D-2, was launched from a closed breech silo to evaluate launch effects and performed a programmed maneuver using both pitch and yaw TVC injection to continue

evaluation of the performance of the flight control system. Data were obtained on silo heating rates, silo pressures, and the effect of silo pressure on rocket motor exhaust gas flow. Accurate pitch and yaw control was obtained with reference to vehicle body axes. Sabot base pressure is discussed and pictorial representations of the sabot and vehicle are included.

- 364 "HIBEX Flight Test Report Vehicle D-3;" (Confidential Report), The Boeing Co. Report No. D2-99579-6, 17 January 1966, AD 368 691L.

(Unclassified Abstract) This report presents the results of the sixth flight test of the HIBEX (High-g Boost Experiment) vehicle. The vehicle, designated D-3, was launched from a closed breech silo of reduced plenum volume from the preceding silo launch test to evaluate launch effects at relatively high silo pressure. Following vehicle exit from the silo, a programmed maneuver using liquid injection thrust vector control was performed to continue evaluation of the performance of the flight control system and to obtain rocket motor performance data at high lateral accelerations and aerodynamic data at large angles of attack. An external burning experiment was incorporated into the second stage to provide an indication of the effectiveness of this technique for controlling guided missiles. Data were obtained relative to all flight objectives. The external configuration of the D-3 vehicle and sabot assembly was the same as that of the D-2 assembly.

D-8 TERMINAL BALLISTICS STUDIES

- 365 "Development of Sabot for Firing Spherical Munitions from the Range 72E Air Gun, Work Assignment B-5; (Unclassified Report) Chicago Midway Laboratories, Technical Note No. CML-57-TN-M107.4, 1 January 1957.

(Unclassified Abstract) Development work and testing involved to determine feasibility of using an air gun to launch a spherical munition are described. Velocities of 200 fps were obtained. Purpose of launching was to obtain terminal ballistic data. Sabot development and stripping are described. Photographs of sabot and stripper are given.

- 366 Partridge, William S.: "Construction of a High Velocity Gun for Propelling Small Irregular-Shaped Pellets; (Unclassified Report) University of Utah, Interim Technical Report No. 8, March 1957, AD 142 784.

(Unclassified Abstract) A .22 calibre accelerator capable of firing irregular shaped fragments weighing 1/2 to 15 grains was constructed. The gun barrel was made in two sections joined together with an O-ring seal and flange. The barrel was smooth-bored and had an adapter on the muzzle to allow evacuation of the barrel with a mechanical vacuum pump. The gun was chambered for a standard .220 Swift shell and fired electrically by means of a 110 volt a-c solenoid.

To fire the irregular shaped pellets, a sabot was constructed to carry the pellets and separate from them within 36 inches from the end of the barrel. The problem of measuring the velocity of these small pellets is discussed and three systems are described which were used successfully.

By evacuating the barrel and using 1/2 grain pellets, velocities of more than 9,000 feet per second were obtained. Five-grain pellets were accelerated to a velocity of approximately 8,000 feet per second.

Drawings and photos are included of the gun and sabot.

- 367 Warren, H. R.: "Aeroballistic Range Tests of the CF-105 Phase 1-Rounds 1 to 10 ;"(Secret Report 27), CARDE Report No. TM AB-43, March 1958, AD 301 144.
- 368 Genevese, F.; Editor; "Third Symposium on Hypervelocity;" (Unclassified Report) Volume 1- February 1959, Held 7-9 October 1958, Chicago, AD 233 487.

Table of Contents (U)

- (1) "Microsecond Framing Camera Observations of High Velocity Impact," M. A. Cook and R. T. Keyes
- (2) "Electrostatic Accelerator for Impact Studies," C. D. Hendricks, H. Shelton and R. F. Wuerker
- (3) "Cratering by High Velocity Microparticles," G. D. Anderson, D. G. Doran, F. S. Hempy and M. C. Kells
- (4) "An Analysis of Microparticle Cratering in a Variety of Target Materials," J. W. Gehring, Jr.
- (5) "Perforation and Penetration Effects of Thin Targets," W. S. Partridge, C. R. Morris and M. D. Fullmer
- (6) "An Empirical Study of Residual Velocity Data for Steel Fragments Impacting on Four Materials," D. Malick
- (7) "High-Speed Impact of Metal Projectiles in Targets of Various Materials," J. L. Summers and A. C. Charters
- (8) "The Anomalous Behavior of Lead-to-Lead Impact," H. B. Vanfleet, W. S. Partridge and E. T. Cannon
- (9) "Volume-Energy Relation for Crater Formed by High-Velocity Projectiles," F. L. Culp
- (10) "An Experimental Study of Crater Formation in Lead," J. H. Kineke, Jr.
- (11) "Dinner Address" - Today's Military Technology - Ultra-modern, M. Schilling, Deputy Chief, Research and Development Division, Redstone Arsenal.

- (12) "Hypervelocity Penetration Studies," W.W. Atkins
- (13) "Volume-Energy Relations from Shaped Charge Jet Penetrations," J.B. Feldman, Jr.
- (14) "Surface Roughness Caused by Meteoroid Impacts," M. Kornhauser
- (15) "High-Velocity Impact of Small Metal Spheres Upon Flat Metal Targets," R.J. McKenzie, F.F. Martin, H.M. Kenworthy
- (16) "A Review of the Theories Concerning Crater Formation by Hypervelocity Impact," F.E. Allison
- (17) "Interplanetary Dust Distribution and Erosion Effects," D.B. Beard
- (18) "Variation of Emissive Properties of Surfaces Due to Atomic Molecular Bombardment," R.P. Stein
- (19) "Experimental Studies of Penetration by Shaped Charge Jets," H.J. James and J.S. Buchanan
- (20) "Sputtering from Hypersonic Vehicles in the Free Molecule Flow Region," G.D. Magnuson and D.B. Medved
- (21) "Experimental Techniques Developed for Impact Studies of Microparticles," M.C. Kells, F.B. Burkdoll, G.D. Anderson, D.E. Davenport, D.G. Doran, F.S. Hempy, and T.C. Poulter, Jr.
- (22) "Facilities and Instrumentation of the NRL Hypervelocity Laboratory," S.O. Bailey, A.B.J. Clark, D.A. Hall and H.F. Swift
- (23) "Calibration of Micrometeoritic Detectors Used in Satellites and Rockets," H.A. Cohen, A. Corman and M. Dubin
- (24) "The Utah Light-Gas Gun," W.A. Boyd, W.S. Partridge and E.T. Cannon
- (25) "An Experimental Study of the Input Parameters for an NRL-Type H-Gun," G.C. Crews
- (26) "An Expendable High-Explosive, Light-Gas Gun for Projecting High-Velocity Projectiles," J.W. Gehring, Jr.
- (27) "High-Explosive Hypervelocity Projectors," R. Stresau and J. Savitt

- (28) "EM Accelerators," D. L. Wennersten
- (29) A Critical Study of the Air Cavity Technique for Projecting Intact Hypervelocity Fragments," L. Zernow, K. N. Kreyenhagen, P. G. McManigal and A. W. Hall
- (30) "Some Results of Hypervelocity Explosive Charge Investigations," E. N. Clark and A. MacKenzie
- (31) "A Multi-Stage H. E. -Actuated Hypervelocity Gun," F. J. Willig and H. W. Semon
- (32) "Aerodynamic Heating of Missiles -- Experimental Determination of Heat Transfer Coefficients," K. H. Abbott
- (33) "Observations of Projectile Impacts of Sand Particles at Velocities Ranging from 2,900 ft/sec to 7,000 ft/sec," J. P. McDonough and E. N. Hegge
- (34) "The Hyperballistics Launcher at A. R. D. R. Fort Halstead and Preliminary Results on Impact Phenomena," R. N. Cox and W. A. Clayden
- (35) "Multi-Phase Magnetic Propulsion of Projectiles," W. W. Salisbury
- 369 "Hypervelocity Impact, Fourth Symposium, April 26, 27, 28, 1960;" (Unclassified Report), Air Proving Ground Center, APGC-TR-60-39 (I), September 1960, AD 244 275

Table of Contents - Volume I (U)

- (1) "Hypervelocity Gun for Micrometeorite Impact Simulation Employing Capacitor Discharge in a Condensed Phase," Charles N. Scully and David L. Cowan
- (2) "An Exploding Wire Hypervelocity Projector," V. E. Scherrer and P. I. Richards
- (3) "Acceleration of Projectiles with the Sequenced High-Explosive Impulse Launcher," W. E. Fogg and C. W. Fleischer
- (4) A Multi-Stage Hypervelocity Projector," M. H. Bengson, T. K. Slaweki, and F. J. Willig
- (5) "Electroballistic Techniques," H. F. Swift

- (6) "Experimental Production of Hypervelocity Pellets by Means of Condenser Discharges in Hydrogen," D. Bloxom, Jr.
- (7) "The Addition of Electrical Energy to Helium," James R. Kymer
- (8) "The Fexitron - A New, Short-Pulse, High-Intensity X-Ray Tube," F.J. Grundhauser and W.P. Dyke
- (9) "Studies of Hypervelocity Impact on Lead," E.N. Clark, A. Mackenzie, F.H. Schmitt, and I.L. Kintish
- (10) "An Experimental Study of Crater Formation in Metallic Targets," John H. Kineke, Jr.
- (11) "Hypervelocity Penetration Studies," W.W. Atkins
- (12) "Mechanics of Hypervelocity Impact of Solids," H.G. Hopkins and H. Kolsky
- (13) "Cratering; Experiment and Theory," E.P. Palmer, R.W. Grow, D.K. Johnson, and G.H. Turner
- (14) "Effects of Target Temperature on Hypervelocity Cratering," F.E. Allison, K.R. Becker, and R. Vitali
- 370 "Hypervelocity Impact - Fourth Symposium, April 26, 27, 28, 1960;" (Unclassified Report) Air Proving Ground Center, September 1960, APGC-TR-60-39 (III), AD 244 477.

Table of Contents - Volume III (U)

- (1) "Framing Camera Observations of Ultra-High Velocity Penetration in Transparent Targets and A Mechanism for Crater Expansion," R.T. Keys, R.W. Bartlett, and M.A. Cook
- (2) "An Analytical Approach to Hypervelocity Impact Mechanics," M. Zaid
- (3) "Impact Crater Formation in Rock," William C. Mauerer and John S. Rinehart
- (4) "A Model of Oblique Impact," G.M. Bryan
- (5) "Further Studies of Micro-Particle Cratering in a Variety of Target Materials," J. William Gehring, Jr., and L.G. Richards

- (6) "A Metallurgical Approach to the Hypervelocity Problem,"
Coy M. Glass and Robert B. Pond
- (7) "High-Velocity-Projectile Drag Determination,"
S. Halperson, P. T. Boltz, and D. A. Hall
- (8) "Experimental Investigation of Spray Particles Producing
the Impact Flash," R. W. Grow, R. R. Kadesch,
E. P. Palmer, W. H. Clark, J. S. Clark and R. E. Blake
- (9) "An Investigation of Spalling and Crater-Formation by
Hypervelocity Projectiles," C. J. Maiden, J. Charest,
and H. P. Tardif
- (10) "Ballistic Impacts by Microscopic Projectiles,"
J. F. Friichtenicht and B. Hamermesh
- (11) "The Penetration of Thin Rods into Aluminum,"
R. E. Slattery and W. G. Clay
- (12) "A Sequential Electrical Discharge-Light Gas Gun,"
V. F. Volpe and F. J. Zimmerman
- 371 Oliver, Alfred G.; Brown, Bernard J.; Merkler, Jules M.:
"Wound Ballistics of the 0.85-Grain Steel Disk "; (Secret
Report) . Chemical Warfare Laboratories Technical Report
CWLR 2372, May 1960, AD 317 999.
- 372 Bilek, Andrew G.: "Hypervelocity Impact Studies - Improvement
of APGC 37 -mm Light-Gas (Helium) Projector"; (Unclassified
Report), Air Proving Ground Center Report No. APGC-TR-
60-29, July 1960, AD 240 378.

(Unclassified Abstract) This project was conducted to determine the causes of difficulties encountered in the operation of the APGC 37-mm light gas (helium) projector, to effect corrective measures, and to discover methods for increasing the velocity obtainable with the projector.

Velocities obtainable with the gun were increased substantially through a series of modifications. New projectile launch and velocity measuring techniques were developed.

Improvements to the gun made during and subsequent to this test have resulted in firings with projectile velocities in excess of 18,000 fps.

Sabot design and testing, plus some discussion of sabot materials and problems, are included. Photographs of the sabot and other components are given.

- 373 Fendick, R.B.: "Hypervelocity Impact Facility - Light Gas Projector"; (Unclassified Report), Air Proving Ground Center Report No. APGC-TN-60-102, November 1960, AD 246 789L.

(Unclassified Abstract) Development efforts on the APGC light gas projector from March to August 1960 were conducted to meet specific test requirements. The major objective of the development program during the interval reported here was to upgrade the velocity capability of the APGC light gas projector to meet test requirements for current and future projects. Effort has been centered on:

- Sabot investigation
- Lightweight pistons
- Projectile barrel adapters
- Cal .60 projectile barrels (120-in. length)
- Propellant powder
- Pressure measurements.

The section concerning sabot investigation includes:

- The material used,
- Purpose of sabot,
- Design of sabot (pictorially shown), and
- The sabot stripping device.

- 374 Hegge, E.N.; McDonough, J.P.: "Watertown Arsenal Light-Gas Gun"; (Unclassified Report), Watertown Arsenal Laboratories, Technical Report No. WAL TR 761/64, December 1960, AD 249 527.

(Unclassified Abstract) A simple, practical, low-cost light-gas gun was developed to conduct terminal-ballistic studies in the velocity range of 6000 to 13,000 ft/sec. Standard cartridge cases and propellants are used to propel a lightweight plastic piston to compress the light gas (helium). The light gas is shaped to flow uniformly behind the projectile through the launching tube or rifled barrel by a disposable cone of plastic material which also serves as a buffer to decelerate the piston without appreciable damage to any major structural component. Either full-calibre conventional shear-type projectiles or subcalibre projectiles, fragments, and other irregularly shaped missiles can be fired, the latter by means of plastic-discarding-carrier techniques, in either smoothbored launching tubes or rifled barrels.

The light gas gun, projectile, and sabot designs are pictorially shown and discussed.

- 375 "Weapon System 107 A-2"; (Confidential Report), Research and Advanced Development Division AVCO Corporation, Progress Report No. 4 of RAD-SR-61-25, 28 February 1961, AD 326391L, Prepared for Air Force Ballistics Missile Division.

(Unclassified Abstract) This report contains only the appendixes of the complete report. The appendixes contain 28 papers concerning different phases of the program. The appendix in which this study is most interested is entitled "The Development of Sabots for Hypervelocity Guns." The present sabot design is adequate for launching projectiles of tungsten carbide, at least at velocities up to 15,000 ft/sec.

- 376 Zimmerman, F. J.; Barbarek, L. A. C.: "Hypervelocity Weapon Feasibility Study - Volume II"; (Unclassified Report), Illinois Institute of Technology, Report No. WADD-TR-61-203 (II), April 1961, AD 255 805 L, for APGC.

(Unclassified Abstract) This is the appendix portion of report of same title (Vol. I). The appendix consists of three parts: (1) catalog of hypervelocity projector types. Included in this section is a general definition of the sabot along with a pictorial representation. (2) Analysis of performance requirements for hypervelocity guns. The purpose of this theoretical analysis is to determine the design characteristics that will insure the adequate performance of a hypervelocity gun in a co-planar tactical situation. (3) The ARF traveling charge gun program.

- 377 Fendick, R. B.: "Hypervelocity Impact Facility - Light-Gas Projector Development"; (Unclassified Report), Air Proving Ground Center, Report No. APGC-TR-61-31, June 1961, AD 263 373.

(Unclassified Abstract) The major accomplishment during this reporting period was the launch of a 1/8-in. diameter aluminum projectile at a velocity of 22,030 fps. Refinements were made in saboting techniques producing clean projectile impacts on the target. Launching 1/4-in. diameter tungsten carbide projectiles was successful up to 12,800 fps and 1/4-in. diameter aluminum projectiles to 16,000 fps. Modifications to the light-weight piston (4 oz) were responsible for achieving higher velocities.

A discussion of sabot development and design, accompanied by pictorial representations, is given. Also included is sabot stripping and intercepting techniques.

- 378 Austin, D. W.: "Vulnerability of Mark III Nose Cone Materials (Phase 2) (U)*; (Secret Report)²⁶, Air Proving Ground Center, Report No. APGC-TDR-61-28, July 1961, AD 344 345.
- 379 Heerema, C. E.: "Carde Support Program, Tasks, I, II, III, V"; (Confidential Report), (Bendix Systems Division), Report No. BSC-22748, March 1961, AD 346 217, for CARDE.

(Unclassified Abstract) Under the CARDE support program, the Bendix Systems Division of the Bendix Corporation provides a supporting staff to the Army Rocket and Guided Missile Agency (ARGMA) Project Officer, an operating budget for on-site expenses administered by the ARGMA Project Office, and a technical supporting staff integrated into the existing CARDE organization.

This report is divided into five (5) sections. The first describes the basic elements of a hypervelocity test range. The second describes the basic elements of a ballistic range. The third considers the status of each range currently in use or under development at CARDE. The fourth describes the status of the various tests complete or in process which are of concern of the project officer. The fifth is a summary of services provided by the Bendix Corporation to the Project Office.

Included are brief comments on the sabot used in light-gas gun launching, the problems to be concerned with re-sabot design, and the function of the sabot. No technical discussions are included.

- 380 "Carde Support Program, Tasks I, II, and III"; (Unclassified Report), The Bendix Corporation, Report No. BSR-543, June 1961, AD 261 934, for CARDE.

(Unclassified Abstract) This report covers the period 1 January to 30 June 1961 of the CARDE support program. The report is comprised of four sections. The first describes the level of activity maintained in the project office staff and the technical support staff. The second describes the status and progress of the facilities during this report period. The third gives the status of the various programs in progress. The contract is summarized in the fourth section.

Included are brief comments on the sabot, the type used, and the problems of discarding.

- 381 "CARDE Support Program 1961"; (Unclassified Report), The Bendix Corporation, Report No. BSC-29473, December 1961, AD 424 196, for CARDE.

Range instrumentation and status are discussed. Programs being carried out either by U. S. sponsorship or otherwise are discussed, and CARDE support is discussed.

Brief mention is made of the use of sabots in light-gas gun launching.

- 382 Cowan, P. L.; Roney, P. L.: "CARDE Impact Studies Progress Report "; (Secret Report)²⁸, CARDE Report No. TM 620/61, August 1961, AD 326 113.

- 383 Solnoky, P.: "Some Recent Developments in Projectile Launching Techniques at CARDE"; (Unclassified Report), CARDE T.M. 727/62, November 1962, AD 299 606.

(Unclassified Abstract) This paper deals with some of the methods used in hypersonic ranges for the launching of sabot projectiles. Three techniques are described: the ramp deflector, the arrestor tube, and the air tube. These provide the basic means to satisfy these requirements over a wide range of velocity, range pressure, and gun size when using basic aerodynamic shapes such as spheres, cones, and slender rods as projectiles. Photographs of sabots and models are included. Sabots are described.

- 384 McKay, William L.: "Performance of a Three-Stage Arc Heated Light Gas Gun"; (Confidential Report), AVCO Corp., Technical Memorandum RAD-TM-62-40, 28 July 1962, AD 331 262, Prepared for Air Force Ballistic Systems Division Air Force Systems Command.

(Unclassified Abstract) A launcher was designed to accelerate fragile projectiles to high velocities (15,000-20,000 fps) without distortion. This has been accomplished by coupling an arc heating stage to the calibre 0.600 light gas gun. A program of developmental firings was completed, from which performance data were obtained. The result and analysis of the firings are presented in this report. A brief description of the 4 piece delux sabot is given.

- 385 Grabarek, Chester; Herr, Louis: "Performance of Long Rods Against Steel Armor Targets"; (Confidential Report), BRL Memorandum, Report No. 1442, January 1963, AD 334 319.

(Unclassified Abstract) Penetration data are provided for 1 and 1.36-lb. tungsten carbide rod penetrators, length-to-diameter ratio of 25, tested against single and spaced tripartite targets. The present data for single targets are combined with published data on small scale rod-type projectiles against rolled homogeneous armor at 60-degree obliquity to indicate the scaling law. A curve of the ratio of target thickness to rod body diameter is presented as a function of the specific limit energy for a single target at 60°. A description and photograph of the push-pull type sabot used to launch the rods from a 90-mm smoothbore gun are given.

- 386 "Development of a Saboting Technique for Light Gas Hypervelocity Projectors"; (Unclassified Report), MB Associates, Report No. MB-R-63/14, February 1963, AD 605 836.

(Unclassified Abstract) A sabot, using internal gas expansion to separate its halves, was developed for use in the launching of hypervelocity projectiles. Most sabots are designed so that aerodynamic forces will strip parts away from the projectile. Here, separation was achieved by burning a propellant inside the sabot while it traveled down the gun barrel. Upon launch, the high pressure gases imparted lateral velocity to the halves by expansion.

It was desired to achieve separation velocities of 1.5×10^4 cm/sec. At this velocity, each half of the sabot would be displaced 10 cm from the trajectory at 6 meters from launch when fired at a velocity of 29,500 feet per second. A total of 33 experimental firings was carried out from cal 0.60 powder and light gas guns. Both aluminum and fiberglass sabots were used.

- 387 "Hypervelocity Capability and Impact Research"; (Unclassified Report), NRL Memo Report 1412, March 1963, AD 410 310L.

(Unclassified Abstract) The primary objective of this program is to launch a controlled shape projectile weighing approximately two grams to a velocity of 9.5 km/sec. Studies of impacts by high velocity projectiles on a variety of target configurations also are carried out. Studies are presented of the use of electrical energy pulses for augmenting the performance of light-gas guns. A positive augmentation effect was measured when the gun was operated under reduced parameters and electrical energy was added to the driver gas during the compression stroke. This report also contains the results of an effort to develop explosively separating sabots for carrying sub-calibre projectiles during light-gas gun launches. The sabots are made in two segments and contain an explosive-filled cavity as well as the projectile. The acceleration of the sabot during its launch in the gas gun ignites the explosive which generates a high gas pressure within the sabot cavity. This pressure causes the sabot segments to separate upon leaving the launch tube.

- 388 Chandler, Robert L.: "The Effects of Physical Projectile Properties on Thin Target Damage at Hypervelocities"; (Confidential Report), IIT Research Institute Technology Center, Report No. ASD-TDR-63-4, March 1963, AD 335 636.

(Unclassified Abstract) Projectiles of various metallic materials (including tungsten, nickel, Armco iron, steel, and tin) were fired at a standard spaced aluminum plate target configuration. Impact velocities varied from 15,000 to 19,000 fps for the 0.5-gram projectiles. The objective of the firings was to determine the material property or properties contributing most to the maintenance of projectile integrity after first hypervelocity impact.

Experimental results and techniques are presented. Preliminary indications of material properties are discussed. Pictorial representation of a mechanical sabot stripper adapter is given.

- 389 "Proceedings of the Sixth Symposium on Hypervelocity Impact"; Cleveland, Ohio, April 30, May 1, 2, 1963, Sponsored by the Firestone Tire and Rubber Co., Akron, Ohio

Table of Contents - Volume II, Part I

AD 423 063

- (1) Review of Physical Processes in Hypervelocity Impact and Penetration
Robert L. Bjork
- (2) Hydrodynamics of Hypervelocity Impact
J.M. Walsh and J.H. Tillotson
- (3) Visco-Plastic Solution of Hypervelocity Impact Cratering Phenomenon
T.E. Riney
- (4) The Calculation of Stress Waves in Solids
Mark L. Wilkins and Richard Giroux
- (5) A Hypervelocity Impact Model for Completely Deforming Projectiles
J.L. Luttrell
- (6) A Blast-Wave Theory of Crater Formation in Semi-Infinite Targets
William J. Rae and Henry P. Kirchner
- (7) Spherical Shock Waves and Cavity Formation in Metals
N. Davids, H.H. Calvit, and O.T. Johnson
- (8) Properties of Spherical Shock Waves Produced by Hypervelocity Impact
Ray Kinslow
- (9) Shock Front Variation in Time for High Speed Impact Into Water
James F. Heyda

Table of Contents - Volume II, Part 2

AD 423 064

- (10) Hypervelocity Cratering Data and a Crater-Depth Model
for the Regime of Fluidity
Olive G. Engel
- (11) Fluid Impact Craters and Hypervelocity -- High-Velocity
Impact Experiments in Metal and Rocks
H. J. Moore, R. W. MacCormack, and D. E. Gault . . .
- (12) Energy Balances in Hypervelocity Penetration
R. B. Pond, C. Mobley, and C. M. Glass
- (13) The Partition of Energy for Hypervelocity Impact
Craters Formed in Rock
Donald E. Gault and Ezra D. Heitowit
- (14) Transient Observations of Crater Formation in Semi-
Infinite Targets
J. H. Kineke, Jr., and Richard Vitali
- (15) Influence of Target Strength on Hypervelocity Crater
Formation in Aluminum
J. H. Kineke, Jr., and L. G. Richards
- (16) Some Phenomena Associated with Impacts into Aluminum
S. M. Halperson
- (17) Particle-Solid Impact Phenomena
E. H. Goodman and C. D. Lites
- (18) Investigation of the Impact of Copper Filaments into
Aluminum Targets at Velocities to 16,000 Feet Per
Second
C. Robert Nysmith, James L. Summers and
B. Pat Denardo
- (19) Ionization Associated with Hypervelocity Impact
J. F. Fritchenicht and J. C. Slattery
- (20) Investigation of Impact Flash at Low Ambient
Pressures
Robert W. MacCormack
- (21) An Investigation of the Phenomena of Impact Flash and
Its Potential Use as a Hit Detection and Target
Discrimination Technique
J. W. Gehring and R. L. Warnica

Table of Contents - Volume III

AD 423 802

- (22) Two Dimensional Analysis of a Hypervelocity Impact
upon a Visco-Plastic Plate
H. Kraus
- (23) A Meteoroid Bumper Design Criterion
P. E. Sandorff
- (24) Experimental and Theoretical Results Concerning the
Protective Ability of a Thin Shield Against Hypervelocity
Projectiles
O. J. Maiden
- (25) Effects of 3 to 12 KM/SEC Impacts on Finite Targets
R. B. Mortensen, J. E. Ferguson, J. P. Joyce, and
K. N. Kreyenhagen
- (26) Thin Plate Perforation Studies with Projectiles in the
Velocity Range from 2 to 5 KM/SEC
R. W. Watson, K. R. Becker, and F. C. Gibson
- (27) A New System of Protection from Hypervelocity
Particles
B. W. Reynolds and R. H. Emmons
- (28) Hypervelocity Puncturing of Self-Sealing Structures
Philip J. D'Anna
- (29) An Investigation of the Penetration of Hypervelocity
Projectiles into Composite Laminates
A. R. McMillan
- (30) Meteoroid Effects on Nuclear Rocket Space Vehicle
Mission Success
William H. Sterbentz and Loren L. Long

Table of Contents - Volume IV

AD 345 054

- (31) (Secret) Application Aspects of Hypervelocity Impact
1963 (U)
J. M. Brown and P. K. Margous
- (32) (Confidential) Jet Pellet Projection Technique (U)
S. Kronman
- (33) (Confidential) Hypervelocity Projectile Investigation
for Multiple Thin Plate Penetration (U)
R. L. Chandler, T. Watmough and F. J. Zimmerman . . .

Table of Contents - Volume IV (Continued)

- (34) (Secret) Lethality of Hollow Shapes (U)
W.H. Dittrich, D.R. Christman, J.W. Gehring,
K.N. Kreyenhagen, and R.B. Mortensen
- (35) (Confidential) A Warhead Concept for Defeat of Hard
Targets in Space (U)
Dale M. Davis
- (36) (Secret) Aimed Warhead Concepts (U)
Samuel D. Stein, George M. Gaydos,
and Edmund M. Harrity
- (37) (Confidential) Hypervelocity Impact Experiments
with Laminated Complex Targets (U)
C.M. Cox and E.S. Thorn
- (38) (Secret-No Foreign) Hypervelocity Impacts into
Ablative Materials (U)
Mario A. Persechino
- (39) (Confidential) Determination of Perforation Energies
for Composite Targets (U)
Murray Rockowitz and Charles A. Carey
- (40) (Secret) A Short Review of the Status of the Aero-
Thermal Phase of the Hypervelocity Kill Mechanisms
Program (U)
Coleman duP. Donaldson
- (41) (Secret-No Foreign) Lethality of Small Fragments Versus
ICBM Re-entry Vehicles (U)
James J. Dailey
- (42) (Secret-No Foreign) Vulnerability of Large Missile Systems
During the Launch Phase (U)
H.S. Zimney, R.B. Mortensen, W.A. Rhea,
and R.B. Coley
- (43) (Confidential) Free, A Hypervelocity Rocket Weapon (U)
D.C. Lane
- (44) (Confidential) Armour Research Foundation Traveling
Charge Gun (U)
Louis A.G. Barbarek

- 390 Dmitrieff-Koklive, A.: "Spectrographic Studies of the Radiation Emitted by Hypersonic Projectiles"; (Unclassified Report), CARDE Technical Note 1564, May 1963, AD 417 898.

(Unclassified Abstract) Some preliminary results are presented of spectrographic observations of the distribution of intensities emanating from the environment of hypersonic projectiles. An account is given of the development of a spectrographic system suitable for operation under range conditions. Experimental results are given, together with some discussion on their interpretation.

Mention is made that sabots are used in launching and several drawings of sabots are given.

- 391 Taylor, G.: "Sabot-Launching Systems for Experimental Penetrators"; (Unclassified Report), BRL Memorandum Report No. 1505, August 1963, AD 428 223.

(Unclassified Abstract) Performance details for special purpose, high velocity sabots are described. These sabots were designed and developed for launching high-density projectiles, of rod form, with overall length to diameter ratios varying from less than one to twenty-five.

Sabot systems for a rod penetrator device of the base-push type and combinations of push and pull are described. Many in-flight photographs of sabot separation are included.

- 392 "Effect of Projectile Physical Properties on Thin Target Damage at Hypervelocities (C)"; (Confidential Report), IIT Research Institute Technology Center, Report No. ASD-TDR-63-36, September 1963, AD 341 871.

(Unclassified Abstract) An investigation of the effects of projectile material and shape on thin plate impact at hypervelocities is being conducted. This report covers the results of the materials phase of this work.

One-half gram projectiles of various materials were sabot-launched in the velocity regime of 15,000 to 20,000 fps at 0.1 in. thick 2014-T6 aluminum sheets spaced 24 inches apart. The impact effects, photographically shown, were monitored with a sequential flash X-ray device and by post-fire examination of the target and witness plates. A large number of materials were tried to determine the effects of melting point, strength, toughness, density, latent heat of fusion, liquid metal surface tension, and latent heat of vaporization. Appendix A considers the viscosity of molten metals.

- 393 "Hypervelocity Kill Mechanisms Program ARPA Order 149"; (Secret Report), Dynamics Branch Mechanics Division, NRL (Naval Research Laboratory) NRL 6032, October 1963, AD 344 803L.

- 394 Condon, J. J.; Halperson, S. M.: "Hypervelocity Kill Mechanisms Program ARPA Order No. 149-60 Impact Damage Phase", (Secret Report), NRL (Naval Research Laboratories) NRL NR 1492, February 1964, AD 348 245L.
- 395 Cable, A. J.: "Experimental Studies of the Oblique Hypervelocity Impact of Inert and Explosive Projectiles on Thin Targets"; (Confidential Report), Royal Armament and Development Establishment Memo 17/64, April 1964, AD 350 908.

(Unclassified Abstract) Inert and explosive projectiles were fired at a velocity of 13,500 ft./sec. against targets consisting of copper sheets inclined at 15° to the line of flight. The experiments show that under these circumstances enhanced damage is caused by the use of explosive projectiles of the same mass and velocity as inert projectiles. The area of hole produced by inert projectiles is proportional to the kinetic energy of the projectile for each thickness of target.

Little is said concerning the hole of the sabot. However, a drawing of the projectile and sabot is given. This work is in support of project Helmet.

- 396 Nagaoka, H. H.: "Spaced Armor Penetration Studies"; (Confidential Report), IIT Research Institute Technology Center Technical Report No. ATL-TR-64-69, 9 November 1964, AD 354 600.

(Unclassified Abstract) An experimental and analytical program was conducted to investigate the effectiveness of the composite laminated projectile concept in the hypervelocity penetration of a standard aluminum spaced target plate configuration. Representative projectile configurations designed, fabricated, and evaluated included a rigid-core composite projectile, a tubular projectile, a plastic capsular projectile, and a plastic capsulated tubular projectile. The projectile-target interaction phenomenon was investigated analytically. One-dimensional effects were considered to gain insight into attenuator response. The kinematics of interaction of an impact shock in the attenuator material with the unloading wave originating from the stress-free periphery of the projectile were studied.

Mention is made that the projectiles were sabot-launched.

- 397 Malik, Donald: "The Characteristics of Particles Formed During the Perforation of Steel Armor by Steel Fragments". (Confidential Report), BRL Technical Report No. 57, December 1964, AD 358 893.

(Unclassified Abstract) When steel fragments impact on and perforate a structural material, one or more particles are emitted from the rear

surface of the material under attack. An analysis is made of the weight, speed, and spatial distributions and the number of these particles when the structural material is steel armor. Empirical formulas are provided relating certain characteristics of these distributions to selected parameters defining the impact conditions.

Mention is made only of the fact that sabots were used for high-speed launching. Velocities of 13,000 F/S were obtained.

- 398 "Proceedings of the Seventh Hypervelocity Impact Symposium"; Tampa, Florida, 17-19 November 1964. Sponsored by Eglin Air Force Base.

Table of Contents - Volume II - Theory

AD 463 228

- (1) On the Theory of Hypervelocity Impact
J. M. Walsh and W. E. Johnson
- (2) Hypervelocity Impact Calculations
T. D. Riney and J. F. Heyda
- (3) Late-Stage Equivalence and Similarity Theory for One-Dimensional Impacts
John K. Dienes
- (4) The Strong Plane Shock Produced by Hypervelocity Impact and Late-Stage Equivalence
P. C. Chou, H. S. Sidhu, and L. J. Zajac

Table of Contents - Volume III, Theory

AD 463 229

- (1) Impact of a Porous Aluminum Projectile on Aluminum at 20 and 72 KM/Sec
M. H. Wagner, N. B. Brooks, and R. L. Bjork
- (2) Numerical Solution of Oblique Impacts
K. N. Kreyenhagen, R. L. Bjork, and Nancy B. Brooks . .
- (3) Peak Axial Pressures in Semi-Infinite Media Under Hypervelocity Impact
J. F. Heyda and T. D. Riney
- (4) An Investigation of Crater Formation by Hypervelocity Impact
S. W. Yuan and R. W. Courter
- (5) Hypervelocity Impact - A Series Solution
P. Marnell, M. Soifer, and M. Zaid

- (6) On the Mechanics of Indentation and Cratering in Solid Targets of Strain-Hardening Metal by Impact of Hard and Soft Spheres
J. N. Goodier
- (7) A Penetration Method for Determining Impact Yield Strength
N. Davids, R. Minnich, and J. Sliney

Table of Contents - Volume IV - Theory

AD 463 230

- (1) A Physical Basis for Scaling Hypervelocity Impact
Robert J. Naumann
- (2) Change of Effective Target Strength with Increasing Size of Hypervelocity Impact Craters
H. J. Moore, D. E. Gault, and E. D. Heitowit
- (3) A Linear-Elastic Treatment of the Spall-Fracture Problem
W. J. Rae
- (4) Thin Sheet Impact
C. J. Maiden, A. R. McMillan, and R. E. Sennett III
- (5) A Study by a Perturbation Method of the Hypervelocity Impact of Rod-Like Projectiles Upon a Thin Viscoplastic Plate
Lit S. Han and Raymond E. Hess
- (6) Hypervelocity Impact of End-Oriented Rods
R. L. Bjork and M. Rosenblatt

Table of Contents - Volume V - Experiments

AD 463 231

- (1) Calculation of Maximum Hypervelocity Impact Damage from Material Properties
Andrew M. Dietrich, R. B. Pond, and C. M. Glass
- (2) Energy Partitioning in High-Velocity-Impact Cratering in Lead
E. P. Palmer and G. K. Turner
- (3) The Application of Metallurgical Gaging for Hypervelocity Impact Studies
P. E. Kyle and G. Gerard
- (4) Energy Balances for Hypervelocity Targets
C. E. Mobley, Jr., and R. B. Pond
- (5) Electron Microprobe Study of a Crater and Ejecta Produced by Hypervelocity Impact Against a Ni-Fe Target
Richard A. Schmidt, Klaus Keil, and Donald E. Gault

- (6) The Behavior of Wax Targets Subjected to Hypervelocity Impacts
J. T. Frasier, B. G. Karpov, and L. S. Holloway
- (7) Experimental Studies of Impact Phenomena and Correlation with Theoretical Models
J. W. Gehring, C. L. Meyers, and J. A. Charest
- (8) Mechanics of Hypervelocity Impact
F. E. Allison
- (9) Comparisons Between Hydrodynamic Theory and Impact Experiments
S. M. Halpern
- (10) Determination of the Yield Strength as an Effective Mechanical Strength Property in the Catering Process of Hypervelocity Impact
R. Piacesi, R. H. Waser, V. C. D. Dawson
- (11) Effect of Target Material Yield Strength on Hypervelocity Perforation and Ballistic Limit
Robert G. Thomson and E. T. Druszewski

Table of Contents - Volume VI - Experiments

AD 463 232

- (1) The Effect of Material Properties on Threshold Penetration
Richard H. Fish and James L. Summers
- (2) Brittle Behavior of Beryllium, Graphite, and Lucite Under Hypervelocity Impact
J. H. Diedrich, I. J. Loeffler, and F. S. Stepka
- (3) Observations of Hypervelocity Impact of Transparent Plastic Targets
Ray Kinslow
- (4) Impact Flash Investigations to 15.4 km/sec
F. D. Rosen and C. N. Scully
- (5) Hypervelocity Impact on Single Thin Sheet Structures Incipient Perforation Conditions
E. P. Bruce
- (6) Penetration Mechanisms of High-Velocity Rods
D. R. Christman, A. B. Wenzel, and J. W. Gehring

- (7) Investigation of Catastrophic Fracturing and Chemical Reactivity of Liquid-Filled Tanks When Impacted by Projectiles of High Velocity
Francis S. Stepka, Robert P. Dengler, and C. Robert Morse
 - (8) Systematic Investigation of Crater Formation in Metals
Neil R. Sorensen
 - (9) Dustwall Shielding Against Meteoroids
Dr. Carl N. Klahr
 - (10) Scaling Relationships for Microscale to Megascale Impact Craters
Donald E. Gault
- 399 "Proceedings of the Seventh Hypervelocity Impact Symposium - Volume VII - Applications"; (Secret Report), February 1965, AD 365 243. Sponsored by Eglin Air Force Base.

(Unclassified Abstract) Included in this volume are six different papers on hypervelocity impact and its applications. Under the topic, "The Role of Projectile Material Properties in the Hypervelocity Penetration of Thin Plates," brief discussion is made of sabot materials and sabot stripping techniques.

Under the topic, "Spaced Armor Penetration Studies," various sabot projectile configurations are shown and briefly discussed.

The other sections do not relate any pertinent information on sabots.

Table of Contents

- (1) Military Uses of Hypervelocity Impact Research
R. L. Hayford and J. M. Brown
- (2) The Role of Projectile Material Properties in the Hypervelocity Penetration of Thin Plates
R. L. Chandler and T. Watmough
- (3) Spaced Armor Penetration Studies
H. H. Nagoaka and T. A. Zaker
- (4) Effect of Projectile Geometry and Impact Angle on the Vulnerability of Multiple Sheet Targets
R. L. Warnica and D. R. Christman
- (5) Rod Lethality Studies
J. J. Condon
- (6) Hypervelocity Penetration of Thin Targets by Long Rods
S. Kronman, C. M. Glass, and M. Gorrell

Volume VIII - Applications (U); (Secret Report), February
1965, AD 365 244. Sponsored by Eglin Air Force Base.

(Unclassified Abstract) Hypervelocity system applications. No sabot launching mentioned.

Table of Contents

(1)	The Air Force Program in Hypervelocity Weapons D. M. Davis
(2)	Stabilized Rod Warhead P. A. Saigh and R. E. Stern
(3)	Radially Expanding Fragmentation Warhead Study William R. Porter
(4)	Preliminary Development of an Automatic Light - Gas Weapon E. Ashley, D. M. Jeffreys, and E. Poston
(5)	A Traveling Charge Type Hypervelocity Projector L. A. C. Barbarek
(6)	Hypervelocity Penetration of Composite Targets R. W. Watson, K. R. Becker, and F. C. Gibson
(7)	Massive Impact into Ablative Structures C. D. Porter
(8)	Hypervelocity Impact into Composite Targets with One Megajoule Pellets C. M. Cox and E. R. Berus
(9)	Hypervelocity Impact on Thin Plate Targets; Spall Particles Distribution B. VanZyl
(10)	Impact Failure of Pressure Vessels J. F. Lundeberg, G. T. Burch, Jr., and D. H. Lee
400	"Electrical Augmentation of a Light Gas Gun"; (Unclassified Report), Arnold Engineering Development Center Report No. AEDC-TR-65-32, January 1965, AD 455 811.

(Unclassified Abstract) This report covers the experimental and analytical research directed toward the development of a system for electrical augmentation of a light gas launcher.

The first phase involved the use of a medium performance light gas launcher and served the purpose of developing techniques and providing proof that electrical augmentation was experimentally practical. In the second phase, a high-performance launcher was used and optimization of these augmentation techniques was attempted.

Higher efficiency of augmentation was obtained in the Phase I work where the sabot was heavier and normal launch velocity was lower. The highest velocity obtained with the augmented launcher was 8.23 kilometers per second, representing a velocity increase of .98 kilometers per second and a sabot kinetic energy increase of 2.68 kilojoules.

- 401 "Annual Report of the Canadian Armament Research and Development Establishment"; (Confidential Report), Canadian Armament Research and Development Establishment, CARDE Technical Report 523/65, March 1965.

(Unclassified Abstract) Included in this report on the activities at CARDE during 1964 is mention of a type of sabot capable of withstanding pressures and "g" loading experienced when firing a light-gas gun. An exceptional in-flight photo of the sabot discard is shown.

Considerable emphasis is being placed on designing a lightweight sabot used primarily for the 105-mm tank gun.

Included also is a complete list of technical reports and technical notes published by CARDE in 1964, and a list of lectures given by CARDE scientists during the same period.

- 402 Condon, J. J. : "Rod Lethality Studies"; (Confidential Report), Naval Research Lab Report No. ATL-TR-65-18, March 1965, AD 358 533.

(Unclassified Abstract) Data are presented for the loss in rod length of aluminum rods, with length-to-diameter ratios equal ten, after normal impact at 4.6 km/sec and perforation of each plate in a spaced array. Various thickness aluminum plates were impacted, but each plate in an array was of constant thickness. The rod consumption values are compared with calculations based on one-dimensional analysis. Progress is summarized toward a solution of a two-dimensional hydro-dynamic numerical analyses for the same experimental parameters. The deceleration of the rod because of plate impact, plate perforation diameter, and semi-infinite target penetration are compared with published analytical and semi-empirical expressions. Preliminary results on the effect of plate and rod orientation also are examined.

All rods were sabot-launched. Brief mention of rod stability and sabot launching is given. Photographs of sabots and launching are given.

- 403 Sodickson, Lester A.; Carpenter, Jock W.; Davidson, Gilbert: "A New Method of Producing High Speed Molecular Beams"; (Unclassified Report), American Science and Engineering, Inc. Report No. AFCRL-65-337, 17 March 1965, AD 617 142, for Air Force Cambridge Research Laboratories, Office of Aerospace Research, United States Air Force, Bedford, Massachusetts.

(Unclassified Abstract) A new method of producing a pulsed, cold beam of high velocity neutral molecules is shown to be feasible. A hollow container filled with a chosen gas is mechanically accelerated to a high velocity in a rifle or light gas gun. The container (called a sabot) is

subsequently opened to allow the gas to emerge. The sabot then is slowed or deflected. Velocities up to about 3 km/sec can be achieved with a Super Swift rifle and up to about 10 km/sec with a light gas gun. It appears feasible to produce a pulsed beam at 10 km/sec with an angular divergence of $\pm 2.5^\circ$ and a spread in velocity of ± 4 percent. A μ sec pulse with an instantaneous intensity of the order of 2×10^{23} molecules/cm²-sec can be achieved. A beam of N₂ crossed with a low velocity beam of CO or CO₂ produces vibrationally excited molecules in sufficient quantity to be detected with state-of-the-art techniques. It appears feasible to measure the cross sections for collisional excitation of the vibrational levels of CO₂ and CO by N₂ and the cross sections for the exchange of vibrational energy between N₂ and CO₂ or CO. The total cross section, which gives the mean free path, also can be obtained.

Pictorial representations of the sabot are given. Proposed techniques for sabot opening are shown.

- 404 Chandler, R.L.; Watmough, T.; "Effect of Projectile Physical Properties on Thin Target Damage at Hypervelocities," (Confidential Report), IIT Research Institute Technology Center, Report No. ATL-TR-65-95, December 1965, AD 368899.

(Unclassified Abstract) Experimental firings using light-gas guns were conducted as part of studies to provide a basis for maximizing the lethal effectiveness of hypervelocity fragments for specialized warhead applications. The overall program was divided into two phases: projectile material investigations and projectile configuration investigation.

The materials investigation was designed to determine material properties contributing most to the maintenance of projectile integrity after hypervelocity impact on a thin target plate.

The configuration investigation consisted of experimental firings to determine the lethal effectiveness of specific projectile configurations designed to defeat specified thin-plate targets. A complete section on the role of various sabot types, including photographs and pictorial representation, is included.

- 405 Payne, J. J.; "The Impact of Thin Disks into Semi-Infinite Aluminum Targets," (Unclassified Report), AEDC Report No. AEDC-TR-66-35, May 1966, AD 482038.

(Unclassified Abstract) Hypervelocity impact tests were performed using aluminum targets and projectiles comprising low-fineness-ratio disks of 1100-0 aluminum, commercially pure titanium, mild steel, and Kennertium. To ensure the desired projectile attitudes upon impact, rifled launch tubes were used to produce spin stabilization. These tubes allowed the establishment of the desired projectile orientation, and the removal of a multi-pieced sabot, without a mechanical stripping device.

A photograph of the sabot is given and a description of its function is included.

- 406 McLaughlin, W. L.; Armistead, D. M.; Partington, R. L.; Pascoe, R. A.: "Small-Scale Sabot Separation Test Program;" (Confidential Report), BOEING Report No. D2-36383-13, September 1966, AD 376505.

(Unclassified Abstract) The objectives of the Small-Scale Sabot Test program were to: (1) develop design criteria for two BSD-supplied sabot/missile separation concepts, (2) conduct parametric and subscale demonstration testing and design studies, (3) produce preliminary design drawings, a material and processes report, and a reliability report, and (4) submit a performance specification. In-flight sabot/missile separation consisted of bleeding eject-launch gases through an opening into the volume between the missile base and the sabot precharge volume. Pre-charge volume pressure then ejected the sabot axially away from the missile upon exit from the launch tube and decay of the eject gas pressures under the sabot. In-silo sabot retention involved stopping the sabot at the top of the launch tube by engaging the sabot with a retention mechanism that absorbs sabot arrest energy by crushing a crushable material. It may be concluded from the overall design analysis presented in this final report that a feasible full-scale separation design can be completed for either of the two concepts developed and tested in this program.

- 407 Braun, Walter F.; "Feasibility of Launching Micron-Size Particles at Speeds of 12,000 ft/sec To 18,000 ft/sec;" (Unclassified Report), BRL Memorandum Report No. 1780, September 1966, AD-643537

(Unclassified Abstract) A technique is described whereby a light gas gun was used to launch micron-size spherical particles of the stable isotope of a radioactive salt at velocities up to 18,000 ft/sec. The required sabot was successively retarded, deflected, and stopped before reaching the range area. It was a 0.2 inch lexan cylinder a few thousandth inch overbore diameter. Spark shadowgraph and streak camera techniques were used to observe the particles in free flight.

- 408 Berus, E. R.; "HYPERVELOCITY IMPACT STUDIES," Firestone Tire & Rubber Co., Defense Research Div., Report No. DRD-6, (AD 387 269)
- 409 Brooks, P. N.; "ON THE DESIGN OF A MINIMUM WEIGHT SABOT FOR THE BALLISTIC LAUNCHING OF SPHERES," Canadian Armament Research and Development Establishment, Report No. CARDE-TR-490/64, August 1964.
- 410 Cross, Bruce, Ralston, Margaret, "HYPERVELOCITY GUNS," Product Engineering, Vol. 33, November 12, 1962, pp. 116-117.

Describes sabot used by Armour Research Foundation in a light gas gun. The sabot is a bullet-shaped nylon case surrounding the projectile. Sabot is stripped away in a blast tank after leaving the launch tube.

- 411 Gehring, J. W.; "PENETRATION MECHANISMS OF HIGH-VELOCITY PROJECTILES," General Motors Defense Research Laboratories, Technical Report No. TR-65-50, 1965. (AD 829 635)

- 412 Murphy, J. R. B.; "EXPERIMENTAL INVESTIGATION OF A SABOT STRIPPING METHOD FOR A 0.5 INCH LIGHT GAS GUN. FINAL REPORT," Computing Devices of Canada, Ltd., Report 7457/R1, Sup. 1, NASA CR 90503, 24 October 1967.

An experimental program to develop a sabot stripping method for an 0.5 inch light gas gun is described. Sabots carrying spherical projectiles of various densities and sizes were employed, at velocities in excess of 20,000 feet per second. Dispersion of the sabot fragments was required within a length of less than two feet. It was found that a combination of a gasdynamic decelerator tube and a cruciform configuration of wedge shaped tungsten pins provided best results. The decelerator tube separated the sabot and projectile, and the pins interfered with the sabot to produce high energies and pressures which dissipate the sabot material.

- 413 Pereshino, Mario A.; Schlemmer, Harold V.; "AUGMENTOR AND SABOT STRIPPER FOR HYPERVELOCITY LIGHT GAS GUN (NAVY)," U. S. Patent Office, No. 3,212,208.

The hypervelocity augmentor and sabot stripper is a two-stage device designed to eliminate the sabot and to provide velocity augmentation to a projectile fired from a light-gas gun by utilizing the kinetic energy in the carrier of sabot. The hypervelocity augmentor and sabot stripper is secured to the end of a gun muzzle by use of screw threads or a suitable bolt and nut or screw arrangement.

- 414 Porter, C. D.; Swift, H. F.; Fuller, R. H.; "SUMMARY OF NRL HYPERVELOCITY ACCELERATOR DEVELOPMENT," Proceedings of the Fifth Symposium on Hypervelocity Impact, Denver, Vol. I, Part I, October 30-November 1, 1961, pp. 23-52.

A study is made of high-performance gas-powered accelerators for ballistic research studies. Research is necessary in order to produce velocities in excess of 6 km/sec with sufficiently low pressure and acceleration to avoid breakup of fragile sabot packages. Experimental work is continuing to increase mass, size, and velocity capabilities using sabot projectiles for impact research. Use of isometric charts to interpolate Narec results to a new set of design parameters representing a specific gun has resulted in about 95 % agreement with experimental results. Increased energy storage and distribution capabilities and development of electric ballistic techniques will considerably extend the scope of electro-ballistics.

- 415 Teng, R. N.; "ADVANCES IN LIGHT-GAS GUN MODEL-LAUNCHING TECHNIQUES," AIAA Journal, Vol. 5, November 1967, pp. 2082-2084.

Description of a light-gas-gun model launching technique which appears to have the advantages of both the aerodynamic and mechanical methods of stripping the sabots from the models. If the driving pressure is relieved when the projectile approaches the muzzle, the friction and drag forces begin to impede the sabot. At first a minute separation between the model and the sabot is achieved, principally because of wall friction. Thereafter, the aerodynamic drag on the projectile vanishes, so that both friction and aerodynamic drag on the sabot work to increase the separation distance. After an adequate separation is achieved, a ramp, for example, can be placed at the muzzle to deflect the sabot away from the trajectory of the model. Significant gains in launch velocity capability were obtained.

- 416 "DEVELOPMENT OF AN EXPLOSIVE SABOTING TECHNIQUE FOR LIGHT GAS GUNS," MB Associates, First Progress Report, April 15, 1962.

The feasibility of an explosive sabot for use in light-gas hyper-velocity guns that fire into an evacuated range is being investigated. The sabot is designed to fit a 0.60-caliber bore and carry a spherical steel projectile. The sabot consists of two halves split longitudinally, with a hollowed out cavity that contains a small explosive charge with an appropriate initiation system. Upon firing the gun, the explosive charge is detonated, creating a very high pressure in the cavity, which causes the sabot halves to fly apart, thus separating from the projectile. The projectile is then free to travel down the range and strike a target without having the effects on the target obscured by parts of the sabot. The major problem, is in initiating the explosive charge without causing the sabot halves to separate. Another problem is in saboting a light-gas gun to carry a high density projectile, such as steel, without the acceleration effects causing the projectile to damage the sabot.

- 417 "HYPERVELOCITY CAPABILITY AND IMPACT RESEARCH," Naval Research Laboratory, Memorandum No. MR-1412, Semi-annual technical progress report, covering period 1 July - 31 December 1962, March 1963. (AD 410 310L)

D-9 FREE FLIGHT AERODYNAMIC TESTING

- 418 Clancy, T. M. ; Chaplin, H.R.: "Wind-Tunnel Investigation of the Body of a Fin-Stabilized, Discarding-Sabot Projectile (U); (Unclassified Report), U.S. Naval Ordnance Laboratories, Aeroballistic Research Report No. 128, 24 September 1952. AD 76103.

(Unclassified Abstract) Wind tunnel tests were conducted to obtain stability data for the body of the FSDS, and to investigate the differences in drag, normal force, and location of center of pressure, because of a groove in the projectile head and a buttress thread at midbody.

- 419 Gamblin, W. E. S.; Bertrand, G.: "1/8-Scale Missile Model Tests with 5.9-Inch Smoothbore Gun (Sabot Type B-1) (U);" (Confidential Report), CARDE Report No. N-44-132, 1 April 1953, AD 365979.

(Unclassified Abstract) Following the development of a sabot for launching 1/16" scale guided missile models, a request was given to design a sabot to launch 1/8" scale guided missile models at velocities ranging from 1200 f/s to 2400 f/s.

This new design is described, test results are given, and sabot and model photographs are included.

- 420 Gamblin, W. E. S.; Peacock, W. B.; Bertrand, G.: "Sabot Design for 1/16-Scale Model 3-In. Smoothbore Gun (U);" (Confidential Report), CARDE, Technical Letter No. N-44-110, 10 February 1953, AD 365980.

(Unclassified Abstract) Presented is a means of launching 1/16" scale guided missile models for aerodynamic study. A radially discarding sabot was designed to meet the following requirements: (1) capable of being fired from a 3.125 in. smoothbore gun at velocities up to 2500 f/s, (2) sabot must support the model rigidly during shot travel, (3) separation must occur as soon as possible after shot ejection, and the sabot must not interfere with the model during separation, and (4) sabot must be as light as possible.

Nine sabot designs are included and are verbally and photographically described.

- 421 Cohen, J.: "Supersonic Wind Tunnel Tests on Scale Models of Two F.S.D.S. Projectiles (U);" (Confidential Report), CARDE Memorandum (B) 26/56, September 1956, AD 116280.

(Unclassified Abstract) The results of test on exact scale models of the 5.0"/2.32" and 5.0"/1.78" F.S.D.S. projectiles are presented. Normal force and pitching moment coefficients and centers of pressure are given for Mach numbers between 2.0 and 4.0 and compared with "theoretical" estimates given by methods currently in use.

Aerodynamic characteristics are graphically presented and discussed for the fin-stabilized discarding sabot projectile bodies.

- 422 Loeb, Alfred A.: "Static Longitudinal Stability and Drag of a 105/40 mm Delta-Fin Shell at Mach Numbers of 4.00, 4.53, and 4.89 (U):" (Confidential Report) Picatinny Arsenal. Technical Report 2422, June 1957, AD 133 377.

(Unclassified Abstract) Wind tunnel tests were performed at Mach numbers of 4.00, 4.53, and 4.89, on full-scale models of a delta-finned, 105/40-mm projectile. Static longitudinal stability and drag information was obtained for this configuration at angles of attack from -42 to 10°, with experimental measurements of normal force, pitching moment, and drag. The material received from BRL represents experimental data. This report presents the data, as well as an analysis.

Mention is made that the projectile is sabot-supported.

- 423 Seiff, Alvin: "The Use of Gun-Launched Models for Experimental Research at Hypersonic Speeds (U):" (Unclassified Report). Advisory Group for Aeronautical Research and Development. Report No. 138, July 1957, AD 150315.

(Unclassified Abstract) The purpose of this paper is to discuss the difficulties and the advantages associated with doing high mach number research and also to discuss the high performance gun, which extends the capabilities of the technique far out into the hypersonic regime.

Two methods of attaining hypervelocities are discussed: (1) launching upstream in a wind tunnel, and (2) light-gas gun launching. Use of a sabot is mentioned.

- 424 Fontenot, John E. Jr.: "Free Flight Model Tests for Drag and Stability of Three Cone-Cylinder-Flare Configurations (U):" (Confidential Report) AVCO Corporation Report No. 26, May 1960, AD 321 809

(Unclassified Abstract) Three ICBM shapes were fired to determine drag, stability, and pressure distribution in a Mach number range of 4.0 to 8.0. Possible real gas effects also were noted in the drag coefficient of the bluntest shape above Mach 7.

This report also discusses launching difficulties incurred in Mach 8 firings.

Aerodynamic data are presented in graph form. Models of sabots are shown. Sabot materials are mentioned. Launching difficulties and aerodynamic coefficients are discussed.

- 425 Scott, E. R.: "Stability Derivative from Minuteman Aeroballistic Range Tests (U):" (Confidential Report), Boeing. Document No. D2-9557, 14 April 1961, AD 364619.

(Unclassified Abstract) Subscale free-flight stability tests of the Minuteman missile were conducted during late fall and early winter of 1960 to 1961. In the tests, models of the basic missile were launched at high speed on the CARDE Aeroballistic Range. The models were sabot-launched via a 4 inch smoothbore powder gun. The tests were made at nominal Mach and Reynolds numbers of about 5.5 and 30 million respectively. Stability data have been reduced by assumptions of both linear and nonlinear pitching-moment characteristics. Data obtained from the initial aeroballistic tests are presented.

Description of the sabot, along with a photograph and a pictorial representation, is given.

- 426 Cheers, B.: "Aeroballistics Range Test on the Transonic Drag of Spherically-Blunted Cones (U);" (Confidential Report), CARDE Technical Memorandum 654/61, November 1961, AD 328789.

(Unclassified Abstract) Tests were conducted to determine the variations, due to body geometry, of drag coefficient and shock-wave detachment distance, in the transonic region, of a series of seven spherically-blunted cone configurations.

The models had cone half-angles of 10, 13.5, and 15 degrees and nose radii varying from 0.2 to 0.5 of the base radius. The Mach number range covered in the tests was from 0.8 to 1.5 giving a corresponding variation in Reynolds number from 1×10^6 to 1.8×10^6 , based on model base diameter. Twenty-four models were fixed and all provided useful data points.

Mention is made and photographs are shown of the 4-petal saw-cut aluminum cup-shaped sabots used to launch the cones.

- 427 "Status Report on the Reentry Physics Program, December 31, 1962 (U);" (Unclassified Report), Staff of the Radiation Physics Section, Aero/Physics Wing, CARDE Technical Memorandum 740, January 1963, AD 403 391.

(Unclassified Abstract) This report is a description of progress achieved up to 31 December 1962 in the present C.A.R.D.E. re-entry physics program. A brief description is given of the instrumentation employed in the radiation measurements. Some of the results obtained are presented. Supporting theoretical research at C.A.R.D.E. is discussed. An appendix describes the status of hypersonic range technology at C.A.R.D.E. as it affects the re-entry physics program. The results presented consist essentially of raw data only. One drawing and brief mention of sabot used in launching are the only two references to sabots.

- 428 Cowan, P. L.: "A Simple Sabot Retarding Device for Light Gas Launchers (U);" (Unclassified Report), CARDE Technical Note 1549, April 1963, AD 415821.

(Unclassified Abstract) This report presents a description of a sabot-retarding device for separating the sabot and model in a light gas launcher. The device consists basically of a column of air contained in the launch tube at the muzzle. The shock pressure generated by the projectile in the tube separates the sabot and projectile. Operating curves are presented for determining the loading conditions for any particular sabot discard problem. An application of the technique for the Launching of cone models in the CARDE 20-mm launcher is described.

- 429 Golbghat, G.; Lemay, A.: "Temperature Measurement of the Near Wake Generated by Hypervelocity Bodies (U);" (Unclassified Report). CARDE T.R. 502/64, July 1964, AD 448749.

(Unclassified Abstract) The wake radiation associated with hypervelocity ablating (Ioxan) one-inch diameter spheres fired from light gas guns into a pressurized range facility was found to be grey body within detectable limits. A two wavelength temperature method then was used to measure the color temperature of the radiation of the wake from immediately behind the body, through the recompression zone to approximately seven body diameters. The temperature results, as well as the emissivity values, are given for initial range pressures varying from 30 to 150 millimeters for sphere velocities of approximately 15,000 feet per second. A photograph of the sabot and projectile is given.

- 430 Bertrant, G.; Brooks, P.: "Parametric Study for Light Gas Gun Models (U);" (Confidential Report). CARDE T.R. 411/64, August 1964, AD 356609.

(Unclassified Abstract) This report covers a parametric study on the design of very light projectiles for use with hypervelocity launchers. Three basic model configurations, the sphere, the Atlas XV cone, and the Blue Streak GW-20, and one type of sabot, the "cup" sabot which discards radially under air drag, are considered. Theoretical approaches to projectile and sabot design are given. General comment on materials and high strain rate are included.

- 431 Crogan, L.E.: Drag & Stability Obtained from Free-Flight Firings of a Spherically Blunted 10-Degree Semi-Angle Cone with Four Variations in Base Geometry (U) ;" (Secret Report) Report No. NOLTR 62-136, 13 August 1964, AD 373 233.
- 432 Normand, M.: "A Review of Model Design for Free Flight Aerodynamic Studies (U);" (Unclassified Report). CARDE Technical Note 1657, February 1965, AD 461279.

(Unclassified Abstract) This report presents the design aspect of some scaled models that were successfully fired in the CARDE Aeroballistic Range: (1) 30° bimetal cone with sabot, (2) Apollo Launch Escape System, (3) Apollo Command Module, (4) Armad Configuration, (5) Half cone lifting vehicle, and (6) Delta wing.

The subject matter is presented according to the following inter-related topics: (1) description of range facilities, (2) description of guns, (3) design philosophy for sabots and models, and (4) classification of models. Of particular interest is the design philosophy for sabots. Several in-flight photographs of sabot separation are given.

- 433 Ball, Henry W.: "Initial Operation of the Pilot Counterflow Test Unit (1) (U)," (Unclassified Report), AEDC Report No. AEDC-TR-65-132, July 1965, AD 465893.

(Unclassified Abstract) A small counterflow test unit consisting of a shock tunnel and a hypervelocity launcher is being evaluated at the VKF, AEDC. The results of the shock tunnel calibration, the performance of the model launcher system, counterflow operating experiences, and some preliminary measurements of shock-cap radiation are reported. The shock tunnel calibration data for a room-temperature, helium driver gas are shown to confirm theoretical calculations and indicate clean uniform flow during a 4- to 5-msec run time. Aluminum spheres of 0.95-cm diam (0.375 in.) were sabot-launched with a 2-stage, light-gas gun at velocities between 4.0 and 5.5 km/sec (13,000 and 18,000 fps). During counterflow runs, relative velocities up to 7.5 km/sec (25,000 fps) were attained. Measurements of total radiation from the shock-caps of the small spheres are in reasonable agreement with theories and previous measurements from free-flight and shock-tube facilities.

- 434 Madagan, A. N.; Welsh, C. J.: "Free-Flight Range Tests of a Missile Configuration at Hypersonic Speeds (U);" (Confidential Report), Report No. AEDC-TR-66-98, May 1966, AD 372 309.

(Unclassified Abstract) Results are presented of free-flight range test of an AMICOM missile configuration, with and without fins, at hypersonic speeds. Drag coefficients and static and dynamic stability derivatives were measured. The tests were conducted over a Mach number range of 5.6 to 10.9 and Reynolds numbers of 7.3 to 33.6 by 10^6 . The models were light-gas gun launched by a 4-piece sabot. Photographs of the sabot and model are given.

- 435 Barrett, Benjamin J.; Rogers, Walter K.: "Second Interim Report on GM DRL'S 2-1/4 Inch Gun Project (U);" (Unclassified Report), General Motors Report No. TR66-01P, September 1966, AD 800958, for G.M. and Advanced Research Projects Agency.

(Unclassified Abstract) This report contains an account of the results of firing rounds five through seven of the 2-1/4" light-gas gun. Sphere and cone firing test results, shadowgraphs of launch, and sphere and sabot photographs are included.

- 436 "Third Technical Progress Report Hypervelocity Range Program (HYRAP 11) (1 May through 31 August 1966) (U);" (Confidential Report), General Motors Corporation, Report No. BSD-TR-66-366, November 1966, AD 377774.

(Unclassified Abstract) This report describes work conducted at GM Defense Research Laboratories between 1 May and 31 August 1966 on an extension (HYRAP II) of the original Hypervelocity Range Program (HYRAP). This is the final progress report on the HYRAP II program that extended from 1 September 1965 through 31 August 1966. The broad objective of the program is the study of re-entry observables on slender bodies in a free-flight ballistic range. Work described in the present report includes radar scattering from wakes, wake growth and transition, wake ionization studies and radiation measurements, theoretical ionization calculations, and results of shock-tube studies and molecular beam experiments. A bibliography of technical reports generated under this program is included in an appendix.

- 437 Brooks, P. N.; "ON THE DESIGN OF A LIGHT-WEIGHT SABOT WITH HEMISPHERICAL BASE FOR LAUNCHING AEROBALLISTIC MODELS," Canadian Armament Research and Development Establishment, Report No. CARDE TR 493/64, April 1964, (AD 441 868)

The design of a hemispherical-base sabot for launching near-full-bore aeroballistic models is presented. Two cases are considered: (a) the base has a constant thickness, (b) the base thickness is varied with rotational symmetry so as to provide a first approximation to a constant stress base. In both cases, the stress in the base is calculated for the inertial loads of the model, the cylindrical sabot wall and the material of the base itself. All pertinent information is given in terms of physical parameters and is expressed as dimensionless functions of the critical length of the sabot material and the combined weight of the model and cylindrical sabot wall. Finally a comparison is made between the two cases and also the standard cup sabot when used to launch a model of the Atlas XV nose cone.

- 438 Charters, A. C.; Curtis, John S.; "HIGH VELOCITY GUNS FOR FREE-FLIGHT RANGES," GM Defense Research Laboratories, Technical Memorandum No. TM 62-207, April 1962. (AD 203 473)
- 439 Curtis, John S.; "SABOTS," GM Defense Research Laboratories, Report No. CTN 64-04, August 1964. (AD 448 061)

This report describes a successful and novel sabot which has been developed for the gun launching of aerodynamic models at GM Defense Research Laboratories, Flight Physics Region. The sabot satisfies all requirements and operates in a satisfactory and reliable manner. It is constructed of a vacuum-annealed polycarbon resin (LEXAN). Sabot separation is achieved by aerodynamic forces, muzzle blast effects, and elastic rebound of the sabot. Using this sabot, both cones and spheres have been launched at velocities in excess of 24,000 feet per second.

- 440 Fedenia, John N.; Carter, Hilton, L.; Chamberline, Amy A.; "EXPERIENCES IN THE LAUNCHING OF FRAGILE AERODYNAMIC SHAPES IN THE NOL 1,000 FT. HYPERBALLISTICS RANGE NO. 4," Third Hypervelocity Techniques Symposium, Denver, March 17-18, 1964, pp. 517-550.

The technique of launching aerodynamic models at hypersonic speeds with a two-stage gun has been under development in the NOL 1,000 ft. Hyperballistic Range No. 4. Severe accelerating conditions to obtain high speeds makes it difficult to launch fragile aerodynamic shapes such as slender cones and thin-walled models. To investigate the projectile launching conditions, an analysis has been made of several modes of operation of the 1.6 in two-stage gas-gun. The gun cycle was investigated using three pump tube piston weights and projectile release pressures. Calculated performance is compared with experimental results. Typical model and sabot construction and experiences in launching are described. Various model and sabot designs have been launched at velocities from 13,000 to 20,000 ft. per second.

- 441 Glass, I. I.; "RESEARCH FRONTIERS AT HYPERVELOCITIES," Canadian Aeronautics and Space Journal, Vol. 13, Nos. 8/9, October/November 1967, pp. 347-426.

Report summarizes several facets of hypervelocity, real gas flow and presents work on the use of stable, explosive-driven implosion waves as drivers for shock tubes and hypervelocity launchers that theoretically possess very impressive hypervelocity performance capabilities. In practice, however, loss mechanisms and the projectile-integrity problem may limit the actual attainable hypervelocities of shock waves and projectiles. These problems are now under investigation.

- 442 MacAllister, L. C.; "ON THE USE OF PLASTIC SABOTS FOR FREE FLIGHT TESTING," Ballistic Research Laboratories, Memorandum Report No. MR-782, May 1954. (AD 44 457)

A description of the use of sabots to adapt winged and/or finned projectiles for gun-launching in free flight range testing is given. Examples of adaptations for 20-mm, 37-mm, 57-mm, 90-mm, and 155-mm guns are described.

Good photographs of sabots and models are included. Several muzzle exit and sabot separation photographs are also given.

- 443 Motomura, F.; "CONE LAUNCHING TECHNIQUES AT C. A. R. D. E.," Canadian Armament Research and Development Establishment, Report No. CARDE-TN-1604/64, July 1964.

This note deals with some of the experiments carried out to launch aerodynamically stable cones at velocities of 13,500 fps-14,500 fps. This was achieved in a 20-mm light gas gun at the range pressures in excess of 40 mm of Hg. The design concepts for the projectiles and the launch techniques used are presented, together with graphs that show the effect of pressure range on the stability of the cones. Efforts made to trace and analyze the source of destabilization, both by theoretical and experimental methods, are also discussed in detail.

- 444 Seigel, Arnold E.; "A TWO-INCH LAUNCHER FOR AERO-DYNAMIC MODELS," Journal of the Aerospace Sciences, Vol. 29, November 1962, pp. 1383-1384.

Description of the design and principles of an aerodynamic-model launcher, which has been firing regularly into a 1,000-ft hyperballistic range since January 1962. Fragile models have been fired at velocities in excess of 18,000 ft/sec.

- 445 Slattery, R. E.; Clay, W. G.; Stevens, R. R.; "INTERACTIONS BETWEEN A HYPERSONIC WAKE AND FOLLOWING HYPERSONIC PROJECTILE," AIAA Journal, Vol. 1, April 1963, pp. 974-975.

The presence of the sabot in the wake of a spin-stabilized cone radically altered the flow around the cone. The base section of the sabot is partially split, so that normally it breaks upon leaving the gun muzzle and the pieces are separated from the cone's flight path by centrifugal forces. When the sabot base fails to split, as sometimes occurs, it continues down range along the same path as the cone, slowly falling behind it because of the difference in drag. Photographs show cone after firing with the base of the sabot located in the wake of the cone changing the normal flow about the cone. Interpretation is that the sabot is immersed in a fluid with respect to which it has a subsonic velocity. It can propagate energy back up the cone's trail, countercurrent to the flow in the trail, and alter the characteristic flow about the cone.

- 446 Taylor, G.; Murphy, C. H.; "AN INTERESTING SABOT DESIGN," Ballistic Research Laboratories, Memorandum Report No. MR-1304, September 1960. (AD 247 270)

The design and performance of a sabot making use of internal support (as opposed to the conventional wrap-around or external variety) are described. The sabot makes use of an internal string for support and the expanding gun gases for separation.

Drawings and photographs of the sabot are given. Photographs of sabot discarding are also included.

- 447 "BALL VALVE DOUBLES AS GATE FOR PROJECTILE IN TEST FIRING," Product Engineering, Vol. 37, October 24, 1966, p. 38.

Problem was to provide a quick-opening tunnel gate that would let a test model of a projectile pass through yet would stop the debris following close behind. Work done by CARDE was to simulate space vehicle performance at 40-mi. elevation by shooting a test projectile at ground level into a vacuum tank. Projectile wrapped in a plastic sabot begins its flight in the muzzle of a 264-ft. hypersonic gas gun. It then passes through two tanks leaving plastic sabot in first tank where it has peeled away from the projectile.

D-10 GUN DEVELOPMENT STUDIES

- 448 Nelson, R. H.; Whitcraft, J. S.: "Accuracy and Erosion Studies of Modified T254 Series Gun Tubes for 105-mm Gun, M68 (U)"; (Confidential Report), APG Report No. DPS-469, February 1962, AD 328 368.
- 449 "Preliminary Final Report Project Helmet (U)"; (Confidential Report) ARPA Division, Army Missile Command, Report RN-62-1, 31 December 1962, AD 337 575.

(Unclassified Abstract) The technical and economic feasibility of two high-performance methods of delivering heavy payloads to specified altitudes are analyzed. Limitations of each approach are considered in relationship to the state of art in each subsystem area. A total delivery cost model is described showing the pattern of costs for wide variations in payload weight and peak acceleration.

The final variation of the undergun involves fitting a 24-foot sabot to the projectile to increase the area exposed to the high-pressure propellant gases. With such a large sabot, the problem arises of controlling the falling pieces to avoid damage to the surrounding area.

- 450 "Final Report of Helmet Delivery Study (U)"; (Confidential Report), AMF Document No. G-16262A, 19 April 1963, AD 336 483.

(Unclassified Abstract) Volume 1 of this report summarized the conclusions and recommendations resulting from the Helmet delivery feasibility study conducted by AMF. This document presents the analytical background to support conclusions reported in the first volume. The program reported here was initiated to evaluate the feasibility of using an under-ground gun to deliver the Helmet AICBM payload. In the Helmet program, a systematic investigation was undertaken to determine the technical and economic feasibility of delivering large pellet payloads--in the range of tens to thousands of tons--from ground-based launch facilities.

- 451 Comer, Richard H.; Jones, Richard N.; Shearer, Robert B.: "Predicted Performance of a High-Pressure, High-Velocity Liquid Propellant (U)"; (Confidential Report), BRL Memorandum Report No. 1573, July 1964, AD 354 590.

(Unclassified Abstract) Extrapolation of BRL 37-mm data, and other data from 30, 77, and 90-mm firings, indicates that an 8-pound projectile might be launched at about 7000 ft/sec from a 120-mm gun.

- 452 Haden, H.G.: "A Note on Swedish Additive (U)"; (Confidential Report), Royal Armament Research and Development Establishment Memorandum 43/64, September 1964, AD 354 196.

(Unclassified Abstract) Substances such as titanium dioxide, in a finely powdered state, placed around the propellant in a gun charge, markedly reduce the wear of the gun. This note sketches a theory on one possible mode of action of the additive, the theory that it affects the transmission of heat from the main gas stream across the boundary layer to the bore surface.

- 453 Wolff, Robert O.: "Reduction of Gun Erosion, Part II, Barrel Wear-Reducing Additive"; (Unclassified Report), August 1963, Picatinny Arsenal Technical Report 3096, AD 416 237.

(Unclassified Abstract) The superiority of the additive method over the laminar coolant method in reducing barrel wear was demonstrated in firings of the M392 Round with the M68 Gun. Tungsten trioxide (WO_3) and titanium dioxide (TiO_2) additives were considered. Titanium dioxide was chosen for intensive evaluation on the basis of effectiveness and cost. The use of the additive did not degrade ballistics, storage, or handling characteristics of the rounds tested. Similar results were obtained for TiO_2 additive with the 105-mm cartridge, HEAT-T, M456 (also TP-T, XM490) and the 90-mm cartridge, HEAT-T, M431. Technical Data Packages were modified to include the additive for all future production of these rounds. The 105-mm cartridge APDS-T, M392, was used as the vehicle for the preliminary work to provide direct comparison with laminar coolant.

- 454 Temchin, J.R.; Nicol, W.R.; Edwards, J.B.; Fauth, M.I.; Richardson, A.C.; Heinen, F.J.; Gauthier, C.J.: "Survey of Developments in Gun Propulsion (U)"; (Confidential Report), NAVWEPS Report 8693, 30 June 1965, AD 366 968.

(Unclassified Abstract) A state-of-the-art survey on various phases of gun propulsion technology is presented. Current gun systems and recent developments in cartridge cases, gun-barrel erosion, liquid gun systems, gun-boosted rockets, and hypervelocity systems are included, as well as a note on possible future artillery applications.

It is concluded that (1) hypervelocity systems offer a means of developing more effective gun systems, and (2) lightweight or sabot-type projectiles, combined with standard or smoothbore barrels, would increase muzzle velocity with standard charges.

Included are pictorial representations and an extensive bibliography.

- 455 Sylvester, David; Lehner, Robert: "Naval Gun Study (U)"; (Confidential Report), Aircraft Armaments, Inc. Report No. ER-4434, July 1966, AD 374 741.

(Unclassified Abstract) This study was conducted to investigate an improved and more versatile gun system and types of ammunition for surface vessels. The ammunition family investigated included a sabot-launched Arrow projectile (slap) round, a multiple projectile antiaircraft (AA) round, an anti-submarine warfare (ASW) round consisting of four rocket-assisted sub-projectiles, and a massive high-explosive round for landing support operations (LSO).

Many pictorial representations and several photographs of the different types of ammunition, including sabots to be used in the enlarged bore, are given. The sabot and its technique of operation are described in the body of the study.

- 456 Baker, J. R.; Condon, J. J.; Porter, C. D.; Swift, H. F.; "NRL HYPERVELOCITY ACCELERATOR DEVELOPMENT," Proceedings of the Sixth Symposium on Hypervelocity Impact, Cleveland, April 30 - May 2, 1963, Vol. 1, August 1963, pp. 175-246.

Present accelerators are light-gas guns of the semi-expandable-central-breech design which vary in size from 0.830 in., 0.30 in. units to an 8.2 in., 2.5 in. gun. The current launch capability of the facility ranges from 0.1 g at 9.35 km/sec to 250 g at 5.6 km/sec. The operation of gas guns is being studied theoretically with a computer program. An experimental study of various aspects of gun operations including projectile release, driver gas leakage, projectile-bore friction, and sabot breakup is also being conducted.

- 457 Bertrand, G.; Gallagher, G.; Maroney, J. J.; "A HIGH PERFORMANCE EXPERIMENTAL SMOOTH BORE GUN," Canadian Armament Research and Development Establishment, Technical Report No. CARDE TR-484/64, August 1964. (AD 451 971)
- 458 Carn, Robert E.; Stinson, Anna B.; "HANDBOOK OF TRAJECTORY DATA FOR SPIN STABILIZED PROJECTILES, TYPICAL FIN STABILIZED FLECHETTES, SPHERES AND CUBES," Ballistic Research Laboratories, Report No. R-1336, August 1966. (AD 809 904)
- 459 Crosby, John K.; Gill, Stephen P.; "FEASIBILITY STUDY ON AN EXPLOSIVE GUN," Stanford Research Institute, April 1967.

The component requirement for a gun with near-optimum performance were specified as (1) low detonation velocity in the first stages to allow the use of a short, high pressure helium

reservoir; (2) a transition section around the original projectile position to allow containment of high pressures during the low velocity stages of projectile acceleration; and (3) detonation velocities increasing gradually to very high values as the acceleration proceeds. The experimental work performed on these three problems is discussed, along with experiments on a constant velocity-constant wall thickness gun using thin-walled, high strength steel tubing. Different modes of gun operation were studied using the artificial viscosity computer code. A theoretical design of an explosive system, which will provide a piston with constant acceleration, is proposed. Theoretical calculations are presented on ionization, radiative cooling, and boundary layer effects along with calculations on the NASA-Ames 4"-1" deformable piston light gas gun. It was concluded that the gun operation was experimentally demonstrated, and that fair agreement between theoretical and experimental performance was shown.

- 460 Darpas, J. G.; "TRANSVERSE FORCES ON PROJECTILES WHICH ROTATE IN THE BARREL," Ballistic Research Laboratories, Memorandum Report No. 1208, March 1959. (AD 218 873)
- 461 de Stefano, Leonard A.; "A DIGITAL COMPUTER SIMULATION OF BREECH-LAUNCHED ROCKETS," Frankford Arsenal, Report No. M67-18-1, January 1967. (AD 648 152)

The report documents a digital computer simulation of solid propellant breech-launched rockets. The equations describing the system are presented and solved by Runge-Kutta methods programmed in Fortran for the Univac Solid State 90 digital computer. The computer program, its input and output formats, and comparison with experimental performance are also presented. It is also shown how the program can be used to simulate certain other ballistic devices.

- 462 Frankle, J. M.; "AN INTERIOR BALLISTIC STUDY OF A 24-INCH GUN FOR PROJECT HARP," Ballistic Research Laboratories, Technical Note No. 1606, May 1966. (AD 486 743)
- 463 Frankle, Jerome M.; "INTERIOR BALLISTICS OF HIGH VELOCITY GUNS: EXPERIMENTAL PROGRAM PHASE I," Ballistic Research Laboratories, Memorandum Report No. 1879, (AD 830 408)
- 464 Geldmacher, R. C.; Roach, T. M., Jr.; "MEASUREMENTS OF GUN AND SHELL STRAINS DURING FIRING," General Technology Corporation, Research and Development, Technical Report No. 1-13, February 1960.

- 465 Goodall, A. M.; "GUNS USING LIQUID PROPELLANTS," Armament Research and Development Establishment, Propulsion Munitions Division, Progress Report No. 6, covering period 1 January - 30 June 1957, Report No. (P)48/57, September 1957. (AD 146 319)
- 466 Goode, J. B.; "DEFINITIONS OF PRESSURES FOR USE IN THE DESIGN AND PROOF OF GUNS AND AMMUNITION," Royal Armament Research and Development Establishment, Guns and Ammunition Division, Memorandum No. 11/66, April 1966. (AD 481 141)
- 467 Howell, W. G.; Ipson, T. W.; Recht, R. F.; "HYPERVELOCITY AUGMENTATION TECHNIQUES," Proceedings of the Sixth Symposium on Hypervelocity Impact, Cleveland, April 30 - May 2, 1963, Vol. 1, August 1963, pp. 305-316.

This paper presents analytical and experimental results from an initial investigation of a light-gas-gun projection system, a third stage is added to the end of the launch tube of a conventional two-stage light-gas projector. This third stage is designed to make use of the kinetic energy which is available in the sabot at the time that a sabot-projectile combination is normally fired from the launch tube. It has a convergent section which acts as an acceleration chamber leading into a final launch tube having a smaller bore. The projectile is carried centrally on the face of the sabot and fits the bore of the final launch tube.

- 468 Howell, W. G.; Kottenstette, J. P.; "ELECTRICAL AUGMENTATION OF A LIGHT GAS GUN," Denver Research Institute, Mechanics Division, January 1965.

This report covers the experimental and analytical research directed toward the development of a system for electrical augmentation of a light gas launcher. The first phase involved the use of a medium performance light gas launcher to develop techniques and prove that electrical augmentation was experimentally practical. The second phase used a high performance launcher to attempt optimization of these augmentation techniques.

- 469 Kaufman, William F., Jr.; "PROJECTILE (ARMY)," U. S. Patent Office, No. 3,216,356, November 9, 1965.

The caseless round is used in a recoilless rifle. A somewhat elastic ring is secured to the projectile and is fitted within a groove rearwardly of the projectile rotating band to extend radially outward far enough for engaging an inwardly extending ledge within the chamber of the gun. This ring is preferably of a plastic having an ultimate shear strength of about 20,000 pounds per square inch, so that on rupture of the ring, the projectile is

given more rapid acceleration and velocity for a given propellant than it would have had with a metal cartridge case having a conventional base flange arrangement.

- 470 Kennedy, Bruce; "MUZZLE VELOCITY MEASUREMENT," Atmospheric Sciences Laboratory, Report No. ECOM 5083, October 1966. (AD 642 859)
- 471 Lorimor, George; "ANALYSIS OF CARRIAGES SUITABLE FOR 7-INCH HARP GUN," Rock Island Arsenal, Report No. 3-65, January 1965.
- 472 McCluney, E. L.; "PROJECTILE DISPERSION AS CAUSED BY BARREL DISPLACEMENT IN THE 5-INCH GUN PROBE SYSTEM," Atmospheric Sciences Laboratory, Report No. ECOM 5060, July 1966. (AD 639 960)
- 473 Moore, E. T., Jr.; "EXPLOSIVE HYPERVELOCITY LAUNCHERS," Physics International Company, Final Report No. FR-051, NASA CR-982, February 1968.
- 474 Nelson, R. H.; "FIRST PARTIAL REPORT OF A STUDY TO SUMMARIZE PRESSURE AND VELOCITY DISPERSION CHARACTERISTICS FOR SEVERAL ARTILLERY WEAPONS," Aberdeen Proving Ground, Development and Proof Services, Report No. DPS-1343, June 1964. (AD 442 313L)
- 475 Oskay, Vural; "PROOF TESTING AND COMPUTER ANALYSIS OF BRL 81/26 MM LIGHT-GAS GUN," Ballistic Research Laboratories, Memorandum Report No. 1855, July 1967. (AD 661 289)

A computer program and its use to simulate the performance of a light-gas gun is described. This technique is applied to simulate proof tests of the 81/26 mm light-gas gun. The analysis is extended to determine performance characteristics and maximum muzzle velocity attainable with a 29-gram launch weight. Results of computer analysis indicate that a sabot/model combination of that weight could be launched at a velocity above 21,000 ft./sec. if it could be designed to withstand about 1,000,000-g acceleration loads.

- 476 Parkinson, G. V.; "SIMPLE INTERNAL BALLISTICS THEORY FOR SINGLE AND DOUBLE CHAMBER GUNS," Space Research Institute, McGill University, Report No. SRI-H-TN-4, August 26, 1966.

The equations of the well-known simple one-dimensional unsteady gas dynamics model for the internal ballistics of a conventional gun, assuming instantaneous uniform density throughout the propellant gas volume, are presented for use in HARP project. The

principal equations give ratios of breech and space mean pressures to projectile base pressure in terms of charge to projectile weight ratio. The theory is extended to cover the problem of a double chamber gun system, with the chambers separated by a free piston. Again, results are given in the form of relations among the various significant gas pressure ratios in terms of charge to projectile and piston weight ratios.

- 477 Seigel, Arnold E.; "THE THEORY OF HIGH SPEED GUNS," Advisory Group for Aerospace Research and Development, Report No. AGARDograph-91, May 1965.

This monograph summarizes the gas dynamics of high-speed guns, utilizing a gas of low molecular weight at high temperature. Theory and test results are presented. The reader is assumed to be an advanced student in engineering. The fundamental ideas and equations are fully developed.

- 478 Swotinsky, J. M.; Spiess, I.; Long, J. A.; Lombardi, C. A.; "DESIGN AND USE OF A CLOSED BREECH LAUNCH SIMULATOR FOR THE SHILLELAGH GUIDED MISSILE," Bulletin of 20th Interagency Solid Propulsion Meeting, Vol. IV, July 1964, pp. 413-426, Confidential.
- 479 Thurnborg, S., Jr.; Ingram, G. E.; Graham, R. A.; "COMPRESSED GAS GUN FOR CONTROLLED PLANAR IMPACTS OVER A WIDE VELOCITY RANGE," Review of Scientific Instruments, Vol. 35, January 1964, pp. 11-14.

A description is given of the mechanical characteristics and performance of a compressed gas gun capable of accelerating precisely aligned flat-faced projectiles over a wide velocity range. Predetermined reproducible velocities may be achieved between 150 and 5700 ft/sec with an angular misalignment between the impacting surfaces as small as 1.3×10^{-4} rad. The impact occurs in a vacuum with pressures as low as 10^{-4} mm Hg. The gun has an inside diameter of 2-1/2 in., a length of 100 ft., and uses either air or helium at pressures as high as 5000 psi. The gun is particularly suited for experiments in which a well-defined impact is desired. (The projectile is grooved for a hard rubber O-ring with Teflon back-up rings.)

- 480 "HYDROSTATIC COMBUSTION SEAL DEMONSTRATION FEASIBILITY," Aerojet-General Corporation, Progress Report No. AGC 10784-Q-1, covering period 7 March - 15 September 1965, October 15, 1965, Confidential.
- 481 "INVESTIGATION OF THE EFFECT OF RAM FORCE ON BREECH PRESSURE AND MUZZLE VELOCITY IN THE 16.5" SMOOTHBORE GUN," Inspection Services, Canadian DND, Technical Note No. 4/65, February 1965.

D-11 MUZZLE BLAST EFFECTS

- 482 Zaroodny, S. J.: "On Jump Due to Muzzle Disturbances (U)"; (Unclassified Report), BRL Report No. 703, June 1949, AD 805 876.

(Unclassified Abstract) A review of the current approach to the problem is given. Formulas are compiled giving jump as a function of the muzzle disturbances, and which can also be used for analysis of the jump, i. e., for evaluating these disturbances from the observed motion of the shell (in particular, its yawing motion). Muzzle disturbances are assumed to consist of three planar vector quantities: a lateral linear momentum, an initial yaw, and an initial yawing. In this way the restrictive assumptions that have been customary with respect to the jump are removed, and the way is open for experimental verification of these assumptions and for further analysis of jump.

- 483 Witt, Jr., W. R.: "Spark Shadowgraph Pictures from Tests with Two 20-mm Muzzle Blast Reducers (U)"; (Unclassified Report), NAVORD Report 5759, November 1957, AD 162 939.

(Unclassified Abstract) An investigation of the performance of two muzzle blast reducers for a 20-mm barrel was carried out in the Naval Ordnance Laboratory Block Mount Range. Spark shadowgraph pictures were taken to obtain a qualitative measure of the muzzle blast intensity. No analysis of the data was made at the Naval Ordnance Laboratory. However, because of the considerable interest shown by many people in the spark pictures and the limited number of such pictures appearing in the literature, several shadowgraphs are presented comparing the muzzle blast patterns for the case of no reducer with those obtained with the two reducer designs.

- 484 Berry, John: "Development of UBU Muzzle Brake as Applied to the 105-mm Howitzer, XM102 (U)"; (Unclassified Report), Rock Island Arsenal Research & Engineering Division Report No. TR-64-2560, August 1964, AD 448 463.

(Unclassified Abstract) A design, development, and test program was conducted to determine what effect a Upward Blast Utilizer (UBU) muzzle brake would have on overall weapon performance with regard to: (1) overall stability during firing, (2) obscuration during firing, (3) overpressure in the gun crew area, and (4) accuracy of the weapon.

- 485 Salsbury, Mark J.: "Experimental Test of Reservoir-Type Muzzle Brake (U)"; (Unclassified Report), Rock Island Arsenal Research & Engineering Division Technical Report 65-1517, June 1965, AD 466 201.

(Unclassified Abstract) The object of this test was to evaluate a reservoir-type muzzle brake as a blast suppression device for artillery pieces, the theory being that by throttling the gases the mass rate of discharge would be smoothed out and overpressures reduced. The value of this type of muzzle brake test lies in the fact that very little actual firing data is available dealing with the theoretical aspects of a muzzle brake design instead of one specific brake.

- 486 Oswatitsch, K.: "Intermediate Ballistics"; (Unclassified Report), U.S. Army Foreign Science and Technology Center Report No. FSTC 381-T65-372 October 1965, AD 473 249.

(Unclassified Abstract) Intermediate ballistics means the transitional phenomena between "interior ballistics" and "exterior ballistics," near the muzzle. This stage is marked by the emission of gas from the barrel in front of the projectile and by the discharge of the propellant gases behind the projectile. Here the use of the momentum of the propellant gas and the effect on the delivery of the projectile are of special interest. The present paper gives a first brief exposition of "intermediate ballistics."

- 487 Donselman, R.W.; Johnson, R.R.: "Hardening Technology Studies: Ballistic Range Test Data and Analysis Report"; (Unclassified Report), LMSC Report No. BSD TR-66-96, 30 September 1965, AD 480 644.

(Unclassified Abstract) A ballistic range test program was conducted as part of the Hardening Technology Studies (HARTS). Purpose of this test was to obtain experimental data on a re-entry vehicle flying through a blast, these data then to be used to correlate with and confirm analytical prediction techniques. This report discusses the test program, the test technique, the instrumentation used, the test facility, and the data obtained. Aluminum pushers and wooden (pine) sabots were used to support the launchings. Basic drawings are given.

- 488 Townsend, Philip E.: "Development of a Gas Gun to Investigate Obscuration Effects"; (Unclassified Report), Rock Island Arsenal, Research & Engineering Division Technical Report 66-3281, November 1966, AD 804 815.

(Unclassified Abstract) The objective of this study was to develop a method for obscuration investigation. A serious problem associated with artillery firings is the obscuration of the target by the cloud of smoke, dust, and debris raised by the muzzle blast. In an attempt to study this problem a development program was outlined and initiated on a model basis under laboratory conditions. A gas gun was designed and tested in conditions modeling a prototype test using flat plates as blast deflectors.

Three items of discussion are presented: (1) generation of the muzzle blast, (2) raising of the dust cloud with the muzzle blast, and (3) use of an inert-gas gun as an approach in the investigation of gas deflection to minimize obscuration.

- 489 Berry, John M.; "ACCURACY COMPARISON FIRINGS OF 5-K AND UBU 105 MM MUZZLE BRAKES," Rock Island Arsenal, Report No. RIA-68-267, 1968. (AD 828 858L)
- 490 Berton, I. P. T. T.; "ON THE TRIGGER ACTION OF X-RAY APPARATUS AT THE MUZZLE OF A GAS TUBE TO STUDY THE BEHAVIOR OF A PROJECTILE LAUNCHED BY A LIGHT GAS GUN," Laboratoire de Recherches Balistiques et Aerodynamiques, Report No. LRBA-E.1023-NT-12, November 20, 1967 (in French).

Details are given on an experiment in which X-ray photography was used to study the containment and separation of the protective sabot within the mouth of an ejection tube in a light gas gun. Using a gas laser as a light source, an X-ray apparatus was placed at the mouth and intermediate chambers of the gas gun to study the passage of projectiles through the tube. It was concluded that the combined use of the gas laser with the X-ray equipment resulted in effective studies of the mechanism of sabot separation and conditions which cause the separation.

- 491 Francis, David J.; "ENGINEER DESIGN TEST OF CHARGE, PROPELLING, 155-MM, XM119E4 (BLAST STUDY)," Aberdeen Proving Ground, Development and Proof Services, Final Report No. DPS-1964, March 1966. (AD 479 856)
- 492 Schlenker, George; "THEORETICAL STUDY OF THE BLAST FIELD OF ARTILLERY WITH MUZZLE BRAKES," Rock Island Arsenal, Technical Report No. 62-4257, December 1962. (AD 296 587)
- 493 Spalinger, R. E.; "SOUND AND PRESSURE LEVEL MEASUREMENTS OF THE HARP-BARBADOS 16.5-INCH GUN WITH A 51 FT. MUZZLE EXTENSION," Eglin Air Force Base, Report No. APGC-TR-65-50, July 1965. (AD 467 721)
- 494 Taylor, Wayne L.; "REDUCTION OF BLAST OVERPRESSURE FIRING EXTENDED RANGE AMMUNITION IN THE 155MM M109 SP HOWITZER," Picatinny Arsenal, Ammunition Engineering Directorate, Technical Report No. TR-3499, December 1966. (AD 805 582)
- 495 White, C. E.; "SOUND PRESSURE LEVEL MEASUREMENTS OF THE HARP 16.5" SMOOTHBORE GUN AT BARBADOS DURING THE FIRINGS IN DECEMBER 1964," Inspection Services, Canadian Department of National Defence, Report No. TN 1/65, January 1965.

- 496 "DETERMINATION OF BLAST PRESSURE WITHIN A SUB-TERRANEAN WOODEN BUNKER WHILE FIRING A 106 MM RECOILLESS RIFLE," Aberdeen Proving Ground, Development and Proof Services, Report No. TS4-4020-28, March 1958. (AD 159 775)
- 497 "INVESTIGATION OF MUZZLE BLAST OF HOWITZER, 155-MM, M1A2E3," Aberdeen Proving Ground, Development and Proof Services, Report No. DPS-169, March 1961. (AD 251 955)

D-12 MATERIAL PROPERTIES

- 498 Tardif, H. P.; Erickson, Wm.: "The Mechanical Properties of Metals Under Dynamic Loading"; (Unclassified Report), CARDE, PCC No. D46-95-35-08, April 1958, AD 210 559.

(Unclassified Abstract) This report is a general survey of published literature on the effects of rate of loading on the mechanical properties of metals. It is generally known that properties such as yield stress and ultimate stress increase with an increase in the rate of load application. However, it is believed that this effect seldom is taken into account for design purposes. Were this effect of sufficient magnitude, there would be an advantage in using it to lighten the weight of structures submitted to dynamic loading.

The purpose of this report was to survey and assess metal dynamic properties published to date. Properties were found for mild steel, medium carbon steel, quenched and tempered alloy steels, aluminum alloys, and a few other metals. Although the yield stress of mild steel may be increased during dynamic deformation by as much as 2 or 3 times its static value, the increase in most other metals is much smaller, of the order of approximately 0 to 30%.

- 499 Hendrix, R. E.: "Microwave Measurements of Projectile Kinematics Within Launcher Barrels"; (Unclassified Report), AEDC Report No. AEDC-TDR-62-213, November 1962, AD 104 637.

(Unclassified Abstract) Microwave reflectometry has been applied successfully to the study of the kinematic behavior of projectiles within launcher barrels and of pistons within compression (pump) tubes in the Hypervelocity Pilot Range of the von Karman Gas Dynamics Facility. Well-defined mathematical treatment enables the calculation of an accurate time history of projectile position inside the launcher barrel. Microwave excitation in extraneous modes has been attenuated, resulting in an increase in the accuracy of the reflectometer system.

- 500 Mescall, John F.: "Thin Cylindrical Shells Under Local Axial Loadings"; (Unclassified Report), U.S. Army Materials Research Agency Technical Report AMRA TR 64-39, December 1964, AD 456 337.

(Unclassified Abstract) The linear equations due to Flugge for thin elastic circular cylindrical shells are solved by use of the finite Fourier transform for the case of distributed tangential (axial) loading with simply supported edge conditions. This solution supplements prior results obtained by Bijlaard for radial (normal) distributed loadings.

Combining Bijlaard's results with the solutions obtained in this report permits discussion of localized loadings having components both normal and tangential to the shell's middle surface. Such an application is discussed and numerical results are provided.

- 501 Cable, A. J.: "An Examination of Failing Loads in Model Launching Experiments"; (Unclassified Report), AEDC Report No. AEDC-TR-65-54, March 1965, AD 457 907.

(Unclassified Abstract) Tests were conducted to evaluate the structural adequacy of the design of a 9-degree semi-angle, blunted cone to be launched from light-gas guns in aeroballistic ranges. Because of the high accelerations of the model necessary if muzzle velocities of interest are to be attained, structural design constitutes a prominent part of the overall problem. Measurements of model accelerations during launch, using microwave reflectometers, compared favorably with accelerations arrived at analytically, and have allowed determination of failing loads during launching. These dynamic loads were correlated both with static compression tests and theoretical estimates. The failing accelerations for 7075-T6 aluminum models have ranged from $1.6 \times 10^5 g$ for a 1.75-in. (44.5-mm) caliber cone to $6 \times 10^5 g$ for a 0.45-in. (11.4-mm) caliber cone. Drawings of the cone model and four-petaled sabot are given.

- 502 Huffington, Norris J., Jr (Ed): "Behavior of Materials Under Dynamic Loading"; (Unclassified Report), American Society of Mechanical Engineers (ASME), 1965

(Unclassified Abstract) Recently, technology has made differences in material properties under dynamic and static conditions increasingly significant. This book concentrates attention on intense transient loading, such as is produced by impact or explosives, where departures of material behavior from the static case should be maximal. It covers the range of impact velocities from those just sufficient to exceed the linear elastic regime up through those attainable with hypervelocity particle projectors.

The papers of this Colloquium principally employ the "macro-analytical", or phenomenological, approach. The advantages of this procedure are two-fold: there is the prospect of greater short-term progress in systematizing information regarding dynamic material behavior, as well as the natural expression of new developments in terms of the macroscopic (continuum) variables which the dynamics analyst wishes to employ.

The papers of this Colloquium were prepared by recognized authorities who have presented their views on the following topics:

- (1) The Propagation of Mechanical Pulses in Anelastic Solids, H. Kolsky.

(Unclassified Abstract) Stress wave propagation in linear visco-elastic solids is discussed for one dimensional propagation along rods or filaments and in blocks where dilatational waves are propagated. The information such experimental studies give with regard to suitable constitutive relations for real polymers under conditions of triaxial loading is described. The use of numerical Fourier methods for treating pulse propagation also is discussed. A short account of plastic wave propagation and the information plastic wave experiments give about strain-rate effects is included.

- (2) The Dynamic Plasticity of Metals at High Strain Rates: An Experimental Generalization, James F. Bell.

(Unclassified Abstract) "Extended quasi-static" impact and indirect dynamic impact experiments are compared critically with direct dynamic experiments. The success of the direct dynamic experiments in establishing the applicability of the finite amplitude wave theory to a variety of metals is described. In such direct experiments diffraction grating measurement of dynamic plastic strain and wave speeds in the symmetrical free-flight impact of polycrystals may be used to predict the stage III deformation of nearly 400 aluminum, copper, nickel, lead, gold, and silver single crystals in the metal physics literature. This fact is evidence of the generality of these results.

Recent experiments on initially work-hardened metals are discussed. These data include a brief description of the success of the writer's linearly temperature-dependent generalized parabolic stress-strain law governing strain rate independent finite amplitude wave propagation in predicting dynamic ultimate strength data of numerous earlier experimentalists.

- (3) Dynamic Deformation of Metals, Ulric S. Lindholm.

(Unclassified Abstract) Mechanical testing of metals over a wide range in strain rates is discussed. The experimental methods described are the split Hopkinson pressure bar for uniaxial compression testing and a new pneumatic machine for dynamic testing under combined stress conditions. Results are presented for a number of metals. Theoretical aspects of rate-sensitive plastic deformation of metals are discussed briefly in terms of thermally activated dislocation mechanisms.

- (4) Dynamic Plastic Behavior of Aluminum, Copper, and Iron, E. A. Ripperger.

(Unclassified Abstract) Aluminum, copper, and iron all are strain-rate sensitive in that (1) they are capable of developing stresses appreciably higher than the stresses at corresponding strains under static conditions, and (2) the dynamic yield stress increases with strain rate and is appreciably higher than the static yield stress. It is also shown that extensive cold-working of high-purity aluminum does not appreciably affect the strain-rate sensitivity. The presence of a hydrostatic stress component during rapid straining of copper and iron has an appreciable effect on strain-rate sensitivity. The experimental results presented indicate a logarithmic relation between plastic strain rate and the dynamic overstress ratio. For solid cylindrical specimens, it is shown that lateral inertia has no appreciable influence on dynamic yield stress.

- (5) Experimental Studies of Strain-Rate Effects and Plastic-Wave Propagation in Annealed Aluminum, L. E. Malvern.

(Unclassified Abstract) Dynamic compressive stress-strain measurements on annealed aluminum specimens and longitudinal compressive plastic-wave propagation experiments on long bars of the same material are described and discussed in relation to the rate-dependent theory of plastic-wave propagation. At room temperature the material exhibits very little rate dependence, but the rate dependence increases with temperature in tests up to 550° C. In the wave-propagation studies at room temperature, particle velocity measurements with an electromagnetic transducer are correlated well by a single dynamic stress-strain curve slightly above the static curve.

- (6) Strain Rate Effects in Dynamic Loading of Structures, S. R. Bodner.

(Unclassified Abstract) Approximations made in analytical determination of the inelastic response of structures to dynamic loading are discussed, with particular reference to the applicability of rigid-plastic theory. A brief review of the dynamic properties of structural metals is given from the viewpoint of the methods of incorporating the properties in structural response analyses. The importance of strain rate effects in such analyses and in experimental results is considered in detail. References are made to theoretical and experimental investigations that consider materials with strain rate dependent yield stresses.

- (7) Viscoplastic Behavior in Response of Structures to Dynamic Loading, P. S. Symonds.

(Unclassified Abstract) Methods to analyze plastic deformations of structures under dynamic loads are reviewed, with experimental evidence from tests on mild steel and aluminum alloy beams. An approximate method for quickly estimating final deflections, taking account of strain rate sensitivity and strain hardening, is outlined and comparisons made with relevant test results. The use of simple representations of strain rate sensitivity in dynamic structural analysis is discussed in the light of recent experiments on the behaviour of various metals.

- (8) Spherical Elasto-Plastic Waves in Materials, N. Davids and P. K. Mehta.

(Unclassified Abstract) Expansion of spherical cavities in impulsively loaded thick metal spheres is investigated analytically and experimentally. The method of analysis is one bypassing formulation in terms of differential equations and associated boundary conditions which, due to their intractable form, would have to be solved by coding for automatic computation. Rather, the computer program is constructed directly from the physical laws and the finite formulation of the material constitutive relations. The results show that spherical plastic waves propagate at the speed of bulk compressional waves as long as discontinuities persist across the boundary.

- (9) Wedge Penetration in a Thick Target, W. G. Soper.

(Unclassified Abstract) Analysis of a wedge penetration into a thick aluminum target is compared with penetration experiments at velocities from 1 to 500 ft/sec. The penetration data follow the "rough" wedge solution at low velocity but approach the frictionless case at several hundred ft/sec. This behavior is ascribed to adiabatic heating and consequent softening of target material adjacent to the penetrator. It is concluded that a strain-rate-insensitive Tresca maximum shear stress provides a satisfactory specification of the dynamic material properties, but that work-hardening and thermal phenomena must be included for accurate analysis.

- (10) Hypervelocity Impact, R. J. Eichelberger.

(Unclassified Abstract) Impact phenomenology at high velocities is discussed in detail and supported by a summary of pertinent theoretical and experimental studies. Emphasis is placed upon the current understanding of the transient events leading to crater formation. The relative importance of material properties and of impact conditions in determining the form and dimensions of the crater is considered, and the formulas derived from both theory and experiment are described and evaluated.

- 503 Kendall, David P.; Davidson, Thomas E.: "The Effect of Strain Rate on Yielding in High-Strength Steels"; (Unclassified Report), Watertown Arsenal Report No. WVT-6618, May 1966, AD 637 217.

(Unclassified Abstract) Effect of strain rates ranging from 10^{-4} to 10 in./in./sec on yield strengths of several high-strength alloy steels is investigated.

Quenched and tempered-type alloys exhibit two regions of strain rate sensitivity, with the strain rate dividing the sensitive and insensitive regions varying from 0.5 to greater than 10 in/in/sec, depending on composition, microstructure, and grain size. At the higher rates, a power law relationship is found which is consistent with a yielding model involving breakaway of dislocations from solute atmospheres.

Maraging steel exhibits a continuous power law strain rate sensitivity over the entire range. The ratio of static (yield strength) to dynamic strength is given for aluminum, copper, magnesium, titanium, plastic and fiberglass.

- 504 Groeneveld, T.P.: "Review of Recent Developments in High-Strength Steels"; (Unclassified Report), Defense Metals Information Center, 22 March 1967, AD 810 150.

(Unclassified Abstract) A review is presented of nine recent developments in high-strength steels. In particular, the effect of strain rate on yielding in high-strength steels is discussed. An equation is given describing the relationship between strain rate and yield stress. Brief comment on strain rate as a function of material grain size is included.

- 505 Beebe, Wayne M.; "AN EXPERIMENTAL INVESTIGATION OF DYNAMIC CRACK PROPAGATION IN PLASTIC AND METALS," Air Force Materials Laboratory, Research and Technology Division, Report No. AFML TR 66-249, November 1966.

Crack propagation experiments were conducted in polyester resin sheets containing a central crack. Uniaxial tension loading at several loading rates was applied perpendicular to the crack direction. Two types of experiments were conducted: (1) High loading rate tests at 24°C and -45°C, with a constant loading rate to study the acceleration characteristics of cracks running in a glassy material, and (2) High temperature-low loading rate tests to study slow crack propagation when appreciable viscous dissipation could occur.

During crack propagation, full frame photographs were taken of the photoviscoelastic isochromatic patterns and crack tip position at framing rates from 250 to 100,000 frames per second. The principal conclusions were as follows: (1) Even at loading rates exceeding 10^5 psi per sec, isochromatic patterns prior to crack propagation compare closely with static patterns. (2) Constant crack velocities were achieved in the high loading rate tests and it was found that the isochromatic patterns compare closely with the theoretical solution of Broberg. (3) During the crack acceleration period, the experimental data could not be represented adequately by the Berry elastic theory. (4) For the early phase of the slow (viscous) crack growth period, the crack length could be predicted using a simple theory proposed by Schapery and Williams.

Several tests were conducted on silicon-iron metal sheets; it was concluded that the same testing technique can be applied to the study of crack growth in metals.

- 506 Bodner, S. R.; "CONSTITUTIVE EQUATIONS FOR DYNAMIC MATERIAL BEHAVIOR," Material Mechanics Laboratory, Technion, Sci. Report No. 7, MML Report No. 10, September 1967. (AD 659 369)

The constitutive equations that have been developed for the dynamic behavior of materials presuppose the existence of a reference "static" yield criterion. An alternative formulation motivated by the work on dislocation dynamics considers the total deformation to consist of elastic and plastic components throughout the deformation history. This procedure permits the consideration of large deformations (finite strains) in a direct manner. The present paper outlines an elastic-viscoplastic theory based on this approach and includes numerical results for an internally pressurized thick walled sphere.

- 507 Campbell, J. D.; "PLASTIC INSTABILITY IN RATE-DEPENDENT MATERIALS," Brown University, ARPA E44, June 1967. (AD 656 732)

The paper presents a theoretical analysis of the time variation of strain gradients in a tensile specimen of rate dependent material, the analysis being based on the assumption that the strain rate in the material is a function of the local values of stress and strain. The theory is used to determine the criterion for the growth of strain gradients, and it is shown that for a given material there exists a region of the stress-strain plane in which these gradients increase indefinitely with time. The theory is applied to materials with specific types of rate-dependence, and the results are related to experimental data obtained at constant rates of strain.

- 508 Chu, Boa-Teh; "RESPONSE OF VARIOUS MATERIAL MEDIA TO HIGH VELOCITY LOADINGS, II. FINITE ELASTIC DEFORMATION," General Applied Science Laboratories, Technical Report No. TR 475, March 1, 1966. (AD 803 659)

Analytical prediction of the stress and finite deformation produced by an intense pressure step moving on one face of a slab of a perfectly elastic material at a speed greater than the wave propagation speeds in the medium are studied. Analytic solutions are given for the case when the slab occupies a half space. Depending on the nature of the material, a fast and/or a slow shock may be produced, or there may be no shocks at all. The characteristic theory is then presented. Its application to the computation of stress and deformation fields in a finite slab is discussed.

- 509 Jones, Norman; "FINITE DEFLECTIONS OF A SIMPLY SUPPORTED RIGID-PLASTIC ANNULAR PLATE LOADING DYNAMICALLY," International Journal of Solids and Structures, Vol. 4, No. 6, June 1968, pp. 593-603.

A theoretical analysis is presented for the dynamic behavior of a simply supported rigid, perfectly plastic annular plate subjected to a rectangular pressure pulse. It is shown that this theory, which considers the simultaneous influence of membrane forces and bending moments, predicts final deformations which are considerably smaller than those given by the corresponding bending theory even when maximum deflections only of the order of the plate thickness are permitted. It is believed that this theoretical analysis could be developed further in order to describe the behavior of plates having other support conditions and different dynamic loading characteristics.

- 510 Jones, N. . "INFLUENCE OF STRAIN-HARDENING AND STRAIN-RATE SENSITIVITY ON THE PERMANENT DEFORMATION OF IMPULSIVELY LOADED RIGID-PLASTIC BEAMS." Brown University. ARPA E46, July 1967. (AD 657 129)

A simple method is presented for estimating the combined influence of strain-hardening and strain-rate sensitivity on the permanent deformation of rigid-plastic structures loaded dynamically. A study is made of the particular case of a beam supported at the ends by immovable frictionless pins and loaded with a uniform impulse. The results of this work indicates that considering strain-hardening alone when appropriate or strain-rate sensitivity alone gives permanent deformations which are similar to those predicted by an analysis retaining both effects simultaneously.

- 511 Kramer, I. R.; "SURFACE EFFECTS ON MECHANICAL PROPERTIES OF METALS," Air Force Materials Laboratory. Report No. AFML TR 67-75, May 1967. (AD 816 627)

The research reported was conducted in three separate parts. First the stress associated with the surface layer was determined for iron and molybdenum. The measurements show that the surface layer plays a very important role in the plastic deformation of b. c. c. metals.

Secondly, the effect of diameter on the flow stress of polycrystalline aluminum (99.997 %) was studied. The increase in flow stress is attributed to an increase in the surface layer stress with decreasing specimen size.

Finally, the low temperature transient creep behavior of polycrystalline aluminum was investigated in terms of the recovery of the surface layer stress. The creep compliance was found to vary exponentially with time.

- 512 Kramer, I. R.; "RELATIONSHIP OF SURFACE EFFECTS TO THE MECHANICAL BEHAVIOR OF METALS." Air Force Materials Laboratory. Report No. AFML TR 66-2. January 1966. (AD 630 661)

The role of the surface is discussed in terms of its effect on the mechanical behavior of metals. There is adequate evidence which demonstrates that a region of high dislocation concentration exists in the region at the surface of a deformed metal. This dislocation rich layer impedes the movement of mobile dislocations. It was shown in aluminum by means of strain rate cycling tests that for a given applied stress, the average velocity of the dislocations is affected by the surface. It appears possible to explain the surface effects in terms of stress field associated with the surface layer, and the m^* values, where $V \propto \tau^* m^*$, V is the dislocation velocity and τ^* is the effective stress. For aluminum crystals additional internal dislocation barriers were not formed in Stage I and it was possible to show that Stage I ends when the difference between the applied stress and the surface stress on the secondary slip system equals the critical resolved shear stress.

The effect of the surface was found to be greater on polycrystalline specimens than on single crystals. For Armco iron, the surface stress was almost twice as great as that due to internal obstacles.

It is also shown that the yield point in high purity metals is associated with the surface layer.

- 513 Nicholas, T.; "THE MECHANICS OF BALLISTIC IMPACT -- A SURVEY," Air Force Materials Laboratory, Report No. AFML TR 67-208, July 1967. (AD 820 356)

A major portion of this report is devoted to a summary of the response of materials to dynamic loading. A list of 245 references is included.

- 514 Perrone, Nicholas; "IMPULSIVELY LOADED STRAIN-RATE-SENSITIVE PLATES," Journal of Applied Mechanics, Transactions of ASME, Series E, Vol. 34, No. 2, June 1967, pp. 380-384. (AD 657 221)

The response of an impulsively loaded, isotropically rate-sensitive annular plate is calculated via "exact" and approximate viewpoints. For a typical example, numerical results differed by about 3%. The essence of the approximate approach which represents a natural extension of a previously one-dimensional analysis, is that the initial stress profile remains substantially constant during the dominant portion of plastic flow.

- 515 Perrone, Nicholas; El-Kasrawy, Tamim; "COMPLETE DYNAMIC RESPONSE OF RATE-SENSITIVE STRUCTURES," Catholic University of America, Report No. 2, October 1966. (AD 643 282)

Recently a simplified general method was developed to determine the response of impulsively loaded, perfectly plastic, rate-sensitive structures with highly non-linear yield stress-strain laws.

In the present paper this approach is extended to encompass the dynamic load application phase. In other terms, a mathematical model closer to the physical situation is considered, namely, a pressure loaded rather than an impulsively loaded structural element.

As the prototype of a general structure the dynamically loaded thin ring is considered. For a constant pressure pulse, exact and approximate responses are calculated and differ by only a few percent. In the approximate solution the yield stress is taken to be a constant associated with the peak strain rate (which occurs at the instant of load termination).

The results suggest that one should be able to determine the complete response of a complex structure with arbitrary load pulse by enforcing an impulse/momentum change condition, while neglecting forces arising owing to deformation, to determine the initial strain rate distribution. The associated yield stress distribution may be calculated and assumed to be constant at each field point during the entire motion. This enormous simplification should bring a wide variety of practical physical problems within the scope of accurate solution via relatively modest effort.

- 516 Thurston, G. A.; "EIGHTH QUARTERLY REPORT OF TECHNICAL PROGRESS: CENTER FOR HIGH ENERGY FORMING," Martin Marietta Corporation, Denver Division, Report No. AMRA CR 66-05/9, July 1, 1967. (AD 655 521)

A parametric study was initiated using the computer program to predict strains in blanks formed into ellipsoidal dies. Techniques and instrumentation for dynamic strain measurements have been checked out.

Brief descriptions of papers on shock hardening, high-strain-rate ductility, explosive welding, and strain-rate experiments that were presented at the First International Conference of the Center for High Energy Forming are in this report. Papers presented by representatives of the Center at the conference will be included in the Second Annual Report of the Center. The complete proceedings of the conference will be edited and published at a later date.

D-12.1 Experimental Techniques

- 517 Beach, Norman E.; "GUIDE TO TEST METHODS FOR PLASTICS AND RELATED MATERIALS," Plastics Technical Evaluation Center, Picatinny Arsenal, Plastec Note 17, August 1967.

A listing of test methods pertaining to plastics materials and processes is presented. They are identified from lists of existing standards and test methods, promulgated by various government and national groups; and from physical examination of specifications relating to plastics. Thus there are included standardized methods and those which exist only as within-specification write ups. The citations are presented in alphabetical order, by test-subject ("Creep") rather than by material tested ("cushioning material"). The work covers 1000 test subjects and over 4000 citations.

- 518 Nicholas, T.; "A NOTE ON TENSILE TESTING AT HIGH STRAIN RATES," Air Force Materials Laboratory, Report No. AFML TR 66-341, October 1966. (AD 809 825)

The response of an elastic uniaxial tension specimen to a constant velocity applied at one end is presented. The application to the problem of testing specimens with high rate testing machines where the velocity of the ram approaches the dilatational wave velocity of the material is discussed. The concept of high strain rates is shown to break down under high loading rates.

- 519 Perrone, Nicholas; "ON THE USE OF THE RING TEST FOR DETERMINING RATE SENSITIVE MATERIAL CONSTANTS," Catholic University of America, Report No. 3, November 1966. (AD 646 609)

An explosive ring test is reappraised in light of recently developed material behavior models and analytical predictive techniques. It is demonstrated in complete detail how this test may be utilized to determine the uniaxial flow laws of rate sensitive perfectly plastic and strain hardening materials.

- 520 Rand, James L.; Marshall, John M.; "STRESS WAVE PROPAGATION IN A STRAIN-RATE SENSITIVE MATERIAL," Naval Ordnance Laboratory, Report No. NOLTR 65-11, Ball. Res. 143, April 1965. (AD 626 634)

It is known that some materials will behave differently when subjected to dynamic loading than when loaded statically. The purpose of this study is to examine the one-dimensional strain rate independent theory of T. von Karman and G. I. Taylor and the plastic rigid theory of E. H. Lee for material response, utilizing the dynamic stress-strain properties of these "rate sensitive" materials. All the predictions made from the theories were verified experimentally. An air gun was used to accelerate small lexan cylinders to a constant velocity, impacting them against a high strength target. The deformation, as well as the propagation of the stress wave resulting from the impact was observed. The predicted deformations by the plastic rigid theory, and the one-dimensional theory were within 7.0% and 8.7% of the measured deformations, respectively. The stress predicted by the one-dimensional theory was within 8.5% of the average measured stress.

- 521 Stewart, Wayne Lee; Rowe, Pierce Edward; Pahl, Peter Jan; "DYNAMIC TESTS OF MODEL STEEL STRUCTURES," Massachusetts Institute of Technology, Report No. R65-32, November 1965. (AD 628 063)

The objective of this research project is to investigate the effect of strain rate on the resistance function of structural elements and to develop modeling techniques for steel structures.

The dynamic loading machine capable of rise times of 3 milliseconds or more and maximum loads of 2000 pounds was developed. This machine can also be used for static loadings.

The beam tests indicate that the resistance function in bending for SAE 1113 steel models of 8 WF 67 sections is essentially independent of the strain rate. An equivalent single degree of freedom system yields good predictions of the experimental deflection-time curves for the beams. The consistency of tests on essentially identical beams was good. Tests on SAE 1020 steel models of 14 WF 103 beams indicate that for this steel, the resistance function in bending is strain rate dependent.

The frame tests confirm the observations made during the beam tests.

D-12.2 Steels and Refractory Metals

- 522 Asche, W. H.; Gross, M. R.; "EFFECT OF TEMPERING ON THE STRENGTH HARDNESS, AND NOTCH TOUGHNESS OF HY-130/150, 5Ni-Cr-Mo-V STEEL," U. S. Navy Marine Engineering Laboratory, Phase Report 72/66, March 1966. (AD 630 464)

The effect of tempering in the range of 900 to 1150F on the tensile properties, hardness, and Charpy V-notch toughness of HY-130/150, 5Ni-Cr-Mo-V steel was investigated. The investigation confirmed high tempering resistance claimed for the steel. The strength and hardness properties were found to be similar over a tempering range of 900 to 1050F. The notch toughness, however, increased with increasing tempering temperature.

- 523 Bartlett, E. S.; Barth, V. D.; et al; "REFRACTORY METALS (Cb, Ta, Mo, W), " Defense Metals Information Center, Battelle Memorial Institute, Review of Recent Developments, April 22, 1966; July 27, 1966; November 9, 1966; January 26, 1967; July 28, 1967; November 3, 1967; January 19, 1968; October 4, 1968.

Reviews recent developments relating to Columbium, Tantalum, Molybdenum and tungsten. Information presented includes properties, processing characteristics, and applications.

- 524 Boulger, F. W. et al; "METAL DEFORMATION PROCESSING, VOLS. II AND III: A SURVEY CONDUCTED AS PART OF THE METALWORKING PROCESS AND EQUIPMENT PROGRAM (MPEP), " Defense Metals Information Center, Battelle Memorial Institute, Reports 226 and 243, July 7, 1966 and June 10, 1967.

As part of the Metalworking Processes and Equipment Program, information was collected on deformation characteristics of metals and their effect on processing operations. This report presents the information collected from technical engineering reports on Government contracts and from general engineering and metallurgical publications. The objective is to help the non-specialist in recognizing the implications of scientific findings and in applying them in specific operations. This report contains a series of articles covering the following subjects: Ductile Fracture; Application of High Pressure to the Forming of Brittle Metals; Superplasticity; Lubrication in Metal-Deformation Processes; Swaging; Adiabatic Conditions in Deformation Processing; Residual Stresses Produced by Deformation. These subjects are treated in two ways: (1) generalized discussions of common processes point out why specific variables must be modified in order to deform certain types of metals satisfactorily; and (2) data on the more difficult-to-form metals are used to illustrate the principles, limitations, and effects of the processes.

- 525 Buttner, F. H.; Hale, R. W.; "THE REFRACTORY METALS -- AN EVALUATION OF AVAILABILITY, " Defense Metals Information Center, Battelle Memorial Institute, Memorandum 235, March 1968.

This memorandum discusses the supply, production, consumption, and applications of the refractory metals, columbium, tantalum, molybdenum, tungsten, and rhenium. List of manufacturers of mill products of these metals are included.

- 526 Campbell, J. E.; "MECHANICAL PROPERTIES OF METALS, " Defense Metals Information Center, Battelle Memorial Institute, Reviews of Recent Developments, October 22, 1965 (AD 803 124); May 13, 1966; August 5, 1966; November 23, 1966 (AD 803 357); February 3, 1967 (AD 807 491); May 24, 1967 (AD 814 796); August 22, 1967; November 8, 1967; February 16, 1968; May 10, 1968; July 19, 1968.

Review of the latest properties for steels, titanium alloys, aluminum, etc.

- 527 Caywood, W. C.; Rivello, R. M.; "STRUCTURAL EFFICIENCY OF VARIOUS MATERIALS AT ELEVATED TEMPERATURES," Johns Hopkins University, Applied Physics Laboratory, Report No. APL/JHU CF-2578, October 1956. (AD 657 110)

Curves are presented for determining the relative efficiencies of several structural materials at elevated temperatures for various loading conditions. The materials considered are:

Aluminum:	6061-T6, 2024-T4
Steel:	NAX (high strength low alloy steel made by Great Lakes Steel Corp.)
Stainless Steel:	301-1/2H, 321 Annealed, 17-7PH Condition TH1050, 17-7PH Condition RH950
High Nickel Alloy:	Inconel X Solution treated
Magnesium:	HK31A-T6, HM21XA-T8
Titanium:	6AL-4V

These materials were examined for (1) tensile ultimate strength; (2) tensile yield strength; (3) bending stiffness of thin-walled cylinders; (4) thin-walled cylinders under compression, bending, and pressure loadings; and (5) buckling of thin flat plates.

- 528 Clark, H. T.; Manfre, J. A.; "BASIC METALLURGY OF TITANIUM," Defense Metals Information Center, Battelle Memorial Institute, Memorandum 234, April 1, 1968, pp. 1-7.

A survey of the properties and applications of titanium and titanium alloys.

- 529 DeFries, Richard S.; "AN EVALUATION OF ELEVATED TEMPERATURE MATERIALS FOR THE 81MM MORTAR TUBE," Watervliet Arsenal, Report No. WVT 6629, November 1966. (AD 807 425)

An evaluation of test results for room and elevated temperatures and their effect on the mechanical properties of seven steel alloys for application to the 81mm Mortar Tube was made. Elevated temperature yield strength, ductility, impact and fracture toughness, and fatigue properties are discussed. Availability and cost of materials are also compared. Results of elevated temperature testing of the seven alloys reveals yield strength decreases rapidly with temperature and slightly with time at temperature. INCO 718 steel exhibited the best combination of properties to warrant its use in the 81mm Mortar Tube.

- 530 Groeneveld, T. P.; "HIGH STRENGTH STEELS," Defense Metals Information Center, Battelle Memorial Institute, Review of Recent Developments, December 16, 1966 (AD 804 273); September 1, 1967; December 20, 1967; March 20, 1968.

Summary of recent developments relating to high strength steels including properties, strengthening mechanisms, weldability, corrosion characteristics, etc.

- 531 Gurev, Harold S.; "HIGH-ENERGY-RATE PROCESSES," Defense Metals Information Center, Battelle Memorial Institute, Review of Recent Developments, February 17, 1967; August 23, 1967; January 12, 1968 (AD 824 959).

Periodic reviews and summaries of reports relating to such high-energy-rate processes as explosive forming, explosive welding, shock treatment, powder compaction, etc. Often summarizes mechanical properties of materials, such as, maraging steel, alloy steels, titanium, etc.

- 532 Kalish, D.; Kulin, S. A.; "THERMOMECHANICAL TREATMENTS APPLIED TO ULTRA-HIGH-STRENGTH STEELS," Manlabs Inc., Final Report, April 1965. (AD 614 806)

The response of 9% nickel and 4% cobalt steels to thermomechanical treatments was evaluated with particular emphasis on fracture toughness. Two carbon contents, 0.25 and 0.45%, were studied. The thermomechanical treatments involved austenite deformation processes and strain-tempering processes with either martensite or bainite being the transformation product. The properties of undeformed structures were also measured for comparison purposes.

Thermal and strain-tempering treatments applied to 9-4-45 develop two bands of precracked Charpy impact energy versus yield strength, one for martensites and one for bainites. In the yield strength range 20,000 to 340,000 psi the bainites possess substantially higher impact strengths than the martensites at equivalent strength levels. Austenite deformation processes do not improve the impact strength of 9-4-45 for treatments involving 50% deformation. Strain-tempering of the 9-4-25 steel develops yield strengths from 200,000 to 300,000 psi. At these strength levels this steel has higher impact energies than the 0.45% carbon steel.

The level of both K_{IC} and yield strength in the 9-4-xx steels may be increased by thermomechanical treatments, such that combinations of K_{IC} and yield strength are obtained that are equivalent or superior to those developed in the 18 nickel maraging alloy.

- 533 Lannelli, Armando A.; Rizzitano, F. J.; "NOTCHED PROPERTIES OF HIGH STRENGTH ALLOYS AT VARIOUS LOAD RATES AND TEMPERATURES," U. S. Army Materials Research Agency, Technical Report AMRA TR 66-13, July 1966. (AD 647 884)

Tests have been conducted to determine the notched and unnotched strengths of aluminum alloys 7001-T6 and 7075-T6, titanium alloy 6Al-6V-2Sn, uranium alloy 8Mo-0.5Ti, Rocoloy steels and 18% Ni maraging steel at load durations of 10 milliseconds to 5 minutes, and at temperatures from -320°F to 500°F.

At room temperatures, as load duration was increased from 10 milliseconds to 5 minutes, the notched and unnotched tensile strengths of these materials were maintained within 10%, except that they increased approximately 30% for the notched aluminum alloys, and decreased 30% for the unnotched uranium alloy.

The notched strength of Rocoloy steel is less than its unnotched strength over the entire test temperature range. Notched strengths of all the other alloys tested are less than their unnotched strengths in the lower test temperature range but exceed the unnotched strengths in the higher temperature range.

- 534 Maykuth, Daniel J.; Hanby, Kenneth R.; "CURRENT AND FUTURE TRENDS IN THE UTILIZATION OF TITANIUM," Defense Metals Information Center, Battelle Memorial Institute, Memorandum 226, October 27, 1967.

This report has been prepared almost entirely from information available in trade magazines, newspapers, and press releases. The report points out trends in the application of titanium and its alloys, and provides some statistics on the current availability of titanium sponge, ingot, and mill product. A final section points out some of the factors which will be involved in the future supply-demand situation, and provides a preliminary assessment of that situation. In the appendix, price data as well as detailed data on the availability of specific mill forms is given.

- 535 Owen, W. S.; Averbach, B. L.; Cohen, M.; "BRITTLE FRACTURE OF MILD STEEL IN TENSION AT -196C," Massachusetts Institute of Technology, Report No. SSC-109, November 5, 1967. (AD 635 082)

The tensile fracture behavior of a mild steel at -196C has been studied in some detail. With the aid of long thin strip specimens loaded at controlled crosshead speeds between 8.9×10^{-4} and 1.6×10^{-1} in./min, the strain pattern and microscopic changes preceding fracture were observed, and the magnitude local strain was measured. Specimens heat-treated to alter the tendency toward brittle behavior, but maintaining ferrite-pearlite structures, were also examined.

Under these conditions, all the Lüder's bands display micro-cracks in some ferrite grains. However, the as-received and normalized specimens do not fracture at low yield stresses (slow loading speeds) during the spread of the Lüder's bands. By raising the loading speed, a critical stress is reached when fracture occurs after a delay time. The formation of micro-cracks and fracture is always preceded by gross yielding. On further increasing the loading rate, the fracture stress rises along with the yield stress.

Deductions from the dislocation pile-up theory of fracture in polycrystalline metals are not compatible with the experimental data. It is concluded that the microcrack model suggested by Low is more appropriate.

Some observations on the creep occurring in Lüder's bands during their propagation at -196 C are included.

- 536 Polosatkin, G. D.; Kudriavtseva, L. A.; Glazkov, V. M.; "STUDY OF THE DYNAMIC YIELD POINT OF METALS AT SHOCK VELOCITIES TO 1000 M/SEC," Lockheed Missiles & Space Company, 1966 (AD 644 178); Translation from Izv. AN SSSR, Metally, No. 5, 1966, pp. 121-124.

The dynamic yield point was determined for a steel alloy and aluminum using three different methods, i. e., the residue strain, motion picture, and strain gages. All methods agree. The dynamic yield point was found to rise in both materials as the impact velocity increased up to 250 m/sec. The dynamic yield point then remained constant up to 1000 m/sec.

- 537 Prosvirin, V. I.; Zaytsev, A. I.; Mortikov, V. D.; "INFLUENCE OF WORKING TEMPERATURES ON PROPERTIES OF ALLOY EI-437," Foreign Technology Division, Air Force Systems Command, "Studies of Steels and Alloys (Selected Articles)", Machine Translation No. FTD-MT-65-383, June 30, 1966. (AD 640 724)

Translation of AN SSSR Nauchnyy Sovet Po Probleme Zharoprochnykh Splavov (Russian). Issledovaniya Staley I Splavov, 1964, pp. 166-171. This article is an investigation of the effect of prolonged heating in the temperature range of 550° to 700°C upon the properties of a Russian heat-resisting alloy designated EI-437. The alloy is used in gas-turbine engines.

- 538 Puzak, P. P.; Lloyd, K. B.; "METALLURGICAL CHARACTERISTICS OF HIGH STRENGTH STRUCTURAL MATERIALS," Naval Research Laboratory, Report No. NRL 6364, August 1965. (AD 625 374)

A progress report covering research studies in high strength structural materials conducted in the period May 1965 to July 1965 is presented. The report includes fracture toughness studies on the 12 Ni maraging and 9Ni-4Co-XXC steels, a variety of titanium alloy MIG, EB, and plasmarc weldments, and some aluminum alloys. The current fracture toughness index diagrams are presented for steels, titanium alloys, and aluminum alloys. Results are presented of (1) a study of the plane-strain fracture toughness of the alloys Ti-6Al-4V and Ti-6Al-6V-2.5Sn over respective yield strength ranges of 130-140 ksi and 147-186 ksi; (2) heat-treatment studies on several titanium alloys; and (3) a low cycle fatigue crack propagation study of 5Ni-Cr-Mo-V steel in dry and wet environments in which considerable microcrack formation and growth was encountered.

- 539 Sessler, J. G.; Weiss, V. (editors); AEROSPACE STRUCTURAL METALS HANDBOOK, Air Force Materials Laboratory, Vols. I, II, and IIA, Report No. ASD-TDR 63-741 (in 3 volumes), March 1963, with supplements issued yearly (Vol. IIA, Suppl. 3, AD 802 121; Vol. I, Suppl. 4, AD 819 736; Vol. II, Suppl. 4, AD 819 792).

The Aerospace Structural Metals Handbook consists of three volumes I, II and IIA. Volume I contains data for 66 ferrous alloys. Volume II contains data on 56 light metal alloys. Volume IIA contains data on 54 non-ferrous heat resistant alloys.

- 540 Severdenko, V. P.; Kal'nitskiy, R. M.; "PLASTICITY AND STRENGTH OF TUNGSTEN DURING SHORT TIME TESTS," Foreign Technology Division, Air Force Systems Command, "Studies of Steels and Alloys (Selected Articles)", Machine Translation No. FTD-MT-65-383, June 30, 1966, pp. 1-7 (AD 640 724)

Translation of AN SSSR Nauchnyy Sovet Po Probleme Zharoprochnykh Splavov (Russian). Issledovaniya Staley I Splavov, 1964, pp. 114-117. This is a study of the plasticity and strength of preliminary deformed cermet tungsten. Tests were conducted at strain rates of from 2.36×10^{-2} to 5.55×10^{-1} and over the temperature range of 20-1000°C.

- 541 Simmons, W. F.; "RUPTURE STRENGTHS OF SELECTED HIGH-IRON, NICKEL-BASE, COBALT-BASE, AND REFRACTORY METAL ALLOYS," Defense Metals Information Center, Battelle Memorial Institute, Memorandum 236, May 1, 1968.

Rupture strengths, in graphical form, are presented for selected superalloys at 100 hours and 1000 hours, and for selected refractory metal alloys at 10 hours and 100 hours. Nominal chemical compositions are tabulated for all of the alloys covered.

- 542 St. Germain, F.; "EVALUATION OF RMSRP TUNGSTEN SHEET," Solar, Report No. ER 1399-6, July 9, 1965. (AD 617 733)

The final report of a study to determine the metallurgical uniformity, mechanical properties, forming characteristics, and fabrication properties of tungsten sheet. Data presented includes tensile properties over the ambient to 3000°F temperature range, five different joining techniques, and optimum temperatures for brake forming, dimpling, corrugating, joggling, and deep drawing processes.

- 543 Strohecker, D. E.; "FORMING OF TITANIUM AND TITANIUM ALLOYS," Defense Metals Information Center, Battelle Memorial Institute, Report 238, September 1, 1967.

This report represents a portion of the information contained in the March, 1967, revised edition of the "Aircraft Designer's Handbook for Titanium and Titanium Alloys" which was prepared by the Defense Metals Information Center under the joint sponsorship of the U. S. Air Force Research and Technology Division, and the Federal Aviation Agency.

The important techniques discussed include: (1) brake forming, (2) stretch forming, (3) deep drawing, (4) trapped-rubber forming, (5) tube bulging, (6) bending, (7) drop-hammer forming, (8) roll forming, (9) roll bending, (10) spinning and (11) shear forming, (12) dimpling, (13) joggling, and (14) hot sizing. Auxiliary metalworking operations, preparation for forming, blank heating methods, lubricants for forming and tooling materials are discussed. Other data available in the open literature have been summarized and referenced to present a comprehensive picture on the state of the art of these fabrication methods as related to titanium and its alloys.

- 544 Wagner, H. J.; Simmons, W. F.; "NICKEL- AND COBALT-BASE ALLOYS," Defense Metals Information Center, Battelle Memorial Institute, Review of Recent Developments, November 3, 1966; January 20, 1967; May 3, 1967; August 11, 1967; October 27, 1967; January 31, 1968; May 15, 1968.

Surveys and summarizes recent reports on the properties, physical metallurgy, process development, and applications of nickel- and cobalt-based alloys.

- 545 Weinberg, Mark H.; "TENSILE TESTING OF PEARLITIC MALLEABLE CAST IRON PROJECTILE BODY, 81MM, M362A1," Picatinny Arsenal, Report No. PA-TR-3390, July 1968. (AD 673 691)

A detailed study is made of the mechanical properties of 81MM pearlitic malleable cast iron projectile bodies, using a precise method for measuring elongation of tensile specimens. A critical analysis is made of the minimum percentage elongation requirement as an acceptance criterion. A high degree of inhomogeneity is found with respect to percentage elongation. Recommendations are made to eliminate the percentage elongation requirement, replace with other material characteristics.

- 546 Weiss, V.; Kot, R.; Krause, G.; "INVESTIGATION OF PHENOMENON OF SUPERPLASTICITY IN METALS," Syracuse University, Final Report, October 1966. (AD 807 264)

The influence of stress on the deformation of Ti-6Al-4V specimens was investigated during cycling through the phase transformation. A linear relationship between deformation per cycle and stress was observed. The experimental slope value $(\delta\epsilon/\delta\sigma) = 2.22 \times 10^{-5} (\text{psi})^{-1}$ was in excellent agreement with the theoretical predictions of the Greenwood-Johnson pseudo-creep theory. Isothermal creep tests, required for comparison with the above theory, were conducted on the same specimen geometry and in the same test stand as that used for the temperature cycling tests. A change of the deformation mechanism at a constant temperature, just below the transformation temperature for stress levels, causing the same flow rate as that observed in the cycling test, was observed from these creep tests.

Static room temperature tension tests were performed on Ti-6Al-4V specimens after repeated temperature cycling through the phase change under various stresses and performing the usual aging treatment. The mechanical properties were measured and compared with those of specimens given the conventional solution treatment and the same aging treatment. The specimens cycled through the phase change exhibited a small decrease of Young's modulus, strength and ductility.

- 547 Wood, R. A.; Maykuth, D. J.; "TITANIUM AND TITANIUM ALLOYS," Defense Metals Information Center, Battelle Memorial Institute, Review of Recent Developments, November 16, 1966; February 24, 1967; August 24, 1967; December 5, 1967; May 29, 1968; August 23, 1968.

Reviews recent developments in the properties, processability, metallurgy, and applications of titanium and titanium alloys.

- 548 "MECHANICAL-PROPERTY DATA HP 9Ni-4Co-25C STEEL: TEMPERED PLATE," Air Force Materials Laboratory, October 1965. (AD 803 546)

This data sheet was prepared by Battelle Memorial Institute. It contains mechanical property data for a nickel-cobalt quenched and tempered martensitic steel which exhibits excellent toughness at yield-strength levels up to about 200 ksi. The alloy is available as sheet, plate, wire, rod, bar, and forging.

See also: Abstract No. 520

D-12.3 Lead

- 549 Gondusky, J. M.; Duffy, J.; "THE DYNAMIC STRESS-STRAIN RELATION OF LEAD AND ITS DEPENDENCE ON GRAIN STRUCTURE," Brown University, Technical Report 53, May 1967.

Several specimens of commercial and high-purity lead of various grain size and crystallographic orientation were loaded dynamically in compression by means of the split Hopkinson bar. Strain rate was held constant at approximately 1200 sec^{-1} for strains up to about 15%. The dynamic stress-strain curves were found to lie approximately 50% higher than the corresponding static curves.

The compression tests described formed part of a larger project whose purpose was to determine dynamic values of Tabor's constant for lead and its dependence on crystal orientation. For this purpose the results of the compression tests were combined with those of dynamic indentation tests previously performed on the same lead specimens. It was found that dynamic values of Tabor's constant range from 2.4 to 6.0 depending upon grain size and orientation. These values are approximately equal to the corresponding static values. They may be compared to the value of 2.8 obtained by Tabor and other investigators for numerous fine-grained polycrystalline materials, including lead, and for strains up to about 20%.

See also: Abstract No. 525

D-12.4 Light Alloys

- 550 Bodner, S. R.; Rosen, A.; "DISCONTINUOUS YIELDING OF COMMERCIALLY PURE ALUMINUM," Israel Institute of Technology, Sci. Rpt. No. 2, MML Rpt. No. 2, September 1966 (AD 641 990); See also: Journal of the Mechanics and Physics of Solids, Vol. 15, 1967, pp. 63-77 (AD 652 082 and AD 641 995).

The discontinuous, repeated yielding of commercially pure aluminum under slowly applied dead weight loading is examined as a dynamic instability problem. The destabilizing factor is shown to be the negative slope of the flow stress-strain rate relation which, for aluminum, is a consequence of rapid strain aging. The essentials of the phenomenon are illustrated by a dry friction model which incorporates a counterpart of strain hardening. More generalized models show the equivalent of progressive yielding over the specimen length and delayed yielding under incremental loading. A stepped stress-strain curve is derived from the experimental flow stress-strain rate relation which agrees well with the observations in dead weight loading tests. Additional experiments on an Instron testing machine were performed with variable machine flexibility and strain gage recording. These test results support the explanation of the origin of the stepped stress-strain curves.

- 551 Grant, Nicholas J.; Blucher, Joseph T.; Ritter, Donald L.; "RESEARCH ON THE ROLE OF STRAIN RATE AND TEMPERATURE IN FATIGUE," Air Force Materials Laboratory, Report No. AFML TR 66-39, January 1967. (AD 813 619)

This study is concerned with the roles of strain rate and temperature on fatigue behavior. For the purposes of the immediate work pure aluminum and an aluminum - 10% zinc alloy were selected. To simplify analyses of the observed behavior, an axial fatigue machine was designed to eliminate strain rate and stress gradients in the specimen cross-section. Strain rates of 5 and 150% per minute strains of $\pm 1\%$, and temperatures from 80 to 900°F were the variables studied. A number of grain sizes were utilized to evaluate the role of alloy structure. Other strain rates, strains and structures, including two phase systems, are being examined to extend the studies. Thermal fatigue behavior will be examined and the results compared with the present observations in mechanical fatigue.

- 552 Hallowell, J. B.; "ALUMINUM AND MAGNESIUM," Defense Metals Information Center, Battelle Memorial Institute, Review of Recent Developments, October 17, 1967; April 26, 1968.

Survey of recent developments including alloying agents, properties, applications, etc.

- 553 Kenig, Marvin Jerry, "EXPERIMENTS ON ANNEALED ALUMINUM," Princeton University, Report No. 737, AFOSR 65-0983, 1965. (AD 618 088)

The stress-strain relationship for biaxial stressing of an annealed, commercially pure aluminum were determined under quasi-static and dynamic conditions. The main points

of the report are that (1) all existing commonly used theories of plasticity cannot possibly apply to mechanically unstable materials such as the 1100 aluminum tested, and (2) all experimentally observed wave speeds can be predicted by shock wave and the Karman-Taylor theory with respect to strain rate effects.

- 554 Ritter, D. L.; "EFFECT OF TEMPERATURE ON DEFORMATION AND FRACTURE OF ALUMINUM DURING HIGH AMPLITUDE CYCLIC STRAIN," Air Force Materials Laboratory, Report No. AFML TR 67-85, March 1967. (AD 816 195)

Low cycle axial fatigue tests were performed on high purity aluminum and an Al-10% Zn alloy. Constant strain rates of 5 and 150% per minute were employed at a strain amplitude of 2% ($\pm 1\%$) over the temperature interval 20 to 482°C. Electron microscopy was applied extensively, utilizing improved replication techniques, to study crack initiation, crack growth and failure. A number of crack growth curves were established.

At temperatures above 260°C, where grain boundary sliding and migration become active, the one to one migration-cycles process (for fine grained materials yielded an activation energy of 18.5 k cal/mol, approximately equal to that for self-diffusion along boundaries).

Double kinking in single crystals, orthogonal boundary diffusion and fracture at very high temperatures, and the role of strain rate are discussed in considerable detail.

- 555 Smith, S. H. et al; "FATIGUE-CRACK-PROPAGATION AND FRACTURE-TOUGHNESS CHARACTERISTICS OF 7079 ALUMINUM-ALLOY SHEETS AND PLATES IN THREE AGED CONDITIONS," The Boeing Company (Renton Division), NASA CR-996, February 1968.

See also: Abstract Nos. 526, 536, and 539

D-12.5 Plastics and Rubbers

- 556 Eichenberger, T. W.; "MECHANICAL PROPERTY AND FRACTURE TOUGHNESS EVALUATION OF 2219-T6E46 FOR CRYOGENIC APPLICATIONS," The Boeing Company, Final Report, August 15, 1964. (AD 455 312)

Mechanical properties and fracture toughness characteristics were determined for 2219-T6E46 aluminum alloy plate and forged ring material from room temperature to -423°F. Static tension tests; notched tension, fatigue and creep tests; and center cracked tear resistance tests were conducted at room temperature, -109°, -320°, and -423°F.

Design Allowable tensile strengths, plane strain fracture toughness and flaw growth characteristics, and plane stress tear resistance characteristics were determined for cryogenic applications.

- 557 Landrock, Arthur H.; "PROPERTIES OF PLASTICS AND RELATED MATERIALS AT CRYOGENIC TEMPERATURES," Plastics Technical Evaluation Center, Picatinny Arsenal, Plastic Report No. 20, July 1965.

This report reviews the effects of cryogenic temperatures on plastics and such related materials as elastomers and adhesives. It presents an annotated bibliography of 319 references from the open literature, government project and contract reports, and conference papers. A detailed subject index and a number of supplemental indexes are included. Topics covered are: molded polymeric materials (plastics); cryogenic insulation; structural plastic laminates; elastomers, seals, and sealants; adhesives; plastic films, film laminations and vapor barriers; fibers; electrical applications; wear and friction; liquid oxygen (LOX) compatibility; radiation and combined effects; and miscellaneous applications. Test Methods are not treated in the discussion, but the subject index refers to many references with information on test procedures and apparatus.

- 558 Lifshitz, J. M.; Kolsky, H.; "NON-LINEAR VISCOELASTIC BEHAVIOR OF POLYETHYLENE," Brown University (AD 652 537); see also International Journal of Solids and Structures, Vol. 3, 1967, pp. 383-397.

The response of viscoelastic solids to quasi-static loading, under conditions where non-linear theories have to be used, are discussed. Creep measurements of tension and of torsion in polyethylene specimens are described. Step loading was used and the deformations were measured optically by means of traveling microscopes for the tension experiments and by the reflection of light beams from mirrors for the torsion experiments. The deformations were too large for the theory of linear viscoelasticity to hold and the constitutive relations used were of multiple integral form; some of the kernels involved have been determined. It was found that for the loading range used, two kernels were sufficient to describe pure shear deformations and three kernels were required for tension. Some experiments in which two loading steps were applied are also described and discussed.

- 559 Nicholas, T.; Freudenthal, A. M.; "THE EFFECT OF FILLER ON THE MECHANICAL PROPERTIES OF AN ELASTOMER AT HIGH STRAIN RATES," Columbia University, Technical Report No. 36, November 1966. (AD 807 737)

Results are presented which show the effect of filler size and content on the stress-strain curves of an elastomer at high strain rates. An equation is proposed for the prediction of the apparent increase in modulus of an elastomer due to the addition of rigid spherical particles.

- 560 Rand, J. L.; Hinckley, W.; "DYNAMIC COMPRESSION TESTING OF SHOCK MITIGATING MATERIALS," Naval Ordnance Laboratory, Report No. NOLTR 66-39, Ball. Res. Rpt. No. 156, January 9, 1966. (AD 639 062)

The purpose of this report is to present the stress-strain relations of a variety of materials obtained at room temperature in compression and at rates of strain in excess of those achievable by standard testing techniques. The data are presented in the same form as most structural materials (stress versus strain) for the purpose of comparison with the conventional "static" relationship. Types of materials tested include rubbers, molded thermoplastics, and cast resins.

- 561 Rand, J. L.; Yang, J. C. S.; Marshall, J. M.; "DYNAMIC COMPRESSION TESTING OF A STRAIN-RATE MATERIAL," Naval Ordnance Laboratory, Report No. NOLTR 65-10, Ball. Res. Rpt. No. 142, October 1, 1965. (AD 477 279)

Complete compressive stress, strain and strain-rate data have been obtained at room temperature for annealed Lexan, a typical polycarbonate material, for strain-rates of 1.6×10^{-3} in/in/sec to 4×10^3 in/in/sec. It has been observed that although this material is violently sensitive to the rate of loading at lower strain-rates, this sensitivity becomes negligible as the rate of strain is increased and the resulting stress-strain relation may be considered to be a limiting curve. The existence of this limiting curve is an extremely significant characteristic of the material since it will permit a rate independent analysis to be used to predict material response at extremely high rates of strain.

- 562 Roberts, J.; "POLYMER MOLECULAR STRUCTURE AND MECHANICAL PROPERTIES," Explosives Research and Development Establishment (AD 612 979); see also Philosophical Magazine, Vol. II, No. 109, 1965, pp. 1-9.

The theoretical problem of relating the mechanical properties of a polymer to molecular structure is considered for the simplest case where an amorphous polymer is subjected to a hydrodynamic stress system at high rates of deformation. The theoretical basis is that under such conditions the mechanical properties can be attributed to the London forces between nearest atoms on neighbouring chain molecules.

For the amorphous polymers polymethylmethacrylate and polystyrene the calculations give room temperature values of maximum bulk modulus, triaxial and uniaxial brittle fracture strengths and probable brittle fracture strain. Theoretical values of bulk modulus are also obtained for polyethylenes of various degrees of crystallinity by considering strain in the amorphous regions only.

It is indicated how time dependent or viscoelastic effects might be introduced into the analysis to describe mechanical properties at much lower rates of deformation.

- 563 Sollenberger, Goerge H.; "GENERAL PROPERTIES OF THE NEW SUPERPOLYETHYLENES," Paper presented at Fourth Annual Wire and Cable Symposium, December 1955. (AD 656 389)

Lists the properties of superpolyethylene and discusses possible applications.

- 564 Stiles, E. Parker; "EXTRUDING HIGH DENSITY POLYETHYLENE FOR QUALITY AND SAVINGS," Paper presented at Eleventh Wire and Cable Symposium, November 1962. (AD 656 065)

High density polyethylene has proved itself to be an excellent wire and cable resin from both an electrical and a mechanical point of view. There are some extrusion technique modifications necessary in order to fully utilize the superior characteristics of this material. Improved polymer technology has developed the wherewithal to produce a very stable material capable of long term reliable service under the most severe environments.

Mechanical properties of both high and low density polyethylene are presented.

- 565 Titus, Joan B.; "EFFECT OF LOW TEMPERATURE (0 to -65°F) ON THE PROPERTIES OF PLASTICS," Plastics Technical Evaluation Center, Picatinny Arsenal, Plastec Report No. 30, July 1967.

The effects of low temperature on the mechanical, electrical and thermal properties of plastics is discussed. Data are given at three temperatures; namely, low temperature, about -65°F room temperature and around 160°F to permit complete evaluation. The material is presented by plastic family (in alphabetical order) and is divided into three parts: thermoplastics, thermosets and foams.

See also: Abstract No. 519

D-13 SEALS AND OBTURATORS

- 566 Ewbank, W. J.; "DYNAMIC SEALS -- A REVIEW OF THE RECENT LITERATURE," American Society of Mechanical Engineers Winter Annual Meeting and Energy Systems Exposition, Paper No. 67-WA/LUB-24, Pittsburgh, November 12-17, 1967.

This paper is an attempt to review and discuss all the significant papers which have been printed since 1952 on rotary shaft seals, both of the flat face and of the circumferential type. Seals for reciprocating motion are included. Discrepancies between reported results are pointed out where noted, and suggestions are made for needed future experimental work.

- 567 Jepsen, Robert E.; "INVESTIGATION OF MATERIALS AND DESIGN CONCEPTS FOR LONG LIFE RECIPROCATING PISTON SEALS," Air Force Flight Dynamics Laboratory, Report No. AFFDL TR-66-212, September 1966. (AD 814 784)

This report covers the effort involved in the investigation of material combinations and designs for 3/8 diameter unlubricated pistons and seals for use in miniature cryogenic pistons and reciprocating compressors.

- 568 Larsen, A. E.; "A DYNAMIC SEAL TESTER FOR PROPELLANT ACTUATED DEVICES," Frankford Arsenal, Report No. R-1753 SEG-TR-65-11, April 1965.

A study was conducted concerning the conception, design, fabrication, and preliminary evaluation of a test fixture to measure the static and dynamic performance of seals applicable to propellant actuated devices (PAD). Efforts were directed toward determination of the quantitative performance of seals, sealing materials, and sealing techniques. Three separate seal testing devices were conceived; one of these concepts was placed on contract for detail design, fabrication, and preliminary performance testing.

- 569 "HYDROSTATIC COMBUSTION SEAL DEMONSTRATION FEASIBILITY," Aerojet-General Corporation, Progress Report No. AGC 10784-Q-1, covering period 7 March - 15 September 1965, October 15, 1965, Confidential.

- 570 "SEALS REFERENCE ISSUE, 3RD EDITION," Machine Design, Vol. 39, No. 6, March 9, 1967.

A part of the Machine Design Reference Issue series, this issue is devoted to seals. Both design data and a product

directory are presented. Types of seals covered include (1) felt radial seals, (2) radial positive-contact seals, (3) exclusion devices, (4) clearance seals, (5) split-ring seals, (6) circumferential seals, (7) axial mechanical seals, (8) compression packings, (9) molded packings, (10) diaphragm seals, (11) static O-ring seals, (12) nonmetallic gaskets, (13) metallic gaskets, and (14) sealants.

See also: Abstract No. 3

D-14 UNCLASSIFIED ABSTRACTS FROM CLASSIFIED DOCUMENTS

- 571 Barrieres, Elie L.: "First Report on Ammunition Development for the US/FRG Main Battle Tank -- Feasibility Study of the 120mm Delta Shot (U)"; (Secret Report), Picatinny Arsenal Technical Report 3249, July 1965, AD 364 536.

(Unclassified Abstract) The Joint US/FRG Exploratory Development testing program for the 120mm Delta Shot evaluated five models for metal parts security, component functioning, aerodynamic characteristics and armor penetration. The ignition and burning characteristics of the propulsion components were determined at ambient and extreme temperature conditions.

During the metal parts security phase, five sub-projectile designs and four sabot designs were evaluated -- utilizing flash X-ray in the muzzle blast, smear, and framing cameras and recovery of fired parts to form conclusions. Armor penetration firings were conducted to obtain protection ballistic limits against heavy armor targets on three penetrator designs. Model and test results are given. Photographs and drawings of sabots and projectiles are given.

- 572 "Research Test of 120mm Delta System (with Prototype Gun)(U)"; (Secret Report), Aberdeen Proving Ground, Report No. DPS-1326, June 1964, AD 351 586.

(Unclassified Abstract) All testing was conducted with the Delta Prototype Gun No. 2. Tests of various cartridge case-primer assemblies with various lots and web sizes of propellants, T28, T28E1, and T36, MP, were performed with the Delta proof slugs. Tests were conducted to determine the exterior ballistics of four series of base-driven Delta shots. These tests were conducted with and without the muzzle gas diffuser attached to the prototype gun.

Drawings of projectile and sabot, Models 13 and 14, are included.

- 573 "Research Test of Shot, APFSDS, Delta, Models 11 and 12 (Armor Penetration Phase)(U)"; (Secret Report), Aberdeen Proving Ground, Report No. DPS-1109, November 1963, AD 344 980L.

(Unclassified Abstract) Models 11 through 20 of the 120/40mm APFSDS were tested to evaluate the following projectile properties: armor penetration, exterior ballistics, metal parts security, and discard characteristics of the sabot.

Drawings and photographs of the various sabot and projectile configurations are given.

- 574 Heinemann, Robert W.; Schimmel, Robert T.: "Development of a Bridgewire Initiator for the 105mm Tripartite Round (U)"; (Secret Report), Picatinny Arsenal, Technical Memorandum ORDBB-TE-31, August 1960, AD 319 754.

(Unclassified Abstract) The results of a study in developing a bridgewire igniter to replace the United Kingdom conductive composition cap in the 105mm Tripartite Round are given. Low-energy premature initiation was experienced in the British cap.

- 575 "Report of Project No. 2167 Service Test of Cartridge, 105mm, APDS-T, M392E1 (U)"; (Secret Report), U.S. Army Armor Board, Fort Knox, Kentucky, 14 December 1961, AD 326 862.

(Unclassified Abstract) Ammunition was fired and achieved satisfactory results at 1,000 and 1,500 meters. Gunner zeroing inaccuracy and line-of-sight parallax caused most misses. The test ammunition performance was similar to that of the British ammunition except for tracer burnout. Empty cartridge cases were not consistently ejected. Dispersion was satisfactory except in the desert firing, where USCONARC criteria were exceeded.

- 576 Sissom, B; Lamon, Lt. H.; Anderson, H. B.: "Visit to Fort Hood, Texas, Regarding Inaccuracy of the M60 Tank-Gun-Ammunition System (U)"; (Secret Report), Aberdeen Proving Ground, Report No. DPS-64, September 1960, AD 319 077.

(Unclassified Abstract) Troop tests with the M60 tank system led to reports of inaccuracy. This trip report concluded that the main difficulty during the troop test had been inability to zero the 105mm gun. The establishment of an emergency zeroing procedure was recommended.

105mm, APDS, T382 and UK, L36A1, rounds were used in the test. Photographs of a cutaway and complete T382 round were shown. Photographs of both U.S. and U.K. sabots and petals that were recovered are shown.

- 577 "Report on XM60 Weapon System Evaluation (U)"; (Secret Report), D&PS Aberdeen Proving Ground, First Report on Project TW-419, October 1958, AD 327 007.

(Unclassified Abstract) A weapon system evaluation for the XM60 tank was conducted to provide a basis for selection of a gun-ammunition combination. The following aspects were covered: (1) armor penetration test, (2) rate and accuracy of fire, (3) terminal effectiveness, and (4) overall system capabilities. Results are included and discussed. Conclusions and recommendations are given.

- 578 Bertrand, G.; Hansen, Capt. P.: "Improved APDS Shot for Tank Guns (U)"; (Secret Report), Canadian Armament Research and Development Establishment, CARDE T.N. 1601/64, July 1964, AD 357 466.

(Unclassified Abstract) Tests of the M392 APDS projectile were conducted to evaluate plate penetration, accuracy, and bridgewire initiator. Test results are given.

- 579 Hubbard, F. T.: "A Summary of Development on the Minnow Project from February 1956 to March 1957 (U)"; (Secret Report), Canadian Armament Research and Development Establishment, Technical Memorandum No. 144/57, April 1957, AD 300 017.

(Unclassified Abstract) The Minnow project represents a Canadian contribution to the Tripartite effort on the defeat of armor. The project supplements and extends work being done in the U. S. A. on the "Arrow" shell launched from a smoothbore gun.

The object of the Minnow project is to establish: (1) principles upon which a kinetic energy APFSDS projectile can be designed for smoothbore guns; and (2) the method of application of these principles to the use of larger cores in AP projectiles fired from rifled bore guns.

The following areas of interest are discussed:

- (a) Internal ballistics
- (b) Core movement
- (c) Aerodynamic characteristics
- (d) Penetration
- (e) Miscellaneous investigations
- (f) Future program

The transport zone and some of the basic problems concerned with it are discussed under the topic aerodynamic characteristics. An analytical method for the calculation of a fin-stabilized round of non-uniform density with optimum aerodynamic performance is presented. Sectioned representatives of the projectile and sabot are given; launch photographs are included.

- 580 Hubbard, F. T. : "A Summary of the Development of the Minnow Project from April 1957 to March 1958 (U)"; (Secret Report), Canadian Armament Research and Development Establishment, CARDE Technical Memorandum 187/58, April 1958, AD 302 575.

(Unclassified Abstract) Two types on projectiles, the moving-core Minnow and the hanging-fin Minnow, were investigated during the year. Serious doubts as to the practicability of the moving-core Minnow arose and concentration was placed on the hanging-fin concept.

Discussion of the following points is given:

- (1) Plating trials
- (2) Aeroballistic range tests
- (3) Plastic sabot

Photographs of launches, projectiles, and sabots are given.

- 581 Permuter, L.; Temple, E. P.; James, S. M. : "Uranium Alloy and Tungsten Alloy Cores for APDS Shot, Comparative Plating Trials in 105mm and 120mm Calibres (U)"; (Secret Report), Royal Armament Research and Development Establishment, CARDE Memorandum (P) 13/63, February 1963, AD 337 629.

(Unclassified Abstract) Comparative plating trials were fired with uranium alloy (98% U/2% Mo) cored APDS with tungsten alloy (90% W/7.5% Ni-2.5% Cu) cored APDS with the object of testing the relative efficiency of the two alloys. A 3/4 scale sectioned view of the 120mm APDS L15A3 shot is given.

- 582 "152mm Gun-Launcher Cannon, XM150 Series (U)"; (Secret Report), University of Pittsburgh, Technical Information Report 27.3.2.1, February 1967, AD 380 824, for Army Materiel Command.

(Unclassified Abstract) The XM150 152mm gun-launcher cannon is the principal armament of the XM70 main battle tank being jointly developed by the United States and the Federal Republic of Germany. This cannon has a separable-chamber breech and fires, selectively, a high explosive antitank (HEAT) guided missile or conventional rounds with combustible cartridge cases. This report discusses the gun-launcher and the different types of ammunition used.

- 583 "Development of Ammunition for M68 105mm Gun Cannon (U)"; (Secret Report), University of Pittsburgh, Technical Information Report 27.3.3.1, January 1966, AD 369 753, for Army Materiel Command.

(Unclassified Abstract) This report is a description of the ammunition for the M68 gun cannon of the M60 and M60A1 105mm gun full-tracked combat tanks. (See October 1963 report on same subject.)

- 584 "152mm Gun/Launcher Full-Tracked Combat Tank, XM70 (MBT-70)(U)"; (Secret Report), University of Pittsburgh, Information Report 27.3.1.1, August 1966, AD 376 323.

(Unclassified Abstract) The United States and the Federal Republic of Germany are jointly developing XM70 152mm gun/launcher full-tracked combat tank. This tank fires both the Shillelagh extended-range guided missile and five kinds of conventional ammunition. It is also armed with a 20mm automatic gun that can be retracted in the turret and a coaxial 7.62mm machine gun. The crew of three, stationed in the turret, not only have armor protection against projectiles but protection against radiation and chemical and bacteriological agents as well. The XM70 can ford streams and can submerge for concealment or for protection against nuclear effects. This report describes the systems and capabilities of the XM70 tank.

- 585 "Evaluation of Single Flechette (U)"; (Secret Report), Army Infantry Board, Fort Benning, Georgia, Report of Project Nr. 2876, 18 March 1960, AD 316 128.

(Unclassified Abstract) An evaluation of the .22 calibre single flechette is given and recommendations are made.

A complete description of the cartridge, flechette, and sabot is given in regard to material and operation. A sectioned view of the assembled projectile is given. The single flechette is a prototype round developed for Frankford Arsenal by Aircraft Armaments, Inc., to meet a requirement to replace standard small arms ammunition.

- 586 Dziemian, Arthur J.; Oliver, Alfred G.; McDonald, Walter C.: "Wound Ballistics of SPIW Flechettes (U)"; (Secret Report), Edgewood Arsenal - Army Chemical Research & Development, Report No. CRDLR 3308, July 1965, AD 364 425.

(Unclassified Abstract) All the work done in C.R.D.L.R. on Flechettes specifically designed for S.P.I.W. has been connected and analyzed for this report.

The S.P.I.W. program uses lightweight lethal arms for launching the arrow-like Flechette. The pull-type sabots supporting the Flechette are briefly described under the topic materials and methods.

- 587 MacMillan, J. T.: "Final Summary Report to Develop and Supply Experimental Shotgun Ammunition (U)"; (Secret Report), Remington Arms Company, Inc., Report No. AB 64-19, October 1964, AD 354 449.

(Unclassified Abstract) A 12-gauge shotshell with explosively charged No. 4 buckshot (.240 dia.) was developed and tested as an antipersonnel ammunition. Sabot systems (complete rounds) for firing single No. 4 buckshot are shown for both .12 gauge and .410 gauge guns.

- 588 "Summary Report Volume I - Design, Manufacturing and Testing of Canister Fillers (U)"; (Secret Report), Whirlpool Corporation, October 1959, AD 315 434.

(Unclassified Abstract) The design, manufacture and test of antipersonnel ammunition fillers (Flechettes) for use in flapper and beehive rounds is presented. Drawings of the pushers and sabots in launching the Flechettes up to velocities of 4000 fps are included. Material and round loading procedures are given.

- 589 Austin, D. W.: "Vulnerability of Mark III Nose Cone Materials (Phase 2)(U)"; (Secret Report), Eglin Air Force Base, Report No. APGC-TDR-61-28, July 1961, AD 344 345.

(Unclassified Abstract) Information is presented on the results of 32 good data shots which were fired against target specimens of three different ablating materials. The targets were either cut from a General Electric Mark III re-entry vehicle or were constructed to resemble portions of the actual vehicle. Spherical projectiles of aluminum, stainless steel, and tungsten-carbide were fired against the targets at velocities ranging from 10,000 to 20,000 fps and at three different angles of impact. Twenty-two shots were fired against targets at room temperature and 10 against targets which had been heated to the char point. An ultra high-speed framing camera was used to obtain the projectile velocity prior to impact.

A description of the types of sabots and the stripping techniques used is given.

- 590 Warren, H. R.: "Aeroballistic Range Tests of the CF-105 Phase 1 - Rounds 1 to 10 (U)"; (Secret Report), Canadian Armament Research and Development Establishment, Report No. TM AB-43, March 1958, AD 301 144.

(Unclassified Abstract) The present report describes a preliminary series of tests of the CF-105 supersonic, delta-winged aircraft consisting of 10 rounds using 1/120th scale models fired at a Mach number of about 1.6. The models were launched from a 5.9-inch smoothbore gun. The launching techniques and sabot are described.

- 591 Cowan, P.L.; Roney, P.L.: "CARDE Impact Studies Progress Report (U)"; (Secret Report), Canadian Armament Research and Development Establishment, Report No. TM 620/61, August 1961, AD 326 113.

(Unclassified Abstract) A comparison is made between the damage caused to targets by active and inert pellets. Two types of targets are used. The first is a steel plate of semi-infinite thickness, and the second a phenolic glass fiber laminate, backed with aluminum to simulate an ablative re-entry nose cone. No difference in damage is noted for the impact of inert and active pellets of the same density (1.78 g/cc) into steel.

In the case of the ablative targets, damage is found to vary with pellet material for inert pellets. Crater volume in the ablative targets seems to be dependent on pellet velocity, but independent of pellet density for a wide range of the latter (pellet mass constant). Penetration is strongly dependent on pellet density. Detonation of the active pellets is not definitely established for impact into either type of target. No difference is noted between impact in vacuum and in atmospheric air.

The sabots for launching the pellets are shown. The sabots were made of zelux plastic. Sabot separation techniques are described.

- 592 "Parametric Study of Gun-Launched Anti-Missile Defense System (GADS) (U)"; (Secret Report), U. S. Naval Ordnance Laboratory, Report No. NOLTR 62-56, 3 September 1963, AD 350 416.

(Unclassified Abstract) This is a report of a theoretical investigation into the feasibility of using a gun-launched projectile as a system for Ballistic Missile Defense.

The report describes a method and contains graphs for simple, adequate estimates of gun parameters to obtain a desired muzzle velocity with a given projectile weight. The parameters are: propellant sound speed, gun length, area of bore and chamber pressure. This method is applied to a 500-pound 8-inch projectile - 100 calibre 16-inch gun - Al - H₂O₂ - H₂ propellant system. The resulting gun system is described and rough cost estimates made. The conclusion is: the system is technically feasible but economically not useful.

Brief general discussion of the sabot and its function in launching is given. Two fin-stabilized discarding sabot (FSDS) projectiles for a 16-inch gun are proposed. A schematic of the 16-inch sabot and projectile is included.

- 593 "Polaris Progress Reports (U)"; (Secret Report), U. S. Naval Ordnance Laboratory, 1 April 1964 to 1 July 1964, AD 359 904.

(Unclassified Abstract) This abstract covers Polaris Progress Reports in general from 1 April 1964 to 30 June 1965, four reports being covered.

These reports deal with aerodynamic studies, pressure distribution, drag, pitching moment, normal force, turbulent wake investigation, etc., of various cone and missile shapes launched from light gas guns. Test results are given and discussed.

Launching techniques, model and sabot designs are discussed. Brief general descriptions are given of several different sabots.

- 594 "Polaris Progress Reports (U)"; (Secret Report), U. S. Naval Ordnance Laboratory, 1 July 1964 to 30 September 1964, AD 359 891.

(Unclassified Abstract) A discussion and results of the hypervelocity wake. A general discussion of the launching techniques and the sabots used in given.

- 595 "Polaris Progress Reports (U)"; (Secret Report), U. S. Naval Ordnance Laboratory, 1 October 1964 to 31 December 1964, AD 373 547.

(Unclassified Abstract) A discussion of model launching and aerodynamic characteristics/wake characteristics. Brief mention of launching techniques and sabot design.

- 596 "Polaris Progress Reports (U)"; (Secret Report), U. S. Naval Ordnance Laboratory, 1 April 1965 to 30 June 1965, AD 374 499.

(Unclassified Abstract) The aerodynamic characteristics of cones and cone shapes are discussed. Brief discussion of launching and range improvements.

- 597 Jusino, J. B. : "Experimental Data Obtained from Free-Flight Tests of a SARV Configuration (U)"; (Secret Report), U. S. Naval Ordnance Laboratory Technical Report 63-189, 8 March 1965, AD 363 890L.

(Unclassified Abstract) Drag and stability coefficients obtained from free-flight tests of a SARV vehicle configuration are given. Shadowgraphs of the model in flight are given and a still photograph of the vehicle and sabot is included. Sabots were manufactured from ethocel.

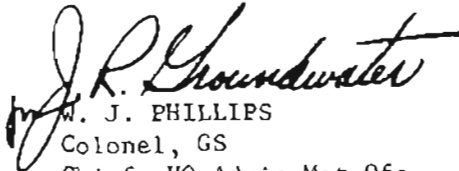
- 598 Condon, J.J.; Halperson, S.M.: "Hypervelocity Kill Mechanisms Program ARPA Order No. 149-60 Impact Damage Phase (U)"; (Secret Report), U.S. Naval Research Laboratory, NR 1492, February 1964, AD 348 245L.

(Unclassified Abstract) In this reporting period emphasis was placed on the perforation characteristics of different types of ablative materials. The targets were flat ablative plates bonded to metal plates for simulation of R/V outer construction. The ablation materials impacted were laminated and random-chopped phenolic refracil and nylon and G.E. Series 124A. The thickness varied from 2-inches to 0.5-inch. The majority of the materials used in these impact experiments were one-inch thick. For the phenolics the back-up materials were steel, aluminum and magnesium varying in thickness from 1/8-inch to 1/4-inch. For the G.E. Series 124A, the back-up was a one-inch aluminum honeycomb. The projectiles were solid steel, aluminum and plastic spheres. The tests were made primarily with steel spheres. The projectile velocity ranged from 3 to 7 km/sec and angles of obliquity from 90 degrees (normal impact) to 15 degrees. Correlations of the hole size with target thickness and composition, projectile energy, velocity, size and density were examined for each of the composite targets. Some comparisons are made between impacts into an actual ablative structure and the simulated flat plate targets. Photographs of all impacted targets discussed in the text are shown in the Appendix. A brief description is given of a solid sabot and stripping device which was developed during this period for higher velocity impacts. Also included as a separate topic are data and discussion on steel into steel impacts. These data were gathered from materials used as targets in firings in the development of a sabot for firing dense projectiles. A drawing of the sabot is included.

(AMCRD-TV)

FOR THE COMMANDER:

OFFICIAL:


W. J. PHILLIPS
Colonel, GS
Chief, HQ Admin Mgt Ofc

CHARLES T. HORNER, JR.
Major General, USA
Chief of Staff

DISTRIBUTION:
Special

